UNIVERSIDADE FEDERAL DO RIO GRANDE DO SUL
ESCOLA DE ENGENHARIA
PROGRAMA DE PÓS-GRADUAÇÃO EM ENGENHARIA ELÉTRICA

RAFAEL DA SILVEIRA CASTRO

OUTPUT REGULATION OF RATIONAL NONLINEAR SYSTEMS WITH INPUT SATURATION

Porto Alegre
2019

RAFAEL DA SILVEIRA CASTRO

OUTPUT REGULATION OF RATIONAL NONLINEAR SYSTEMS WITH INPUT SATURATION

Thesis presented to Programa de Pós-Graduação em Engenharia Elétrica of Universidade Federal do Rio Grande do Sul in partial fulfillment of the requirements for the degree of Doctor in Electrical Engineering.
Minor: Control and Automation

ADVISOR: Prof. Dr. Jeferson Vieira Flores

COADVISOR: Prof. Dr. Aurélio Tergolina Salton

Porto Alegre
2019

RAFAEL DA SILVEIRA CASTRO

OUTPUT REGULATION OF RATIONAL NONLINEAR SYSTEMS WITH INPUT SATURATION

This thesis was considered adequate for the awarding of the degree of Doctor in Electrical Engineering and approved in its final form by the Advisor and the Examination Committee.

Advisor: _____
Prof. Dr. Jeferson Vieira Flores, UFRGS
Doctor by Universidade Federal do Rio Grande do Sul – Porto Alegre, Brazil

Examination Committee:

Prof. Dr. Alexandre Trofino Neto, DAS-UFSC
Doctor by Institut National Polytechnique de Grenoble – Grenoble, France

Prof. Dr. Romeu Reginatto, UNIOESTE
Doctor by Universidade Federal de Santa Catarina – Florianópolis, Brazil

Prof. Dr. Alexandre Sanfelici Bazanella, PPGEE-UFRGS
Doctor by Universidade Federal de Santa Catarina – Florianópolis, Brazil

Prof. Dr. Lucíola Campestrini, PPGEE-UFRGS
Doctor by Universidade Federal do Rio Grande do Sul – Porto Alegre, Brazil

Prof. Dr. Diego Eckhard, PPGEE-UFRGS
Doctor by Universidade Federal do Rio Grande do Sul – Porto Alegre, Brazil

Coordinator of PPGEE: _____
Prof. Dr. João Manoel Gomes da Silva Jr.

Porto Alegre, January 2019.

ACKNOWLEDGEMENTS

I would like to thank my advisors Prof. Dr. Jeferson Vieira Flores and Prof. Dr. Aurélio Tergolina Salton for the immense technical support and cooperation during this research. My sincere gratitude also goes to my parents, who encouraged me in this journey.

ABSTRACT

This thesis deals with the output regulation of rational nonlinear systems with input saturation. The output regulation problem considers a controlled plant subject to non-vanishing perturbations or reference signals produced by an exogenous autonomous system, where the goal is to ensure asymptotic convergence to zero of the plant output error. This work develops systematic methodologies for stability analysis and design of anti-windup compensated dynamic output feedback stabilizing controllers able to solve the output regulation problem for rational nonlinear systems with saturating inputs. In order to obtain these results, the proposed method employs the differential-algebraic representation, a theoretical framework that treats rational nonlinear systems by a differential equation combined with an equality relation. This tool is utilized in order to cast the stability analysis and control synthesis into optimization problems subject to linear matrix inequality constraints. Towards ensuring asymptotic output regulation, it is initially assumed the prior knowledge of an exact solution to the regulator equations, which represent an invariant and zero-error steady-state manifold. This assumption is later relaxed, where the results are extended for the practical regulation problem. In this last scenario, any numerically approximated solution to the regulator equations may be considered and the devised methodology ensures ultimate boundedness of the output error. Overall, the main innovation of this thesis is the application of the differential-algebraic representation into the nonlinear output regulation context, in turn providing a solution to a new set of problems intractable by state-of-the-art nonlinear methods.

Keywords: Output regulation, differential-algebraic representation, linear matrix inequalities, rational nonlinear systems, input saturation, anti-windup.

RESUMO

Esta tese trata da regulação de saída de sistemas não-lineares racionais com saturação na entrada. O problema de regulação de saída considera uma planta sujeita a sinais persistentes de distúrbio ou referência produzidos por um sistema exógeno autônomo, onde o objetivo é garantir a convergência assintótica do erro de saída da planta para zero. Este trabalho desenvolve metodologias sistemáticas para análise de estabilidade e projeto de controladores estabilizantes dinâmicos de realimentação de saída com compensadores *anti-windup* para sistemas não-lineares racionais com saturação no contexto de regulação de saída. O método proposto utiliza principalmente a representação algébrico-diferencial, uma abordagem teórica que trata sistemas não-lineares racionais por meio de uma equação diferencial combinada com uma igualdade algébrica. Para assegurar a regulação assintótica de saída, inicialmente assume-se o conhecimento de um modelo interno e uma solução exata para as equações do regulador, que representa um conjunto invariante de regime permanente onde o erro de saída é zero. Esta suposição é posteriormente relaxada, onde os resultados são estendidos para o contexto de regulação de saída prática.

Os desenvolvimentos principais desta tese estão divididos nos seguintes capítulos: Regulação de Saída de Sistemas Não-Lineares Racionais; Regulação de Saída de Sistemas Não-Lineares Racionais com Saturação de Entrada e Extensão para Regulação de Saída Prática. O primeiro capítulo mencionado introduz a proposta de base deste trabalho, que consiste no emprego da representação algébrico-diferencial para a dinâmica do erro de regulação entorno do conjunto invariante descrito pelas equações do regulador. Com base nesta formulação, teoremas de estabilidade e desempenho são obtidos com condições na forma de desigualdades matriciais, permitindo o uso de otimização numérica para análise e síntese de controladores estabilizantes. No próximo capítulo, a formulação é estendida para a presença de saturação no sinal de controle, onde uma nova condição de setor é proposta para tratar esta não-linearidade adicional. Desta forma, novos teoremas são obtidos tanto para análise quanto para síntese de controladores estabilizantes incluindo compensadores *anti-windup*. No capítulo final da metodologia, considera-se uma abordagem de regulação prática onde soluções numéricas aproximadas podem ser consideradas para as equações do regulador. Novos teoremas de estabilidade voltados para análise e síntese também são obtidos dentro deste panorama prático, onde garante-se um conjunto terminal para a trajetória do erro de saída. Em geral, a grande importância deste trabalho é a possibilidade de solucionar um novo conjunto de problemas de regulação de saída não-linear, anteriormente intratáveis por métodos do estado-da-arte.

Palavras-chave: Regulação de saída, representação algébrico-diferencial, desigualdades matriciais lineares, sistemas não-lineares racionais, saturação de entrada, *anti-windup*.

CONTENTS

LIST OF FIGURES 8

LIST OF TABLES 11

LIST OF ABBREVIATIONS 12

LIST OF SYMBOLS 13

1 INTRODUCTION 14
1.1 Contribution of the Thesis 15
1.2 Outline of the Text 16

2 PRELIMINARIES 17
2.1 Stability of Nonlinear Systems 17
2.2 LMI based Stability and Control Design 18
2.2.1 Dynamic Output Feedback Control 18
2.2.2 Stability of Systems with Control Input Saturation 21
2.2.3 Stability of Rational Nonlinear Systems 24
2.3 Output Regulation of Nonlinear Systems 26
2.3.1 Internal Model Design 30
2.3.2 Design of Stabilizing Components 34
2.4 Final Remarks 36

3 OUTPUT REGULATION OF RATIONAL NONLINEAR SYSTEMS . . . 37
3.1 Problem Statement 37
3.2 Control Structure 38
3.3 Main Results 41
3.3.1 Regulation Error Coordinates 41
3.3.2 Differential-Algebraic Representation 43
3.3.3 Analysis Conditions 45
3.3.4 Design Conditions 47
3.4 Numerical Examples 51
3.4.1 Polynomial Nonlinear Plant with a Harmonic Exosystem 52
3.4.2 Rational Nonlinear Plant with a Chaotic Exosystem 59
3.5 Final Remarks 63

4 OUTPUT REGULATION OF RATIONAL NONLINEAR SYSTEMS WITH INPUT SATURATION 67
4.1 Problem Statement 67
4.2 Control Structure 67
4.3 Main Results 70
4.3.1 Regulation Error Coordinates 70
4.3.2 Differential-Algebraic Representation 72
4.3.3 Sector Conditions 73
4.3.4 Analysis Conditions 75
4.3.5 Design Conditions 78
4.4 Numerical Examples 81
4.4.1 Polynomial Nonlinear Plant with a Harmonic Exosystem 81
4.4.2 Rational Nonlinear Plant with a Chaotic Exosystem 85
4.5 Final Remarks 91

5 EXTENSION FOR THE PRACTICAL OUTPUT REGULATION 92
5.1 Problem Statement 93
5.2 Practical Control Framework 93
5.3 Main Results 96
5.3.1 Practical Regulation Error System 96
5.3.2 Differential-Algebraic Representation 97
5.3.3 Analysis Conditions 98
5.3.4 Design Conditions 102
5.4 Numerical Example 104
5.4.1 Approximate Solution of the Regulator Equations 105
5.4.2 Stabilizing Stage Design 107
5.4.3 Extended Design with Input Saturation and Anti-Windup 116
5.5 Final Remarks 118

6 CONCLUSION AND PERSPECTIVES 121
6.1 Overview of the Thesis 121
6.2 Future Perspectives 121

REFERENCES 123

APPENDIX A COMPLEMENTARY MATERIAL 127
A.1 Linear Matrix Inequalities 127
A.2 Bilinear Matrix Inequalities 130

LIST OF FIGURES

Figure 1: Block diagram of a linear dynamic output feedback control. 19

Figure 2: Block diagram of a Lur'e System with a saturation function. 21

Figure 3: The nonlinear output regulation framework. 27

Figure 4: Block diagram of the closed-loop system with the considered control structure. 38

Figure 5: On top: the output regulation error signal $e(t)$. On bottom: the control input signal (solid line) $u(t)$ compared to the zero-error steady-state signal $c(w(t))$ (dashed line). 56

Figure 6: Phase portrait depicting the system trajectory (x_1, x_2, u) (thin line) compared to the zero-error steady-state trajectory $(\pi_1(w), \pi_2(w), c(w))$ (thick line). 56

Figure 7: Plant and controller states $x(t)$ and $\xi(t)$ (solid lines) compared to the zero-error steady-states $\pi(w(t))$ and $\sigma(w(t))$ (dashed lines). 57

Figure 8: Representation of the set $\mathcal{D}$ in the x-state-space. The black contour is the region border for the default exosystem initial state. The gray contours denote borders for a myriad of exosystem initial states $w(0) \in \mathcal{W}$. 58

Figure 9: Output error signals $e(t)$ for initial conditions on the border of the domain of attraction estimate $\mathcal{D}$. Shades denote trajectories for different plant initial states. 58

Figure 10: On top: the output regulation error signal $e(t)$. On bottom: the control input signal (solid line) $u(t)$ compared to the zero-error steady-state signal $c(w(t))$ (dashed line). 64

Figure 11: Phase portrait depicting the internal model trajectory ξ_m (thin line) compared to the zero-error steady-state trajectory $\sigma_m(w)$ (thick line). 64

Figure 12: Plant and controller states $x(t)$ and $\xi(t)$ (solid lines) compared to the zero-error steady-states $\pi(w(t))$ and $\sigma(w(t))$ (dashed lines). 65

Figure 13: Representation of the set $\mathcal{D}$ in the x-state-space. The black contour is the region border for the default exosystem initial state from (230). The gray patches denote borders for a myriad of exosystem initial states $w(0) \in \mathcal{W}$. 66

Figure 14: Output error signals $e(t)$ for initial conditions on the border of the domain of attraction estimate $\mathcal{D}$. Shades denote trajectories for different plant initial states. 66

Figure 15: Control structure with saturation and anti-windup loops. 68

Figure 16: On top: the output regulation error signals $e(t)$. On bottom: the control input signals $u(t)$ compared to the zero-error steady-state signals $c(w(t))$ (dashed line). Shades denote different initial conditions on the border of $\mathcal{D}$. 84
Figure 17: Zoomed in depiction of the control inputs $u(t)$ from Figure 16. The top plot details the initial saturated period, while the bottom graph shows the control signals approaching the steady-state waveform. . . 84
Figure 18: Representation of the set $\mathcal{D}$ in the x-state-space. The black contour is the region border for the default exosystem initial state. The gray contours denote borders for a myriad of exosystem initial states $w(0) \in \mathcal{W}$. 85
Figure 19: On top: the output regulation error signals $e(t)$. On bottom: the control input signals $u(t)$ compared to the zero-error steady-state signals $c(w(t))$ (dashed line). Shades denote different initial conditions on the border of $\mathcal{D}$. 88
Figure 20: Zoomed in depiction of the control inputs $u(t)$ from Figure 19. Top plot details the initial saturated period, while bottom graph focuses on the steady-state. 88
Figure 21: Phase portrait depicting transient internal model trajectories ξ_m for different plant initial conditions. The thick lines indicate activation of the control input saturation. 89
Figure 22: Phase portrait depicting internal model trajectories ξ_m in the steady-state. 89
Figure 23: Representation of the set $\mathcal{D}$ in the x-state-space. The black contour is the border of $\mathcal{D}$ for the default exosystem initial state from (230). The gray patches denote borders of $\mathcal{D}$ for a myriad of exosystem initial states $w(0) \in \mathcal{W}$. 90
Figure 24: The contour denotes the region $\mathcal{D}$, where output regulation is guaranteed with the complete proposed design. Crosses represent initial conditions for which the closed-loop system simulation becomes unstable if the anti-windup compensation is deactivated. The small dot is an initial condition which does not produce input saturation, whereas circles denote cases which produce saturation and the closed-loop system simulation without anti-windup still achieves output regulation. 90
Figure 25: Graphical representation of the residual function $\Delta_{f_2}(w)$ respectively for the zero, second and fourth-order internal model case. 108
Figure 26: Projection of the ultimate bound region $\mathcal{B}_\infty$ into the z_x-plane for different internal model orders. 113
Figure 27: Projection of the initial condition region $\mathcal{D}$ into the z_x-plane for different internal model orders. 113
Figure 28: Transient output error signals $e(t)$ (on top) and control signals $u(t)$ (on bottom). 115
Figure 29: Steady-state output error signals $e(t)$ (on top) and control signals $u(t)$ (on bottom). The dashed line denotes the steady-state approximation $\tilde{c}(w(t))$ as used in the last scenario. 115
Figure 30: Approximated zero-error steady-state trajectories $(\tilde{\pi}_1(w), \tilde{\pi}_2(w), \tilde{c}(w))$ for the different evaluated cases. The thin black line denotes an actual simulated trajectory considering the last scenario. 116

Figure 31: Projection of the ultimate bound region $\mathcal{B}_\infty$ into the z_x-plane for different internal model orders when the controllers are subject to input saturation. 119
Figure 32: Projection of the initial condition region $\mathcal{D}$ into the z_x-plane for different internal model orders when the controllers are subject to input saturation. 119
Figure 33: Transient output error signals $e(t)$ (on top) and control signals $u(t)$ (on bottom) when the controllers are subject to input saturation. . . . 120
Figure 34: Steady-state output error signals $e(t)$ (on top) and control signals $u(t)$ (on bottom) when the controllers are subject to input saturation. . . . 120

LIST OF TABLES

Table 1: Accuracy measure of the regulator equations approximate solutions for different internal model orders. Lower values indicate a better approximation. 107

Table 2: Theoretical upper bounds η_τ of the Lypunov function $V(\mathbf{z})$ according to the internal model order. 114

Table 3: Theoretical upper bounds γ_τ of the output error norm $||e||$ according to the internal model order. 114

Table 4: Theoretical ultimate bound η_∞ of the Lypunov function $V(\mathbf{z})$ for each internal model order case when the controllers are subject to input saturation. 118

Table 5: Theoretical ultimate bound γ_∞ of the output error norm $||e||$ for each internal model order case when the controllers are subject to input saturation. 118

LIST OF ABBREVIATIONS

DAR	Differential-Algebraic Representation
LMI	Linear Matrix Inequality
SDP	Semidefinite Programming

LIST OF SYMBOLS

$\dot{x}$	time derivative $\mathrm{d}x/\mathrm{d}t$
$\ddot{x}$	second order time derivative $\mathrm{d}^2x/\mathrm{d}t^2$
$\overset{(n)}{x}$	n-th order time derivative $\mathrm{d}^nx/\mathrm{d}t^n$
$\|\|x\|\|$	euclidean norm $\sqrt{x^\intercal x}$.
x_i	i-th element of vector x
$A_{[i]}$	i-th row of matrix A
$A_{[i,j]}$	term located at the i-th row and j-th column of matrix A
I	identity matrix
$A^\intercal$	transpose of matrix A
A^{-1}	inverse of matrix A
$A^{-\intercal}$	transpose of the inverse of matrix A
$\mathrm{tr}(A)$	trace of matrix A
$\mathcal{H}\{A\}$	symmetric block $A + A^\intercal$
$\mathrm{diag}\{A, B\}$	block diagonal matrix formed with A and B
$A \succ 0$	matrix A is positive-definite
$A \prec 0$	matrix A is negative-definite
$(\star)$	symmetric elements in a matrix
$(\cdot)$	hidden elements in a matrix
$\mathrm{Co}\{\mathcal{V}\}$	convex hull formed by the set of vertices $\mathcal{V}$
$\mathbb{N}$	set of natural numbers
$\mathbb{R}$	set of real numbers
$\mathbb{R}^n$	set of real-valued vectors with n elements
$\mathbb{R}^{n\times m}$	set of real-valued matrices with n rows and m columns
$\mathrm{int}\{\mathcal{X}\}$	interior of the set $\mathcal{X}$

1 INTRODUCTION

Ensuring output tracking of reference signals and rejection of exogenous perturbations is a fundamental control engineering problem with several applications, for example: robotic manipulators (CICEK; DASDEMIR; ZERGEROGLU, 2015), power converters (KIM et al., 2015), secure communication systems (SENOUCI et al., 2015), wind turbines (CASTRO et al., 2017), stabilizing platforms (YANG; LI, 2018), electric motors (CASTRO; FLORES; SALTON, 2018) and spacecraft (XIA et al., 2019). In practice, most of these applications exhibit both nonlinear dynamics and physical limitations from the actuators, such as input saturation. Naturally, it is of major interest to develop robust and systematic control design methodologies able to address all these intrinsic characteristics.

The theoretical foundation of output regulation is the internal model principle (FRANCIS; WONHAM, 1976). This result demonstrated that asymptotic tracking is achieved if the control loop is stable and incorporates the dynamics of the exosystem generating the reference and disturbance signals, in the case of linear time-invariant systems. Later studies have focused on expanding this result in order to consider time-varying parameters and nonlinearities. A remarkable contribution in this context is the work of ISIDORI; BYRNES (1990), which provides necessary and sufficient conditions to the solvability of a nonlinear output regulation problem. Further developments in this subject include extensions to time-delay systems (FRIDMAN, 2003), discrete systems (HUANG, 2004) and multi-agent systems (SU; HUANG, 2012).

General guidelines have been proposed in order to approach a nonlinear output regulator control problem, which are based on decoupling the design procedure into two distinct phases (HUANG; CHEN, 2004). In the first step, one should determine an internal model that matches with the so-called regulator equations, a set of conditions representing an invariant and zero-error manifold. Afterwards, a stabilization problem should be solved to ensure attractiveness of system trajectories with respect to the target steady-state manifold. There is however no solution entirely systematic and general for both of these steps (ISIDORI; MARCONI; SERRANI, 2012). The state-of-the-art on output regulator synthesis is consequently composed by a myriad of methods focused on different classes of problems, on different ways to design internal models capable of handling parametric uncertainties and also on different procedures to solve the stabilization problem. For example, MARINO; TOMEI (2013) proposed an adaptive error feedback scheme for a class of minimum-phase uncertain nonlinear systems. On the other hand, LU; HUANG (2015) proposed ways to design nonlinear internal models in order to address systems with non-polynomial nonlinearities. More recently, XU; WANG; CHEN (2016) showed a method for output regulation of normal form nonlinear systems with exponential convergence properties, while XU; CHEN; WANG (2017) dealt with nonlinear cascaded systems

with integral dynamic uncertainties. Even though these remarkable developments were achieved, the existent methods still show some limitations. For instance, the presence of actuator constraints, such as input saturation, is often disregarded in the context of nonlinear output regulation. Moreover, most of the literature in this sense is limited to nonlinear systems described in a normal form (CHEN; HUANG, 2015), where structural restrictions are imposed with respect to the system differential equations.

An alternative way to approach the nonlinear output regulation problem is referred in the literature as practical output regulation (MARCONI; PRALY, 2008), where the output error is just required to be ultimately bounded, thus not necessarily asymptotically convergent to zero. The main purpose of this relaxation is to allow the use of reduced order internal models, seeking to minimize the control implementation complexity and also to deal with problems where an infinite-order dynamic compensator would be required for perfect asymptotic regulation. In this sense, novel methodologies could also be explored in order to address input saturation and unstructured systems.

A well-established theory for control design and stability analysis of nonlinear systems is the differential-algebraic representation (TROFINO, 2000; TROFINO; DEZUO, 2014), which consists in representing a nonlinear system by a differential equation combined with an equality relation. This approach is capable of addressing systems with rational nonlinearities (products and quotients of polynomial functions) and it allows the characterization of a nonlinear control problem in terms of a convex optimization problem subject to linear matrix inequalities (BOYD et al., 1994). The fundamental procedure in this context is to lump all nonlinearities into a new vector variable subject to an algebraic constraint. Afterwards, the Finsler's lemma is considered in order to incorporate this algebraic constraint into stability conditions derived by the usual Lyapunov theory. Methodologies based on this theoretical framework have been extensively investigated in many different scenarios and with several improvements for conservatism reduction. Initially, a method for stabilization and domain of attraction estimation was developed for rational nonlinear systems (COUTINHO et al., 2004), and was subsequently extended for systems subject to input saturation (COUTINHO; GOMES DA SILVA JR, 2007). Later on, these methods were refined so as to include static anti-windup design (GOMES DA SILVA JR et al., 2014) and dynamic anti-windup design (GOMES DA SILVA JR; LONGHI; OLIVEIRA, 2016). A similar design approach was also proposed for the input-to-state stabilization problem in the presence of actuator saturation (SOUZA; COUTINHO; GOMES DA SILVA JR, 2015) and event-triggered control (MOREIRA et al., 2017). Furthermore, (TROFINO; DEZUO, 2014) brought a complete overview of the differential-algebraic theory, focusing on criteria for local, regional and global asymptotic stability of uncertain rational nonlinear systems. In spite of all these important studies based on the differential-algebraic representation, further investigations related to the nonlinear output regulation context are still to be made.

1.1 Contribution of the Thesis

In contrast to the aforementioned works, this thesis employs the differential-algebraic representation in the nonlinear regulation problem, providing a systematic framework for designing dynamic output feedback controllers for the output regulation of rational nonlinear systems. As pointed out earlier, state-of-the-art methods on nonlinear output regulation design are restricted to input affine nonlinear systems representable in a normal form. On the other hand, the proposed methodology is able to address a new class of

nonlinear plants and exosystems, i.e., cases where the regulation error dynamics is rational – not necessarily in a normal form – and where the control input is possibly subject to the saturation effect. Besides ensuring stability and asymptotic output error convergence, the devised approach provides transient performance guarantees, such as a minimum exponential decay rate.

The proposed methodology is initially based on the traditional internal model approach widely employed for output regulation problems, where the solution of regulator equations are performed *a priori* and the stabilizing components of the controller are designed subsequently (HUANG; CHEN, 2004). This work mainly focuses on the construction of such stabilizing components, which must ensure the attractiveness of system trajectories in relation to the zero-error steady-state manifold. For this purpose, the differential-algebraic representation of the system equations is developed in a modified state-space frame, subsequently referred as regulation error coordinates. As a result, the achieved theorems allow the synthesis of stabilizing and anti-windup parameters by numerical optimization routines, which in general are subject to bilinear matrix inequality constraints. Nevertheless, there exist particular scenarios to be illustrated where the solution can be achieved by usual convex optimization problems subject to linear matrix inequality constraints.

Beyond these developments, the main results of the thesis are also extended for the practical output regulation context (MARCONI; PRALY, 2008). This extension is especially useful for cases where the exact internal model solution is unknown, or also when the required compensator order is infinite. In this sense, the main innovation to be presented is a practical stabilization framework, which is in output feedback form and allows the usage of numerically approximated internal models and steady-state manifolds. Towards this formulation, the fundamental development is the characterization of an invariant bounding region, where the regulation error trajectory is ultimately confined within.

1.2 Outline of the Text

Prior to introducing the novel material of the thesis, Chapter 2 details some fundamental theory on nonlinear systems stability and most importantly on the output regulation of nonlinear systems. In the sequence, the main methodology divides into three major chapters. The first one, i.e. Chapter 3, is dedicated to introducing the proposed concepts with a simpler framework, where the scope is restricted to rational nonlinear systems with unbounded control input. The following Chapter 4 then extends all results to a more general setup, where the effects of input saturation are considered into the stability analysis and the anti-windup compensation proposed by GOMES DA SILVA JR et al. (2014) is also investigated. Lastly in Chapter 5, the results are generalized for the practical output regulation problem. Each of these chapters present in the end some numerical examples so as to illustrate the theoretical results and proposed design approaches. Chapter 6 states ending remarks and shows perspectives for future research. Appendix A at the very end also shows some complementary material about matrix inequalities.

2 PRELIMINARIES

This chapter introduces preliminary topics for the main content of this thesis. The stability of nonlinear systems in the Lyapunov sense is primarily demonstrated in Section 2.1. Afterwards, Section 2.2 presents an overview of some LMI based methods for stability analysis of nonlinear systems and control design. In the end, Section 2.3 will provide a detailed insight on output regulation of nonlinear systems and internal model based control.

2.1 Stability of Nonlinear Systems

Consider an autonomous nonlinear system described by

$$\dot{x} = f(x)\,, \tag{1}$$

where $x \in \mathcal{X} \subseteq \mathbb{R}^n$ is the system state and $f : \mathcal{X} \to \mathbb{R}^n$ is a local Lipschitz map from $\mathcal{X}$ into $\mathbb{R}^n$. Without loss of generality, suppose that the origin is an equilibrium point of (1), that is $f(0) = 0$ and $\{0\} \subset \mathrm{int}\{\mathcal{X}\}$. If the equilibirum point of (1) is not zero, it is always possible to consider a change of coordinates such that the equilibirum point is displaced to the origin. Definition 2.1 formalizes basic concepts of stability and asymptotic stability. Subsequently, Theorem 2.1 presents a fundamental Lyapunov result (KHALIL, 2002).

Definition 2.1. The origin of the system (1) is said to be:

- *stable* if, for each $\epsilon > 0$, there is some $\ell > 0$ such that

$$||x(0)|| < \ell \;\Rightarrow\; ||x(t)|| < \epsilon \;\; \forall\, t > 0\,. \tag{2}$$

- *asymptotically stable* if it is *stable* and ℓ can be chosen such that

$$||x(0)|| < \ell \;\Rightarrow\; \lim_{t\to\infty} ||x(t)|| = 0\,. \tag{3}$$

- *globally asymptotically stable* if previous condition holds for all $\ell > 0$.

Theorem 2.1. *Let $\mathcal{X} \subseteq \mathbb{R}^n$ be a domain containing the origin and assume that $f : \mathcal{X} \to \mathbb{R}^n$ satisfies $f(0) = 0$. Suppose there exists a smooth function $V : \mathcal{X} \to \mathbb{R}$ such that*

$$V(0) = 0\,,\; V(x) > 0 \;\; \forall\, x \in \mathcal{X}\,,\; x \neq 0\,, \tag{4}$$

$$\dot{V}(x) \triangleq \frac{\partial V(x)}{\partial x} f(x) \leq 0 \;\; \forall\, x \in \mathcal{X}\,, \tag{5}$$

then the origin of the system (1) *is stable. Furthermore, if*

$$\dot{V}(x) < 0 \;\; \forall\, x \in \mathcal{X}\,,\; x \neq 0\,, \tag{6}$$

then the origin is asymptotically stable. Moreover, if $\mathcal{X} = \mathbb{R}^n$ *and* $V(x)$ *is radially unbounded*[1]*, then the origin is globally asymptotically stable.*

Proof. See KHALIL (2002). □

Following the result presented by Theorem 2.1, any level set of the Lypunov function $V(x)$ contained in $\mathcal{X}$, e.g.

$$\mathcal{D} = \left\{ x \in \mathbb{R}^n : V(x) \leq \epsilon \right\} \subset \mathcal{X}\,, \tag{7}$$

for some $\epsilon > 0$, is said to be *positively invariant* with respect to system (1), meaning that $x(0) \in \mathcal{D} \Rightarrow x(t) \in \mathcal{D}\; \forall\, t > 0$. Furthermore, if condition (6) is true, then this region is also a *domain of attraction estimate* (KHALIL, 2002), since all trajectories staring in $\mathcal{D}$ are thus attracted towards the origin.

2.2 LMI based Stability and Control Design

This section presents an overview of fundamental preliminary methodologies to the main contribution of this work, which will be later presented in Chapters 3, 4 and 5. The material to be detailed here includes:

- Dynamic Output Feedback Control (SCHERER; GAHINET; CHILALI, 1997);
- Stability of Systems with Control Saturation (GOMES DA SILVA JR; TARBOURIECH, 2005);
- Stability of Rational Nonlinear Systems (TROFINO; DEZUO, 2014).

One common characteristic of the above-mentioned works is the characterization of stability conditions in the form of linear matrix inequalities (LMIs). Appendix A.1 may be examined for a brief introduction about this topic.

2.2.1 Dynamic Output Feedback Control

Consider a linear system described by

$$\left\{ \begin{array}{rcl} \dot{x} & = & A\,x + B\,u \\ y & = & C\,x \end{array} \right. \tag{8}$$

where $x \in \mathbb{R}^{n_x}$ is the system state, $u \in \mathbb{R}^{n_u}$ is the control input and $y \in \mathbb{R}^{n_y}$ is the system output. The system input is supposedly provided by a dynamic output feedback controller of the form:

$$\left\{ \begin{array}{rcl} \dot{\xi} & = & F\,\xi + G\,y \\ u & = & H\,\xi + K\,y \end{array} \right. \tag{9}$$

where $\xi \in \mathbb{R}^{n_\xi}$ is the controller state. All matrices $A \in \mathbb{R}^{n_x \times n_x}$, $B \in \mathbb{R}^{n_x \times n_u}$, $C \in \mathbb{R}^{n_y \times n_x}$, $F \in \mathbb{R}^{n_\xi \times n_\xi}$, $G \in \mathbb{R}^{n_\xi \times n_y}$, $H \in \mathbb{R}^{n_u \times n_\xi}$ and $K \in \mathbb{R}^{n_u \times n_y}$ are considered constant. The closed-loop topology of (8) and (9) is demonstrated on Figure 1.

[1] A function $V(x)$ is said to be radially unbounded if $V(x) \to \infty$ as $||x|| \to \infty$.

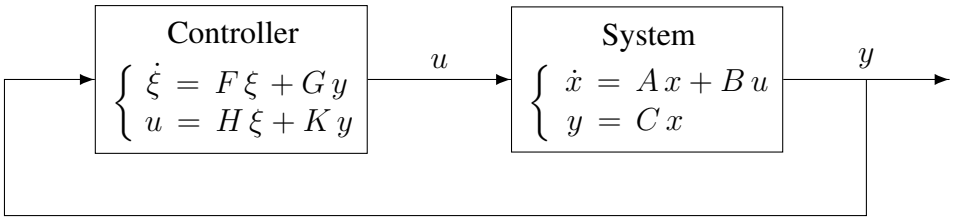

Figure 1: Block diagram of a linear dynamic output feedback control. Source: the author.

Problem 2.1. Design controller parameters F, G, H and K such the origin of the closed-loop system (8), (9) is globally asymptotically stable.

An LMI based solution has been proposed in order to solve Problem 2.1 (SCHERER; GAHINET; CHILALI, 1997). Towards this solution, first step is to represent the closed-loop dynamics in the augmented form

$$\dot{\mathbf{x}} = \mathbf{A}\,\mathbf{x}\,, \tag{10}$$

where $\mathbf{x} = [x^\mathsf{T} \quad \xi^\mathsf{T}]^\mathsf{T} \in \mathbb{R}^{n_a}$, $n_a = n_x + n_\xi$, is the augmented state and $\mathbf{A} \in \mathbb{R}^{n_a \times n_a}$ is

$$\mathbf{A} = \begin{bmatrix} A + BKC & BH \\ GC & F \end{bmatrix}\,. \tag{11}$$

The global asymptotic stability of (10) is addressed by the following theorem directly derived from Theorem 2.1.

Theorem 2.2. *Suppose there exists a symmetric matrix $P \in \mathbb{R}^{n_a \times n_a}$ such that*

$$P \succ 0\,, \tag{12}$$

$$P\mathbf{A} + \mathbf{A}^\mathsf{T} P \prec 0\,. \tag{13}$$

Then the origin of system (10) *is globally asymptotically stable.*

Proof. Consider a quadratic Lyapunov candidate function

$$V(\mathbf{x}) = \mathbf{x}^\mathsf{T} P\,\mathbf{x}\,. \tag{14}$$

If P is symmetric and positive-definite, i.e. (12), then $V(\mathbf{x}) > 0\ \forall\,\mathbf{x} \in \mathbb{R}^{n_a}$, $\mathbf{x} \neq 0$. The derivative of (14) along the trajectories of the system (10) can be expressed as:

$$\dot{V}(\mathbf{x}) = \mathbf{x}^\mathsf{T}(P\mathbf{A} + \mathbf{A}^\mathsf{T} P)\,\mathbf{x}\,. \tag{15}$$

So, if (13) is true, $\dot{V}(\mathbf{x}) < 0\ \forall\,\mathbf{x} \in \mathbb{R}^{n_a}$, $\mathbf{x} \neq 0$. From Theorem 2.1, since $V(\mathbf{x})$ is radially unbounded, the origin of system (10) is globally asymptotically stable. □

The set of inequalities (12) and (13) can be considered LMIs only if all controller terms F, G, H and K are *a priori* fixed and not regarded as decision variables. However, SCHERER; GAHINET; CHILALI (1997) have proposed a method to linearize these inequalities with respect to all controller parameters, thus providing an approach able to cast Problem 2.1 as a single LMI feasibility problem. Such result, as presented next, is based on congruence transformations (Lemma A.1) and the introduction of some new variables.

Theorem 2.3. *Suppose $n_\xi = n_x$ and there exist matrices $X = X^\intercal \in \mathbb{R}^{n_x \times n_x}$, $Y = Y^\intercal \in \mathbb{R}^{n_x \times n_x}$, $\hat{F} \in \mathbb{R}^{n_x \times n_x}$, $\hat{G} \in \mathbb{R}^{n_x \times n_y}$, $\hat{H} \in \mathbb{R}^{n_u \times n_x}$ and $K \in \mathbb{R}^{n_u \times n_y}$ such that*

$$\begin{bmatrix} X & I \\ \star & Y \end{bmatrix} \succ 0 \,, \tag{16}$$

$$\mathcal{H}\left\{ \begin{bmatrix} AX + B\hat{H} & A + BKC \\ \hat{F} & YA + \hat{G}C \end{bmatrix} \right\} \prec 0 \,. \tag{17}$$

Then the origin of the closed-loop system (8)*,* (9) *is globally asymptotically stable with parameters F, G and H obtained from*

$$\begin{cases} F &= N^{-1}(\hat{F} + YBKCX - \hat{G}CX - YB\hat{H} - YAX)M^{-\intercal} \\ G &= N^{-1}(\hat{G} - YBK) \\ H &= (\hat{H} - KCX)\, M^{-\intercal} \end{cases} \tag{18}$$

where $M, N \in \mathbb{R}^{n_x \times n_x}$ are non-singular solutions to

$$MN^\intercal = I - XY \,. \tag{19}$$

Proof. Consider $n_\xi = n_x$ and suppose Theorem 2.2 holds with matrix P and its inverse defined as

$$P = \begin{bmatrix} Y & N \\ N^\intercal & \cdot \end{bmatrix}, \;\; P^{-1} = \begin{bmatrix} X & M \\ M^\intercal & \cdot \end{bmatrix}, \tag{20}$$

where X, Y are symmetric matrices and M, N are non-singular square matrices. Since $P^{-1}P = I$, then condition (19) must be satisfied because

$$P^{-1}P = \begin{bmatrix} X & M \\ M^\intercal & \cdot \end{bmatrix} \begin{bmatrix} Y & N \\ N^\intercal & \cdot \end{bmatrix} = \begin{bmatrix} XY + MN^\intercal & \cdot \\ \cdot & \cdot \end{bmatrix} = \begin{bmatrix} I & 0 \\ 0 & I \end{bmatrix} \,. \tag{21}$$

Consider the congruence transformation blocks $Z_1 \in \mathbb{R}^{n_a \times n_a}$ and $Z_2 \in \mathbb{R}^{n_a \times n_a}$ defined by

$$Z_1 \triangleq \begin{bmatrix} X & I \\ M^\intercal & 0 \end{bmatrix}, \;\; Z_2 \triangleq \begin{bmatrix} I & Y \\ 0 & N^\intercal \end{bmatrix}, \tag{22}$$

which satisfy identity $PZ_1 = Z_2$. Then, post- and pre-multiplying (12) by Z_1 and its transpose leads to

$$Z_1^\intercal P Z_1 = Z_2^\intercal Z_1 = \begin{bmatrix} X & I \\ I & Y \end{bmatrix} \,, \tag{23}$$

therefore (12) is equivalent to (16). Similarly,

$$Z_1^\intercal P \mathbf{A} Z_1 = Z_2^\intercal \mathbf{A} Z_1 = \begin{bmatrix} AX + B\hat{H} & A + BKC \\ \hat{F} & YA + \hat{G}C \end{bmatrix}, \tag{24}$$

when considering the following change of variables:

$$\begin{cases} \hat{F} &= Y\,(A + BKC)\,X + NGCX + YBHM^\intercal + NFM^\intercal \\ \hat{G} &= YBK + NG \\ \hat{H} &= KCX + HM^\intercal \end{cases} . \tag{25}$$

Thus, (13) is also equivalent to (17). At last, from straightforward inversion of the variable transformations in (25), one obtains (18). As a conclusion, Theorem 2.3 is equivalent to Theorem 2.2 when $n_\xi = n_x$. □

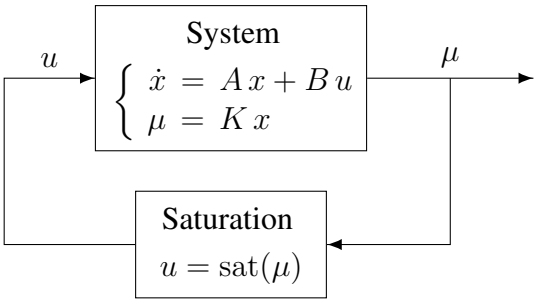

Figure 2: Block diagram of a Lur'e System with a saturation function. Source: the author.

Remark 2.1. There will always exist non-singular solutions M and N satisfying (19) as long as the condition (16) holds (SCHERER; GAHINET; CHILALI, 1997). In order to efficiently determine a solution pair M and N, one can apply singular value decomposition into $I - XY$, which should result $USV^{\top} = I - XY$ where $U \in \mathbb{R}^{n_x \times n_x}$, $V \in \mathbb{R}^{n_x \times n_x}$ are orthogonal matrices and $S \in \mathbb{R}^{n_x \times n_x}$ is a diagonal matrix. In this case, a balanced solution for M and N is $M = US^{1/2}$, $N = VS^{1/2}$ and their inverses are $M^{-1} = S^{-1/2}U^{\top}$ and $N^{-1} = S^{-1/2}V^{\top}$.

2.2.2 Stability of Systems with Control Input Saturation

Consider a closed-loop nonlinear system defined by

$$\begin{cases} \dot{x} &= A\,x + B\,u \\ \mu &= K\,x \\ u &= \mathrm{sat}(\mu) \end{cases} \tag{26}$$

where $x \in \mathbb{R}^{n_x}$ is the system state, $u \in \mathbb{R}^{n_u}$ is the saturated control input and $\mu \in \mathbb{R}^{n_u}$ is the unsaturated control input. The nonlinear function $\mathrm{sat} : \mathbb{R}^{n_u} \to [-\overline{u}_1, \overline{u}_1] \times \ldots \times [-\overline{u}_{n_u}, \overline{u}_{n_u}]$ is defined as

$$\mathrm{sat}(\mu_j) \triangleq \begin{cases} \overline{u}_j & \text{if} \quad \mu_j \geq \overline{u}_j \\ -\overline{u}_j & \text{if} \quad \mu_j \leq -\overline{u}_j \\ \mu_j & \text{if} \quad \text{otherwise} \end{cases} . \tag{27}$$

This is a particular case of Lur'e Systems (SUYKENS; VANDEWALLE; DE MOOR, 1998), where the static feedback nonlinearity is restricted to a saturation function. The block diagram of Figure 2 demonstrates the topology of the closed-loop system (26).

Problem 2.2. Determine a domain of attraction estimate $\mathcal{D}$ in which the origin of the closed-loop system (26) is asymptotically stable.

In order to solve Problem 2.2 using LMI based tools, GOMES DA SILVA JR; TARBOURIECH (2005) proposed to rewrite the saturation function as a deadzone type nonlinearity

$$\psi(\mu) \triangleq \mu - \mathrm{sat}(\mu) . \tag{28}$$

By introducing this definition, the closed-loop system (26) can be written as

$$\dot{x} = \hat{A}\,x - B\,\psi(Kx) , \tag{29}$$

where $\hat{A} \triangleq A + BK$. In order to deal with this deadzone function $\psi(\cdot)$, a generalized sector condition has also been proposed according to the following lemma.

Lemma 2.1. *Consider vector functions $\theta, \vartheta : \mathbb{R}^{n_x} \to \mathbb{R}^{n_u}$. If $x \in \mathcal{S}$, where $\mathcal{S}$ is the polyhedral set*

$$\mathcal{S} = \left\{ x \in \mathbb{R}^{n_x} : |\, \theta_j(x) - \vartheta_j(x) \,| \,\leq\, \overline{u}_j \,,\; j = 1, 2, \ldots, n_u \right\}, \tag{30}$$

then it verifies that

$$\psi^{\mathsf{T}}(\theta(x))\, T \left(\psi(\theta(x)) - \vartheta(x) \right) \leq 0 \tag{31}$$

for any diagonal and positive-definite matrix $T \in \mathbb{R}^{n_u \times n_u}$.

Proof. Consider the three possible cases that follows:

(a) $-\overline{u}_j \leq \theta_j(x) \leq \overline{u}_j$. In this case, $\psi(\theta_j(x)) = 0$ and then

$$\psi^{\mathsf{T}}(\theta_j(x))\, T_{[j,j]} \left(\psi(\theta_j(x)) - \vartheta_j(x) \right) = 0 \,. \tag{32}$$

(b) $\theta_j(x) \geq \overline{u}_j$. In this case, $\psi(\theta_j(x)) = \theta_j(x) - \overline{u}_j > 0$. If $x \in \mathcal{S}$, then $\theta_j(x) - \vartheta_j(x) \leq \overline{u}_j$, therefore it follows that $\psi(\theta_j(x)) - \vartheta_j(x) \leq 0$. Consequently, one gets that

$$\psi^{\mathsf{T}}(\theta_j(x))\, T_{[j,j]} \left(\psi(\theta_j(x)) - \vartheta_j(x) \right) \leq 0 \,. \tag{33}$$

(c) $\theta_j(x) \leq -\overline{u}_j$. In this case, $\psi(\theta_j(x)) = \theta_j(x) + \overline{u}_j < 0$. If $x \in \mathcal{S}$, then $\theta_j(x) - \vartheta_j(x) \geq -\overline{u}_j$, therefore it follows that $\psi(\theta_j(x)) - \vartheta_j(x) \geq 0$. Consequently, one also gets that (33).

From these three cases, provided that $x \in \mathcal{S}$ and that matrix T is diagonal and positive-definite, condition (31) is verified. □

Following the result of Lemma 2.1, it is straightforward to apply the S-Procedure (Lemma A.5) in order to obtain the stability criteria for the closed-loop system. An additional condition, as shown by (35) in the next theorem, ensures that the domain of attraction estimate $\mathcal{D}$ is contained inside the polyhedral region where the sector condition holds, i.e. $\mathcal{D} \subset \mathcal{S}$.

Theorem 2.4. *Suppose there exists a symmetric matrix $\hat{P} \in \mathbb{R}^{n_x \times n_x}$, a diagonal matrix $\hat{T} \in \mathbb{R}^{n_u \times n_u}$ and a matrix $\hat{R} \in \mathbb{R}^{n_u \times n_x}$ such that $\hat{P} \succ 0$, $\hat{T} \succ 0$,*[2]

$$\begin{bmatrix} \mathcal{H}\{\hat{A}\hat{P}\} & \hat{R}^{\mathsf{T}} - B\hat{T} \\ \star & -2\hat{T} \end{bmatrix} \prec 0 \,, \tag{34}$$

$$\begin{bmatrix} \overline{u}_j{}^2 & \hat{K}_{[j]} - \hat{R}_{[j]} \\ \star & \hat{P} \end{bmatrix} \succ 0 \;\; \forall\, j \in \{1, 2, \ldots, n_u\} \,, \tag{35}$$

where $\hat{K} \triangleq K\hat{P}$. Then the origin of the system (29) *is asymptotically stable in*

$$\mathcal{D} = \left\{ x \in \mathbb{R}^{n_x} : x^{\mathsf{T}} \hat{P}^{-1} x \leq 1 \right\}. \tag{36}$$

[2] In (35), $\hat{K}_{[j]}$ and $\hat{R}_{[j]}$ are denoting the j-th row of matrices $\hat{K}$ and $\hat{R}$.

Proof. Consider the Lyapunov candidate function $V(x) = x^{\mathsf{T}} P x$. If $P \succ 0$ then $V(x) > 0 \; \forall \, x \in \mathbb{R}^{n_x}$, $x \neq 0$. The derivative of $V(x)$ along the trajectories of system (29) is $\dot{V}(x) = \zeta^{\mathsf{T}}(x) \, \Delta_1 \, \zeta(x)$ where:

$$\Delta_1 \triangleq \begin{bmatrix} \mathcal{H}\{P\hat{A}\} & -PB \\ \star & 0 \end{bmatrix} , \quad \zeta(x) \triangleq \begin{bmatrix} x \\ \psi(Kx) \end{bmatrix} . \tag{37}$$

From Lemma 2.1 and considering $\theta(x) = Kx$ and $\vartheta(x) = R\,x$, for some $R \in \mathbb{R}^{n_u \times n_x}$, it follows that if $x \in \mathcal{S}$ then (31), or equivalently $\zeta^{\mathsf{T}}(x) \, \Delta_2 \, \zeta(x) \geq 0$ where:

$$\Delta_2 \triangleq \begin{bmatrix} 0 & 0 \\ TR & -T \end{bmatrix} . \tag{38}$$

It consequently verifies that $\dot{V}(x) < 0 \; \forall \, x \in \mathcal{S}$, $x \neq 0$ if

$$\dot{V}(x) + \mathcal{H}\big\{\zeta^{\mathsf{T}}(x) \, \Delta_2 \, \zeta(x)\big\} < 0 \;\; \forall \, x \neq 0 \, . \tag{39}$$

By plugging $\dot{V}(x) = \zeta^{\mathsf{T}}(x) \, \Delta_1 \, \zeta(x)$ into (39) and factorizing the vector $\zeta(x)$, one should obtain

$$\begin{bmatrix} \mathcal{H}\{P\hat{A}\} & R^{\mathsf{T}}T - PB \\ \star & -2T \end{bmatrix} \prec 0 \, . \tag{40}$$

Post- and pre-multiplying (40) by the congruence transformation $\mathrm{diag}\{P^{-1} \, , \, T^{-1}\}$ and applying the following change of variables $\hat{P} = P^{-1}$, $\hat{T} = T^{-1}$ and $\hat{R} = RP^{-1}$ leads to condition (34). Moreover, $\hat{P} \succ 0$ and $\hat{T} \succ 0$ ensure that $P \succ 0$ and $T \succ 0$.

The candidate domain of attraction estimate and positively invariant region of system (29) is given by (7), which here is the ellipsoidal set $\mathcal{D} = \{x \in \mathbb{R}^{n_x} : x^{\mathsf{T}} P x \leq 1\}$. In order to guarantee that $x(0) \in \mathcal{D} \Rightarrow x(t) \in \mathcal{S} \; \forall \, t > 0$, for the validity of Lemma 2.1, one must ensure that the region $\mathcal{D}$ is contained inside the polyhedral set $\mathcal{S}$. In turn, Lemma A.6 implies that $\mathcal{D} \subset \mathcal{S}$ if and only if

$$\begin{bmatrix} \overline{u}_j{}^2 & K_{[j]} - R_{[j]} \\ \star & P \end{bmatrix} \succ 0 \;\; \forall \, j \in \{1, 2, \ldots, n_u\} \, , \tag{41}$$

where $K_{[j]}$ and $R_{[j]}$ are denoting the j-th row of matrices K and R. Lastly, post- and pre-multiplying (41) by the congruence transformation $\mathrm{diag}\{1 \, , \, P^{-1}\}$ leads to (35). □

One possibility to solve Problem 2.2 is by minimizing the trace of $\hat{P}^{-1}$ subject to LMIs $\hat{P} \succ 0$, $\hat{T} \succ 0$, (34) and (35). In order to linearize this objective function, one can consider a symmetric matrix $\tilde{P} \in \mathbb{R}^{n_x \times n_x}$ which satisfies $\tilde{P} > \hat{P}^{-1}$, or equivalently by Schur Complement (Lemma A.2):

$$\begin{bmatrix} \tilde{P} & I \\ \star & \hat{P} \end{bmatrix} \succ 0 \, . \tag{42}$$

The solution is hence obtained by solving the following SDP problem:

$$\min_{\tilde{P}, \hat{P}, \hat{T}, \hat{R}} \; \mathrm{tr}(\tilde{P}) \;\; \text{s.t.} \;\; \big\{\hat{P} \succ 0 \, , \, \hat{T} \succ 0 \, , \, (34) \, , \, (35) \, , \, (42)\big\} \, . \tag{43}$$

One may also employ alternative objective functions as presented in (TARBOURIECH et al., 2011). In case it is also intended to design the feedback gain matrix K, one should simply set $\hat{K}$ from (35) as a free decision variable. The feedback parameters are then reconstructed as $K = \hat{K}\hat{P}^{-1}$.

2.2.3 Stability of Rational Nonlinear Systems

Consider an autonomous system described by a differential-algebraic representation (DAR):

$$\begin{cases} \dot{x} &= A(x)\,x + \Phi(x)\,\varphi(x) \\ 0 &= \Psi(x)\,x + \Omega(x)\,\varphi(x) \end{cases}, \tag{44}$$

where $x \in \mathcal{X} \subseteq \mathbb{R}^{n_x}$ is the system state, $\varphi : \mathcal{X} \to \mathbb{R}^{n_\varphi}$ is a rational function and the matrices $A : \mathcal{X} \to \mathbb{R}^{n_x \times n_x}$, $\Phi : \mathcal{X} \to \mathbb{R}^{n_x \times n_\varphi}$, $\Psi : \mathcal{X} \to \mathbb{R}^{n_\varphi \times n_x}$ and $\Omega : \mathcal{X} \to \mathbb{R}^{n_\varphi \times n_\varphi}$ are affine functions with respect to x. Moreover, $\Omega(x)$ is supposedly non-singular inside $\mathcal{X}$, i.e. $\det\{\Omega(x)\} \neq 0\ \forall\, x \in \mathcal{X}$. Every autonomous system originally described as (1), whose function $f(x)$ is a regular rational function[3] in $\mathcal{X}$, can be represented in the form of (44) (TROFINO; DEZUO, 2014).

An LMI based method has been proposed by TROFINO; DEZUO (2014) in order to analyze the stability of nonlinear systems described by (44), therefore providing a systematic solution to the following problem.

Problem 2.3. Determine a domain of attraction estimate $\mathcal{D}$ in which the origin of the system (44) is asymptotically stable.

Since $A(x)$, $\Phi(x)$, $\Psi(x)$ and $\Omega(x)$ are affinely dependent on x, the first step towards the solution of Problem 2.3 is to define the set $\mathcal{X}$ by a convex hull of vertices:

$$\mathcal{X} = \mathrm{Co}\{\mathcal{V}_x\} \ \subseteq \mathbb{R}^{n_x}. \tag{45}$$

Without loss of generality, one may also denote $\mathcal{X}$ in the polyhedral form

$$\mathcal{X} = \left\{ x \in \mathbb{R}^{n_x} : |\, p_k^{\mathsf{T}}\, x\,| \ \leq 1\,,\ k = 1, 2, \ldots, n_k \right\}, \tag{46}$$

for some vector $p_1, p_2, \ldots, p_{n_k} \in \mathbb{R}^{n_x}$. From a collection of vertices $\mathcal{V}_x$, an equivalent representation (46) can always be obtained (COUTINHO; GOMES DA SILVA JR, 2007). Given the above mentioned definitions, the asymptotic stability of (44) is addressed by the following theorem.

Theorem 2.5. *Suppose there exist some matrices $P = P^{\mathsf{T}} \in \mathbb{R}^{n_x \times n_x}$ and $L \in \mathbb{R}^{n_\varphi \times n_\varphi}$ such that $P \succ 0$,*

$$\mathcal{H}\left\{ \begin{bmatrix} PA(x) & P\Phi(x) \\ L\Psi(x) & L\Omega(x) \end{bmatrix} \right\} \prec 0 \ \ \forall\, x \in \mathcal{V}_x\,, \tag{47}$$

$$\begin{bmatrix} 1 & p_k^{\mathsf{T}} \\ \star & P \end{bmatrix} \succ 0 \ \ \forall\, k \in \{1, 2, \ldots, n_k\}\,. \tag{48}$$

Then the origin of the system (44) *is asymptotically stable in*

$$\mathcal{D} = \left\{ x \in \mathbb{R}^{n_x} : x^{\mathsf{T}} P x \leq 1 \right\}. \tag{49}$$

Proof. Consider the Lyapunov candidate function $V(x) = x^{\mathsf{T}} P x$. If $P \succ 0$ then $V(x) > 0\ \forall\, x \in \mathbb{R}^{n_x}$, $x \neq 0$. The derivative of $V(x)$ along the trajectories of system (44) is $\dot{V}(x) = \zeta^{\mathsf{T}}(x)\,\Delta_1(x)\,\zeta(x)$, where

$$\Delta_1(x) \triangleq \mathcal{H}\left\{ \begin{bmatrix} PA(x) & P\Phi(x) \\ 0 & 0 \end{bmatrix} \right\}, \quad \zeta(x) \triangleq \begin{bmatrix} x \\ \varphi(x) \end{bmatrix}. \tag{50}$$

[3] A function $f(x)$ is said to be rational if it can be expressed as a fraction of polynomial functions and it is also regular in $\mathcal{X}$ if it has no singularities $\forall\, x \in \mathcal{X}$.

Note the equality constraint in (44) can be expressed as $\Delta_2(x)\,\zeta(x) = 0\;\forall\, x \in \mathcal{X}$, where

$$\Delta_2(x) = \begin{bmatrix} \Psi(x) & \Omega(x) \end{bmatrix} . \tag{51}$$

It verifies that $\dot{V}(x) < 0\;\forall\, x \in \mathcal{X}$, $x \neq 0$ if, for some matrix $L \in \mathbb{R}^{n_\varphi \times n_\varphi}$,

$$\dot{V}(x) + \mathcal{H}\{\varphi^{\mathsf{T}}(x)\, L \Delta_2(x)\, \zeta(x)\} < 0 \;\; \forall\, x \in \mathcal{X}\,,\; x \neq 0\,. \tag{52}$$

By plugging $\dot{V}(x) = \zeta^{\mathsf{T}}(x)\,\Delta_1(x)\,\zeta(x)$ into (52) and factorizing $\zeta(x)$, this expression becomes equivalent to

$$\mathcal{H}\left\{\begin{bmatrix} PA(x) & P\Phi(x) \\ L\Psi(x) & L\Omega(x) \end{bmatrix}\right\} \prec 0 \;\; \forall\, x \in \mathcal{X}\,, \tag{53}$$

and then, from Lemma A.3, (47) $\Leftrightarrow$ (53).

In order to complete this proof, the candidate domain of attraction estimate $\mathcal{D}$, as in (49), must additionally be contained the polyhedral set $\mathcal{X}$, as defined in (46). By direct application of Lemma A.6, $\mathcal{D} \subset \mathcal{X}$ is equivalent to (48). Based on Theorem 2.1 consequently, $P \succ 0$, (47) and (48) ensure that the trajectory of (44) asymptotically approaches the origin for any initial condition starting in $\mathcal{D}$. □

According to Theorem 2.5, the solution of Problem 2.3 is obtained by solving the following SDP:

$$\min_{P,L}\; \mathrm{tr}(P) \;\; \text{s.t.} \;\; \{P \succ 0\,,\, (47)\,,\, (48)\}\,. \tag{54}$$

Example 2.1. Consider a rational nonlinear system described as

$$\begin{cases} \dot{x}_1 &= x_2 + \dfrac{x_1^3}{1+x_1^2} \\ \dot{x}_2 &= a\,x_1 + b\,x_2 + \dfrac{x_1^2 x_2^2}{1+x_1^2} \end{cases} \tag{55}$$

where $a, b \in \mathbb{R}$ are constant parameters. A possible choice in order to represent (55) in the form of (44) is to consider $\varphi(x)$ as:

$$\varphi(x) = \begin{bmatrix} \dfrac{x_1}{1+x_1^2} & \dfrac{x_1^2}{1+x_1^2} & \dfrac{x_1^2 x_2}{1+x_1^2} \end{bmatrix}^{\mathsf{T}} . \tag{56}$$

The corresponding matrices $A(x)$, $\Phi(x)$, $\Psi(x)$ and $\Omega(x)$ can be arranged as:

$$\begin{aligned} A &= \begin{bmatrix} 0 & 1 \\ a & b \end{bmatrix}, \quad \Phi(x) = \begin{bmatrix} 0 & x_1 & 0 \\ 0 & 0 & x_2 \end{bmatrix}, \\ \Psi &= \begin{bmatrix} -1 & 0 \\ 0 & 0 \\ 0 & 0 \end{bmatrix}, \quad \Omega(x) = \begin{bmatrix} 1 & x_1 & 0 \\ -x_1 & 1 & 0 \\ 0 & -x_2 & 1 \end{bmatrix}. \end{aligned} \tag{57}$$

One should notice that $\Omega(x)$ is non-singular $\forall\, x \in \mathbb{R}^2$, since $\det\{\Omega(x)\} = 1 + x_1^2 \geq 0$. The next step is to define the convex region $\mathcal{X} \subseteq \mathbb{R}^2$, which may be built by $\mathcal{X} = \mathrm{Co}\{\mathcal{V}_x\}$, where the set of vertices is

$$\mathcal{V}_x = \left\{ \begin{bmatrix} -\overline{x}_1 & -\overline{x}_2 \end{bmatrix}^{\mathsf{T}}, \begin{bmatrix} -\overline{x}_1 & \overline{x}_2 \end{bmatrix}^{\mathsf{T}}, \begin{bmatrix} \overline{x}_1 & -\overline{x}_2 \end{bmatrix}^{\mathsf{T}}, \begin{bmatrix} \overline{x}_1 & \overline{x}_2 \end{bmatrix}^{\mathsf{T}} \right\}, \tag{58}$$

for some scalars $\overline{x}_1, \overline{x}_2 > 0$, which denote the maximum admissible value of $|x_1(t)|$ and $|x_2(t)| \; \forall \, t \geq 0$. The equivalent definition of $\mathcal{X}$ according to (46) is obtained with

$$p_1 = \left[\begin{array}{cc} \overline{x}_1{}^{-1} & 0 \end{array} \right], \;\; p_2 = \left[\begin{array}{cc} 0 & \overline{x}_2{}^{-1} \end{array} \right]. \tag{59}$$

Given this setup phase and provided that all system parameters are numerically defined, it remains to solve (54) in order to compute the optimal P which defines the domain of attraction estimate $\mathcal{D}$ for the system origin.

2.3 Output Regulation of Nonlinear Systems

The set of problems so far presented have basically involved conditions for asymptotic stability with respect to the origin. A much more complex set of problems in the field of control and dynamic systems, which will be dealt in this section, is the output regulation (ISIDORI; BYRNES, 1990). In this context, the system to be controlled is perturbed by non-vanishing signals generated by an exogenous system, which may represent unmeasured disturbances or even reference signals to be tracked. For instance, consider a nonlinear system described by

$$\left\{ \begin{array}{rcl} \dot{x} & = & f(x, w, u) \\ y & = & g(x, w) \\ e & = & h(x, w) \end{array} \right. \tag{60}$$

where $x \in \mathbb{R}^{n_x}$ is the system state vector, $u \in \mathbb{R}^{n_u}$ is the control input, $y \in \mathbb{R}^{n_y}$ is the output measurement vector and $e \in \mathbb{R}^{n_e}$ is the output error. This system is supposedly perturbed by an exogenous signal $w \in \mathbb{R}^{n_w}$ generated by an autonomous exosystem:

$$\dot{w} = s(w) \; . \tag{61}$$

The goal now is to ensure that all system trajectories are bounded for all positive time and the output error asymptotically converges to zero. In turn, the system control input is provided by a nonlinear output feedback controller of the form

$$\left\{ \begin{array}{rcl} \dot{\xi} & = & \phi(\xi, y) \\ u & = & \theta(\xi, y) \end{array} \right. \tag{62}$$

where $\xi \in \mathbb{R}^{n_\xi}$ is the controller state vector. The block diagram on Figure 3 presents the closed-loop topology of (60), (61) and (62).

Assumption 2.1. Nonlinear functions $f : \mathbb{R}^{n_x} \times \mathbb{R}^{n_w} \times \mathbb{R}^{n_u} \to \mathbb{R}^{n_x}$, $g : \mathbb{R}^{n_x} \times \mathbb{R}^{n_w} \to \mathbb{R}^{n_y}$, $h : \mathbb{R}^{n_x} \times \mathbb{R}^{n_w} \to \mathbb{R}^{n_e}$, $s : \mathbb{R}^{n_w} \to \mathbb{R}^{n_w}$, $\phi : \mathbb{R}^{n_\xi} \times \mathbb{R}^{n_y} \to \mathbb{R}^{n_\xi}$, and $\theta : \mathbb{R}^{n_\xi} \times \mathbb{R}^{n_y} \to \mathbb{R}^{n_u}$ satisfy $f(0, 0, 0) = 0$, $g(0, 0) = 0$, $h(0, 0) = 0$, $s(0) = 0$, $\phi(0, 0) = 0$ and $\theta(0, 0) = 0$.

The concept of achieving output regulation is defined on the sequence (ISIDORI; BYRNES, 1990).

Definition 2.2. The closed-loop system (60), (61), (62) is said to:

- be *bounded* in $\mathcal{D} \subseteq \mathbb{R}^{n_x} \times \mathbb{R}^{n_\xi} \times \mathbb{R}^{n_w}$ if $\exists \; \epsilon_1, \epsilon_2, \epsilon_3 > 0$ such that

$$\big(x(0), \xi(0), w(0)\big) \in \mathcal{D} \;\; \Rightarrow ||x(t)|| < \epsilon_1 \; , \; ||\xi(t)|| < \epsilon_2 \; , \; ||w(t)|| < \epsilon_3 \;\; \forall \, t > 0 \; ; \tag{63}$$

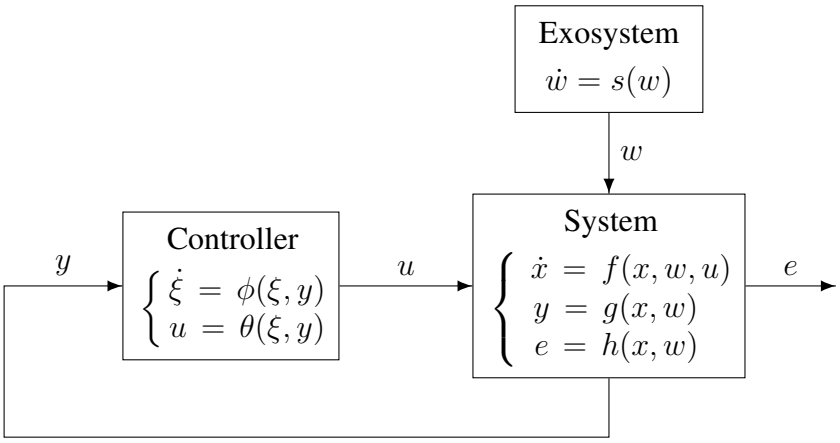

Figure 3: The nonlinear output regulation framework. Source: the author.

- achieve *output regulation* in $\mathcal{D} \subseteq \mathbb{R}^{n_x} \times \mathbb{R}^{n_\xi} \times \mathbb{R}^{n_w}$ if it is *bounded* in $\mathcal{D}$ and furthermore:

$$\big(x(0), \xi(0), w(0)\big) \in \mathcal{D} \;\Rightarrow\; \lim_{t\to\infty} ||e(t)|| = 0\,. \tag{64}$$

A standard assumption in the context of output regulation is the existence of a compact positively invariant set bounding the trajectory $w(t)$. Examples of exosystems within the scope of this assumption are harmonic oscillators, chaotic systems and systems with stable limit-cycles.

Assumption 2.2. There exists a compact and positively invariant set $\mathcal{W} \subset \mathbb{R}^{n_w}$ such that:

$$w(0) \in \mathcal{W} \;\Rightarrow\; w(t) \in \mathcal{W}\ \forall\, t > 0\,. \tag{65}$$

Given the preliminary assumptions and definitions, a general nonlinear output regulation problem is described as follows.

Problem 2.4. Design controller functions $\phi(\xi, y)$ and $\theta(\xi, y)$ such that the closed-loop system (60), (61), (62) achieves output regulation in some region $\mathcal{D} \subseteq \mathbb{R}^{n_x} \times \mathbb{R}^{n_\xi} \times \mathcal{W}$.

Towards the solution of Problem 2.4, one must consider the following fundamental theorem (ISIDORI; BYRNES, 1990).

Theorem 2.6. *The closed-loop system* (60)*,* (61)*,* (62) *achieves output regulation in* $\mathcal{D} \subseteq \mathbb{R}^{n_x} \times \mathbb{R}^{n_\xi} \times \mathcal{W}$ *if there exist smooth mappings* $\pi : \mathcal{W} \to \mathbb{R}^{n_x}$*,* $\sigma : \mathcal{W} \to \mathbb{R}^{n_\xi}$*,* $c : \mathcal{W} \to \mathbb{R}^{n_u}$ *and* $d : \mathcal{W} \to \mathbb{R}^{n_y}$ *satisfying:* $\pi(0) = 0$*,* $\sigma(0) = 0$*,* $c(0) = 0$*,* $d(0) = 0$*,*

$$\begin{cases} \dfrac{\partial \pi(w)}{\partial w} s(w) &= f(\pi(w), w, c(w)) \\ d(w) &= g(\pi(w), w) \\ 0 &= h(\pi(w), w) \end{cases} \quad \forall\, w \in \mathcal{W}\,, \tag{66}$$

$$\begin{cases} \dfrac{\partial \sigma(w)}{\partial w} s(w) &= \phi(\sigma(w), d(w)) \\ c(w) &= \theta(\sigma(w), d(w)) \end{cases} \quad \forall\, w \in \mathcal{W}\,, \tag{67}$$

and also:

$$\big(x(0), \xi(0), w(0)\big) \in \mathcal{D} \;\Rightarrow\; \begin{cases} \lim\limits_{t\to\infty} \big|\big|x(t) - \pi(w(t))\big|\big| = 0 \\ \lim\limits_{t\to\infty} \big|\big|\xi(t) - \sigma(w(t))\big|\big| = 0 \end{cases}. \tag{68}$$

Proof. Consider a manifold region $\mathcal{M}$ denoted by (75) and suppose the following properties are true:

(i) the system output error is zero inside $\mathcal{M}$, i.e.

$$h(x,w) = 0 \;\; \forall\, (x,\xi,w) \in \mathcal{M} \; . \tag{69}$$

(ii) $\mathcal{M}$ is invariant with respect to the closed-loop system trajectory, i.e.

$$\big(x(t_0),\xi(t_0),w(t_0)\big) \in \mathcal{M} \;\; \Rightarrow \;\; \big(x(t),\xi(t),w(t)\big) \in \mathcal{M} \;\; \forall\, t \neq t_0 \, , \, t_0 \geq 0 \; . \tag{70}$$

(iii) every system trajectory starting in $\mathcal{D}$ is asymptotically attracted towards $\mathcal{M}$, i.e.

$$\big(x(0),\xi(0),w(0)\big) \in \mathcal{D} \;\; \Rightarrow \;\; \lim_{t\to\infty} \big(x(t),\xi(t),w(t)\big) \in \mathcal{M} \; . \tag{71}$$

Properties (i), (ii) and (iii) consequently imply that the closed-loop trajectory $(x(t),\xi(t),w(t))$ satisfies (64). Now, observe that property (i) is equivalent to

$$e = h(\pi(w),w) = 0 \;\; \forall\, w \in \mathcal{W} \, , \tag{72}$$

leading to the third equation in (66). Notice next that property (ii) is equivalent to existence of $(\pi(w(t)),\sigma(w(t)),w(t))$ as closed-loop system trajectory when $x(t_0) = \pi(w(t_0))$ and $\xi(t_0) = \sigma(w(t_0)) \; \forall\, t_0 \geq 0$, $w(t_0) \in \mathcal{W}$, which is equivalent to

$$\left\{ \begin{array}{rcl} \dot{\pi}(w) & = & f(\pi(w),w,\theta(\sigma(w),g(\pi(w),w))) \\ \dot{\sigma}(w) & = & \phi(\sigma(w),g(\pi(w),w)) \end{array} \right. \quad \forall\, w \in \mathcal{W} \; . \tag{73}$$

Since $\pi(w)$ and $\sigma(w)$ are smooth mappings, the time-derivatives $\dot{\pi}(w)$ and $\dot{\sigma}(w)$ can be expanded by derivation chain rule

$$\dot{\pi}(w) = \frac{\partial \pi(w)}{\partial w}\dot{w} = \frac{\partial \pi(w)}{\partial w} s(w) \; , \tag{74}$$

and similarly with respect to $\dot{\sigma}(w)$. Hence, the remaining conditions in (66) and (67) are obtained when introducing the additional definitions $c(w) \triangleq \theta(\sigma(w),g(\pi(w),w))$ and $d(w) \triangleq g(\pi(w),w)$. At last, propriety (iii) is directly equivalent to condition (68).

Moreover, since $\pi : \mathcal{W} \to \mathbb{R}^{n_x}$, $\sigma : \mathcal{W} \to \mathbb{R}^{n_\xi}$ and $\mathcal{W}$ is by assumption a compact set, then $\exists\; \epsilon_\pi, \epsilon_\sigma > 0 : ||\pi(w(t))|| < \epsilon_\pi$, $||\sigma(w(t))|| < \epsilon_\sigma \; \forall\, t > 0$ if $w(0) \in \mathcal{W}$. Therefore, (68) also implies boundedness of $(x(t),\xi(t),w(t))$ for every initial state $(x(0),\xi(0),w(0)) \in \mathcal{D}$. As a result, (66), (67) and (68) imply the closed-loop system output regulation in $\mathcal{D}$ according to Definition 2.2. □

Remark 2.2. If $\partial s(w)/\partial w$ is assumed to have all eigenvalues on the imaginary axis $\{z \in \mathbb{C} : \Re(z) = 0\}$ for $w = 0$, then Theorem 2.6 has been proven to be a necessary condition for output regulation as well (ISIDORI; BYRNES, 1990). This however excludes a considerable class of exosystems with stable attractors or limit-cycles. Necessary and sufficient output regulation conditions for the general case are discussed by PAVLOV; WOUW; NIJMEIJER (2006), who modify the error condition from (66) to $h(\pi(w),w) = 0 \;\; \forall\, w \in \mathcal{L}\{\mathcal{W}\}$, where $\mathcal{L}\{\mathcal{W}\} \subseteq \mathcal{W}$ denotes the limit set of the exosystem trajectories starting inside $\mathcal{W}$.

Functions $\pi(w)$ and $\sigma(w)$ introduced by Theorem 2.6 represent the respective zero-error steady-state trajectory of the system and controller states, according to the following invariant manifold:

$$\mathcal{M} = \Big\{ (x, \xi, w) \in \mathbb{R}^{n_x} \times \mathbb{R}^{n_\xi} \times \mathcal{W} \,:\, x = \pi(w) \;,\; \xi = \sigma(w) \Big\} \,. \tag{75}$$

Likewise, $d(w)$ represents the zero-error steady-state trajectory of the output measurement signal and, most importantly, the solution $c(w)$ represents the control function that achieves the desired zero-error and invariant manifold $\mathcal{M}$.

Prior to designing an output regulator, it is necessary to determine mappings $\pi(w)$ and $c(w)$ satisfying the condition (66), which may be attained by considering the system and exosystem functions $f(x, w, u)$, $h(x, w)$ and $s(w)$ solely. These solutions represent the target steady-state specification that must be adressed by the regulator design. In most cases, it verifies that $\pi(w)$ and $c(w)$ can be determined recursively, for instance when system functions $f(x, w, u)$ and $h(x, w)$ are in the form of (CHEN; HUANG, 2015):

$$\left\{ \begin{array}{rcllcl} e & = & h(x_1, w) & & = & \mathrm{a}_0(w) + \mathrm{b}_0(w)\, x_1 \\ \dot{x}_1 & = & f_1(x_1, x_2, w) & & = & \mathrm{a}_1(x_1, w) + \mathrm{b}_1(x_1, w)\, x_2 \\ \dot{x}_2 & = & f_2(x_1, x_2, x_3, w) & & = & \mathrm{a}_2(x_1, x_2, w) + \mathrm{b}_2(x_1, x_2, w)\, x_3 \\ & \vdots & & & \vdots & \\ \dot{x}_n & = & f_n(x_1, \ldots, x_n, w, u) & & = & \mathrm{a}_n(x_1, \ldots, x_n, w) + \mathrm{b}_n(x_1, \ldots, x_n, w)\, u \end{array} \right. \tag{76}$$

for $x_i, e, u \in \mathbb{R}^m \; \forall\, i \in \{1, 2, \ldots, n\}$, $n_x = nm$ with $n, m \in \mathbb{N}$, and nonlinear functions $\mathrm{a}_0 : \mathbb{R}^{n_w} \to \mathbb{R}^m$, $\mathrm{b}_0 : \mathbb{R}^{n_w} \times \to \mathbb{R}^{m \times m}$, $\mathrm{a}_1 : \mathbb{R}^m \times \mathbb{R}^{n_w} \to \mathbb{R}^m$, $\mathrm{b}_1 : \mathbb{R}^m \times \mathbb{R}^{n_w} \to \mathbb{R}^{m \times m}$, $\ldots$, $\mathrm{a}_n : \mathbb{R}^{n_x} \times \mathbb{R}^{n_w} \to \mathbb{R}^m$ and $\mathrm{b}_n : \mathbb{R}^{n_x} \times \mathbb{R}^{n_w} \to \mathbb{R}^{m \times m}$ where $\mathrm{a}_0(0) = 0$, $\mathrm{a}_1(0, 0) = 0$, $\mathrm{a}_2(0, 0, 0) = 0$, etc. In this scenario, $\pi(w)$ and $c(w)$ can be recursively obtained for any exosystem function $s(w)$ according to

$$\left\{ \begin{array}{rcl} \pi_1(w) & = & -\mathrm{b}_0^{-1}(w)\, \mathrm{a}_0(w) \\ \pi_2(w) & = & -\mathrm{b}_1^{-1}(\pi_1(w), w) \left(\mathrm{a}_1(\pi_1(w), w) - \frac{\partial \pi_1(w)}{\partial w} s(w) \right) \\ \pi_3(w) & = & -\mathrm{b}_2^{-1}(\pi_1(w), \pi_2(w), w) \left(\mathrm{a}_2(\pi_1(w), \pi_2(w), w) - \frac{\partial \pi_2(w)}{\partial w} s(w) \right) \\ & \vdots & \\ c(w) & = & -\mathrm{b}_n^{-1}(\pi_1(w), \ldots, \pi_n(w), w) \left(\mathrm{a}_n(\pi_1(w), \ldots, \pi_n(w), w) - \frac{\partial \pi_n(w)}{\partial w} s(w) \right) \end{array} \right. \tag{77}$$

assuming that $\mathrm{b}_0^{-1}(w)$, $\mathrm{b}_1^{-1}(\pi_1(w), w)$, $\mathrm{b}_2^{-1}(\pi_1(w), \pi_2(w), w)$, etc, are non-singular $\forall\, w \in \mathcal{W}$. With the function $\pi(w)$ determined, it readily follows that $d(w) = g(\pi(w), w)$.

In order to tackle next the output regulator design, it is useful to employ the internal model approach (CHEN; HUANG, 2015). So as to concisely demonstrate this methodology, let the controller (62) be expressed as

$$\left\{ \begin{array}{rcl} \dot{\xi} & = & \phi_m(\xi, y) + \phi_s(y) \\ u & = & \theta_m(\xi, y) + \theta_s(y) \end{array} \right. . \tag{78}$$

Functions $\phi_m : \mathbb{R}^{n_\xi} \times \mathbb{R}^{n_y} \to \mathbb{R}^{n_\xi}$ and $\theta_m : \mathbb{R}^{n_\xi} \times \mathbb{R}^{n_y} \to \mathbb{R}^{n_u}$ here are internal model terms and $\phi_s : \mathbb{R}^{n_y} \to \mathbb{R}^{n_\xi}$ and $\theta_s : \mathbb{R}^{n_y} \to \mathbb{R}^{n_u}$ denote stabilizing terms. If one enforces that

$$\left\{ \begin{array}{rcl} 0 & = & \phi_s(d(w)) \\ 0 & = & \theta_s(d(w)) \end{array} \right. \forall\, w \in \mathcal{W} \,, \tag{79}$$

then these stabilizing functions do not influence the solution of regulation condition (67), which simplifies to

$$\left\{ \begin{array}{rcl} \dfrac{\partial \sigma(w)}{\partial w} s(w) & = & \phi_m(\sigma(w), d(w)) \\ c(w) & = & \theta_m(\sigma(w), d(w)) \end{array} \right. \quad \forall\, w \in \mathcal{W}\,. \tag{80}$$

This formulation leads to the following sequential design procedure in order to solve Problem 2.4:

(a) Design internal model functions $\phi_m(\xi, y)$ and $\theta_m(\xi, y)$ such that (80) is satisfied for some $\sigma(w)$.

(b) Design stabilizing functions $\phi_s(y)$ and $\theta_s(y)$ satisfying (79) such that attraction condition (68) holds.

Some traditional methods able to solve step (a) will be presented next in Subsection 2.3.1, while Subsection 2.3.2 shows some useful guidelines in order to solve the stabilization problem of step (b).

2.3.1 Internal Model Design

The internal model represents a dynamical system capable of generating the steady-state control solution $c(w)$, thus establishing a zero-error and invariant manifold $\mathcal{M}$. Classical approaches capable of properly defining internal model functions $\phi_m(\xi, y)$ and $\theta_m(\xi, y)$ are demonstrated by the following lemmas (ISIDORI; MARCONI; SERRANI, 2012).

Lemma 2.2. *(Direct Reconstruction) The internal model functions*

$$\phi_m(\xi) = s(\xi)\,, \qquad \theta_m(\xi) = c(\xi)\,, \tag{81}$$

satisfy the condition (80) *with* $\sigma(w) = w$.

Proof. If $\sigma(w) = w$, then $\partial\sigma(w)/\partial w = I$ and therefore relation (80) becomes

$$\left\{ \begin{array}{rcl} s(w) & = & \phi_m(w, d(w)) \\ c(w) & = & \theta_m(w, d(w)) \end{array} \right. \quad \forall\, w \in \mathcal{W}\,. \tag{82}$$

So, it readily verifies that internal model functions (81) satisfy (82). □

Lemma 2.3. *(Immersion Method) Suppose there exists a number* $\mathrm{q} \in \mathbb{N}$ *and a function* $\zeta : \mathbb{R}^{n_u} \times \ldots \times \mathbb{R}^{n_u} \times \mathbb{R}^{n_y} \to \mathbb{R}^{n_u}$ *such that*

$$\overset{(\mathrm{q})}{c}(w) = \zeta\big(c(w)\,,\, \dot{c}(w)\,,\, \ldots\,,\, \overset{(\mathrm{q}-1)}{c}(w)\,,\, d(w)\big) \;\; \forall\, w \in \mathcal{W}\,. \tag{83}$$

Then for $\xi \in \mathbb{R}^{\mathrm{q}n_u}$, $\xi_i \in \mathbb{R}^{n_u}\; \forall\, i \in \{1, 2, \ldots, \mathrm{q}\}$, *the internal model functions*

$$\phi_m(\xi, y) = \begin{bmatrix} \xi_2 \\ \vdots \\ \xi_n \\ \zeta(\xi_1, \xi_2, \ldots, \xi_n, y) \end{bmatrix}, \;\; \theta_m(\xi) = \xi_1\,, \tag{84}$$

satisfy the condition (80) *with*

$$\sigma(w) = \begin{bmatrix} c(w) \\ \dot{c}(w) \\ \vdots \\ \overset{(\mathrm{q}-1)}{c}(w) \end{bmatrix}. \tag{85}$$

Proof. If $\sigma(w)$ is given as (85), the top-left corner of (80) can be rearranged as

$$\frac{\partial \sigma(w)}{\partial w} s(w) = \dot{\sigma}(w) = \begin{bmatrix} \dot{c}(w) \\ \vdots \\ \overset{(\mathrm{q}-1)}{c}(w) \\ \overset{(\mathrm{q})}{c}(w) \end{bmatrix}, \tag{86}$$

Moreover, if $\phi_m(\xi, y)$ is defined as in (84), the top-right corner of condition (80) can be written as

$$\phi_m(\sigma(w), d(w)) = \begin{bmatrix} \sigma_2(w) \\ \vdots \\ \sigma_{\mathrm{q}}(w) \\ \zeta(\sigma_1(w), \ldots, \sigma_{\mathrm{q}}(w), d(w)) \end{bmatrix} = \begin{bmatrix} \dot{c}(w) \\ \vdots \\ \overset{(\mathrm{q}-1)}{c}(w) \\ \zeta(c(w), \ldots, \overset{(\mathrm{q}-1)}{c}(w), d(w)) \end{bmatrix}. \tag{87}$$

If supposition (83) is true, it verifies that (86) is equal to (87). Beyond this fact, when $\theta_m(\xi) = \xi_1$, the bottom-right corner of (80) can be expressed as $\theta_m(\sigma(w)) = \sigma_1(w) = c(w)$, which readily equals the bottom-left corner of the same relation. Consequently, (80) is satisfied with the internal model design (84) with the mapping $\sigma(w)$ from (85). □

Remark 2.3. If $c(w)$ is a polynomial of finite degree with respect to w and the exosystem function $s(w)$ is linear, then there always exist a positive integer q and a function $\zeta(\cdot)$ such that (83) is satisfied (ISIDORI; MARCONI; SERRANI, 2012). In turn, the required internal model order q is associated with the polynomial degree of $c(w)$.

By using the first design approach of Lemma 2.2, the internal model states ξ will represent the direct estimation of the exosystem states w. If the attraction condition (68) is fulfilled, it follows that $\xi(t) \to w(t)$ as $t \to \infty$ and consequently that $c(\xi(t)) \to c(w(t))$. Even though this is a general method, it is not robust to uncertainties on the control mapping function $c(w)$. In order to get around this issue, the second design method of Lemma 2.3 offers full robustness to any plant parametric uncertainty in $c(w)$, since the design is based on the estimation of $c(w)$ as a whole, meaning that $\xi_1(t) \to c(w(t))$ as $t \to \infty$. This second approach is only applicable though if (83) is true, which is guaranteed to hold just in the particular case described by Remark 2.3. Moreover, the analytical solution of $\zeta(\cdot)$ shows to be highly difficult when the exosystem contains nonlinearities. Another disadvantage of Lemma 2.2 is the required compensator order, which may be much higher then the number of exosystem states.

It may be also possible to design partially robust internal models with alternative approaches in between Lemma 2.2 and Lemma 2.3. For instance, the next method stated on Lemma 2.4 seeks to immerse any scaling factor of $c(w)$ into the mapping $\sigma(w)$ by exploring the use of measurements (CHEN; HUANG, 2015). This alternative method should be tackled when the full immersion function $\zeta(\cdot)$ defined in Lemma 2.3 cannot be determined, which may be the case for nonlinear exosystems.

Lemma 2.4. *Consider a scalar* $\epsilon \in \mathbb{R}$ *and matrix functions* $\mathrm{S} : \mathbb{R}^{n_y} \to \mathbb{R}^{n_w \times n_w}$ *and* $\mathrm{U} : \mathbb{R}^{n_y} \to \mathbb{R}^{n_u \times n_w}$ *such that*

$$\left\{ \begin{array}{rcl} s(w) & = & \mathrm{S}(d(w))\, w \\ c(w) & = & \epsilon\, \mathrm{U}(d(w))\, w \end{array} \right. \quad \forall\, w \in \mathcal{W}\,. \tag{88}$$

Then the internal model functions

$$\phi_m(\xi, y) = \mathrm{S}(y)\, \xi\,, \quad \theta_m(\xi, y) = \mathrm{U}(y)\, \xi\,, \tag{89}$$

satisfy the condition (80) *with* $\sigma(w) = \epsilon\, w$.

Proof. Let $\sigma(w) = \epsilon\, w$ and develop the top-left corner of (80) as follows:

$$\frac{\partial \sigma(w)}{\partial w} s(w) = \epsilon\, s(w)\,. \tag{90}$$

By applying $\phi_m(\xi, y) = \mathrm{S}(y)\, \xi$ to the top-right corner of (80) one obtains:

$$\phi_m(\sigma(w), d(w)) = \mathrm{S}(d(w))\, (\gamma\, w) = \epsilon\, \mathrm{S}(d(w))\, w\,. \tag{91}$$

Supposing $\mathrm{S}(y)$ is defined such that $s(w) = \mathrm{S}(y)\, w$ is true when $y = d(w)\ \forall\, w \in \mathcal{W}$, (91) equals (90) and the top condition in (80) is satisfied. Now develop the bottom-right corner in (80) with $\theta_m(\xi, y) = \mathrm{U}(y)\, \xi$, which leads to:

$$\theta_m(\sigma(w), d(w)) = \mathrm{U}(d(w))\, (\epsilon\, w) = \epsilon\, \mathrm{U}(d(w))\, w\,. \tag{92}$$

If $\mathrm{U}(y)$ is defined such that $c(w) = \gamma\, \mathrm{U}(y)\, w + \eta(y)$ holds for $y = d(w)\ \forall\, w \in \mathcal{W}$, then (92) equals the bottom-left corner side of (80). Therefore, all conditions in (80) verify with the internal model design (89) and the mapping $\sigma(w) = \epsilon\, w$. □

An internal model design example is demonstrated subsequently where all of the discussed methods are employed and robustness properties are analyzed.

Example 2.2. Consider a nonlinear system described by

$$\left\{ \begin{array}{rcl} \dot{x}_1 & = & x_2 \\ \dot{x}_2 & = & a\, x_1^2 x_2 + b\, u \\ e & = & x_1 - w_1 \end{array} \right. \tag{93}$$

where $a, b \in \mathbb{R}$ are constant parameters. Suppose the exogenous state is produced by a harmonic oscillator:

$$\left\{ \begin{array}{rcl} \dot{w}_1 & = & w_2 \\ \dot{w}_2 & = & -w_1 \end{array} \right. . \tag{94}$$

System functions $f(x, w, u)$, $h(x, w)$ and $s(w)$ in this example are

$$f(x, u) = \begin{bmatrix} x_2 \\ a\, x_1^2 x_2 + b\, u \end{bmatrix}, \quad h(x, w) = x_1 - w_1\,, \quad s(w) = \begin{bmatrix} w_2 \\ -w_1 \end{bmatrix}\,. \tag{95}$$

Prior to designing an internal model, it is necessary to find the pair of functions $\pi(w)$ and $c(w)$ satisfying the condition (66). In order to do so, one can write the system equations

into the form (76) with functions $\mathrm{a}_0(w) = -w_1$, $\mathrm{b}_0 = 1$, $\mathrm{a}_1 = 0$, $\mathrm{b}_1 = 1$, $\mathrm{a}_2(x) = a\, x_1^2 x_2$ and $\mathrm{b}_2 = b$. Evaluating the expressions indicated in (77) with these functions, one obtains:

$$\left\{\begin{array}{rcl} \pi_1(w) &=& -\mathrm{b}_0^{-1}\mathrm{a}_0(w) = w_1 \\ \pi_2(w) &=& -\mathrm{b}_1^{-1}\left(\mathrm{a}_1 - \dfrac{\partial \pi_1(w)}{\partial w} s(w)\right) = w_2 \\ c(w) &=& -\mathrm{b}_2^{-1}\left(\mathrm{a}_2(x) - \dfrac{\partial \pi_2(w)}{\partial w} s(w)\right) = -ab^{-1}\, w_1^2 w_2 - b^{-1}\, w_1 \end{array}\right. . \tag{96}$$

Considering the direct reconstruction method presented by Lemma 2.2, the internal model functions are given by:

$$\phi_m(\xi) = \begin{bmatrix} \xi_2 \\ -\xi_1 \end{bmatrix}, \quad \theta_m(\xi) = -ab^{-1}\, \xi_1^2 \xi_2 - b^{-1}\, \xi_1 . \tag{97}$$

The disadvantage of this design is that plant parameters a and b must be exactly known for the implementation of $\theta_m(\xi)$. In order to circumvent this issue, one should consider the immersion design method presented by Lemma 2.3. To do so, it is required to first verify if there exists a positive integer q satisfying (83). This means to successively derive $c(w)$, with respect to time, until a q-th order derivative is found to be a function of the lower derivatives. The multiple time-derivatives of $c(w)$ under $s(w)$ from (95) are evaluated in the following manner:

$$\left\{\begin{array}{rcccl} \dot{c}(w) &=& \dfrac{\partial c(w)}{\partial w} s(w) &=& \dfrac{\partial c(w)}{\partial w_1} w_2 - \dfrac{\partial c(w)}{\partial w_2} w_1 \\ \ddot{c}(w) &=& \dfrac{\partial \dot{c}(w)}{\partial w} s(w) &=& \dfrac{\partial \dot{c}(w)}{\partial w_1} w_2 - \dfrac{\partial \dot{c}(w)}{\partial w_2} w_1 \\ & \vdots & & \vdots & \\ \overset{(\mathrm{q})}{c}(w) &=& \dfrac{\partial^{(\mathrm{q}-1)} c(w)}{\partial w} s(w) &=& \dfrac{\partial^{(\mathrm{q}-1)} c(w)}{\partial w_1} w_2 - \dfrac{\partial^{(\mathrm{q}-1)} c(w)}{\partial w_2} w_1 \end{array}\right. \tag{98}$$

Evaluating (98) up to $\mathrm{q} = 4$, with $c(w)$ obtained from (96) yields:

$$\left\{\begin{array}{rcl} c(w) &=& -ab^{-1}\, w_1^2 w_2 - b^{-1}\, w_1 \\ \dot{c}(w) &=& -2ab^{-1}\, w_1 w_2^2 + \mathrm{a}\, w_1^3 - b^{-1}\, w_2 \\ \ddot{c}(w) &=& 7ab^{-1}\, w_1^2 w_2 - 2\mathrm{a}\, w_2^3 + b^{-1}\, w_1 \\ \overset{(3)}{c}(w) &=& 20ab^{-1}\, w_1 w_2^2 - 7ab^{-1}\, w_1^3 + b^{-1}\, w_2 \\ \overset{(4)}{c}(w) &=& -61ab^{-1}\, w_1^2 w_2 + 20ab^{-1}\, w_2^3 - b^{-1}\, w_1 \end{array}\right. . \tag{99}$$

Observe that the forth order time-derivative of $c(w)$ can be expressed as a function of the lower order derivatives, that is $\overset{(4)}{c}(w) = -9\, c(w) - 10\, \ddot{c}(w)$. Therefore, (83) is true for $\mathrm{q} = 4$ and the immersed internal model functions are:

$$\phi_m(\xi) = \begin{bmatrix} \xi_2 \\ \xi_3 \\ \xi_4 \\ -9\, \xi_1 - 10\, \xi_3 \end{bmatrix}, \quad \theta_m(\xi) = \xi_1 . \tag{100}$$

This immersed design has the property of full robustness with respect to all system parameters a and b, since they are not necessary to compute the internal model functions.

On the other hand, the number of required controller states doubles in comparison to the direct reconstruction.

Now suppose the exogenous signal w_1 is available as an independent measurement, i.e. $y_1 = w_1$ and $d_1(w) = w_1$. In this case, it is possible to use the alternative approach from Lemma 2.4 in order to construct a lower order internal model with partial robustness properties. Observe that functions $s(w) = [w_2 \ -w_1]^\intercal$ and $c(w) = -ab^{-1}\, w_1^2 w_2 - b^{-1}\, w_1$ can be expressed in the form (88) with terms S, $\mathrm{U}(y)$ and ϵ as:

$$\mathrm{S} = \begin{bmatrix} 0 & 1 \\ -1 & 0 \end{bmatrix}, \quad \mathrm{U}(y) = \begin{bmatrix} 1 & a\, y_1^2 \end{bmatrix}, \quad \epsilon = -b^{-1}\,. \tag{101}$$

Therefore according to (89), the following internal model design is also feasible:

$$\phi_m(\xi) = \begin{bmatrix} \xi_2 \\ -\xi_1 \end{bmatrix}, \quad \theta_m(\xi, y) = \xi_1 + a\, y_1^2 \xi_2\,. \tag{102}$$

Despite the parameter a needs to be known in this case, this alternative construction is still robust with respect to b.

2.3.2 Design of Stabilizing Components

Step (b) of the output regulator design method previously shown consists on finding stabilizing functions $\phi_s(y)$ and $\theta_s(y)$ satisfying condition (79) such that the attraction requirement (68) will hold. In order to assist on the solution of this step, an auxiliary vanishing signal $\varepsilon \in \mathbb{R}^{n_\varepsilon}$ can be introduced as (CHEN; HUANG, 2015)

$$\varepsilon = \delta(y)\,, \tag{103}$$

for some function $\delta : \mathbb{R}^{n_y} \to \mathbb{R}^{n_\varepsilon}$ that vanishes inside the regulation manifold, i.e.

$$0 = \delta(d(w)) \ \ \forall\, w \in \mathcal{W}\,. \tag{104}$$

With this definition, controller (78) may be re-expressed in the form of

$$\begin{cases} \dot{\xi} &= \phi_m(\xi, y) + \mathrm{G}(y)\, \varepsilon \\ u &= \theta_m(\xi, y) + \mathrm{K}(y)\, \varepsilon \end{cases}, \tag{105}$$

where $\mathrm{G} : \mathbb{R}^{n_y} \to \mathbb{R}^{n_s \times n_\varepsilon}$ and $\mathrm{K} : \mathbb{R}^{n_y} \to \mathbb{R}^{n_u \times n_\varepsilon}$ are free design matrix functions. One should see that (78) is equivalent to (105) since $\phi_s(y) = \mathrm{G}(y)\, \delta(y)$ and $\theta_s(y) = \mathrm{K}(y)\, \delta(y)$. Also note that (104) ensures the fulfillment of regulation condition (79). Control design step (b) can therefore be separated into the following sub-steps:

(b.1) Choose a steady-state vanishing function $\delta(y)$ satisfying (104).

(b.2) Design matrix functions $\mathrm{G}(y)$ and $\mathrm{K}(y)$ such the attraction condition (68) is verified.

Whenever the output error function $h(x, w)$ can be rearranged in terms of the output measurements, i.e. $h(x, w) = \mathrm{h}(y)$ for $y = g(x, w)$, then a possible choice for sub-step (b.1) is directly

$$\delta(y) = \mathrm{h}(y) \tag{106}$$

since $\delta(d(w)) = \mathrm{h}(d(w)) = h(\pi(w), w) = 0 \; \forall \, w \in \mathcal{W}$. This approach is recommended as a default choice. If the output measurement vector contains more than enough information to implement the output error, the designer can explore this fact in order to augment the output vanishing function $\delta(y)$, thus proving additional degrees of freedom for stabilization purposes. For instance, in a scenario where all system and exosystem states are measured, that is $y = [y_x^{\intercal} \;\; y_w^{\intercal}]^{\intercal} = [x^{\intercal} \; w^{\intercal}]^{\intercal}$, one should consider

$$\delta(y) = y_x - \pi(y_w) \; . \tag{107}$$

This construction may also be used partially, in case only a subset of the system and exosystem states are available. A numerical example subsequently illustrates these design possibilities.

Example 2.3. Consider the same nonlinear system described by (93) where the exogenous state is generated by (94). Recall the error signal was defined as $e = h(x, w) = x_1 - w_1$ and the manifold solution $\pi(w) = [w_1 \;\; w_2]^{\intercal}$ was obtained in (96). Consider also three different output measurement scenarios described by

$$\text{(i)} \;\; y = x_1 - w_1 \; , \quad \text{(ii)} \;\; y = \begin{bmatrix} x_2 \\ w_2 \end{bmatrix} \; , \quad \text{(iii)} \;\; y = \begin{bmatrix} x_1 \\ x_2 \\ w_1 \\ w_2 \end{bmatrix} \; . \tag{108}$$

In case (i), it verifies that $e = h(x, w) = y = g(x, w) = x_1 - w_1$, and so, the output vanishing function can be defined using the default approach from (106):

$$\delta(y) = y \; . \tag{109}$$

On the other hand, a possible setup for case (ii) is the partial usage of expression (107):

$$\delta(y) = y_1 - y_2 \; , \tag{110}$$

since $x_2 - w_2 = 0$ when $x_2 = \pi_2(w) = w_2$. Finally, in the last case (iii), one could use the full definition indicated in (107):

$$\delta(y) = \begin{bmatrix} y_1 - y_3 \\ y_2 - y_4 \end{bmatrix} \; . \tag{111}$$

through the same reasoning employed for case (ii).

After having dealt with sub-step (b.1), the next sub-step (b.2) may be cast as a nonlinear asymptotic stabilization problem by introducing a proper change of coordinates, most commonly (HUANG; CHEN, 2004):

$$z \triangleq \begin{bmatrix} x - \pi(w) \\ \xi - \sigma(w) \end{bmatrix} \; , \tag{112}$$

where $z \in \mathbb{R}^{n_x + n_\xi}$. If one is able to find $\mathrm{G}(y)$, $\mathrm{K}(y)$ and a region $\mathcal{D}$ such that $z(t)$ defined in (112) asymptotically approaches the origin, then Problem 2.4 is finally solved. The Lyapunov stability result presented in Theorem 2.1 is usually employed for this last step (CHEN; HUANG, 2015).

2.4 Final Remarks

Initially, this chapter introduced a selection of LMI based results, including dynamic output feedback control design, stability of nonlinear systems with control input saturation and stability of rational nonlinear systems. The chapter then moved towards the basic theory on nonlinear output regulation, describing fundamental concepts such as steady-state manifolds, regulator equations, internal models and stabilization problems in the regulation sense. The methodology of this thesis subsequently contributes on the basis of all these preliminary topics.

3 OUTPUT REGULATION OF RATIONAL NONLINEAR SYSTEMS

A new output regulation approach for rational nonlinear systems is proposed in this chapter, where a systematic methodology based on the differential-algebraic representation is presented for stability analysis and design of dynamic output feedback controllers.

This chapter is organized in the following manner: Section 3.1 introduces the problem to be tackled, followed by Section 3.2 which explains the controller structure to be considered. The main results are contained in Section 3.3, where stability conditions and design procedures are provided. Afterwards, Section 3.4 demonstrates the proposed methodology with some numerical examples. Final remarks are also given on Section 3.5.

3.1 Problem Statement

The problem dealt in this chapter is equivalent to what has been introduced in Section 2.3, where the nonlinear system to be regulated is described by

$$\left\{ \begin{array}{rcl} \dot{x} & = & f(x,w,u) \\ y & = & g(x,w) \\ e & = & h(x,w) \end{array} \right. \tag{113}$$

with $x \in \mathbb{R}^{n_x}$, $u \in \mathbb{R}^{n_u}$, $y \in \mathbb{R}^{n_y}$ and $e \in \mathbb{R}^{n_e}$ respectively denoting the system state, the control input, the output measurement and the output error. The exogenous perturbation signal $w \in \mathbb{R}^{n_w}$ is generated by an autonomous nonlinear exosystem

$$\dot{w} = s(w)\ , \tag{114}$$

and the system control input is provided by a nonlinear output feedback controller of the form

$$\left\{ \begin{array}{rcl} \dot{\xi} & = & \phi(\xi,y) \\ u & = & \theta(\xi,y) \end{array} \right. , \tag{115}$$

where $\xi \in \mathbb{R}^{n_\xi}$ is the controller state. The standard preliminary Assumptions 2.1 and 2.2 mentioned earlier are also considered here. Given this setup, the problem to be tackled in this chapter is stated as follows.

Problem 3.1. Design controller functions $\phi(\xi,y)$ and $\theta(\xi,y)$ such that the closed-loop system (113), (114), (115) achieves output regulation in some region $\mathcal{D} \subseteq \mathbb{R}^{n_x} \times \mathbb{R}^{n_\xi} \times \mathcal{W}$.

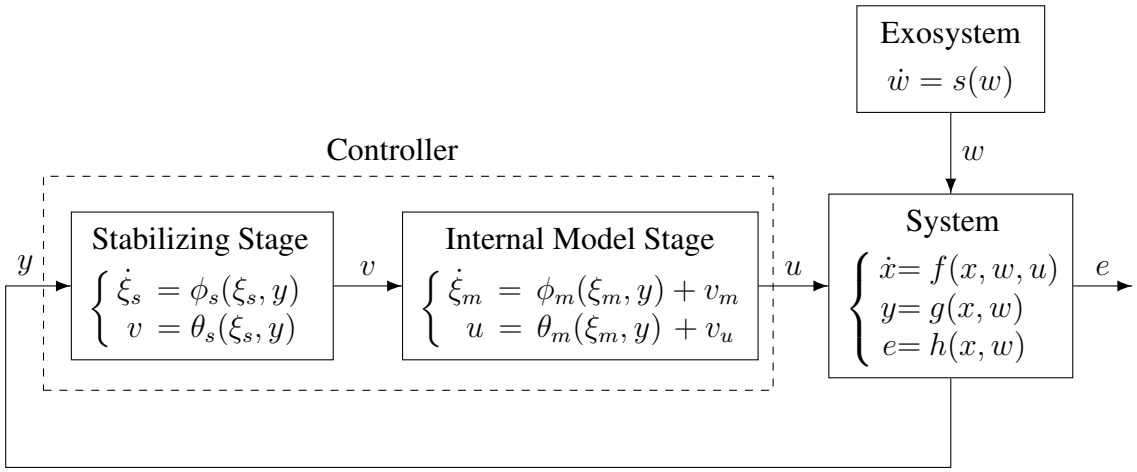

Figure 4: Block diagram of the closed-loop system with the considered control structure. Source: the author.

3.2 Control Structure

In order to construct the dynamic output feedback controller (115), two separate stages are considered: the internal model controller and the stabilizing controller. So as to present such framework, the controller state vector ξ is defined as

$$\xi \triangleq \begin{bmatrix} \xi_m \\ \xi_s \end{bmatrix}, \tag{116}$$

where $\xi_m \in \mathbb{R}^{n_m}$ represents internal model states and $\xi_s \in \mathbb{R}^{n_s}$ denotes the stabilizing controller states. Furthermore, a stabilizing control input $v \in \mathbb{R}^{n_v}$ $(n_v = n_u + n_m)$ is given by

$$v \triangleq \begin{bmatrix} v_u \\ v_m \end{bmatrix}, \tag{117}$$

where the component $v_u \in \mathbb{R}^{n_u}$ is the system stabilizing input and the component $v_m \in \mathbb{R}^{n_m}$ is the internal model stabilizing input. Using the previous definitions (116) and (117), the internal model stage is defined as

$$\begin{cases} \dot{\xi}_m = \phi_m(\xi_m, y) + v_m \\ u = \theta_m(\xi_m, y) + v_u \end{cases}, \tag{118}$$

where $\phi_m : \mathbb{R}^{n_m} \times \mathbb{R}^{n_y} \to \mathbb{R}^{n_m}$ and $\theta_m : \mathbb{R}^{n_m} \times \mathbb{R}^{n_y} \to \mathbb{R}^{n_u}$ are the internal model functions. Likewise, the stabilizing controller stage is defined as

$$\begin{cases} \dot{\xi}_s = \phi_s(\xi_s, y) \\ v = \theta_s(\xi_s, y) \end{cases}, \tag{119}$$

where $\phi_s : \mathbb{R}^{n_s} \times \mathbb{R}^{n_y} \to \mathbb{R}^{n_s}$ and $\theta_s : \mathbb{R}^{n_s} \times \mathbb{R}^{n_y} \to \mathbb{R}^{n_v}$ are the stabilizing controller functions. The block diagram on Figure 4 depicts the considered control framework, which is equivalent to the original output regulation diagram shown by Figure 3. The only difference here is the detailing of the controller with two distinct components: the internal model (118) and the stabilizing stage (119). Considering this particular structure, the sufficient conditions for the output regulation of the closed-loop system (113), (114) are presented by the following lemma, which is directly derived from Theorem 2.6.

Lemma 3.1. *The closed-loop system* (113)*,* (114) *with controller* (118)*,* (119) *achieves output regulation in* $\mathcal{D} \subseteq \mathbb{R}^{n_x} \times \mathbb{R}^{n_m} \times \mathbb{R}^{n_s} \times \mathcal{W}$ *if there exist smooth mappings* $\pi : \mathcal{W} \to \mathbb{R}^{n_x}$*,* $c : \mathcal{W} \to \mathbb{R}^{n_u}$*,* $d : \mathcal{W} \to \mathbb{R}^{n_y}$ *and* $\sigma_m : \mathcal{W} \to \mathbb{R}^{n_m}$ *such that* $\pi(0) = 0$*,* $c(0) = 0$*,* $d(0) = 0$*,* $\sigma_m(0) = 0$*,*

$$\left\{ \begin{array}{rcl} \dfrac{\partial \pi(w)}{\partial w} s(w) & = & f(\pi(w), w, c(w)) \\ d(w) & = & g(\pi(w), w) \\ 0 & = & h(\pi(w), w) \end{array} \right. \quad \forall\, w \in \mathcal{W}\,, \tag{120}$$

$$\left\{ \begin{array}{rcl} \dfrac{\partial \sigma_m(w)}{\partial w} s(w) & = & \phi_m(\sigma_m(w), d(w)) \\ c(w) & = & \theta_m(\sigma_m(w), d(w)) \end{array} \right. \forall\, w \in \mathcal{W}\,, \tag{121}$$

$$\left\{ \begin{array}{rcl} 0 & = & \phi_s(0, d(w)) \\ 0 & = & \theta_s(0, d(w)) \end{array} \right. \quad \forall\, w \in \mathcal{W}\,, \tag{122}$$

and also:

$$\big(x(0), \xi_m(0), \xi_s(0), w(0)\big) \in \mathcal{D} \;\Rightarrow\; \left\{ \begin{array}{l} \lim\limits_{t\to\infty} \big|\big|x(t) - \pi(w(t))\big|\big| = 0 \\ \lim\limits_{t\to\infty} \big|\big|\xi_m(t) - \sigma_m(w(t))\big|\big| = 0 \\ \lim\limits_{t\to\infty} \big|\big|\xi_s(t)\big|\big| = 0 \end{array} \right. . \tag{123}$$

Proof. Observe the first regulation condition (66) of Theorem 2.6 is equivalent to (120). Consider now the second regulation condition (67) with a candidate mapping solution $\sigma(w)$ defined by

$$\sigma(w) = \begin{bmatrix} \sigma_m(w) \\ 0 \end{bmatrix}, \tag{124}$$

for some smooth mapping $\sigma_m : \mathcal{W} \to \mathbb{R}^{n_m}$, $\sigma_m(0) = 0$. The complete controller representation (115) with joined stages (118) and (119) may then be expressed as

$$\left\{ \begin{array}{rcl} \dot{\xi} = \phi(\xi, y) & = & \begin{bmatrix} \phi_m(\xi_m, y) + D_m\, \theta_s(\xi_s, y) \\ \phi_s(\xi_s, y) \end{bmatrix} \\ u = \theta(\xi, y) & = & \theta_m(\xi_m, y) + D\, \theta_s(\xi_s, y) \end{array} \right. \tag{125}$$

where auxiliary matrices $D \in \mathbb{R}^{n_u \times n_v}$ and $D_m \in \mathbb{R}^{n_m \times n_v}$ are

$$D \triangleq \begin{bmatrix} I & 0 \end{bmatrix}\,, \quad D_m \triangleq \begin{bmatrix} 0 & I \end{bmatrix}\,. \tag{126}$$

Using (124) and (125), the regulation condition (67) becomes

$$\left\{ \begin{array}{rcl} \begin{bmatrix} \dfrac{\partial \sigma_m(w)}{\partial w} s(w) \\ 0 \end{bmatrix} & = & \begin{bmatrix} \phi_m(\sigma_m(w), d(w)) + D_m\, \theta_s(0, d(w)) \\ \phi_s(0, d(w)) \end{bmatrix} \\ c(w) & = & \theta_m(\sigma_m(w), d(w)) + D\, \theta_s(0, d(w)) \end{array} \right. . \tag{127}$$

Provided that condition (122) holds, then (127) simplifies to (121). Furthermore, applying (124) into the limit condition (68) leads to (123).

Consequently from Theorem 2.6, the conditions of Lemma 3.1 ensure the output regulation of the closed-loop system defined by (113), (114), (118), (119) with respect to region $\mathcal{D}$. □

An important consequence of Lemma 3.1 is the fact that internal model and stabilizing stages can be designed separately. Observe that equation (121) does not depend on $\phi_s(\xi_s, y)$ and $\theta_s(\xi_s, y)$, therefore one can find an internal model $\phi_m(\xi_m, y)$ and $\theta_m(\xi_m, y)$ as a first step and subsequently design the stabilizing controller so as to ensure the attraction condition (123). This sequential design approach is similar to the case explained in Section 2.3, however, instead of static stabilizing terms, dynamic stabilizing action is being considered here.

Prior to initiating the output regulator design, it is considered that target manifold mappings $\pi(w)$ and $c(w)$ are known, as stated by Assumption 3.1 below[1]. If the system functions $f(x, w, u)$ and $h(x, w)$ are in the form of (76), as discussed in Section 2.3, then $\pi(w)$ and $c(w)$ can be recursively determined by (77). Further guidelines with respect to this procedure may be found in (PAVLOV; WOUW; NIJMEIJER, 2006; CHEN; HUANG, 2015).

Assumption 3.1. There exists a known mapping pair $\pi : \mathcal{W} \to \mathbb{R}^{n_x}$ and $c : \mathcal{W} \to \mathbb{R}^{n_u}$ satisfying $\pi(0) = 0$, $c(0) = 0$ and (120)[2].

Given the presented control framework and preliminary assumptions, the considered design methodology in order to solve Problem 3.1 therefore divides into two distinct steps:

(a) Design internal model functions $\phi_m(\xi_m, y)$ and $\theta_m(\xi_m, y)$ such that (121) is satisfied for some $\sigma_m(w)$.

(b) Design stabilizing functions $\phi_s(\xi_s, y)$ and $\theta_s(\xi_s, y)$ satisfying (122) such that attraction condition (123) holds.

The solution of step (a) can be obtained by any of the internal model design approaches presented in Subsection 2.3.1. Given all assumptions mentioned here, step (a) is guaranteed to be solvable at least by the approach in Lemma 2.2, which is the most general method. However it is recommended to employ the immersion method of Lemma 2.3 whenever possible, because of its additional robustness property.

Towards systematically solving step (b), the general stabilizing controller representation from (119) is henceforth particularized in the form of

$$\left\{ \begin{array}{rcl} \dot{\xi}_s & = & \mathrm{F}(y)\,\xi_s + \mathrm{G}(y)\,\varepsilon \\ v & = & \mathrm{H}(y)\,\xi_s + \mathrm{K}(y)\,\varepsilon \end{array} \right. , \tag{128}$$

where $\mathrm{F} : \mathbb{R}^{n_y} \to \mathbb{R}^{n_s \times n_s}$, $\mathrm{G} : \mathbb{R}^{n_y} \to \mathbb{R}^{n_s \times n_\varepsilon}$, $\mathrm{H} : \mathbb{R}^{n_y} \to \mathbb{R}^{n_u \times n_s}$ and $\mathrm{K} : \mathbb{R}^{n_y} \to \mathbb{R}^{n_u \times n_\varepsilon}$ are free design matrix functions. In (128) also, a steady-state vanishing signal $\varepsilon \in \mathbb{R}^{n_\varepsilon}$ is considered as

$$\varepsilon = \delta(y) \,, \tag{129}$$

where $\delta : \mathbb{R}^{n_y} \to \mathbb{R}^{n_\varepsilon}$ is a function of the output measurement vector y that satisfies

$$0 = \delta(d(w)) \;\; \forall\, w \in \mathcal{W} \,. \tag{130}$$

One should notice that (128) is a particular case of (119) with $\phi_s(\xi_s, y) = \mathrm{F}(y)\,\xi_s + \mathrm{G}(y)\,\delta(y)$ and $\theta_s(\xi_s, y) = \mathrm{H}(y)\,\xi_s + \mathrm{K}(y)\,\delta(y)$, and therefore (130) ensures that the manifold constraint (122) is satisfied. Consequently, (130) will not influence the steady-state solution $c(w)$ rendered by the internal model, provided that $\xi_s \to 0$ as $t \to \infty$.

[1] Assumption 3.1 is relaxed in Chapter 5, where the framework is extended for the practical output regulation.

[2] If mapping $\pi(w)$ is known, one readily obtains the solution of $d(w)$, which is $d(w) = g(\pi(w), w)$.

The reason for choosing the particular stabilizing controller structure from (128) is the linearity with respect to the states ξ_s and the vanishing signal ε. This property will be subsequently useful for synthesis purposes, where a design approach inspired on Subsection 2.2.1 will be employed. Furthermore, in order to provide additional degree of freedom for the design problem, the parameters $\mathrm{F}(y)$, ... , $\mathrm{K}(y)$ are here proposed as possible functions of the available measurements. Also due to convexity arguments, it is proposed an affine parametrization for the stabilizing matrix functions:

$$\begin{bmatrix} \mathrm{F}(y) & \mathrm{G}(y) \\ \mathrm{H}(y) & \mathrm{K}(y) \end{bmatrix} \triangleq \begin{bmatrix} \mathrm{F}_0 & \mathrm{G}_0 \\ \mathrm{H}_0 & \mathrm{K}_0 \end{bmatrix} + \sum_{i=1}^{\mathrm{n}} \begin{bmatrix} \mathrm{F}_i & \mathrm{G}_i \\ \mathrm{H}_i & \mathrm{K}_i \end{bmatrix} \lambda_i(y) \, . \tag{131}$$

In here, $\lambda : \mathbb{R}^{n_y} \to \mathbb{R}^{\mathrm{n}}$ is a free gain scheduling function with arbitrary dimension $\mathrm{n} \in \mathbb{N}$ and $\mathrm{F}_0, \ldots, \mathrm{F}_\mathrm{n} \in \mathbb{R}^{n_s \times n_s}$, $\mathrm{G}_0, \ldots, \mathrm{G}_\mathrm{n} \in \mathbb{R}^{n_s \times n_\varepsilon}$, $\mathrm{H}_0, \ldots, \mathrm{H}_\mathrm{n} \in \mathbb{R}^{n_v \times n_s}$ and $\mathrm{K}_0, \ldots, \mathrm{K}_\mathrm{n} \in \mathbb{R}^{n_v \times n_\varphi}$ are free design matrices.

Given the proposed stabilizing controller structure from (130) and (131), the suggested solution of step (b) then divides into these sub-steps:

(b.1) Choose a steady-state vanishing function $\delta(y)$ satisfying (130).

(b.2) For a given scheduling function $\lambda(y)$, design stabilizing parameters F_0 , ... , K_n such the attraction condition (123) is verified.

The sub-step (b.1) can be systematically addressed using the guidelines discussed Subsection 2.3.2. On the other hand, a novel methodology in order to solve step (b.2) will be proposed in the following subsection, where the main contribution of this chapter is contained.

3.3 Main Results

This section introduces a new method capable of synthesizing the stabilizing parameters explained in the design sub-step (b.2). To do so, Subsection 3.3.1 initially develops the regulation error dynamics, followed by Subsection 3.3.2 which presents a differential-algebraic characterization of the system equations. Stability and transient performance conditions are afterwards derived in Subsection 3.3.3, leading to design conditions later in Subsection 3.3.4.

3.3.1 Regulation Error Coordinates

A change of state-space coordinates is introduced as $z \in \mathbb{R}^{n_z}$ $(n_z = n_x + n_m)$:

$$z \triangleq \begin{bmatrix} z_x \\ z_m \end{bmatrix} \triangleq \begin{bmatrix} x - \pi(w) \\ \xi_m - \sigma_m(w) \end{bmatrix} , \tag{132}$$

henceforth called as regulation error state vector. The vector component $z_x \in \mathbb{R}^{n_x}$ here denotes the deviation between the system state x and the regulation state reference $\pi(w)$, while $z_m \in \mathbb{R}^{n_m}$ denotes the deviation between the internal model state ξ_m and its regulation state reference $\sigma_m(w)$. By combining (132) with the system model (113) and the internal model controller (118), the system equations with respect to z can be written as

$$\left\{ \begin{array}{rcl} \dot{z} & = & f_z(z, w, v) \\ u & = & \theta_z(z, w) + c(w) + v_u \\ y & = & g_z(z, w) + d(w) \\ e & = & h_z(z, w) \\ \varepsilon & = & \delta_z(z, w) \end{array} \right. , \tag{133}$$

where functions $f_z : \mathbb{R}^{n_z} \times \mathbb{R}^{n_w} \times \mathbb{R}^{n_v} \to \mathbb{R}^{n_z}$, $\theta_z : \mathbb{R}^{n_z} \times \mathbb{R}^{n_w} \to \mathbb{R}^{n_u}$, $g_z : \mathbb{R}^{n_z} \times \mathbb{R}^{n_w} \to \mathbb{R}^{n_y}$, $h_z : \mathbb{R}^{n_z} \times \mathbb{R}^{n_w} \to \mathbb{R}^{n_e}$ and $\delta_z : \mathbb{R}^{n_z} \times \mathbb{R}^{n_w} \to \mathbb{R}^{n_\varepsilon}$ are obtained as follows:

$$\begin{aligned} f_z(z,w,v) &\triangleq \begin{bmatrix} f(z_x + \pi(w), w, \theta_z(z,w) + c(w) + v_u) \\ \phi_m(z_m + \sigma_m(w), g_z(z,w) + d(w)) + v_m \end{bmatrix} - \begin{bmatrix} f(\pi(w), w, c(w)) \\ \phi_m(\sigma_m(w), d(w)) \end{bmatrix}, \\ \theta_z(z,w) &\triangleq \theta_m(z_m + \sigma_m(w), g_z(z,w) + d(w)) - c(w)\ , \\ g_z(z,w) &\triangleq g(z_x + \pi(w), w) - d(w)\ , \\ h_z(z,w) &\triangleq h(z_x + \pi(w), w)\ , \\ \delta_z(z,w) &\triangleq \delta(g_z(z,w) + d(w))\ . \end{aligned} \tag{134}$$

If $z = 0$ and $v = 0$, one should note that $\forall\, w \in \mathcal{W}$: $h_z(0,w) = 0$, $g_z(0,w) = 0$, $\delta_z(0,w) = 0$, $\theta_z(0,w) = 0$, $f_z(0,w,0) = 0$. This observation implies that $z = 0$ is an equilibrium point of the sub-system $\dot{z} = f_z(z,w,v)$ when $v = 0$ for every possible exogenous state $w \in \mathcal{W}$. Moreover, the output error $e = h_z(z,w)$ and the function $\varepsilon = \delta_z(z,w)$ vanish to zero at this equilibrium condition.

The proposed stabilizing controller originally defined as (128) can also be expressed with respect to z in the following manner:

$$\left\{ \begin{array}{rcl} \dot{\xi}_s &=& F(z,w)\,\xi_s + G(z,w)\,\varepsilon \\ v &=& H(z,w)\,\xi_s + K(z,w)\,\varepsilon \end{array} \right. . \tag{135}$$

In here, matrix functions $F : \mathbb{R}^{n_z} \times \mathbb{R}^{n_w} \to \mathbb{R}^{n_s \times n_s}$, $G : \mathbb{R}^{n_z} \times \mathbb{R}^{n_w} \to \mathbb{R}^{n_s \times n_\varepsilon}$, $H : \mathbb{R}^{n_z} \times \mathbb{R}^{n_w} \to \mathbb{R}^{n_v \times n_s}$ and $K : \mathbb{R}^{n_z} \times \mathbb{R}^{n_w} \to \mathbb{R}^{n_v \times n_\varepsilon}$ denote the evaluation of $\mathrm{F}(y)$, $\mathrm{G}(y)$, $\mathrm{H}(y)$ and $\mathrm{K}(y)$ for $y = g_z(z,w) + d(w)$, i.e.

$$\begin{bmatrix} F(z,w) & G(z,w) \\ H(z,w) & K(z,w) \end{bmatrix} \triangleq \begin{bmatrix} \mathrm{F}_0 & \mathrm{G}_0 \\ \mathrm{H}_0 & \mathrm{K}_0 \end{bmatrix} + \sum_{i=1}^{\mathrm{n}} \begin{bmatrix} \mathrm{F}_i & \mathrm{G}_i \\ \mathrm{H}_i & \mathrm{K}_i \end{bmatrix} \lambda_i(z,w)\ . \tag{136}$$

where $\lambda : \mathbb{R}^{n_z} \times \mathbb{R}^{n_w} \to \mathbb{R}^{\mathrm{n}}$ is defined similarly to the previous constructions in (134), but now using the controller scheduling function $\lambda(y)$:

$$\lambda(z,w) \triangleq \lambda(g_z(z,w) + d(w))\ . \tag{137}$$

It is desirable that matrices $F(z,w)$, $G(z,w)$, $H(z,w)$ and $K(z,w)$ become affinely dependent on (z,w) in order to take advantage of convexity properties later on. It is possible to enforce this affinity property by simply restricting the choice of $\lambda(y)$ for cases where $\lambda(z,w)$ in (137) become a linear mapping with respect to (z,w), as assumed henceforth.

An augmented system representation must be defined next, incorporating the regulation error state z with the stabilizing controller state ξ_s in a single state vector $\mathbf{z} \in \mathbb{R}^{n_a}$ $(n_a = n_z + n_s)$:

$$\mathbf{z} \triangleq \begin{bmatrix} z \\ \xi_s \end{bmatrix}. \tag{138}$$

By joining (133) with (135), it is possible to express all closed-loop system equations with respect to $(\mathbf{z}, w)$:

$$\left\{ \begin{array}{rcl} \dot{\mathbf{z}} &=& \boldsymbol{f}(\mathbf{z},w) \\ e &=& \boldsymbol{h}(\mathbf{z},w) \end{array} \right. , \tag{139}$$

where functions $\boldsymbol{f} : \mathbb{R}^{n_a} \times \mathbb{R}^{n_w} \to \mathbb{R}^{n_a}$ and $\boldsymbol{h} : \mathbb{R}^{n_a} \times \mathbb{R}^{n_w} \to \mathbb{R}^{n_e}$ are constructed as:

$$\begin{aligned} \boldsymbol{f}(\mathbf{z},w) &\triangleq \begin{bmatrix} f_z(z,w, H(z,w)\,\xi_s + K(z,w)\,\delta_z(z,w)) \\ F(z,w)\,\xi_s + G(z,w)\,\delta_z(z,w) \end{bmatrix}, \\ \boldsymbol{h}(\mathbf{z},w) &\triangleq h_z(z,w)\ . \end{aligned} \tag{140}$$

From previous definitions, it is readily noticeable that $\boldsymbol{f}(0, w) = 0$ and $\boldsymbol{h}(0, w) = 0$ $\forall\, w \in \mathcal{W}$. This implies that $\mathbf{z} = 0$ is an equilibrium point of the augmented system $\dot{\mathbf{z}} = \boldsymbol{f}(\mathbf{z}, w)$, for every possible exogenous state $w \in \mathcal{W}$, and the output error $e = \boldsymbol{h}(\mathbf{z}, w)$ is equal to zero at this equilibrium condition.

The provided change of coordinates will be useful to develop stability conditions, since the original manifold attraction requirement (123) can now be denoted in the more convenient form

$$\big(\mathbf{z}(0), w(0)\big) \in \mathcal{D} \;\; \Rightarrow \;\; \lim_{t\to\infty} ||\mathbf{z}(t)|| = 0 \,, \tag{141}$$

for some region $\mathcal{D} \subseteq \mathbb{R}^{n_a} \times \mathcal{W}$. One should note that $\mathbf{z} = 0$ implies that $x = \pi(w)$, $\xi_m = \sigma_m(w)$ and $\xi_s \to 0$ according to definitions (132) and (138). Because of this reasoning, (123) is equivalent to (141) and the output regulation problem becomes an asymptotic stabilization problem.

3.3.2 Differential-Algebraic Representation

Towards systematically approaching the stabilizing parameters design through numerical optimization, the differential-algebraic representation (DAR) initially introduced in Subsection 2.2.3 will be used. From now on, the scope of the formulation is being restricted to a class of rational nonlinearities, as exposed by the following assumption.

Assumption 3.2. Nonlinear functions $f_z(z, w, v)$ and $\delta_z(z, w)$ of the system (133) can be represented as

$$\begin{aligned} f_z(z, w, v) &= A(z, w)\, z + \Phi(z, w)\, \varphi(z, w) + B\, v \\ \delta_z(z, w) &= C\, z + \Gamma\, \varphi(z, w) \end{aligned} \tag{142}$$

with a rational nonlinear function $\varphi : \mathcal{Z}^+ \times \mathcal{W}^+ \to \mathbb{R}^{n_\varphi}$ satisfying

$$0 = \Psi(z, w)\, z + \Omega(z, w)\, \varphi(z, w) \tag{143}$$

such that:

(i) Sets $\mathcal{Z}^+$ and $\mathcal{W}^+$ satisfy $\{0\} \subset \mathrm{int}\{\mathcal{Z}^+\} \subseteq \mathbb{R}^{n_z}$ and $\mathcal{W} \subseteq \mathcal{W}^+ \subseteq \mathbb{R}^{n_w}$.

(ii) Matrices $A : \mathcal{Z}^+ \times \mathcal{W}^+ \to \mathbb{R}^{n_z \times n_z}$, $\Phi : \mathcal{Z}^+ \times \mathcal{W}^+ \to \mathbb{R}^{n_z \times n_\varphi}$, $\Psi : \mathcal{Z}^+ \times \mathcal{W}^+ \to \mathbb{R}^{n_\varphi \times n_z}$ and $\Omega : \mathcal{Z}^+ \times \mathcal{W}^+ \to \mathbb{R}^{n_\varphi \times n_\varphi}$ are affine with respect to (z, w).

(iii) Matrices $B \in \mathbb{R}^{n_z \times n_v}$, $C \in \mathbb{R}^{n_\varepsilon \times n_z}$ and $\Gamma \in \mathbb{R}^{n_\varepsilon \times n_\varphi}$ are constant.

(iv) Matrix $\Omega(z, w)$ is non-singular $\forall\, (z, w) \in \mathcal{Z}^+ \times \mathcal{W}^+$.

(v) Matrix $A(z, w)$ can be described by

$$A(z, w) = \mathrm{A}_0 + \sum_{i=1}^{\mathrm{n}} \mathrm{A}_i\, \lambda_i(z, w) \,, \tag{144}$$

for constant matrices $\mathrm{A}_0, \ldots, \mathrm{A}_\mathrm{n} \in \mathbb{R}^{n_z \times n_z}$.

Whenever $f_z(z, w, v)$ and $\delta_z(z, w)$ are regular rational functions with respect to $(z, w) \in \mathcal{Z}^+ \times \mathcal{W}^+$, there exists a proper decomposition into the DAR described by Assumption 3.2, satisfying requirements (i) to (iv) (TROFINO; DEZUO, 2014). The choice for this DAR is though not unique and may influence the conservatism of the stability conditions

about to be presented. Guidelines on how to decompose rational functions into DAR have been illustrated and exemplified in Subsection 2.2.3, and further recommendations may be consulted in TROFINO; DEZUO (2014). One should also note that only functions $f_z(z,w,v)$ and $\delta_z(z,w)$ of the regulation error representation (133) are required to be rational, and not necessarily the original system functions $f(x,w,u)$, $g(x,w)$, $h(x,w)$, $s(w)$, etc.

The complementary condition (v) has been included in order to match the definition of $A(z,w)$ with the stabilizing terms $F(z,w)$, $G(z,w)$, $H(z,w)$ and $K(z,w)$ from (136). The purpose of this requirement is to subsequently allow the construction of the stabilizing parameters, which will directly involve $A(z,w)$, similarly to the procedure demonstrated on Theorem 2.3. Nevertheless, there is no loss of generality from (v) because one can always lump the nonlinearities of $f_z(z,w,v)$ entirely into the $\Phi(z,w)\,\varphi(z,w)$ portion of the DAR, i.e. $f_z(z,w,v) = A\,z + \Phi(z,w)\,\varphi(z,w) + B\,v$, defining A as a constant matrix equal to A_0. Although, it should be clear that less conservative results might be obtained if some nonlinearities are decomposed as $A(z,w)\,z$ instead of solely using the $\Phi(z,w)\,\varphi(z,w)$ component.

Sets $\mathcal{Z}^+$ and $\mathcal{W}^+$ specify the validity region of the (z,w) variables of the DAR form (142) and (143). As clearly declared in item (i), the definition of $\mathcal{Z}^+$ must at least include, in its interior, the origin of the z-state-space, which is the equilibrium point of the regulation error system. In turn, set $\mathcal{W}^+$ must at least include the positively invariant region $\mathcal{W}$ where the exosystem trajectory is assumed to be confined in (see Assumption 2.2). As presented in (46), it is convenient to define $\mathcal{Z}^+$ and $\mathcal{W}^+$ as a convex hull of vertices:

$$\mathcal{Z}^+ = \mathrm{Co}\{\mathcal{V}_z\}\;, \qquad \mathcal{W}^+ = \mathrm{Co}\{\mathcal{V}_w\}\;. \tag{145}$$

Without loss of generality, $\mathcal{Z}^+$ is also required to be expressed in the polyhedral form with some vectors $p_1, p_2, \ldots, p_{n_k} \in \mathbb{R}^{n_z}$:

$$\mathcal{Z}^+ = \left\{ z \in \mathbb{R}^{n_z} : |\, p_k^{\mathsf{T}}\, z \,| \leq 1\;,\; k = 1,2,\ldots,n_k \right\}. \tag{146}$$

Given the established DAR framework, the fundamental equations in (133) are now written as

$$\left\{ \begin{array}{rcl} \dot{z} & = & A(z,w)\,z + \Phi(z,w)\,\varphi(z,w) + B\,v \\ 0 & = & \Psi(z,w)\,z + \Omega(z,w)\,\varphi(z,w) \\ \varepsilon & = & C\,z + \Gamma\,\varphi(z,w) \end{array} \right. , \tag{147}$$

and the augmented system dynamics (139) is now expressed as

$$\left\{ \begin{array}{rcl} \dot{\mathbf{z}} & = & \boldsymbol{A}(z,w)\,\mathbf{z} + \boldsymbol{\Phi}(z,w)\,\varphi(z,w) \\ 0 & = & \boldsymbol{\Psi}(z,w)\,\mathbf{z} + \boldsymbol{\Omega}(z,w)\,\varphi(z,w) \end{array} \right. . \tag{148}$$

In here, the augmented matrices $\boldsymbol{A} : \mathcal{Z}^+ \times \mathcal{W}^+ \to \mathbb{R}^{n_a \times n_a}$, $\boldsymbol{\Phi} : \mathcal{Z}^+ \times \mathcal{W}^+ \to \mathbb{R}^{n_a \times n_\varphi}$, $\boldsymbol{\Psi} : \mathcal{Z}^+ \times \mathcal{W}^+ \to \mathbb{R}^{n_\varphi \times n_a}$ and $\boldsymbol{\Omega} : \mathcal{Z}^+ \times \mathcal{W}^+ \to \mathbb{R}^{n_\varphi \times n_\varphi}$ are:

$$\begin{array}{rclcrcl} \boldsymbol{A}(z,w) & = & \begin{bmatrix} A(z,w) + BK(z,w)C & BH(z,w) \\ G(z,w)C & F(z,w) \end{bmatrix}, & \quad & \boldsymbol{\Psi}(z,w) & = & \begin{bmatrix} \Psi(z,w) & 0 \end{bmatrix}, \\ \boldsymbol{\Phi}(z,w) & = & \begin{bmatrix} \Phi(z,w) + BK(z,w)\Gamma \\ G(z,w)\Gamma \end{bmatrix}, & & \boldsymbol{\Omega}(z,w) & = & \Omega(z,w)\,. \end{array} \tag{149}$$

Since all system matrices $A(z,w)$, … , $\Omega(z,w)$, $F(z,w)$, … , $K(z,w)$ were assumed affine with respect to (z,w), the same property is readily inherited by the augmented matrices shown in (149).

3.3.3 Analysis Conditions

On the way to establish a design procedure for stabilizing parameters $\mathrm{F}_0, \ldots, \mathrm{K}_\mathrm{n}$ in (131), the next step is to develop analysis conditions in which the trajectories of the closed-loop system satisfy the desired attraction requirement (141). The starting point to address this objective is the following result based on KHALIL (2002).

Lemma 3.2. *Consider a system* $\dot{\mathbf{z}} = \boldsymbol{f}(\mathbf{z}, w)$ *where* $\boldsymbol{f} : \boldsymbol{\mathcal{Z}}^+ \times \mathcal{W}^+ \to \mathbb{R}^{n_a}$, $\boldsymbol{f}(0, w) = 0$ $\forall\, w \in \mathcal{W} \subseteq \mathcal{W}^+$ *and let* $\{0\} \subset \mathrm{int}\{\boldsymbol{\mathcal{Z}}^+\} \subseteq \mathbb{R}^{n_a}$. *Suppose there exists a smooth function* $V : \boldsymbol{\mathcal{Z}}^+ \to \mathbb{R}$, *such that*

$$V(0) = 0\,,\; V(\mathbf{z}) > 0 \;\; \forall\, \mathbf{z} \in \boldsymbol{\mathcal{Z}}^+\,,\; \mathbf{z} \neq 0\,, \tag{150}$$

$$\dot{V}(\mathbf{z}, w) \triangleq \frac{\partial V(\mathbf{z})}{\partial \mathbf{z}} \boldsymbol{f}(\mathbf{z}, w) < 0 \;\; \forall\, (\mathbf{z}, w) \in \boldsymbol{\mathcal{Z}}^+ \times \mathcal{W}^+\,,\; \mathbf{z} \neq 0\,, \tag{151}$$

$$\boldsymbol{\mathcal{Z}} \triangleq \left\{ \mathbf{z} \in \mathbb{R}^{n_a} : V(\mathbf{z}) \leq 1 \right\} \subset \boldsymbol{\mathcal{Z}}^+\,, \tag{152}$$

then the trajectories $\mathbf{z}(t)$ *asymptotically approach the origin* $\forall (\mathbf{z}(0), w(0)) \in \mathcal{D} = \boldsymbol{\mathcal{Z}} \times \mathcal{W}$.

Proof. Suppose $w(0) \in \mathcal{W}$ and note that $w(t) \in \mathcal{W} \subseteq \mathcal{W}^+$ from Assumption 2.2. Let $\mathbf{z}(t)$ be a solution of $\dot{\mathbf{z}} = \boldsymbol{f}(\mathbf{z}, w)$ with $\mathbf{z}(0) \in \boldsymbol{\mathcal{Z}}$, as defined by (152). From (150) and (151), it follows that $1 \geq V(\mathbf{z}(t)) \geq 0$ and $\dot{V}(\mathbf{z}(0), w(0)) \leq 0\; \forall\, t \geq 0$. Since $V(\mathbf{z}(t))$ is continuous, there exists a limit $\epsilon \in [0, 1]$ such that $V(\mathbf{z}(t)) \to \epsilon$ and $\dot{V}(\mathbf{z}(t), w(t)) \to 0$ as $t \to \infty$. Moreover, it always verify that $\mathbf{z} = 0$ in this limit condition where $\dot{V}(\mathbf{z}, w) = 0$, because (151) and $\boldsymbol{f}(0, w) = 0\; \forall\, w \in \mathcal{W}$. Therefore $\mathbf{z}(t) \to 0$ as $t \to \infty$. □

Besides addressing the fundamental stability condition (141), this work suggests the consideration of additional transient performance criteria (P1) and (P2), as respectively introduced by Definitions 3.1 and 3.2 in the sequence. By the first criterion (P1), it is possible to specify a minimum decay rate for the regulation error state trajectories. On the other hand, the second requirement (P2) implicitly bounds the magnitude of the stabilizing controller gains to be later synthesized, a recommended practice so as to prevent numerical conditioning issues.

Definition 3.1. *Exponential Performance* (P1): the trajectories $\mathbf{z}(t)$ exponentially approach the origin with decay rate faster than $\alpha > 0$, i.e. $\exists\, \epsilon > 0$ such that $||\mathbf{z}(t)|| \leq \epsilon\, \mathrm{e}^{-\alpha t}$ $\forall\, t \geq 0$ for every initial condition $(\mathbf{z}(0), w(0)) \in \mathcal{D}$.

Definition 3.2. *Eigenvalue Clustering* (P2): all eigenvalues of the augmented system matrix $\boldsymbol{A}(z, w)$ are enclosed in the disk $\{\mathrm{s} \in \mathbb{C} : |\mathrm{s}| < r\}$ $\forall (z, w) \in \mathcal{Z}^+ \times \mathcal{W}^+$, where $r > 0$.

The Theorem 3.1 presents the first main result regarding the output regulation of the closed-loop system and the fulfillment of the performance criteria (P1) and (P2).

Theorem 3.1. *Suppose there exist a symmetric matrix* $P \in \mathbb{R}^{n_a \times n_a}$ *and a matrix* $L \in \mathbb{R}^{n_\varphi \times n_\varphi}$ *such that*

$$P \succ 0\,, \tag{153}$$

$$\begin{bmatrix} 1 & \boldsymbol{p}_k^{\mathrm{T}} \\ \star & P \end{bmatrix} \succ 0 \;\; \forall\, k \in \{1, 2, \ldots, n_k\}\,, \quad \boldsymbol{p}_k \triangleq \begin{bmatrix} p_k \\ 0 \end{bmatrix}\,, \tag{154}$$

$$\mathcal{H} \left\{ \begin{bmatrix} P\boldsymbol{A}(z, w) + \alpha P & P\boldsymbol{\Phi}(z, w) \\ L\boldsymbol{\Psi}(z, w) & L\boldsymbol{\Omega}(z, w) \end{bmatrix} \right\} \prec 0 \;\; \forall\, (z, w) \in \mathcal{V}_z \times \mathcal{V}_w\,, \tag{155}$$

$$\begin{bmatrix} -rP & P\boldsymbol{A}(z,w) \\ \star & -rP \end{bmatrix} \prec 0 \;\; \forall\, (z,w) \in \mathcal{V}_z \times \mathcal{V}_w \; . \tag{156}$$

Then the closed-loop system (113)*,* (114) *with controller* (118)*,* (128) *achieves output regulation and satisfies* (P1) *and* (P2) *for every initial condition in*

$$\mathcal{D} = \big\{ (\mathbf{z}, w) \in \mathbb{R}^{n_a} \times \mathcal{W} \,:\, \mathbf{z}^{\mathsf{T}} P\, \mathbf{z} \leq 1 \big\} \; . \tag{157}$$

Proof. Consider the Lyapunov candidate function

$$V(\mathbf{z}) = \mathbf{z}^{\mathsf{T}} P\, \mathbf{z} \; , \tag{158}$$

for $P = P^{\mathsf{T}} \succ 0$, noting that $V(\mathbf{z}) > 0 \; \forall\, \mathbf{z} \in \mathbb{R}^{n_a}$, $\mathbf{z} \neq 0$, as in (150). The derivative of (158) along the trajectories of the system (148) is then given by $\dot{V}(\mathbf{z}, w) = \mathcal{H}\{\mathbf{z}^{\mathsf{T}}\, \boldsymbol{\Delta}_1(z,w)\, \zeta(\mathbf{z}, w)\}$, where

$$\boldsymbol{\Delta}_1(z,w) \triangleq \begin{bmatrix} P\boldsymbol{A}(z,w) & P\boldsymbol{\Phi}(z,w) \end{bmatrix} \; , \quad \zeta(\mathbf{z}, w) \triangleq \begin{bmatrix} \mathbf{z} \\ \varphi(z,w) \end{bmatrix} \; . \tag{159}$$

Using the same vector $\zeta(\mathbf{z}, w)$, the algebraic equality constraint in (148) can be expressed by $\boldsymbol{\Delta}_2(z,w)\, \zeta(\mathbf{z}, w) = 0$, where

$$\boldsymbol{\Delta}_2(z,w) \triangleq \begin{bmatrix} \boldsymbol{\Psi}(z,w) & \boldsymbol{\Omega}(z,w) \end{bmatrix} \; . \tag{160}$$

Now suppose the following inequality holds:

$$\dot{V}(\mathbf{z}, w) + 2\alpha\, V(\mathbf{z}) + \mathcal{H}\big\{ \varphi^{\mathsf{T}}(z,w)\, L \boldsymbol{\Delta}_2(z,w)\, \zeta(\mathbf{z}, w) \big\} < 0 \;\; \forall\, (\mathbf{z}, w) \in \boldsymbol{\mathcal{Z}}^{+} \times \mathcal{W}^{+} \, , \; \mathbf{z} \neq 0 \, , \tag{161}$$

where $\boldsymbol{\mathcal{Z}}^{+} \triangleq \mathcal{Z}^{+} \times \mathbb{R}^{n_s}$ and $L \in \mathbb{R}^{n_\varphi \times n_\varphi}$ is a free matrix. Since $\alpha \geq 0$, $V(\mathbf{z}) > 0$ and $\boldsymbol{\Delta}_2(z,w)\, \zeta(\mathbf{z}, w) = 0 \; \forall\, (\mathbf{z}, w) \in \boldsymbol{\mathcal{Z}}^{+} \times \mathcal{W}^{+}$, $\mathbf{z} \neq 0$, then the satisfaction of (161) implies that $\dot{V}(\mathbf{z}, w) < 0 \; \forall\, (\mathbf{z}, w) \in \boldsymbol{\mathcal{Z}}^{+} \times \mathcal{W}^{+}$, $\mathbf{z} \neq 0$, as in (151). By expressing (161) in the factorized quadratic form $\zeta^{\mathsf{T}}(\mathbf{z}, w)\, \boldsymbol{\Delta}_4(z,w)\, \zeta(\mathbf{z}, w) < 0$, one obtains

$$\boldsymbol{\Delta}_4(z,w) \triangleq \mathcal{H} \left\{ \begin{bmatrix} P\boldsymbol{A}(z,w) & P\boldsymbol{\Phi}(z,w) \\ L\boldsymbol{\Psi}(z,w) & L\boldsymbol{\Omega}(z,w) \end{bmatrix} \right\} \prec 0 \;\; \forall\, (z,w) \in \mathcal{Z}^{+} \times \mathcal{W}^{+} \; . \tag{162}$$

From Lemma A.3 then, one gets that (162) $\Leftrightarrow$ (155) since sets $\mathcal{Z}^{+}$ and $\mathcal{W}^{+}$ have been defined as (145) and $\boldsymbol{A}(z,w)$, . . . , $\boldsymbol{\Omega}(z,w)$ are affine matrix functions. Conditions (153) and (155) consequently ensure that the candidate Lyapunov function (158) is positive-definite and its derivative is negative-definite $\forall\, (\mathbf{z}, w) \in \boldsymbol{\mathcal{Z}}^{+} \times \mathcal{W}^{+}$. So, it must be shown that $(\mathbf{z}(t), w(t)) \in \boldsymbol{\mathcal{Z}}^{+} \times \mathcal{W}^{+} \; \forall\, t > 0$ in order to conclude the proof.

According to Lemma 3.2, the candidate domain of attraction estimate and positively invariant region of system (148) is defined as $\mathcal{D} = \boldsymbol{\mathcal{Z}} \times \mathcal{W}$, where here

$$\boldsymbol{\mathcal{Z}} = \big\{ \mathbf{z} \in \mathbb{R}^{n_a} : \mathbf{z}^{\mathsf{T}} P\, \mathbf{z} \leq 1 \big\} \tag{163}$$

is an ellipsoidal set. Since by assumption $w(0) \in \mathcal{W} \Rightarrow w(t) \in \mathcal{W} \subseteq \mathcal{W}^{+} \; \forall\, t \geq 0$, in order to additionally ensure that $(\mathbf{z}(0), w(0)) \in \boldsymbol{\mathcal{Z}} \times \mathcal{W} \Rightarrow (\mathbf{z}(t), w(t)) \in \boldsymbol{\mathcal{Z}}^{+} \times \mathcal{W}^{+}$ $\forall\, t > 0$, it is necessary to impose the condition $\boldsymbol{\mathcal{Z}} \subset \boldsymbol{\mathcal{Z}}^{+}$. By referring to Lemma A.6 and using the polyhedral definition of $\mathcal{Z}^{+}$ from (146), then it follows that (154) implies $\boldsymbol{\mathcal{Z}} \subset \boldsymbol{\mathcal{Z}}^{+}$.

All conditions from Lemma 3.2 are satisfied if (153), (154) and (155) hold. Consequently, the trajectories $\mathbf{z}(t)$ of the system (139) asymptotically converges to the origin

for every initial condition $(\mathbf{z}(0), w(0)) \in \mathcal{D}$, satisfying (141) which is equivalent to (123). According to Lemma 3.1, it also follows that the closed-loop system (113), (114) with controller (118), (128) achieves output regulation in region $\mathcal{D}$.

Since $\mathcal{D} \subset \boldsymbol{\mathcal{Z}}^+ \times \mathcal{W}^+$, from inequality (161) it also follows that

$$\dot{V}(\mathbf{z}, w) < -2\alpha\, V(\mathbf{z}) \;\; \forall\, (\mathbf{z}, w) \in \mathcal{D}\,,\; \mathbf{z} \neq 0\,, \tag{164}$$

which in turn implies that:

$$V(\mathbf{z}(t)) \leq V(\mathbf{z}(0))\, \mathrm{e}^{-2\alpha t} \leq \mathrm{e}^{-2\alpha t}\; \forall\, (\mathbf{z}(0), w(0)) \in \mathcal{D}\,. \tag{165}$$

Let $\lambda_{min}(P) \in \mathbb{R}$ denote the smallest eigenvalue of P, then $\lambda_{min}(P)\, ||\mathbf{z}||^2 \leq \mathbf{z}^{\mathrm{T}} P\, \mathbf{z} = V(\mathbf{z})$. Thus, (165) leads to

$$||\mathbf{z}(t)|| \leq \lambda_{min}(P)^{-\frac{1}{2}}\, \mathrm{e}^{-\alpha t}\; \forall\, (\mathbf{z}(0), w(0)) \in \mathcal{D}\,, \tag{166}$$

and so, the exponential performance criterion (P1) is satisfied for the given conditions.

In regard of (P2), all eigenvalues of matrix $\boldsymbol{A}(z, w)$ are contained inside the disk $\{\mathrm{s} \in \mathbb{C} : |\mathrm{s}| < r\}\; \forall\, (z, w) \in \mathcal{Z}^+ \times \mathcal{W}^+$ if there exists a matrix $P \succ 0$ such that (156) (BOYD et al., 1994). □

Based on Theorem 3.1, a domain of attraction estimate $\mathcal{D}$ can be found by solving the following SDP:

$$\min_{P,L} \;\; \mathrm{tr}(P) \;\; \text{s.t.} \;\; \big\{(153)\,,\, (154)\,,\, (155)\,,\, (156)\big\}\,. \tag{167}$$

In here, the optimization decision variables are being regarded as P and L only, not including the stabilizing controller gains. The SDP problem (167) can be employed as a stability and performance analysis tool, provided the parameters $\mathrm{F}_0, \ldots, \mathrm{K}_\mathrm{n}$ are given *a priori*.

3.3.4 Design Conditions

In what follows, the methodology is extended for design purposes, where the stabilizing parameters $\mathrm{F}_0, \ldots, \mathrm{K}_\mathrm{n}$ are also regarded as decision variables and initially unknown. By employing a procedure similar to SCHERER; GAHINET; CHILALI (1997), as presented in Subsection 2.2.1, congruence transformations and variables changes are applied to the conditions from Theorem 3.1 in order to linearize the inequalities with respect to the controller parameters. These algebraic manipulations led to the new Theorem 3.2 presented in the sequence. Henceforth, in order to ensure the proper reconstruction of the design parameters, the stabilizing controller order is enforced as equal to the regulation error system order (i.e. $n_s = n_z$).

Theorem 3.2. *Suppose there exist symmetric matrices $X, Y \in \mathbb{R}^{n_z \times n_z}$ and matrices $L \in \mathbb{R}^{n_\varphi \times n_\varphi}$, $\hat{\mathrm{F}}_0, \ldots, \hat{\mathrm{F}}_\mathrm{n} \in \mathbb{R}^{n_z \times n_z}$, $\hat{\mathrm{G}}_0, \ldots, \hat{\mathrm{G}}_\mathrm{n} \in \mathbb{R}^{n_z \times n_\varepsilon}$, $\hat{\mathrm{H}}_0, \ldots, \hat{\mathrm{H}}_\mathrm{n} \in \mathbb{R}^{n_v \times n_z}$ and $\hat{\mathrm{K}}_0, \ldots, \hat{\mathrm{K}}_\mathrm{n} \in \mathbb{R}^{n_v \times n_\varepsilon}$ such that*

$$\begin{bmatrix} X & I \\ \star & Y \end{bmatrix} \succ 0\,, \tag{168}$$

$$\begin{bmatrix} 1 & p_k^{\mathrm{T}} X & p_k^{\mathrm{T}} \\ \star & X & I \\ \star & \star & Y \end{bmatrix} \succ 0 \;\; \forall\, k \in \{1, 2, \ldots, n_k\}\,, \tag{169}$$

$$\mathcal{H}\left\{\begin{bmatrix} A(z,w)X + \\ B\hat{H}(z,w) + \\ \alpha X \end{bmatrix} \begin{bmatrix} A(z,w) + \\ B\hat{K}(z,w)C + \\ \alpha I \end{bmatrix} \begin{bmatrix} \Phi(z,w) + \\ B\hat{K}(z,w)\Gamma \end{bmatrix} \right\} \prec 0 \;\; \forall\, (z,w) \in \mathcal{V}_z \times \mathcal{V}_w \;, \tag{170}$$

$$\begin{bmatrix} -rX & -rI & \begin{matrix} A(z,w)X + \\ B\hat{H}(z,w) \end{matrix} & \begin{matrix} A(z,w) + \\ B\hat{K}(z,w)C \end{matrix} \\ \star & -rY & \hat{F}(z,w) & \begin{matrix} YA(z,w) + \\ \hat{G}(z,w)C \end{matrix} \\ \star & \star & -rX & -rI \\ \star & \star & \star & -rY \end{bmatrix} \prec 0 \;\; \forall\, (z,w) \in \mathcal{V}_z \times \mathcal{V}_w \;, \tag{171}$$

where $\hat{F}(z,w)$*,* $\hat{G}(z,w)$*,* $\hat{H}(z,w)$ *and* $\hat{K}(z,w)$ *denote*

$$\begin{bmatrix} \hat{F}(z,w) & \hat{G}(z,w) \\ \hat{H}(z,w) & \hat{K}(z,w) \end{bmatrix} \triangleq \begin{bmatrix} \hat{\mathrm{F}}_0 & \hat{\mathrm{G}}_0 \\ \hat{\mathrm{H}}_0 & \hat{\mathrm{K}}_0 \end{bmatrix} + \sum_{i=1}^{\mathrm{n}} \begin{bmatrix} \hat{\mathrm{F}}_i & \hat{\mathrm{G}}_i \\ \hat{\mathrm{H}}_i & \hat{\mathrm{K}}_i \end{bmatrix} \lambda_i(z,w) \;. \tag{172}$$

Then the closed-loop system (113)*,* (114) *with controller* (118)*,* (128) *achieves output regulation and satisfies* (P1) *and* (P2) *for every initial condition in* (157) *with* P *given by*

$$P = \begin{bmatrix} I & Y \\ 0 & N^{\intercal} \end{bmatrix} \begin{bmatrix} X & I \\ M^{\intercal} & 0 \end{bmatrix}^{-1} \tag{173}$$

and stabilizing controller parameters F_i*,* G_i*,* H_i *and* K_i $\forall\, i \in \{0, 1, \ldots, \mathrm{n}\}$ *obtained by*

$$\begin{cases} \mathrm{F}_i &= N^{-1}(\hat{\mathrm{F}}_i + YB\hat{\mathrm{K}}_iCX - \hat{\mathrm{G}}_iCX - YB\hat{\mathrm{H}}_i - Y\mathrm{A}_iX)M^{-\intercal} \\ \mathrm{G}_i &= N^{-1}(\hat{\mathrm{G}}_i - YB\hat{\mathrm{K}}_i) \\ \mathrm{H}_i &= (\hat{\mathrm{H}}_i - \hat{\mathrm{K}}_iCX)\, M^{-\intercal} \\ \mathrm{K}_i &= \hat{\mathrm{K}}_i \end{cases} , \tag{174}$$

where the pair $M, N \in \mathbb{R}^{n_z \times n_z}$ *is a non-singular solution to*

$$MN^{\intercal} = I - XY \;. \tag{175}$$

Proof. Suppose conditions from Theorem 3.1 hold for $n_s = n_z$ and for P defined by

$$P = \begin{bmatrix} Y & N \\ N^{\intercal} & \cdot \end{bmatrix}, \;\; P^{-1} = \begin{bmatrix} X & M \\ M^{\intercal} & \cdot \end{bmatrix}, \tag{176}$$

where $X, Y \in \mathbb{R}^{n_z \times n_z}$ are symmetric matrices and $M, N \in \mathbb{R}^{n_z \times n_z}$ are generic square matrices. Since $P^{-1}P = I$, then condition (175) must be satisfied. Consider also the congruence transformation blocks $Z_1 \in \mathbb{R}^{n_a \times n_a}$ and $Z_2 \in \mathbb{R}^{n_a \times n_a}$ as

$$Z_1 \triangleq \begin{bmatrix} X & I \\ M^{\intercal} & 0 \end{bmatrix}, \;\; Z_2 \triangleq \begin{bmatrix} I & Y \\ 0 & N^{\intercal} \end{bmatrix}, \tag{177}$$

where $PZ_1 = Z_2$. Post- and pre-multiplying (153), (154), (155) and (156) respectively with Z_1, $\mathrm{diag}\{1, Z_1\}$, $\mathrm{diag}\{Z_1, I\}$ and $\mathrm{diag}\{Z_1, Z_1\}$ (and their transposes) leads to (168),

(169), (170) and (171) under the following change of variables:

$$\begin{cases} \hat{F}(z,w) \;=\; Y(A(z,w)+BK(z,w)C)X + NG(z,w)CX + YBH(z,w)M^{\intercal} + NF(z,w)M^{\intercal} \\ \hat{G}(z,w) \;=\; YBK(z,w) + NG(z,w) \\ \hat{H}(z,w) \;=\; K(z,w)CX + H(z,w)M^{\intercal} \\ \hat{K}(z,w) \;=\; K(z,w) \end{cases} . \tag{178}$$

Isolating the controller parameters in (178), one obtains

$$\begin{cases} F(z,w) \;=\; N^{-1}(\hat{F}(z,w) + YB\hat{K}(z,w)CX - \hat{G}(z,w)CX - YB\hat{H}(z,w) - YA(z,w)X)M^{-\intercal} \\ G(z,w) \;=\; N^{-1}(\hat{G}(z,w) - YB\hat{K}(z,w)) \\ H(z,w) \;=\; (\hat{H}(z,w) - \hat{K}(z,w)CX)\, M^{-\intercal} \\ K(z,w) \;=\; \hat{K}(z,w) \end{cases} , \tag{179}$$

which leads to (174) by considering the definitions of $F(z,w)$, ... , $K(z,w)$ from (136), of $\hat{F}(z,w)$, ... , $\hat{K}(z,w)$ from (172) and of $A(z,w)$ from (144). Also, matrix P can be reconstructed as (173) since $P = Z_2\, Z_1^{-1}$. As a conclusion, conditions from Theorem 3.1 are equivalent to Theorem 3.2 when considering $n_s = n_z$. □

Considering the initial conditions of the stabilizing controller as $\xi_s(0) = 0$, then it follows that $\mathbf{z}^{\intercal}(0)P\,\mathbf{z}(0) = z^{\intercal}(0)Yz(0)$, since matrix P can be decomposed as (176). Therefore, the original goal of minimizing the measure $\mathrm{tr}(P)$ – in order to enlarge the set of admissible initial states – may be substituted by $\mathrm{tr}(Y)$. The optimal stabilizing controller parameters with respect to this objective function, can then be synthesized by solving the following optimization problem:

$$\min_{X,Y,L,\hat{\mathrm{F}}_0,\ldots,\hat{\mathrm{K}}_{\mathrm{n}}} \; \mathrm{tr}(Y) \;\; \text{s.t.} \;\; \big\{(168)\,,\,(169)\,,\,(170)\,,\,(171)\big\}\,. \tag{180}$$

Observe that (180) is not readily a convex semidefinite optimization problem due to the bilinear terms involving the pair of variables L and X in (170). However, if either L or X is regarded as a constant, then (170) becomes a linear matrix inequality (LMI) and (180) becomes a standard SDP. This idea can be employed in order to iterativelly find a locally optimal solution. A systematic procedure capable of handling this type of optimization problem is presented in Appendix A.2.

It is possible to add extra degree of freedom and also convexify the optimization problem (180) required to synthesize the controllers. To do so however, functions $f_z(z,w,v)$ and $\delta_z(z,w)$ of the regulation error representation must satisfy the subsequent requirements in addition to the original Assumption 3.2.

Assumption 3.3. Assumption 3.2 holds with the following:

(vi) There exists a function $\varphi(y) : \mathbb{R}^{n_y} \to \mathbb{R}^{n_\varphi}$ such that

$$\varphi(z,w) = \varphi(g_z(z,w) + d(w))\,. \tag{181}$$

(vii) Matrix $\Phi(z,w)$ can be described by

$$\Phi(z,w) = \Phi_0 + \sum_{i=1}^{\mathrm{n}} \Phi_i\, \lambda_i(z,w)\,, \tag{182}$$

for constant matrices $\Phi_0, \ldots, \Phi_{\mathrm{n}} \in \mathbb{R}^{n_z \times n_\varphi}$.

What is being stated by Assumption 3.3 is that all nonlinearities contained in $f_z(z,w,v)$ and $\delta_z(z,w)$ can be constructed by a proper arrangement of the measurement vector y. Specifically, item (vi) says that the rational nonlinear function $\varphi(z,w)$ can be exactly remapped as a function of y, i.e. $\varphi(y)$. With this condition, it is then possible to include this function into the stabilizing controller dynamics, as the sequel will illustrate. The complementary item (vii) is included for similar purposes as (v) which regards the choice of matrix $A(z,w)$. In here, the matrix $\Phi(z,w)$ is also being assumed as affinely dependent of the controller scheduling function $\lambda(z,w)$.

In case Assumption 3.3 is true, one should implement the following modified stabilizing controller stage:

$$\left\{ \begin{array}{rcl} \dot{\xi}_s & = & \mathrm{F}(y)\,\xi_s + \mathrm{G}(y)\,\varepsilon + \Lambda(y)\,\varphi(y) \\ v & = & \mathrm{H}(y)\,\xi_s + \mathrm{K}(y)\,\varepsilon + \Theta(y)\,\varphi(y) \end{array} \right. , \tag{183}$$

where the new terms $\Lambda : \mathbb{R}^{n_y} \to \mathbb{R}^{n_s \times n_\varphi}$ and $\Theta : \mathbb{R}^{n_y} \to \mathbb{R}^{n_v \times n_\varphi}$ are free design matrix functions. It is convenient to parameterize $\Lambda(y)$ and $\Theta(y)$ as in (131), i.e.

$$\begin{bmatrix} \Lambda(y) \\ \Theta(y) \end{bmatrix} \triangleq \begin{bmatrix} \Lambda_0 \\ \Theta_0 \end{bmatrix} + \sum_{i=1}^{\mathrm{n}} \begin{bmatrix} \Lambda_i \\ \Theta_i \end{bmatrix} \lambda_i(y) \,, \tag{184}$$

where $\Lambda_0, \ldots, \Lambda_{\mathrm{n}} \in \mathbb{R}^{n_s \times n_\varphi}$ and $\Theta_0, \ldots, \Theta_{\mathrm{n}} \in \mathbb{R}^{n_v \times n_\varphi}$ are free design matrices. The newly proposed stabilizing stage (183) can be also verified to satisfy the regulation requirement (122) from Lemma 3.1, since $\varphi(d(w)) = \varphi(0,w) = 0 \,\forall\, w \in \mathcal{W}$.

A similar approach has been considered in GOMES DA SILVA JR et al. (2013) so as to cast an output feedback stabilization problem by convex optimization, where sector bounded nonlinearities were considered to be implementable with the output measurements. As will be demonstrated later, the stabilizer (183) not only contains extra degree of freedom, but also allows the full linearization of stability and performance conditions, ultimately leading to convex optimization problems in order to synthesize the free design parameters.

Towards new stability results with the controller (183), it is necessary to complement the matrix $\boldsymbol{\Phi}(z,w)$ of the augmented system representation (148), which modifies according to

$$\boldsymbol{\Phi}(z,w) = \begin{bmatrix} \Phi(z,w) + BK(z,w)\Gamma + B\Theta(z,w) \\ \Lambda(z,w) + G(z,w)\Gamma \end{bmatrix}, \tag{185}$$

where $\Lambda(z,w)$ and $\Theta(z,w)$ denote the evaluation of (184) for $y = g_z(z,w) + d(w)$, as in (136). The other terms $\boldsymbol{A}(z,w)$, $\boldsymbol{\Psi}(z,w)$ and $\boldsymbol{\Omega}(z,w)$ remain equal to previous definitions in (149).

The same stability result of Theorem 3.1 is then applicable with respect to the new stabilizer (183), provided the new definition of $\boldsymbol{\Phi}(z,w)$ from (185) is considered. Carrying on from these observations, Theorem 3.2 can be restated as the following corollary.

Corollary 3.1. *Suppose there exist symmetric matrices* $X, Y \in \mathbb{R}^{n_z \times n_z}$ *and matrices* $\hat{L} \in \mathbb{R}^{n_\varphi \times n_\varphi}$, $\hat{\mathrm{F}}_0, \ldots, \hat{\mathrm{F}}_{\mathrm{n}} \in \mathbb{R}^{n_z \times n_z}$, $\hat{\mathrm{G}}_0, \ldots, \hat{\mathrm{G}}_{\mathrm{n}} \in \mathbb{R}^{n_z \times n_\varepsilon}$, $\hat{\mathrm{H}}_0, \ldots, \hat{\mathrm{H}}_{\mathrm{n}} \in \mathbb{R}^{n_v \times n_z}$, $\hat{\mathrm{K}}_0, \ldots, \hat{\mathrm{K}}_{\mathrm{n}} \in \mathbb{R}^{n_v \times n_\varepsilon}$, $\hat{\Lambda}_0, \ldots, \hat{\Lambda}_{\mathrm{n}} \in \mathbb{R}^{n_z \times n_\varphi}$ *and* $\hat{\Theta}_0, \ldots, \hat{\Theta}_{\mathrm{n}} \in \mathbb{R}^{n_v \times n_\varphi}$ *such that* (168)*,*

(169), (171),

$$\mathcal{H}\left\{\begin{bmatrix} A(z,w)X+ & A(z,w)+ & \Phi(z,w)\hat{L}+ \\ B\hat{H}(z,w)+ & B\hat{K}(z,w)C+ & B\hat{\Theta}(z,w) \\ \alpha X & \alpha I & \\ \hat{F}(z,w)+ & YA(z,w)+ & \\ \alpha I & \hat{G}(z,w)C+ & \hat{\Lambda}(z,w) \\ & \alpha Y & \\ \Psi(z,w)X & \Psi(z,w) & \Omega(z,w)\hat{L} \end{bmatrix}\right\} \prec 0 \;\; \forall\,(z,w) \in \mathcal{V}_z \times \mathcal{V}_w \,, \tag{186}$$

where $\hat{F}(z,w)$ *,* $\ldots$ *,* $\hat{K}(z,w)$ *are defined as in* (172) *and* $\hat{\Lambda}(z,w)$*,* $\hat{\Theta}(z,w)$ *are*

$$\begin{bmatrix} \hat{\Lambda}(z,w) \\ \hat{\Theta}(z,w) \end{bmatrix} \triangleq \begin{bmatrix} \hat{\Lambda}_0 \\ \hat{\Theta}_0 \end{bmatrix} + \sum_{i=1}^{\mathrm{n}} \begin{bmatrix} \hat{\Lambda}_i \\ \hat{\Theta}_i \end{bmatrix} \lambda_i(z,w) \,. \tag{187}$$

Then the closed-loop system (113)*,* (114) *with controller* (118)*,* (183) *achieves output regulation and satisfies* (P1) *and* (P2) *for every initial condition in* (157) *with* P *given by* (173) *and stabilizing controller parameters* F_i *,* $\ldots$ *,* K_i *,* Λ_i *,* Θ_i $\forall\, i \in \{0,1,\ldots,\mathrm{n}\}$ *obtained by* (174) *and*

$$\begin{cases} \Lambda_i &= N^{-1}\big((\hat{\Lambda}_i - YB\hat{\Theta}_i)\hat{L}^{-1} + (YB\hat{\mathrm{K}}_i - \hat{\mathrm{G}}_i)\Gamma - Y\Phi_i\big) \\ \Theta_i &= \hat{\Theta}_i\hat{L}^{-1} - \hat{\mathrm{K}}_i\Gamma \end{cases} , \tag{188}$$

where the pair $M, N \in \mathbb{R}^{n_z \times n_z}$ *is a non-singular solution to* (175)*.*

Proof. Consider the same proof presented for Theorem 3.2, except post- and pre-multiply (155) by $\mathrm{diag}\{Z_1, L^{-\intercal}\}$ and its transpose, which yield (186) when considering the change of variables (178), $\hat{L} = L^{-\intercal}$ and

$$\begin{cases} \hat{\Lambda}(z,w) \;=\; \big(Y\Phi(z,w) + YB\Theta(z,w) + YBK(z,w)\Gamma + N\Lambda(z,w) + NG(z,w)\Gamma\big)L^{-\intercal} \\ \hat{\Theta}(z,w) \;=\; \big(\Theta(z,w) + K(z,w)\Gamma\big)L^{-\intercal} \end{cases} . \tag{189}$$

From straightforward inversion of these variable transformations, one obtains

$$\begin{cases} \Lambda(z,w) \;=\; N^{-1}\big(\hat{\Lambda}(z,w)\hat{L}^{-1} - YB\hat{\Theta}(z,w)\hat{L}^{-1} + YB\hat{K}(z,w)\Gamma - \hat{G}(z,w)\Gamma - Y\Phi(z,w)\big) \\ \Theta(z,w) \;=\; \hat{\Theta}(z,w)\hat{L}^{-1} - \hat{K}(z,w)\Gamma \end{cases} , \tag{190}$$

which leads to (188) by considering the previous definitions (182), (184) and (187). □

According to Corollary 3.1, the parameters from stabilizing controller (183) can be synthesized by the following optimization problem in order to attain the largest domain of attraction estimate:

$$\min_{X,Y,\hat{L},\hat{\mathrm{F}}_0,\ldots,\hat{\Theta}_\mathrm{n}} \;\; \mathrm{tr}(Y) \;\; \text{s.t.} \;\; \big\{(168)\,,\,(169)\,,\,(171)\,,\,(186)\big\} \,. \tag{191}$$

In this special case the synthesis problem is always convex, since (186) is now an LMI with respect to decision variables $X, Y, \hat{L}, \hat{\mathrm{F}}_0, \ldots, \hat{\Theta}_\mathrm{n}$.

3.4 Numerical Examples

This section illustrates the previously presented methodologies with two numerical control design examples. The first one will deal with a polynomial nonlinear plant subject to a harmonic exosystem. The second example will address a strictly rational nonlinear system subject to an exosystem with chaotic behavior.

3.4.1 Polynomial Nonlinear Plant with a Harmonic Exosystem

Consider a nonlinear system described by

$$\left\{\begin{array}{rcl}\dot{x}_1 &=& x_2\\ \dot{x}_2 &=& a_1\,x_1^2 x_2 + a_2\,u\end{array}\right. , \qquad y = e = x_1 - w_1\,, \tag{192}$$

where $x \in \mathbb{R}^2$ is the system state vector, $u \in \mathbb{R}$ is the control input, $y \in \mathbb{R}$ is the output measurement, $e \in \mathbb{R}$ is the output error and a_1, a_2 are constant parameters. This plant is supposedly influenced by a harmonic exosystem of the form

$$\left\{\begin{array}{rcl}\dot{w}_1 &=& \omega\,w_2\\ \dot{w}_2 &=& -\omega\,w_1\end{array}\right. , \tag{193}$$

where $w \in \mathbb{R}^2$ is the exosystem state vector and $\omega \in \mathbb{R}$ is a constant parameter denoting the exosystem harmonic frequency. One should note that (193) is able to generate a whole family of sinusoidal signals described by

$$\left\{\begin{array}{rcl}w_1(t) &=& \varrho\sin(\omega t + \rho)\\ w_2(t) &=& \varrho\cos(\omega t + \rho)\end{array}\right. , \tag{194}$$

where ϱ and ρ respectively represent the amplitude and phase of $w(t)$, which are *a priori* unknown and related to the initial state $w(0)$ of the exosystem:

$$\varrho \triangleq \sqrt{w_1^2(0) + w_2^2(0)}\,, \qquad \rho \triangleq \arctan\left(\frac{w_2(0)}{w_1(0)}\right)\,. \tag{195}$$

The objective in this example is to design an output feedback controller such that the error signal $e(t) = x_1(t) - w_1(t)$ asymptotically approaches zero, i.e. $\lim_{t\to\infty} e(t) = 0$.

3.4.1.1 Internal model stage design

According to the control design guidelines previously discussed, the first step towards solving an output regulation problem is to determine a proper internal model. To do so, one must initially know the target mappings $\pi(w)$ and $c(w)$ which describe the invariant and zero-error regulation manifold. Evaluating the expression (77) with $s(w) = [\omega w_1\ -\omega w_2]^{\mathrm{T}}$, $\mathrm{a}_0(w) = -w_1$, $\mathrm{b}_0 = 1$, $\mathrm{a}_1 = 0$, $\mathrm{b}_1 = 1$, $\mathrm{a}_2(x) = a_1\,x_1^2 x_2$ and $\mathrm{b}_2 = a_2$, the following solutions $\pi(w)$ and $c(w)$ are obtained:

$$\pi(w) = \begin{bmatrix} w_1 \\ \omega w_2 \end{bmatrix}\,, \quad c(w) = -a_2^{-1}\big(a_1\omega\,w_1^2 w_2 + \omega^2\,w_1\big)\,. \tag{196}$$

It also follows that the output measurement mapping is $d(w) = 0$, since $y = e$ in this example.

Among the three internal model design options explained on Subsection 2.3.1, it is suggested here to employ the full immersion method of Lemma 2.3 in order to attain a robust internal model implementation independent from the plant parameters a_1 and a_2. Towards employing this methodology, it is necessary to check the multiple time-derivatives of $c(w)$:

$$\left\{\begin{array}{rcl} c(w) &=& -a_2^{-1}(a_1\omega\,w_1^2 w_2 + \omega^2\,w_1)\\ \dot{c}(w) &=& -a_2^{-1}(2a_1\omega^2\,w_1 w_2^2 - a_1\omega^2\,w_1^3 + \omega^3\,w_2)\\ \ddot{c}(w) &=& -a_2^{-1}(7a_1\omega^3\,w_1^2 w_2 - 2a_1\omega^3\,w_2^3 + \omega^4\,w_1)\\ \overset{(3)}{c}(w) &=& -a_2^{-1}(7a_1\omega^4\,w_1^3 - 20a_1\omega^4\,w_1 w_2^2 - \omega^5\,w_2)\\ \overset{(4)}{c}(w) &=& -a_2^{-1}(61a_1\omega^5\,w_1^2 w_2 - 20a_1\omega^5\,w_2^3 + \omega^5\,w_1)\end{array}\right. . \tag{197}$$

One should notice that $\overset{(4)}{c}(w) = -9\omega^4\, c(w) - 10\omega^2\, \ddot{c}(w)$, and thus the internal model stage (118) can be set with the functions

$$\phi_m(\xi_m) = \begin{bmatrix} \xi_{m2} \\ \xi_{m3} \\ \xi_{m4} \\ -9\omega^4\, \xi_{m1} - 10\omega^2\, \xi_{m3} \end{bmatrix}, \quad \theta_m(\xi_m) = \xi_{m1}\,. \tag{198}$$

According to Lemma 2.3, this internal model satisfies the regulation condition (120) with the following mapping $\sigma_m(w)$:

$$\sigma_m(w) = -a_2^{-1} \begin{bmatrix} a_1\omega\, w_1^2 w_2 + \omega^2\, w_1 \\ 2a_1\omega^2\, w_1 w_2^2 - a_1\omega^2\, w_1^3 + \omega^3\, w_2 \\ 7a_1\omega^3\, w_1^2 w_2 - 2a_1\omega^3\, w_2^3 + \omega^4\, w_1 \\ 7a_1\omega^4\, w_1^3 - 20a_1\omega^4\, w_1 w_2^2 - \omega^5\, w_2 \end{bmatrix}. \tag{199}$$

3.4.1.2 Stabilizing stage design

This next phase is dedicated to designing the stabilizing stage, where the proposed DAR based methodology will be illustrated. Prior to performing this stabilizing stage design, there are some preliminary setups to be mentioned. For instance, the output measurement vanishing function $\varepsilon = \delta(y)$ can be set as $\varepsilon = y$, since the output error e is identical to y in this example. For simplicity, the stabilizing controller gain scheduling will be set as inactive, i.e. $\lambda(y) = 0$, since this design concept will be further explored in the next example.

The initial step in this design context is to represent the system equations in the regulation error form (133) using coordinate change (132), which here denotes:

$$\left\{ \begin{array}{rcl} z_1 &=& x_1 - w_1 \\ z_2 &=& x_2 - \omega\, w_2 \end{array} \right. , \quad \left\{ \begin{array}{rcl} z_3 &=& \xi_{m1} + a_2^{-1}(a_1\omega\, w_1^2 w_2 + \omega^2\, w_1) \\ z_4 &=& \xi_{m2} + a_2^{-1}(2a_1\omega^2\, w_1 w_2^2 - a_1\omega^2\, w_1^3 + \omega^3\, w_2) \\ z_5 &=& \xi_{m3} + a_2^{-1}(7a_1\omega^3\, w_1^2 w_2 - 2a_1\omega^3\, w_2^3 + \omega^4\, w_1) \\ z_6 &=& \xi_{m4} + a_2^{-1}(7a_1\omega^4\, w_1^3 - 20a_1\omega^4\, w_1 w_2^2 - \omega^5\, w_2) \end{array} \right. . \tag{200}$$

By developing (134), all the regulation error system functions $f_z(z,w,v)$, $\theta_z(z,w)$, $g_z(z,w)$, $h_z(z,w)$ and $\delta_z(z,w)$ are

$$f_z(z,w,v) = \begin{bmatrix} z_2 \\ a_1\,(z_1^2 z_2 + \omega\, z_1^2 w_2 + 2\omega\, z_1 w_1 w_2 + z_2 w_1^2 + 2\, z_1 z_2 w_1) + a_2\,(z_3 + v_1) \\ z_4 + v_2 \\ z_5 + v_3 \\ z_6 + v_4 \\ -9\omega^4\, z_3 - 10\omega^2\, z_5 + v_5 \end{bmatrix}, \tag{201}$$

$\theta_z(z) = z_3$ and $g_z(z) = h_z(z) = \delta_z(z) = z_1$. Recall that $v_u = v_1 \in \mathbb{R}$ denotes the plant stabilizing input, while $v_m = [v_2\ v_3\ v_4\ v_5]^{\intercal} \in \mathbb{R}^4$ denotes the internal model stabilizing inputs.

The second step is to choose an appropriate differential-algebraic representation for the functions $f_z(z,w,v)$ and $\delta_z(z)$. For this purpose, it is convenient to use the following vector $\varphi(z,w)$ of rational nonlinearities:

$$\varphi(z,w) = \begin{bmatrix} \omega\, w_2 z_1 + 2\, w_1 z_2 + z_1 z_2 \\ 2\omega\, w_2 z_1 + w_1 z_2 \end{bmatrix}. \tag{202}$$

Given this definition, matrices in (142) and (143) can be specified as:

$$A = \begin{bmatrix} 0 & 1 & 0 & 0 & 0 & 0 \\ 0 & 0 & a_2 & 0 & 0 & 0 \\ 0 & 0 & 0 & 1 & 0 & 0 \\ 0 & 0 & 0 & 0 & 1 & 0 \\ 0 & 0 & 0 & 0 & 0 & 1 \\ 0 & 0 & -9\omega^4 & 0 & -10\omega^2 & 0 \end{bmatrix}, \; \Phi(z,w) = a_1 \begin{bmatrix} 0 & 0 \\ z_1 & w_1 \\ 0 & 0 \\ 0 & 0 \\ 0 & 0 \\ 0 & 0 \end{bmatrix}, \; B = \begin{bmatrix} 0 & 0 & 0 & 0 & 0 \\ a_2 & 0 & 0 & 0 & 0 \\ 0 & 1 & 0 & 0 & 0 \\ 0 & 0 & 1 & 0 & 0 \\ 0 & 0 & 0 & 1 & 0 \\ 0 & 0 & 0 & 0 & 1 \end{bmatrix},$$
$$C = \begin{bmatrix} 1 & 0 & 0 & 0 & 0 & 0 \end{bmatrix}, \qquad \Gamma = \begin{bmatrix} 0 & 0 \end{bmatrix},$$
$$\Psi(z,w) = -\begin{bmatrix} \omega\, w_2 & 2\, w_1 + z_1 & 0 & 0 & 0 & 0 \\ 2\omega\, w_2 & w_1 & 0 & 0 & 0 & 0 \end{bmatrix}, \qquad \Omega = \begin{bmatrix} 1 & 0 \\ 0 & 1 \end{bmatrix}, \tag{203}$$

The third step is to define the bounding sets $\mathcal{W} \subseteq \mathcal{W}^+ \subseteq \mathbb{R}^2$ and $\{0\} \subset \mathcal{Z}^+ \subseteq \mathbb{R}^6$ in order to numerically approach the synthesis problem. Regarding the harmonic exosystem (193), it verifies that $w(0) \in \mathcal{W} \Rightarrow w(t) \in \mathcal{W} \; \forall \, t > 0$ for any disk-shaped set of the form

$$\mathcal{W} = \left\{ w \in \mathbb{R}^2 : ||w|| \leq \overline{w} \right\}, \tag{204}$$

where the radius $\overline{w} > 0$ represents the maximum admissible amplitude of sinusoidal trajectories $w_1(t)$ and $w_2(t)$. The convex set $\mathcal{W}^+$ can then be simply defined as a bounding square region where the disk $\mathcal{W}$ is tightly inscribed, e.g. $\mathcal{W}^+ = \mathrm{Co}\{\mathcal{V}_{w_1}\} \times \mathrm{Co}\{\mathcal{V}_{w_2}\}$ for the vertex sets:

$$\mathcal{V}_{w_1} = \mathcal{V}_{w_2} = \{ -\overline{w} \, , \, \overline{w} \} \, . \tag{205}$$

On the other hand, since the z-dependence of $\Phi(z,w)$ and $\Psi(z,w)$ is just involving z_1, the set $\mathcal{Z}^+$ must at least restrict the first dimension of the z-state-space. Therefore one can define $\mathcal{Z}^+ = \mathrm{Co}\{\mathcal{V}_{z_1}\} \times \mathbb{R}^5$ for some vertex set

$$\mathcal{V}_{z_1} = \{ -\overline{e} \, , \, \overline{e} \} \, , \tag{206}$$

where $\overline{e}$ denotes the maximum admissible value of $|z_1(t)| = |e(t)| \; \forall \, t \geq 0$. The equivalent notation of $\mathcal{Z}^+$ is the form of (146) is obtained with $n_k = 1$ and

$$p_1 = \begin{bmatrix} \overline{e}^{-1} & 0 & 0 & 0 & 0 & 0 \end{bmatrix}^{\mathsf{T}}. \tag{207}$$

The system parameters are being regarded as $a_1 = -1$, $a_2 = 1$ and $\omega = 1$. The design constraints for lower bound decay rate and upper bound system matrix eigenvalue are being set respectively as $\alpha = 0.1$ and $r = 10$. Finally, it is being defined $\overline{w} = 1$ and $\overline{e} = 6$ with respect to the bounding sets previously discussed. Given all these numerical values, the optimization problem (180) was considered in order to synthesize the stabilizing controller gains. The iterative procedure in Appendix A.2 was employed here in order to search for a proximate locally optimal solution to this problem. The resulting series of SDP sub-problems were in turn solved by the LMILAB package from software MATLAB. It was necessary to perform 6 iterations in the feasibility phase until achieving an strictly feasible solution. Afterwards, it took 11 iterations in the optimization phase in order to achieve an objective value decrement smaller than 10^{-4} over the last 4 iterations. The ultimately obtained solution has the objective value $\mathrm{tr}(Y) = 0.0645$ and

the following controller parameters[3]:

$$\mathrm{F} = \begin{bmatrix} -1.5035 & -3.6058 & -0.5000 & 165.03 & 11.996 & -0.0014 \\ 0.2477 & -1.6675 & 0.6770 & -3.8422 & -0.2873 & 0.0000 \\ 0.1408 & -0.1716 & -0.4196 & 33.780 & 2.3672 & -0.0001 \\ -0.0465 & 0.0487 & -1.1966 & -9.7660 & -0.1204 & -0.0045 \\ -0.0674 & 0.0335 & 4.5693 & 14.754 & -6.9136 & 0.0635 \\ -0.0002 & 0.0001 & 0.0112 & 0.0182 & -0.0056 & -8.9542 \end{bmatrix}, \quad \mathrm{G} = \begin{bmatrix} -15.127 \\ 1.3386 \\ 24.567 \\ -168.42 \\ 2326.5 \\ 3.4371 \end{bmatrix},$$

$$\mathrm{H} = \begin{bmatrix} -9.2935 & 0.8191 & 0.3851 & 2.1166 & 0.1356 & -0.0009 \\ -12.757 & 3.9066 & 11.408 & 1640.2 & 118.08 & -0.0133 \\ 0.2236 & 59.611 & -14.855 & 306.77 & 22.377 & -0.0020 \\ 7.2186 & -0.2397 & -164.77 & 1381.8 & 102.03 & -0.0047 \\ -0.4364 & 6.6515 & -7.4898 & -843.36 & -60.821 & 0.0080 \end{bmatrix}, \quad \mathrm{K} = \begin{bmatrix} -99.124 \\ 94.718 \\ 149.37 \\ 144.69 \\ -1241.0 \end{bmatrix}. \tag{208}$$

3.4.1.3 Numerical results and discussion

Figures 5, 6 and 7 present the numerical simulation of the closed-loop system response with the designed controller. In these figures, the initial conditions considered for the plant and exosystem are respectively $x(0) = 0$ and $w(0) = [0 \;\; 1]^\intercal$, whereas the initial conditions of the controller are kept as zero, i.e. $\xi_m(0) = 0$, for the internal model states, and $\xi_s(0) = 0$, for the stabilizing states. Using the regulation error coordinates from (200) and matrix Y resultant from the controller synthesis, it was verified that $z^\intercal(0)\, Y z(0) \leq 1$. Since $\xi_s(0) = 0$ and $w(0) \in \mathcal{W}$, it follows that $(\mathbf{z}(0), w(0)) \in \mathcal{D}$ and the output regulation is theoretically ensured for this default setup.

Figure 5 shows on top the system output error signal $e(t)$, demonstrating that $e(t)$ asymptotically approaches zero as $t \to \infty$. On the bottom plot of the same figure one can see the system control input $u(t)$ compared to the excitation signal $c(w(t))$ required to achieve output regulation. The phase portrait of Figure 6 depicts the system transient behavior with respect to the (x_1, x_2, u) tridimensional view compared to the ideal zero-error path $(\pi_1(w), \pi_2(w), c(w))$. In this picture, one can see the system state, initially at rest on the origin, performing an spiral-shaped path in order to synchronize with the zero-error steady-state trajectory shown in thick line. Figure 7 on the other hand shows all system and controller states signals $x(t)$ and $\xi(t)$, respectively compared to their regulation references $\pi(w(t))$ and $\sigma(w(t))$. It is interesting to notice the non-vanishing characteristic of the internal model states ξ_m in contrast to the transient behavior of the stabilizing states ξ_s. One may also notice the first plant state $x_1(t)$ tracking the pure sinusoidal signal $w_1(t)$ produced by the exosystem, which is the expected end result because $e(t) = x_1(t) - w_1(t)$ was defined as the target output error.

Complementary, Figure 8 depicts the domain of attraction estimate attained with the control design, showing all possible plant initial states $x(0)$ for which output regulation is ensured. The black contour in this figure illustrates the border of region $\mathcal{D}$ considering the default exosystem initial state $w(0) = [0 \;\; 1]^\intercal$ and also the default controller initial condition $\xi(0) = 0$. The gray contours in turn represent borders of $\mathcal{D}$ for various exosystem initial states $w(0)$ inside the admissible disk $\mathcal{W}$. It is consequently possible to visualize a subset of plant initial states where output regulation is ensured regardless of the exosystem initial condition inside $\mathcal{W}$, which is denoted by the area inside the gray contours.

[3] Truncated numerical values are being presented.

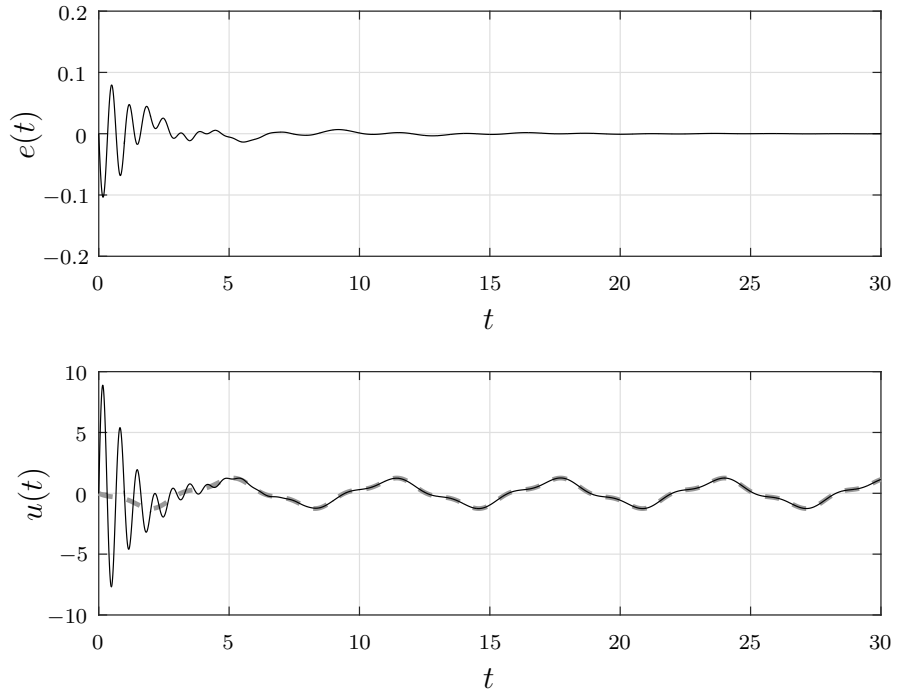

Figure 5: On top: the output regulation error signal $e(t)$. On bottom: the control input signal (solid line) $u(t)$ compared to the zero-error steady-state signal $c(w(t))$ (dashed line). Source: the author.

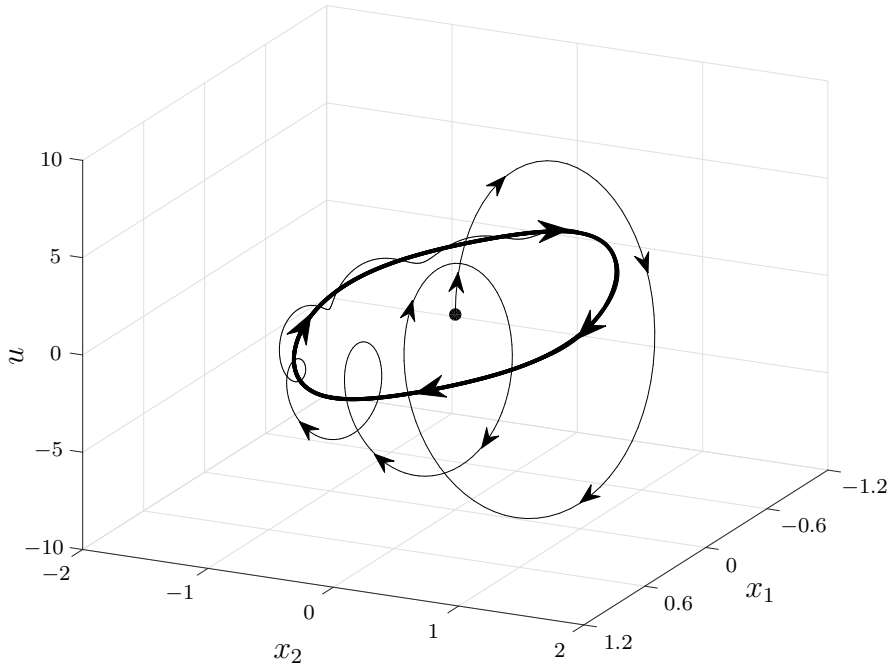

Figure 6: Phase portrait depicting the system trajectory (x_1, x_2, u) (thin line) compared to the zero-error steady-state trajectory $(\pi_1(w), \pi_2(w), c(w))$ (thick line). Source: the author.

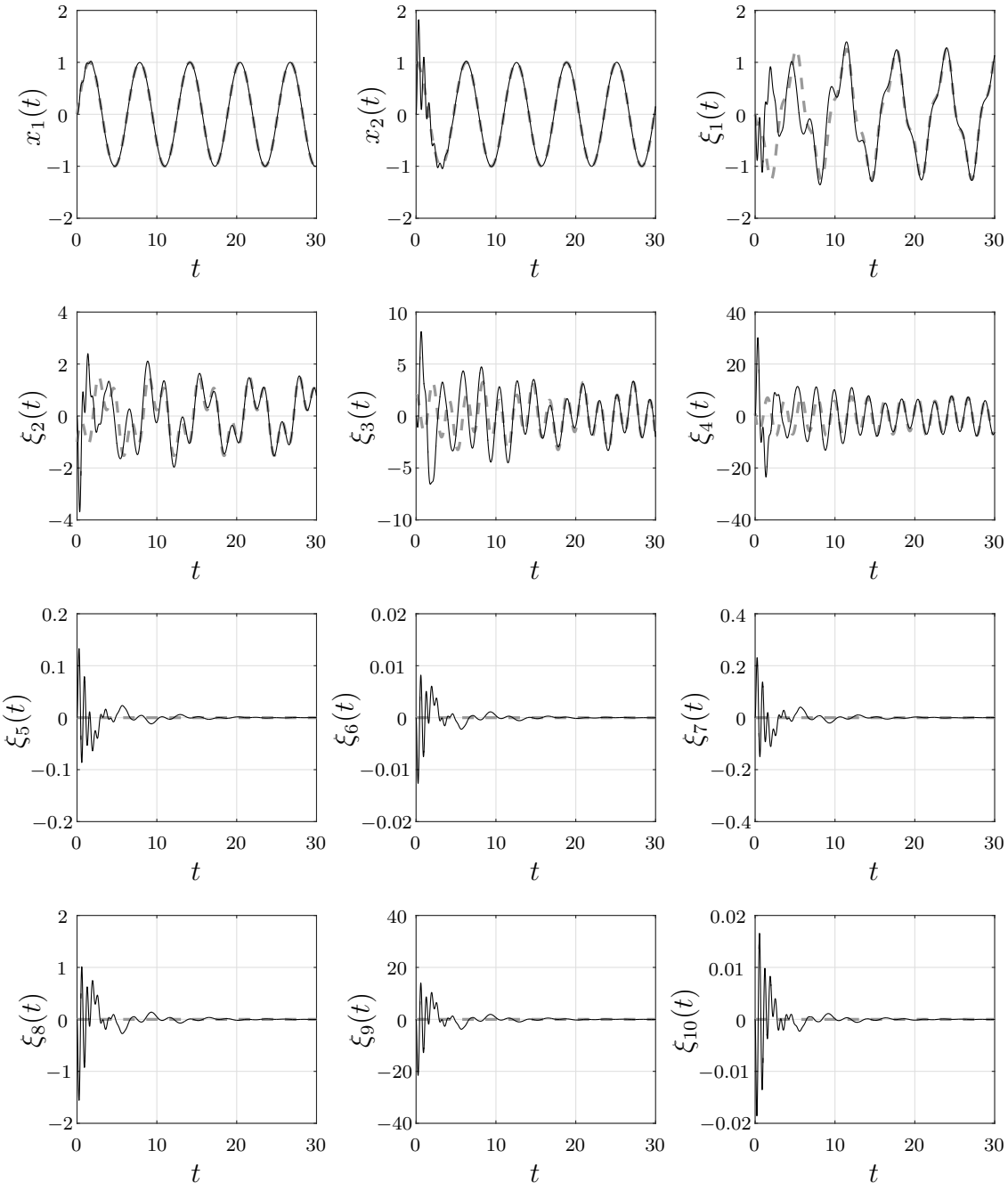

Figure 7: Plant and controller states $x(t)$ and $\xi(t)$ (solid lines) compared to the zero-error steady-states $\pi(w(t))$ and $\sigma(w(t))$ (dashed lines). Source: the author.

Lastly, numerical simulations of the closed-loop system were performed with two initial conditions marginally close to the border of $\mathcal{D}$, as represented by the black dots on Figure 8. Such initial conditions were chosen as $x(0) = [-3 \ -27.11]^\intercal$ and $x(0) = [3 \ \ 29.11]^\intercal$, where $w(0) = [0 \ \ 1]^\intercal$ and $\xi(0) = 0$ in both cases. The resultant output error signals $e(t)$ for each configuration is represented by different shades on Figure 9, where asymptotic convergence can be verified.

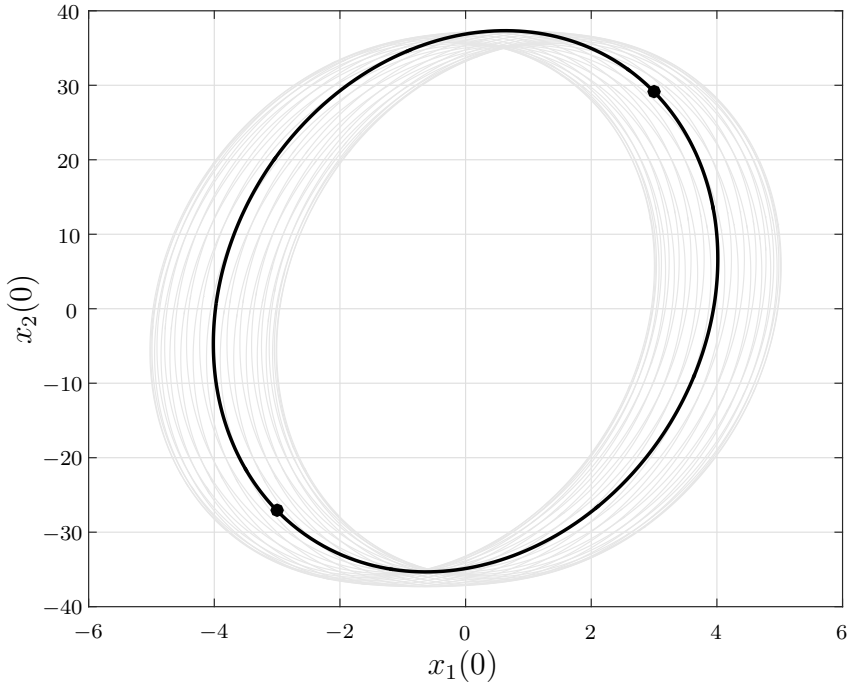

Figure 8: Representation of the set $\mathcal{D}$ in the x-state-space. The black contour is the region border for the default exosystem initial state. The gray contours denote borders for a myriad of exosystem initial states $w(0) \in \mathcal{W}$. Source: the author.

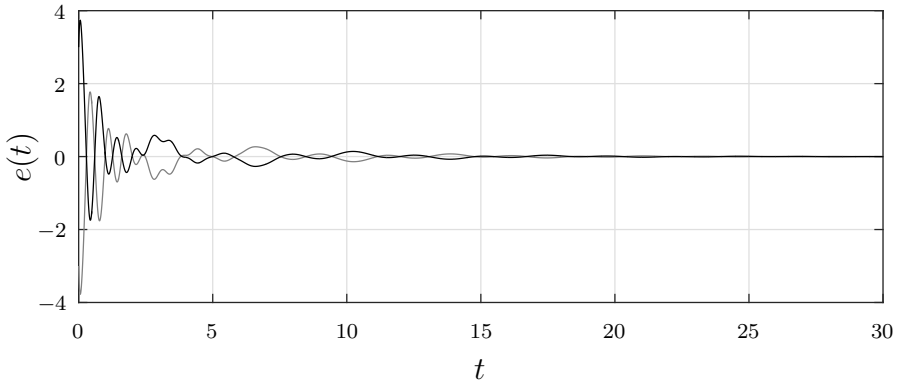

Figure 9: Output error signals $e(t)$ for initial conditions on the border of the domain of attraction estimate $\mathcal{D}$. Shades denote trajectories for different plant initial states. Source: the author.

3.4.2 Rational Nonlinear Plant with a Chaotic Exosystem

Consider a rational nonlinear plant described by

$$\begin{cases} \dot{x}_1 &= a_1 \dfrac{x_1^2}{1+x_1^2} + a_2\, w_2 + x_2 \\ \dot{x}_2 &= a_1 \dfrac{x_1}{1+x_1^2} + a_2\, w_1(1+w_3) + a_3\, u \end{cases} , \quad y = \begin{bmatrix} x_1 \\ w_1 \end{bmatrix} , \quad e = x_1 , \tag{209}$$

where $x \in \mathbb{R}^2$ is the system state vector, $w \in \mathbb{R}^3$ is the exosystem state vector, $u \in \mathbb{R}$ is the control input, $y \in \mathbb{R}^2$ is the output measurement vector, $e \in \mathbb{R}$ is the output error and $a_1, a_2, a_3 \in \mathbb{R}$ are constant parameters. Suppose the dynamics of the exosystem is given by

$$\begin{cases} \dot{w}_1 &= b_1\,(w_2 - w_1) \\ \dot{w}_2 &= b_2\, w_1 - w_2 - w_1 w_3 \\ \dot{w}_3 &= w_1 w_2 - b_3\, w_3 \end{cases} , \tag{210}$$

where $b_1, b_2, b_3 \in \mathbb{R}$ are also constant parameters. This is the so-called Lorenz system, which exhibits chaotic behavior for $b_1 = 10$, $b_2 = 28$ and $b_3 = 8/3$ (LI et al., 2005). The objective here is also to design an output feedback controller which ensures the system output regulation, i.e. $\lim_{t\to\infty} e(t) = 0$.

3.4.2.1 Internal model stage design

Expression (77) can be employed in order to initially determine the target manifold mappings $\pi(w)$ and $c(w)$. By noticing that

$$\mathrm{a}_1(x_1, w) = a_1 \frac{x_1^2}{1+x_1^2} + a_2\, w_2 , \quad \mathrm{a}_2(x_1, w) = a_1 \frac{x_1}{1+x_1^2} + a_2\, w_1(1+w_3) , \tag{211}$$

$\mathrm{a}_1 = 0$, $\mathrm{b}_0 = 1$, $\mathrm{b}_1 = 1$ and $\mathrm{b}_2 = a_3$, equation (77) yields:

$$\pi(w) = \begin{bmatrix} 0 \\ -a_2\, w_2 \end{bmatrix} , \quad c(w) = a_2 a_3^{-1}\big(w_2 - \hat{b}_2\, w_1\big) , \tag{212}$$

where $\hat{b}_2 \triangleq b_2 + 1$. Since $\pi_1(w) = 0$, it also follows that the output measurement mapping is

$$d(w) = \begin{bmatrix} 0 \\ w_1 \end{bmatrix} . \tag{213}$$

Towards designing an internal model, one may choose one of the design options previously explained on Subsection 2.3.1. Because the exosystem is nonlinear however, the full immersion method from Lemma 2.4 is not recommended due to the reasons pointed on Remark 2.3. Between the remaining methods presented by Subsection 2.3.1, the one from Lemma 2.4 is more suited for this case, since robustness with respect to plant parameters can be achieved with a simple design, as illustrated in the sequel.

Using the relation $d_2(w) = w_1$, notice that previously obtained mappings $\pi(w)$ and $c(w)$ can be written in the form of (88) with terms $\mathrm{S}(y)$, $\mathrm{U}(y)$ and ϵ as

$$\mathrm{S}(y) = \begin{bmatrix} -b_1 & b_1 & 0 \\ b_2 & -1 & -y_2 \\ 0 & y_2 & -b_3 \end{bmatrix} , \quad \mathrm{U} = \begin{bmatrix} -\hat{b}_2 & 1 & 0 \end{bmatrix} , \quad \epsilon = a_2 a_3^{-1} . \tag{214}$$

Thus, according to Lemma 2.4, the internal model functions

$$\phi_m(\xi_m, y) = \begin{bmatrix} b_1\,(\xi_{m2} - \xi_{m1}) \\ b_2\,\xi_{m1} - \xi_{m2} - y_2\,\xi_{m3} \\ y_2\,\xi_{m2} - b_3\,\xi_{m3} \end{bmatrix}, \quad \theta_m(\xi_m) = \xi_{m2} - \hat{b}_2\,\xi_{m1}\;, \tag{215}$$

are feasible with the following mapping

$$\sigma_m(w) = a_2 a_3^{-1}\,w\;. \tag{216}$$

3.4.2.2 Stabilizing stage design

In this next design phase the proposed DAR based methodology will be illustrated in order to design a proper stabilizing stage. There are again some preliminary setups to be commented. Specifically, the output vanishing function $\varepsilon = \delta(y)$ may be chosen as $\varepsilon = y_1$ because the first measurement readily vanishes at the target steady-state condition, i.e. $d_1(w) = 0$. Furthermore, a reasonable candidate for the controller gain scheduling function is $\lambda(y) = y_2$, because this second output signal is already being used for the internal model stage implementation previously derived.

The first step required to design the stabilizing stage is to express the system using coordinate change (132), which in this case is:

$$\left\{ \begin{array}{rcl} z_1 &=& x_1 \\ z_2 &=& x_2 + a_2\,w_2 \end{array} \right. , \quad \left\{ \begin{array}{rcl} z_3 &=& \xi_{m1} - a_2 a_3^{-1}\,w_1 \\ z_4 &=& \xi_{m2} - a_2 a_3^{-1}\,w_2 \\ z_5 &=& \xi_{m3} - a_2 a_3^{-1}\,w_3 \end{array} \right. . \tag{217}$$

By developing (134), all the regulation error system functions $f_z(z,w,v)$, $\theta_z(z,w)$, $g_z(z,w)$, $h_z(z,w)$ and $\delta_z(z,w)$ verify to be:

$$f_z(z,w,v) = \begin{bmatrix} a_1\,\dfrac{z_1^2}{1+z_1^2} + z_2 \\ a_1\,\dfrac{z_1}{1+z_1^2} + a_3\,(z_4 - \hat{b}_2\,z_3 + v_1) \\ b_1\,(z_4 - z_3) + v_2 \\ b_2\,z_3 - z_4 - w_1 z_5 + v_3 \\ w_1 z_4 - b_3\,z_5 + v_4 \end{bmatrix}, \quad \begin{array}{l} \theta_z(z) = z_4 - \hat{b}_2\,z_3\;, \\ h_z(z) = \delta_z(z) = z_1\;, \\ g_z(z) = \begin{bmatrix} z_1 \\ 0 \end{bmatrix}. \end{array} \tag{218}$$

The candidate controller scheduling function $\lambda(y) = y_2$ may also be represented in the regulation error form (137) by substituting y with $g_z(z,w) + d(w)$, which in this case yields:

$$\lambda(w) = w_1\;. \tag{219}$$

The next step is to decompose the functions $f_z(z,w,v)$ and $\delta_z(z,w)$ into an appropriate differential-algebraic representation. For instance, one can choose the vector of rational nonlinearities:

$$\varphi(z) = \begin{bmatrix} \dfrac{z_1^2}{1+z_1^2} & \dfrac{z_1}{1+z_1^2} \end{bmatrix}^{\intercal}. \tag{220}$$

Given this definition, the matrices in (142) and (143) can be specified as:

$$A(w) = \begin{bmatrix} 0 & 1 & 0 & 0 & 0 \\ 0 & 0 & -a_3\hat{b}_2 & a_3 & 0 \\ 0 & 0 & -b_1 & b_1 & 0 \\ 0 & 0 & b_2 & -1 & -w_1 \\ 0 & 0 & 0 & w_1 & -b_3 \end{bmatrix}, \quad \Phi = \begin{bmatrix} a_1 & 0 \\ 0 & a_1 \\ 0 & 0 \\ 0 & 0 \\ 0 & 0 \end{bmatrix}, \quad B = \begin{bmatrix} 0 & 0 & 0 & 0 \\ a_3 & 0 & 0 & 0 \\ 0 & 1 & 0 & 0 \\ 0 & 0 & 1 & 0 \\ 0 & 0 & 0 & 1 \end{bmatrix},$$
$$C = \begin{bmatrix} 1 & 0 & 0 & 0 & 0 \end{bmatrix}, \quad \Gamma = \begin{bmatrix} 0 & 0 \end{bmatrix},$$
$$\Psi = -\begin{bmatrix} 0 & 0 & 0 & 0 & 0 \\ 1 & 0 & 0 & 0 & 0 \end{bmatrix}, \quad \Omega(z) = \begin{bmatrix} 1 & -z_1 \\ z_1 & 1 \end{bmatrix}. \tag{221}$$

It is worth noticing that $\Omega(z)$ is non-singular $\forall\, z \in \mathbb{R}^5$ because $\det\{\Omega(z)\} = 1 + z_1^2 \geq 1$, therefore item (iv) of Assumption 3.2 holds for the chosen DAR. Besides, one should observe that item (v) is also true because the specified matrix $A(w)$ can be expressed as $A(w) = \mathrm{A}_0 + \mathrm{A}_1\,\lambda(w)$, where $\lambda(w) = w_1$, according to (219), and matrices A_0 and A_1 are

$$\mathrm{A}_0 = \begin{bmatrix} 0 & 1 & 0 & 0 & 0 \\ 0 & 0 & -a_3\hat{b}_2 & a_3 & 0 \\ 0 & 0 & -b_1 & b_1 & 0 \\ 0 & 0 & b_2 & -1 & 0 \\ 0 & 0 & 0 & 0 & -b_3 \end{bmatrix}, \quad \mathrm{A}_1 = \begin{bmatrix} 0 & 0 & 0 & 0 & 0 \\ 0 & 0 & 0 & 0 & 0 \\ 0 & 0 & 0 & 0 & 0 \\ 0 & 0 & 0 & 0 & -1 \\ 0 & 0 & 0 & 1 & 0 \end{bmatrix}. \tag{222}$$

An important fact of the chosen DAR is that $\varphi(z)$ defined on (220) can be remapped with respect to the output measurement, i.e.

$$\varphi(y) = \begin{bmatrix} \dfrac{y_1^2}{1+y_1^2} & \dfrac{y_1}{1+y_1^2} \end{bmatrix}^{\intercal}. \tag{223}$$

Thus, it verifies the complementary Assumption 3.3 from the special case methodology proposed in Subsection 3.3.3. Due to this observation, it is possible to implement the modified stabilizing stage (183) and the controller synthesis can be addressed by a single convex optimization problem, as indicated in (191).

The last step is to define the bounding sets $\mathcal{W} \subseteq \mathcal{W}^+ \subseteq \mathbb{R}^3$ and $\{0\} \subset \mathcal{Z}^+ \subseteq \mathbb{R}^5$. In (LI et al., 2005), it has been proven that the trajectory $w(t)$ of the Lorenz exosystem (210) is contained in the spherical positively invariant set

$$\mathcal{W} = \left\{ w \in \mathbb{R}^3 : ||w - w_c|| \leq \overline{w} \right\}, \tag{224}$$

where the center point w_c and the sphere radius $\overline{w}$ are calculated as

$$w_c = \begin{bmatrix} 0 & 0 & b_1 + b_2 \end{bmatrix}^{\intercal}, \quad \overline{w} = \frac{(b_1 + b_2)b_3}{2\sqrt{b_3 - 1}}. \tag{225}$$

Considering the default parameters for which the Lorenz exosystem is chaotic (i.e. $b_1 = 10$, $b_2 = 28$ and $b_3 = 8/3$), it follows that $w_c = [0 \;\; 0 \;\; 38]^{\intercal}$ and $\overline{w} = 39.2462$. In turn, the set $\mathcal{W}^+$ can be defined as a bounding box region where the sphere $\mathcal{W}$ is tightly inscribed. Since the DAR matrices only depend on w_1, set $\mathcal{W}^+$ does not need restrictions with respect to w_2 and w_3 dimensions, for instance, one can define $\mathcal{W}^+ = \mathrm{Co}\{\mathcal{V}_{w_1}\} \times \mathbb{R}^2$, where

$$\mathcal{V}_{w_1} = \{-\overline{w}\,,\, \overline{w}\,\}. \tag{226}$$

Similar to the previous numerical example, the set $\mathcal{Z}^+$ must at least ensure the closure of the z_1 dimension of the z-state-space. In this case, one can define $\mathcal{Z}^+ = \mathrm{Co}\{\mathcal{V}_{z_1}\} \times \mathbb{R}^4$, where

$$\mathcal{V}_{z_1} = \{-\overline{e}\,,\, \overline{e}\,\}\,, \tag{227}$$

for some constant $\overline{e} > 0$ which denotes the maximum admissible output error amplitude. The equivalent form of $\mathcal{Z}^+$ as (146) is obtained with $n_k = 1$ and

$$p_1 = \begin{bmatrix}\overline{e}^{-1} & 0 & 0 & 0 & 0\end{bmatrix}^{\intercal}. \tag{228}$$

The numeric values considered for plant parameters and design specifications are $a_1 = 0.5$, $a_2 = 1$, $a_3 = 10^3$, $\overline{e} = 10^2$, $\alpha = 1$ and $r = 1.5 \cdot 10^2$. Provided all these values, the SDP problem (191) was evaluated in order to synthesize the stabilizing controller gains. The optimal objective value $\mathrm{tr}(Y) = 1.23 \cdot 10^{-3}$ was found with the following stabilizing controller gains[4]

$$\mathrm{F}_0 = \begin{bmatrix} -2.9938 & 0.0000 & 0.0000 & -0.0000 & 0.0006 \\ 0.0000 & -43.257 & -3.8295 & 20.479 & 0.0909 \\ -0.0000 & 21.515 & -4.8540 & -14.838 & -0.0788 \\ -0.0000 & -0.0258 & -0.3190 & -179.15 & -0.3429 \\ -0.0000 & -0.0001 & 0.0009 & 0.3926 & -106.31 \end{bmatrix} \mathrm{G}_0 = \begin{bmatrix} -0.0000 \\ 5.7527 \\ -6.1715 \\ -152.54 \\ 0.3394 \end{bmatrix} \Lambda_0 = \begin{bmatrix} -0.0000 & -0.0000 \\ 0.3028 & 0.0058 \\ -0.1938 & -0.0035 \\ -1.1755 & -0.0118 \\ 0.0017 & 0.0000 \end{bmatrix},$$

$$\mathrm{H}_0 = \begin{bmatrix} -0.0000 & 61.541 & -20.511 & -14.815 & -0.0503 \\ 0.0000 & -9.6099 & 106.97 & -4.8997 & 0.0699 \\ 0.0000 & 12.181 & 106.79 & 8.2670 & 0.2987 \\ -12.457 & -0.0000 & 0.0000 & -0.0000 & 0.0237 \end{bmatrix} \mathrm{K}_0 = \begin{bmatrix} -34.118 \\ 10.111 \\ 58.056 \\ -0.0000 \end{bmatrix} \Theta_0 = \begin{bmatrix} -0.1365 & -0.0035 \\ 0.0529 & 0.0081 \\ 0.1421 & 0.0046 \\ -0.0000 & -0.0000 \end{bmatrix},$$

$$\mathrm{F}_1 = \begin{bmatrix} -0.0000 & -0.5192 & -0.8773 & 0.0125 & 0.0007 \\ 1.0768 & 0.0000 & -0.0000 & -0.0000 & -0.0000 \\ 0.7826 & 0.0000 & 0.0000 & 0.0000 & 0.0000 \\ -0.0012 & 0.0000 & -0.0000 & -0.0000 & -0.0000 \\ -0.0000 & 0.0000 & -0.0000 & 0.0000 & -0.0000 \end{bmatrix} \mathrm{G}_1 = \begin{bmatrix} -0.0000 \\ 0.0000 \\ -0.0000 \\ 0.0000 \\ 0.0000 \end{bmatrix} \Lambda_1 = \begin{bmatrix} -0.0000 & -0.0000 \\ -0.0000 & -0.0000 \\ 0.0000 & 0.0000 \\ -0.0000 & -0.0000 \\ 0.0000 & 0.0000 \end{bmatrix},$$

$$\mathrm{H}_1 = \begin{bmatrix} 0.0000 & 0.0000 & -0.0000 & -0.0000 & -0.0000 \\ 1.1252 & 0.0000 & -0.0000 & -0.0000 & -0.0000 \\ 20.474 & 0.0000 & 0.0000 & 0.0000 & 0.0000 \\ 0.0000 & -12.143 & -21.408 & 1.4789 & 0.0283 \end{bmatrix} \mathrm{K}_1 = \begin{bmatrix} 0.0000 \\ 0.0000 \\ -0.0000 \\ 0.6948 \end{bmatrix} \Theta_1 = \begin{bmatrix} -0.0000 & -0.0000 \\ -0.0000 & -0.0000 \\ 0.0000 & 0.0000 \\ 0.0010 & 0.0000 \end{bmatrix}. \tag{229}$$

3.4.2.3 Numerical results and discussion

Results from a numerical simulation of the closed-loop system are presented in Figures 10, 11 and 12. For this analysis, the initial conditions of plant and controller states were kept at the origin, i.e. $x(0) = 0$ and $\xi(0) = 0$. On the other hand, the initial state of the Lorenz exosystem was set with a randomly picked point inside the spherical set $\mathcal{W}$:

$$w(0) = \begin{bmatrix}3.5910 & 6.7150 & 9.4426\end{bmatrix}^{\intercal}. \tag{230}$$

Using the regulation error coordinates from (217) and matrix Y resultant from the controller synthesis, it was verified that $(\mathbf{z}(0), w(0)) \in \mathcal{D}$ and thus that output regulation is theoretically ensured for this default setup. The output error signal $e(t)$ and the control input $u(t)$ obtained with this simulation are both shown on Figure 10. It is interesting to observe the control signal tracking the chaotic waveform $c(w(t))$ required to achieve output regulation. The phase portrait of Figure 11 afterwards compares the internal model trajectory (thin line) with the target zero-error steady-state trajectory (thick line). Because

[4] Since the presentation of numerical values is truncated, elements with order of magnitude lower than 10^{-4} are being hidden, which appear as 0.0000.

$\sigma_m(w(t)) = a_2 a_3^{-1}\, w(t)$, the internal model trajectory is supposed to asymptotically approach the peculiar chaotic trajectory of the Lorenz system scaled the factor $a_2 a_3^{-1}$, what is being illustrated in Figure 11. Complementary, Figure 12 shows the transient temporal response of all system and controller states signals $x(t)$ and $\xi(t)$, respectively compared to their regulation references $\pi(w(t))$ and $\sigma(w(t))$.

So as to illustrate all possible initial states with theoretical convergence guarantee, the attained domain of attraction estimate $\mathcal{D}$ is presented by Figure 13. The black contour is denoting the border of set $\mathcal{D}$ with respect to the x-state-space, when considering $\xi(0) = 0$ and the default exosystem initial state from (230). Furthermore, the gray patches represent several contours of $\mathcal{D}$ with $w(0)$ distributed inside the exosystem invariant sphere $\mathcal{W}$. If $\xi(0) = 0$ and the system initial state $x(0)$ is inside the gray markings, one is sure that output regulation will be achieved for wherever $w(0) \in \mathcal{W}$.

Figure 14 shows complementary numerical simulations with two initial conditions marginally close to the border of $\mathcal{D}$, where $x(0)$ corresponds to the plotted points in Figure 13 and it was considered $\xi(0) = 0$ and (230) in both cases.

3.5 Final Remarks

This chapter presented a methodology for designing dynamic output feedback controllers for output regulation of rational nonlinear systems. The novelty of the material here exposed is mainly the introduction of the differential-algebraic representation into the nonlinear output regulation context. This approach led to the developed of systematic stability analysis and synthesis procedures for stabilizing controllers implemented together with internal model stages. In comparison to the recent literature, the devised nonlinear regulation scheme has the main advantage of not requiring normal form error dynamics and minimum-phase assumptions (XU; WANG; CHEN, 2016; XU; CHEN; WANG, 2017). The research material here presented has originated the following papers:

- CASTRO, R. S.; FLORES, J. V.; SALTON, A. T. *Stability Analysis of Output Regulated of Rational Nonlinear Systems*. In proceedings of the 20th IFAC World Congress, Toulouse, France, 2017.

- CASTRO, R. S.; FLORES, J. V., SALTON, A. T.; CHEN, Z.; COUTINHO, D. F. *A stabilization framework for the output regulation of rational nonlinear systems*. Accepted for publication on the IEEE Transactions on Automation and Control on January of 2019.

This work also paves the way for incorporation of various LMI based results previously focused just for stabilization problems. Particularly, the consideration of saturating actuators and anti-windup design (GOMES DA SILVA JR et al., 2014) can be aggregated, which is the main topic of the subsequent chapter.

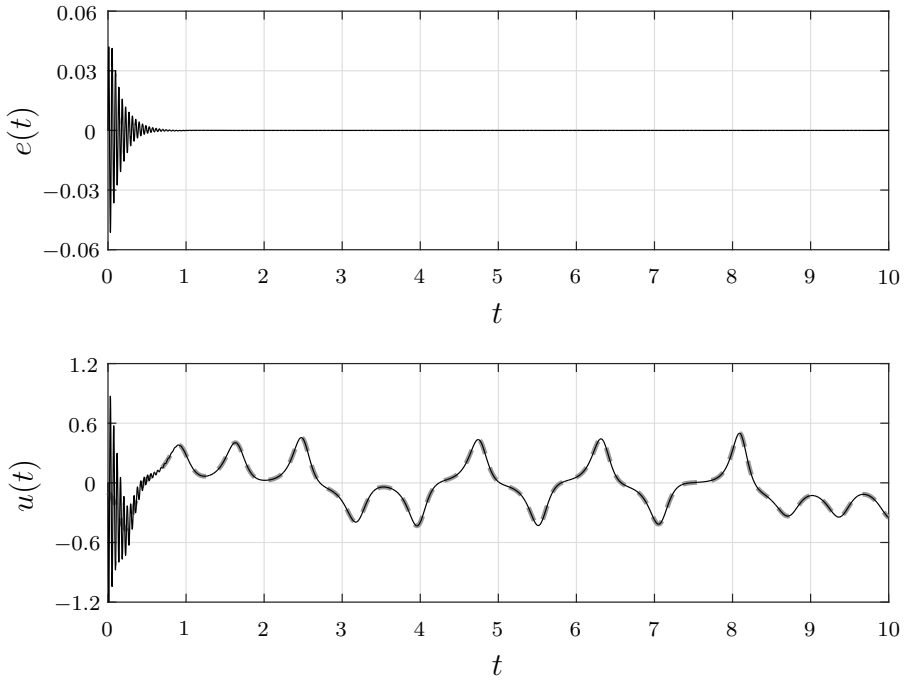

Figure 10: On top: the output regulation error signal $e(t)$. On bottom: the control input signal (solid line) $u(t)$ compared to the zero-error steady-state signal $c(w(t))$ (dashed line). Source: the author.

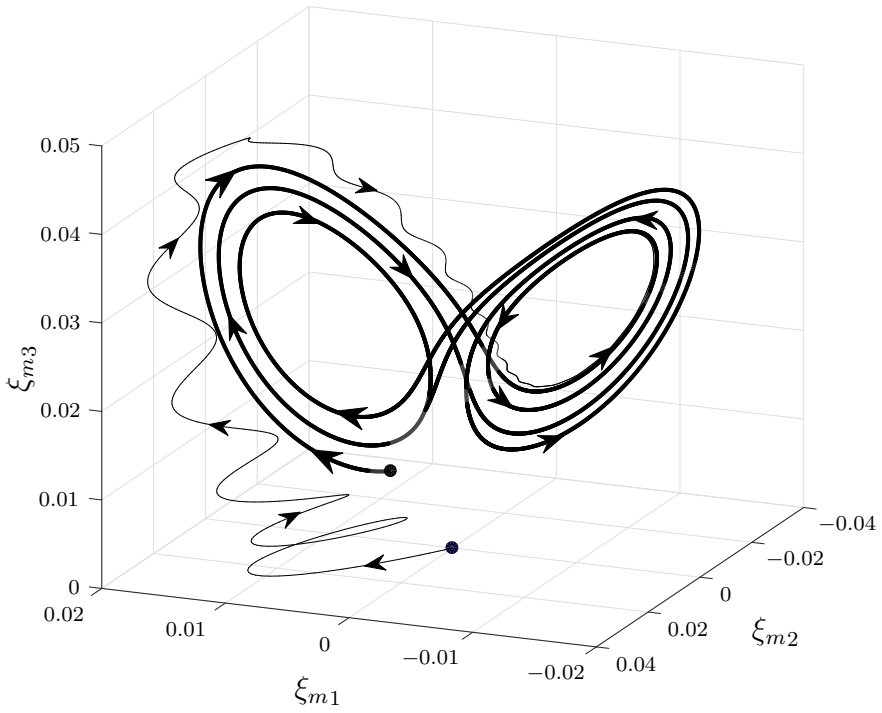

Figure 11: Phase portrait depicting the internal model trajectory ξ_m (thin line) compared to the zero-error steady-state trajectory $\sigma_m(w)$ (thick line). Source: the author.

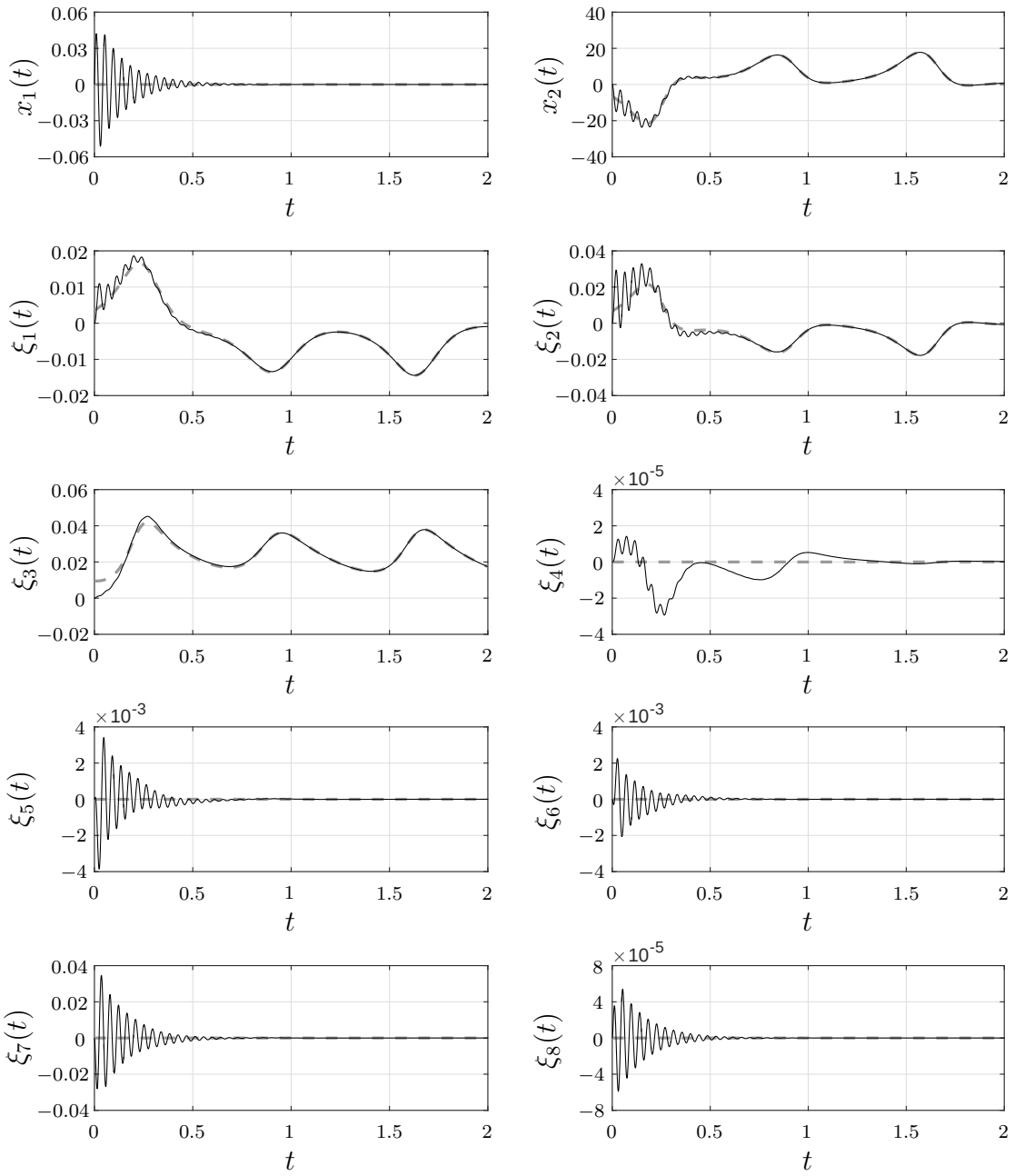

Figure 12: Plant and controller states $x(t)$ and $\xi(t)$ (solid lines) compared to the zero-error steady-states $\pi(w(t))$ and $\sigma(w(t))$ (dashed lines). Source: the author.

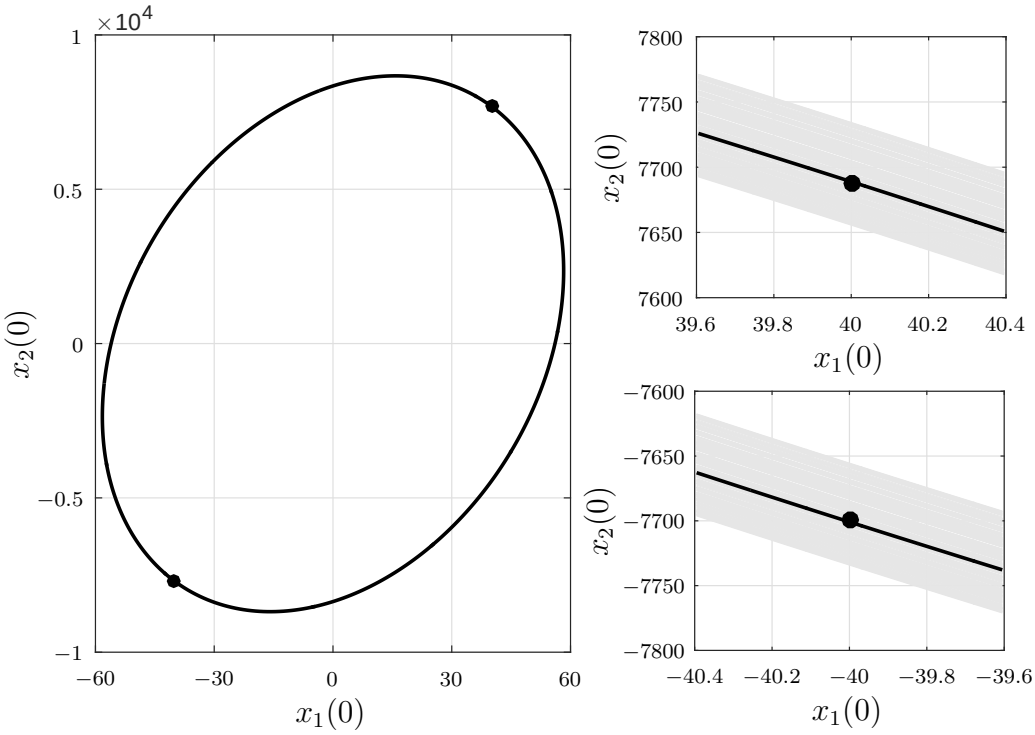

Figure 13: Representation of the set $\mathcal{D}$ in the x-state-space. The black contour is the region border for the default exosystem initial state from (230). The gray patches denote borders for a myriad of exosystem initial states $w(0) \in \mathcal{W}$. Source: the author.

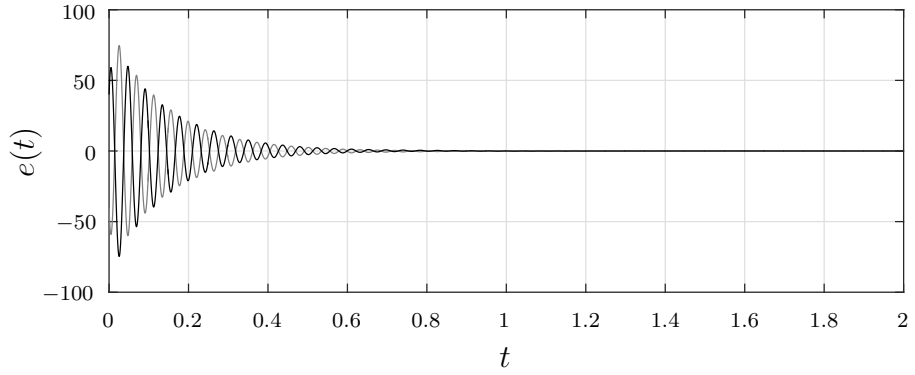

Figure 14: Output error signals $e(t)$ for initial conditions on the border of the domain of attraction estimate $\mathcal{D}$. Shades denote trajectories for different plant initial states. Source: the author.

4 OUTPUT REGULATION OF RATIONAL NONLINEAR SYSTEMS WITH INPUT SATURATION

This chapter extends the proposed output regulation methodologies for systems subject to saturating control inputs. In order to efficiently deal with this problem, a different control framework with anti-windup compensation will be considered. A new set of theorems for stability analysis and control design will be presented, which can be addressed by similar numerical optimization routines as shown before.

In here, Section 4.1 primarily explains the new problem to be solved, followed by Section 4.2 which describes the modified controller architecture to be considered. The development of main theoretical results are contained in Section 4.3. Lastly, Section 4.4 illustrates the proposed methodologies with numerical examples and Section 4.5 provides final remarks.

4.1 Problem Statement

Consider a system, exosystem, and output feedback controller described respectively by (113), (114) and (115). The control signal $u \in \mathcal{U} \subseteq \mathbb{R}^{n_u}$ is now bounded by a region $\mathcal{U}$ of the form

$$\mathcal{U} = [-\overline{u}_1 \, , \, \overline{u}_1] \times [-\overline{u}_2 \, , \, \overline{u}_2] \times \ldots \times [-\overline{u}_{n_u} \, , \, \overline{u}_{n_u}] \subseteq \mathbb{R}^{n_u} \, , \tag{231}$$

where $\overline{u}_j > 0 \; \forall \, j \in \{1, 2, \ldots, n_u\}$ is denoting the maximum admissible value of $|u_j(t)|$ $\forall \, t \geq 0$.

The preliminary assumptions are the same as considered before (i.e. Assumptions 2.1 and 2.2) and the new problem to be tackled is the following.

Problem 4.1. Design controller functions $\phi(\xi, y)$ and $\theta(\xi, y)$ such that the closed-loop system (113), (114), (115) achieves output regulation in some region $\mathcal{D} \subseteq \mathbb{R}^{n_x} \times \mathbb{R}^{n_\xi} \times \mathcal{W}$ with the control input signal restricted to the set (231).

4.2 Control Structure

In order to guarantee that $u \in \mathcal{U}$, the control input is considered to be generated by a saturation function of an unconstrained control signal $\mu \in \mathbb{R}^{n_u}$ supplied by the controller, i.e.

$$u = \mathrm{sat}(\mu) \, , \tag{232}$$

where the nonlinear function $\mathrm{sat} : \mathbb{R}^{n_u} \to \mathcal{U}$ is defined in (27).

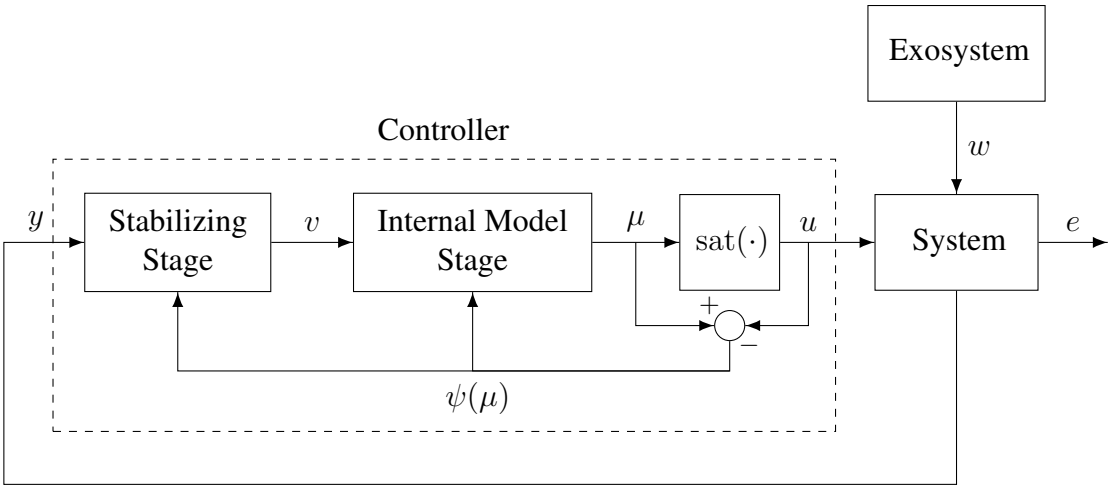

Figure 15: Control structure with saturation and anti-windup loops. Source: the author.

Similarly to the last chapter, the controller state ξ is separated into two components as shown by (116), where ξ_m represents internal model states and ξ_s denotes the stabilizing controller states. Also, an internal stabilizing input $v \in \mathbb{R}^{n_v}$ $(n_v = n_u + n_m)$ is considered as in (117), where the component $v_u \in \mathbb{R}^{n_u}$ is the system stabilizing input and the component $v_m \in \mathbb{R}^{n_m}$ is the internal model stabilizing input. Using these definitions, the proposed internal model controller stage is

$$\left\{ \begin{array}{rcl} \dot{\xi}_m &=& \phi_m(\xi_m, y) + v_m + \mathrm{E}(y)\,\psi(\mu) \\ \mu &=& \theta_m(\xi_m, y) + v_u \end{array} \right. , \tag{233}$$

which is similar to (118), but with a new anti-windup term $\mathrm{E}(y)\,\psi(\mu)$, where $\mathrm{E} : \mathbb{R}^{n_y} \to \mathbb{R}^{n_m \times n_u}$ is a free design matrix function and $\psi(\mu)$ denotes a deadzone function such as defined in (28). One should note that the internal model controller is now responsible for generating the unconstrained input μ which is subsequently saturated by (232). In turn, the stabilizing controller stage is defined as

$$\left\{ \begin{array}{rcl} \dot{\xi}_s &=& \phi_s(\xi_s, y) + \mathrm{W}(y)\,\psi(\mu) \\ v &=& \theta_s(\xi_s, y) \end{array} \right. , \tag{234}$$

similar to (119), but with a new anti-windup term $\mathrm{W}(y)\,\psi(\mu)$ formed by a free design matrix function $\mathrm{W} : \mathbb{R}^{n_y} \to \mathbb{R}^{n_s \times n_u}$.

The block diagram of Figure 15 depicts this considered control architecture with saturation and anti-windup loops. Considering the particular controller structure (232), (233), (234), Lemma 4.1 presents sufficient conditions for output regulation of the closed-loop system with respect to the plant (113) and the exosystem (114).

Lemma 4.1. *The closed-loop system* (113)*,* (114) *with controller* (232)*,* (233)*,* (234) *achieves output regulation in* $\mathcal{D} \subseteq \mathbb{R}^{n_x} \times \mathbb{R}^{n_m} \times \mathbb{R}^{n_s} \times \mathcal{W}$ *if there exist smooth mappings* $\pi : \mathcal{W} \to \mathbb{R}^{n_x}$*,* $c : \mathcal{W} \to \mathcal{U}$*,* $d : \mathcal{W} \to \mathbb{R}^{n_y}$ *and* $\sigma_m : \mathcal{W} \to \mathbb{R}^{n_m}$ *such that* $\pi(0) = 0$*,* $c(0) = 0$*,* $d(0) = 0$*,* $\sigma_m(0) = 0$*,* (120)*,* (121)*,* (122) *and also* (123)*.*

Proof. The first regulation condition (66) of Theorem 2.6 is equivalent to (120), noting here that the available control excursion defined by set $\mathcal{U}$ from (231) must be enough to implement the target steady-state control input $c(w)$ for every exogenous state inside $\mathcal{W}$,

i.e. $c : \mathcal{W} \to \mathcal{U}$. Consider next the second regulation condition (67) with a candidate mapping solution $\sigma(w)$ defined by

$$\sigma(w) = \begin{bmatrix} \sigma_m(w) \\ 0 \end{bmatrix}, \tag{235}$$

for some smooth mapping $\sigma_m : \mathcal{W} \to \mathbb{R}^{n_m}$, $\sigma_m(0) = 0$. Observe that the complete controller representation (115) with stages (232), (233) and (234) can be expressed as

$$\left\{ \begin{array}{rcl} \dot{\xi} = \phi(\xi, y) & = & \begin{bmatrix} \phi_m(\xi_m, y) + D_m\, \theta_s(\xi_s, y) + \mathrm{E}(y)\, \psi(\theta_m(\xi_m, y) + D\, \theta_s(\xi_s, y)) \\ \phi_s(\xi_s, y) + \mathrm{W}(y)\, \psi(\theta_m(\xi_m, y) + D\, \theta_s(\xi_s, y)) \end{bmatrix} \\ u = \theta(\xi, y) & = & \theta_m(\xi_m, y) + D\, \theta_s(\xi_s, y) - \psi(\theta_m(\xi_m, y) + D\, \theta_s(\xi_s, y)) \end{array} \right. \tag{236}$$

where matrices $D \in \mathbb{R}^{n_u \times n_v}$ and $D_m \in \mathbb{R}^{n_m \times n_v}$ are

$$D \triangleq \begin{bmatrix} I & 0 \end{bmatrix}, \quad D_m \triangleq \begin{bmatrix} 0 & I \end{bmatrix}. \tag{237}$$

Using (235) and (236), the regulation condition (67) becomes

$$\left\{ \begin{array}{rcl} \begin{bmatrix} \dfrac{\partial \sigma_m(w)}{\partial w} s(w) \\ 0 \end{bmatrix} & = & \begin{bmatrix} \phi_m(\sigma_m(w), d(w)) + \mathrm{E}(d(w))\, \psi(\theta_m(\sigma_m(w), d(w))) \\ \mathrm{W}(d(w))\, \psi(\theta_m(\sigma_m(w), d(w))) \end{bmatrix} \forall\, w \in \mathcal{W}, \\ c(w) & = & \theta_m(\sigma_m(w), d(w)) - \psi(\theta_m(\sigma_m(w), d(w))) \end{array} \right. \tag{238}$$

considering that stabilizing functions $\phi_s(\xi_s, y)$ and $\theta_s(\xi_s, y)$ vanish at the manifold conditions, according to (122). Moreover, if there exists a mapping $c : \mathcal{W} \to \mathcal{U}$ such that $c(w) = \theta_m(\sigma_m(w), d(w)) \; \forall\, w \in \mathcal{W}$, then it follows that

$$\psi(\theta_m(\sigma_m(w), d(w))) = \psi(c(w)) = c(w) - \mathrm{sat}(c(w)) = 0 \;\; \forall\, w \in \mathcal{W}. \tag{239}$$

Thus, (238) leads to conditions (121) and (122). Furthermore, by applying (235) into the original attraction condition (68), it follows that (123) is obtained.

Consequently, from Theorem 2.6, the conditions of Lemma 4.1 ensure the output regulation of the closed-loop system defined by (113), (114), (232), (234) and (234) with respect to region $\mathcal{D} \subseteq \mathbb{R}^{n_x} \times \mathbb{R}^{n_m} \times \mathbb{R}^{n_s} \times \mathcal{W}$. □

An important observation from Lemma 4.1 and previous conditions is the fact that stabilizing and anti-windup terms do not influence the internal model condition (120). Consequently, the usual internal model approach can be utilized with similar sequential design steps as previously mentioned in Chapter 3.

Prior to initiating the output regulator design, the target manifold mappings $\pi(w)$ and $c(w)$ are again assumed *a priori* known, as stated by Assumption 3.1. If the system functions $f(x, w, u)$ and $h(x, w)$ are in the form of (76), then $\pi(w)$ and $c(w)$ can be recursively determined as in (77). It is additionally assumed here that the maximum control input amplitudes $\overline{u}_1, \ldots, \overline{u}_{n_u}$ are such that the mapping relation $c : \mathcal{W} \to \mathcal{U}$ is feasible, i.e.

$$\sup_{w \in \mathcal{W}} |c_j(w)| < \overline{u}_j \;\; \forall\, j \in \{1, 2, \ldots, n_u\}, \tag{240}$$

so the conditions of Lemma 4.1 can be satisfied.

Given the presented control framework and preliminary assumptions, the proposed design methodology in order to solve Problem 4.1 divides into two distinct steps:

(a) Design internal model functions $\phi_m(\xi_m, y)$ and $\theta_m(\xi_m, y)$ such that (121) is satisfied for some $\sigma_m(w)$.

(b) Design stabilizing functions $\phi_s(\xi_s, y)$ and $\theta_s(\xi_s, y)$ satisfying (122) and anti-windup functions $\mathrm{E}(y)$ and $\mathrm{W}(y)$ such that attraction condition (123) holds.

In order to construct proper stabilizing functions that satisfy (122), an auxiliary definition $\varepsilon \in \mathbb{R}^{n_\varepsilon}$ is again considered as $\varepsilon = \delta(y)$, where $\delta : \mathbb{R}^{n_y} \to \mathbb{R}^{n_\varepsilon}$ is a function that vanishes inside the regulation manifold, i.e. (130). Similar to the methodology in Chapter 3, the stabilizing stage (234) is particularized in the form of

$$\left\{ \begin{array}{rcl} \dot{\xi}_s & = & \mathrm{F}(y)\,\xi_s + \mathrm{G}(y)\,\varepsilon + \mathrm{W}(y)\,\psi(\mu) \\ v & = & \mathrm{H}(y)\,\xi_s + \mathrm{K}(y)\,\varepsilon \end{array} \right. , \tag{241}$$

where $\mathrm{F} : \mathbb{R}^{n_y} \to \mathbb{R}^{n_s \times n_s}$, $\mathrm{G} : \mathbb{R}^{n_y} \to \mathbb{R}^{n_s \times n_\varepsilon}$, $\mathrm{H} : \mathbb{R}^{n_y} \to \mathbb{R}^{n_u \times n_s}$ and $\mathrm{K} : \mathbb{R}^{n_y} \to \mathbb{R}^{n_u \times n_\varepsilon}$ are free design matrix functions. It is again considered the parametrization of $\mathrm{F}(y)\,, \ldots, \mathrm{K}(y)$ with a gain scheduling function $\lambda(y)$ as introduced by (131). Likewise, the new anti-windup terms $\mathrm{E}(y)$ and $\mathrm{W}(y)$ can also be parameterized according to

$$\begin{bmatrix} \mathrm{E}(y) \\ \mathrm{W}(y) \end{bmatrix} \triangleq \begin{bmatrix} \mathrm{E}_0 \\ \mathrm{W}_0 \end{bmatrix} + \sum_{i=1}^{\mathrm{n}} \begin{bmatrix} \mathrm{E}_i \\ \mathrm{W}_i \end{bmatrix} \lambda_i(y)\,, \tag{242}$$

for some free design matrices $\mathrm{E}_0, \ldots, \mathrm{E}_\mathrm{n} \in \mathbb{R}^{n_m \times n_u}$ and $\mathrm{W}_0, \ldots, \mathrm{W}_\mathrm{n} \in \mathbb{R}^{n_s \times n_u}$. The indicated solution of step (b) then divides into these sub-steps:

(b.1) Choose a steady-state vanishing function $\delta(y)$ satisfying (130).

(b.2) For a given scheduling function $\lambda(y)$, design stabilizing parameters $\mathrm{F}_0\,, \ldots, \mathrm{K}_\mathrm{n}$ and anti-windup parameters $\mathrm{E}_0\,, \ldots, \mathrm{W}_\mathrm{n}$ such the attraction condition (123) is verified.

One should recall that sub-step (b.1) can be systematically addressed using the same guidelines discussed Subsection 2.3.2. In turn, the solution of sub-step (b.2) can be obtained by the method to be proposed in the next section, which is an extension of the DAR based formulation previously used in Chapter 3.

4.3 Main Results

This section proposes a new methodology capable of synthesizing the stabilizing and anti-windup parameters mentioned in the sub-step (b.2). Primarily in Subsection 4.3.1, the system equations are re-arranged using a regulation error coordinate change. The differential-algebraic approach is then employed in Subsection 4.3.2. Stability and transient performance conditions are afterwards derived in Subsection 4.3.4, which leads to numerical design procedures in Subsection 4.3.5.

4.3.1 Regulation Error Coordinates

A change of state-space coordinates is introduced as $z \in \mathbb{R}^{n_z}$ $(n_z = n_x + n_m)$, identically to relation (132) already employed before. An auxiliary definition is also introduced according to $\hat{v} \in \mathbb{R}^{n_v}$:

$$\hat{v} \triangleq \begin{bmatrix} \hat{v}_u \\ \hat{v}_m \end{bmatrix} \triangleq \begin{bmatrix} v_u - \psi(\mu) \\ v_m + \mathrm{E}(y)\,\psi(\mu) \end{bmatrix} , \tag{243}$$

where $\hat{v}_u \in \mathbb{R}^{n_u}$ denotes the effective plant stabilizing input, which is v_u subtracted by the control deadzone $\psi(\mu)$. Similarly, $\hat{v}_m \in \mathbb{R}^{n_u}$ denotes the effective internal model stabilizing input, which is v_m added with the internal model anti-windup term $\mathrm{E}(y)\,\psi(\mu)$. The provided definitions allow one to write the system equations in the following manner:

$$\left\{\begin{array}{rcl} \dot{z} &=& f_z(z,w,\hat{v}) \\ \mu &=& \theta_z(z,w) + c(w) + v_u \\ y &=& g_z(z,w) + d(w) \\ e &=& h_z(z,w) \\ \varepsilon &=& \delta_z(z,w) \end{array}\right. , \tag{244}$$

where function $f_z : \mathbb{R}^{n_z} \times \mathbb{R}^{n_w} \times \mathbb{R}^{n_v} \to \mathbb{R}^{n_z}$ is constructed as

$$f_z(z,w,\hat{v}) \triangleq \begin{bmatrix} f(z_x + \pi(w), w, \theta_z(z,w) + c(w) + \hat{v}_u) \\ \phi_m(z_m + \sigma_m(w), g_z(z,w) + d(w)) + \hat{v}_m \end{bmatrix} - \begin{bmatrix} f(\pi(w), w, c(w)) \\ \phi_m(\sigma_m(w), d(w)) \end{bmatrix} , \tag{245}$$

and functions $\theta_z : \mathbb{R}^{n_z} \times \mathbb{R}^{n_w} \to \mathbb{R}^{n_u}$, $g_z : \mathbb{R}^{n_z} \times \mathbb{R}^{n_w} \to \mathbb{R}^{n_y}$, $h_z : \mathbb{R}^{n_z} \times \mathbb{R}^{n_w} \to \mathbb{R}^{n_e}$ and $\delta_z : \mathbb{R}^{n_z} \times \mathbb{R}^{n_w} \to \mathbb{R}^{n_\varepsilon}$ are identical to the definitions in (134).

If $z = 0$ and $\hat{v} = 0$, one should note that $\forall\, w \in \mathcal{W}$: $h_z(0,w) = 0$, $g_z(0,w) = 0$, $\delta_z(0,w) = 0$, $\theta_z(0,w) = 0$, $f_z(0,w,0) = 0$. This observation implies that $z = 0$ is an equilibrium point of the sub-system $\dot{z} = f_z(z,w,\hat{v})$, when $\hat{v} = 0$, for every possible exogenous state $w \in \mathcal{W}$. Additionally, the output error $e = h_z(z,w)$ and the function $\varepsilon = \delta_z(z,w)$ vanish to zero at this equilibrium condition.

The considered stabilizing controller stage originally defined as (241) can also be expressed using the regulation error state z:

$$\left\{\begin{array}{rcl} \dot{\xi}_s &=& F(z,w)\,\xi_s + G(z,w)\,\varepsilon + W(z,w)\,\psi(\mu) \\ v &=& H(z,w)\,\xi_s + K(z,w)\,\varepsilon \end{array}\right. . \tag{246}$$

In (246), matrix functions $F : \mathbb{R}^{n_z} \times \mathbb{R}^{n_w} \to \mathbb{R}^{n_s \times n_s}$, … , $K : \mathbb{R}^{n_z} \times \mathbb{R}^{n_w} \to \mathbb{R}^{n_v \times n_\varepsilon}$ denote the evaluation of $\mathrm{F}(y)$, … , $\mathrm{K}(y)$ using $y = g_z(z,w) + d(w)$, equivalent to (136). In a similar fashion, anti-windup matrix functions $E : \mathbb{R}^{n_z} \times \mathbb{R}^{n_w} \to \mathbb{R}^{n_m \times n_u}$ and $W : \mathbb{R}^{n_z} \times \mathbb{R}^{n_w} \to \mathbb{R}^{n_s \times n_u}$ are defined by

$$\begin{bmatrix} E(z,w) \\ W(z,w) \end{bmatrix} \triangleq \begin{bmatrix} \mathrm{E}_0 \\ \mathrm{W}_0 \end{bmatrix} + \sum_{i=1}^{\mathrm{n}} \begin{bmatrix} \mathrm{E}_i \\ \mathrm{W}_i \end{bmatrix} \lambda_i(z,w) , \tag{247}$$

noting that $\lambda(z,w)$ is the evaluation of the scheduling function $\lambda(y)$ with the variable change $y = g_z(z,w) + d(w)$, similarly to (137). In order to ensure that all controller gain matrices are affinely dependent on (z,w), the choice of the scheduling function is again assumed to be restricted to cases where $\lambda(z,w)$ is a linear mapping, as explained in the previous chapter.

In order to combine the equations from (244) with the stabilizer dynamics in (246), it is necessary to further develop the relation between $\hat{v}$ and v. For instance, one could denote

$$\hat{v} = v + J(z,w)\,\psi(\mu) , \tag{248}$$

where, according to (243), matrix function $J : \mathbb{R}^{n_z} \times \mathbb{R}^{n_w} \to \mathbb{R}^{n_v \times n_u}$ is constructed as

$$J(z,w) \triangleq \begin{bmatrix} -I \\ E(z,w) \end{bmatrix} = D_m^{\mathsf{T}} E(z,w) - D^{\mathsf{T}} , \tag{249}$$

recalling that matrices $D \in \mathbb{R}^{n_u \times n_v}$ and $D_m \in \mathbb{R}^{n_m \times n_v}$ are the same ones defined in (237).

4.3.2 Differential-Algebraic Representation

The next proposed step towards stability conditions is considering a proper differential-algebraic representation of the main system functions from (244), according to the following assumption.

Assumption 4.1. Nonlinear functions $f_z(z, w, \hat{v})$, $\theta_z(z, w)$ and $\delta_z(z, w)$ of the system (244) can be represented as

$$\begin{array}{rcl} f_z(z,w,\hat{v}) & = & A(z,w)\,z + \Phi(z,w)\,\varphi(z,w) + B\,\hat{v} \\ \theta_z(z,w) & = & Q(z,w)\,z + \Upsilon(z,w)\,\varphi(z,w) \\ \delta_z(z,w) & = & C\,z + \Gamma\,\varphi(z,w) \end{array} \tag{250}$$

with a rational nonlinear function $\varphi : \mathcal{Z}^+ \times \mathcal{W}^+ \to \mathbb{R}^{n_\varphi}$ satisfying

$$0 = \Psi(z,w)\,z + \Omega(z,w)\,\varphi(z,w) \tag{251}$$

such that:

(i) Sets $\mathcal{Z}^+$ and $\mathcal{W}^+$ satisfy $\{0\} \subset \text{int}\{\mathcal{Z}^+\} \subseteq \mathbb{R}^{n_z}$ and $\mathcal{W} \subseteq \mathcal{W}^+ \subseteq \mathbb{R}^{n_w}$.

(ii) Matrices $A : \mathcal{Z}^+ \times \mathcal{W}^+ \to \mathbb{R}^{n_z \times n_z}$, $\Phi : \mathcal{Z}^+ \times \mathcal{W}^+ \to \mathbb{R}^{n_z \times n_\varphi}$, $Q : \mathcal{Z}^+ \times \mathcal{W}^+ \to \mathbb{R}^{n_u \times n_z}$, $\Upsilon : \mathcal{Z}^+ \times \mathcal{W}^+ \to \mathbb{R}^{n_u \times n_\varphi}$, $\Psi : \mathcal{Z}^+ \times \mathcal{W}^+ \to \mathbb{R}^{n_\varphi \times n_z}$ and $\Omega : \mathcal{Z}^+ \times \mathcal{W}^+ \to \mathbb{R}^{n_\varphi \times n_\varphi}$ are affine with respect to (z, w).

(iii) Matrices $B \in \mathbb{R}^{n_z \times n_v}$, $C \in \mathbb{R}^{n_\varepsilon \times n_z}$ and $\Gamma \in \mathbb{R}^{n_\varepsilon \times n_\varphi}$ are constant.

(iv) Matrix $\Omega(z, w)$ is non-singular $\forall\,(z, w) \in \mathcal{Z}^+ \times \mathcal{W}^+$.

(v) Matrix $A(z, w)$ satisfies (144) for constant matrices $\mathrm{A}_0, \ldots, \mathrm{A}_\mathrm{n} \in \mathbb{R}^{n_z \times n_z}$.

Assumption 4.1 is similar to Assumption 3.2 considered in the last chapter, and the reader may refer to Subsection 3.3.2 for further explanation with respect to requirements (i) to (v). One should notice though that function $\theta_z(z, w)$ is being additionally included here. The purpose of this complementary consideration is to systematically deal with the deadzone function $\psi(\mu)$ later on, since the unconstrained control input μ is directly described by $\theta_z(z, w)$ as (244) shows.

Regions $\mathcal{Z}^+$ and $\mathcal{W}^+$ are again considered as (145), namely convex sets defined by a convex hull of vertices $\mathcal{V}_z$ and $\mathcal{V}_w$. Furthermore, set $\mathcal{Z}^+$ is again represented as in (146) for some vectors $p_1, p_2, \ldots, p_{n_k} \in \mathbb{R}^{n_z}$.

Provided the DAR of (250) and (251), the main system equations from (244) can be re-written as

$$\left\{ \begin{array}{rcl} \dot{z} & = & A(z,w)\,z + \Phi(z,w)\,\varphi(z,w) + BJ(z,w)\,\psi(\mu) + B\,v \\ \mu & = & Q(z,w)\,z + \Upsilon(z,w)\,\varphi(z,w) + c(w) + D\,v \\ 0 & = & \Psi(z,w)\,z + \Omega(z,w)\,\varphi(z,w) \\ \varepsilon & = & C\,z + \Gamma\,\varphi(z,w) \end{array} \right. , \tag{252}$$

Considering the augmented regulation error state definition $\mathbf{z} \in \mathbb{R}^{n_a}$ as in (138), one is furthermore able express:

$$\left\{ \begin{array}{rcl} \dot{\mathbf{z}} & = & \boldsymbol{A}(z,w)\,\mathbf{z} + \boldsymbol{\Phi}(z,w)\,\varphi(z,w) + \boldsymbol{J}(z,w)\,\psi(\mu) \\ \mu & = & \boldsymbol{Q}(z,w)\,\mathbf{z} + \boldsymbol{\Upsilon}(z,w)\,\varphi(z,w) + c(w) \\ 0 & = & \boldsymbol{\Psi}(z,w)\,\mathbf{z} + \boldsymbol{\Omega}(z,w)\,\varphi(z,w) \end{array} \right. . \tag{253}$$

Augmented matrices $\boldsymbol{A} : \mathcal{Z}^+ \times \mathcal{W}^+ \to \mathbb{R}^{n_a \times n_a}$, $\boldsymbol{\Phi} : \mathcal{Z}^+ \times \mathcal{W}^+ \to \mathbb{R}^{n_a \times n_\varphi}$, $\boldsymbol{\Psi} : \mathcal{Z}^+ \times \mathcal{W}^+ \to \mathbb{R}^{n_\varphi \times n_a}$ and $\boldsymbol{\Omega} : \mathcal{Z}^+ \times \mathcal{W}^+ \to \mathbb{R}^{n_\varphi \times n_\varphi}$ are here defined identically as in (149). In turn, the new matrices $\boldsymbol{Q} : \mathcal{Z}^+ \times \mathcal{W}^+ \to \mathbb{R}^{n_u \times n_a}$, $\boldsymbol{\Upsilon} : \mathcal{Z}^+ \times \mathcal{W}^+ \to \mathbb{R}^{n_u \times n_\varphi}$ and $\boldsymbol{J} : \mathcal{Z}^+ \times \mathcal{W}^+ \to \mathbb{R}^{n_z \times n_u}$ are here denoting:

$$\begin{matrix} \boldsymbol{Q}(z,w) = \begin{bmatrix} Q(z,w) + DK(z,w)C & DH(z,w) \end{bmatrix}, \\ \boldsymbol{\Upsilon}(z,w) = \begin{bmatrix} \Upsilon(z,w) + DK(z,w)\Gamma \end{bmatrix}, \end{matrix} \quad \boldsymbol{J}(z,w) = \begin{bmatrix} BD_m^{\mathsf{T}} E(z,w) - BD^{\mathsf{T}} \\ W(z,w) \end{bmatrix}. \tag{254}$$

4.3.3 Sector Conditions

In order to deal with the deadzone function $\psi(\mu)$, a new modified sector condition is proposed according to the following lemma. This result extends Lemma 2.1 devised by GOMES DA SILVA JR; TARBOURIECH (2005), where the main difference here is the treatment of the non-vanishing steady-state control $c(w)$.

Lemma 4.2. *Consider functions $\boldsymbol{\theta}, \boldsymbol{\vartheta} : \boldsymbol{\mathcal{Z}}^+ \times \mathcal{W}^+ \to \mathbb{R}^{n_u}$, $\mathcal{W} \subseteq \mathcal{W}^+$, and upper bounds $\overline{c}_1, \overline{c}_2, \ldots, \overline{c}_{n_u} \in \mathbb{R}$ such that*

$$\sup_{w \in \mathcal{W}} |c_j(w)| \leq \overline{c}_j < \overline{u}_j \;\; \forall\, j \in \{1, 2, \ldots, n_u\}\,. \tag{255}$$

If $(\mathbf{z}, w) \in \mathcal{S}$, where $\mathcal{S}$ is the set

$$\mathcal{S} = \left\{ (\mathbf{z}, w) \in \boldsymbol{\mathcal{Z}}^+ \times \mathcal{W} : |\, \boldsymbol{\theta}_j(\mathbf{z}, w) - \boldsymbol{\vartheta}_j(\mathbf{z}, w)\,| \;\leq (\overline{u}_j - \overline{c}_j)\,,\; j = 1, 2, \ldots, n_u \right\}, \tag{256}$$

then it follows that

$$\psi^{\mathsf{T}}(\mu)\, T \left(\psi(\mu) - \boldsymbol{\vartheta}(\mathbf{z}, w) \right) \leq 0 \tag{257}$$

is verified for $\mu = \boldsymbol{\theta}(\mathbf{z}, w) + c(w)$ and any diagonal matrix $T \in \mathbb{R}^{n_u \times n_u}$, $T \succ 0$.

Proof. Observe all the possible cases that follows:

(a) $|\, \boldsymbol{\theta}_j(\mathbf{z}, w)\,| \;\leq\; (\overline{u}_j - \overline{c}_j)$. In this case it follows that $|\, \boldsymbol{\theta}_j(\mathbf{z}, w) \pm c_j(w)\,| \;\leq\; \overline{u}_j$ $\forall\, w \in \mathcal{W}$ and then $\psi(\mu_j) = \psi(\boldsymbol{\theta}_j(z, w) + c_j(w)) = 0$. Consequently:

$$\psi^{\mathsf{T}}(\mu_j)\, T_{[j,j]} \left(\psi(\mu_j) - \boldsymbol{\vartheta}_j(\mathbf{z}, w) \right) = 0\,. \tag{258}$$

(b) $|\, \boldsymbol{\theta}_j(\mathbf{z}, w)\,| > (\overline{u}_j - \overline{c}_j)$. In this case there are three possible sub-cases:

(b.1) $|\, \boldsymbol{\theta}_j(\mathbf{z}, w) \pm c_j(w)\,| \;\leq\; \overline{u}_j \;\forall\, w \;\in\; \mathcal{W}$, which is identical to (a) and therefore (258) is verified.

(b.2) $\boldsymbol{\theta}_j(\mathbf{z}, w) \pm c_j(w) > \overline{u}_j \;\forall\, w \in \mathcal{W}$. In this sub-case $\psi(\mu_j) = \psi(\boldsymbol{\theta}_j(z, w) + c_j(w)) = \boldsymbol{\theta}_j(z, w) + c_j(w) - \overline{u}_j > 0$. If $(\mathbf{z}, w) \in \mathcal{S}$, then $\boldsymbol{\theta}_j(\mathbf{z}, w) - \boldsymbol{\vartheta}_j(\mathbf{z}, w) \leq (\overline{u}_j - \overline{c}_j)$ and also $\boldsymbol{\vartheta}_j(\mathbf{z}, w) \geq \boldsymbol{\theta}_j(\mathbf{z}, w) \pm c_j(w) - \overline{u}_j \;\forall\, w \in \mathcal{W}$. Therefore it follows that $\psi(\mu_j) - \boldsymbol{\vartheta}_j(\mathbf{z}, w) = \boldsymbol{\theta}_j(z, w) + c_j(w) - \overline{u}_j - \boldsymbol{\vartheta}_j(\mathbf{z}, w) \leq 0$ $\forall\, w \in \mathcal{W}$. Consequently:

$$\psi^{\mathsf{T}}(\mu_j)\, T_{[j,j]} \left(\psi(\mu_j) - \boldsymbol{\vartheta}_j(\mathbf{z}, w) \right) \leq 0\,. \tag{259}$$

(b.3) $\boldsymbol{\theta}_j(\mathbf{z}, w) \pm c_j(w) < -\overline{u}_j \;\forall\, w \in \mathcal{W}$. In this sub-case $\psi(\mu_j) = \psi(\boldsymbol{\theta}_j(z, w) + c_j(w)) = \boldsymbol{\theta}_j(z, w) + c_j(w) + \overline{u}_j < 0$. If $(\mathbf{z}, w) \in \mathcal{S}$, then $\boldsymbol{\theta}_j(\mathbf{z}, w) - \boldsymbol{\vartheta}_j(\mathbf{z}, w) \geq -(\overline{u}_j - \overline{c}_j)$ and also $\boldsymbol{\vartheta}_j(\mathbf{z}, w) \leq \boldsymbol{\theta}_j(\mathbf{z}, w) \pm c_j(w) + \overline{u}_j \;\forall\, w \in \mathcal{W}$. Therefore it follows that $\psi(\mu_j) - \boldsymbol{\vartheta}_j(\mathbf{z}, w) = \boldsymbol{\theta}_j(z, w) + c_j(w) + \overline{u}_j - \boldsymbol{\vartheta}_j(\mathbf{z}, w) \geq 0$ $\forall\, w \in \mathcal{W}$ and (259) is again verified.

From all these cases, provided that $(\mathbf{z}, w) \in \mathcal{S}$ and that $T \succ 0$, relation (257) is true. $\square$

It is assumed that magnitude bounds $\overline{c}_1, \overline{c}_2, \ldots, \overline{c}_{n_u}$, as defined by (255), are known prior to the evaluation of analysis and design conditions to be later shown. In cases where the mapping $c(w)$ is rational, these bounds can be efficiently computed by a DAR based procedure proposed in the sequence. This sub-problem to be dealt is formally stated as follows.

Problem 4.2. For a given function $c : \mathbb{R}^{n_w} \to \mathbb{R}^{n_u}$ and a given compact set $\mathcal{W} \subset \mathbb{R}^{n_w}$, determine estimates $\overline{c}_1, \overline{c}_2, \ldots, \overline{c}_{n_u} \in \mathbb{R}$, $\overline{c}_1, \overline{c}_2, \ldots, \overline{c}_{n_u} > 0$, such that:

$$\sup_{w \in \mathcal{W}} |c_j(w)| \leq \overline{c}_j \ \ \forall\, j \in \{1, 2, \ldots, n_u\} \, . \tag{260}$$

In order to solve this sub-problem, it is considered employing a similar DAR based approach from the main proposal. In turn, the scope is being restricted to cases where the mapping $c(w)$ is a regular rational function in $\mathcal{W}$, according to the following assumption.

Assumption 4.2. Nonlinear function $c(w)$ can be represented as

$$c(w) = \tilde{Q}(w)\, w + \tilde{\Upsilon}(w)\, \tilde{\varphi}(w) \tag{261}$$

with a rational nonlinear function $\tilde{\varphi} : \mathcal{W}^+ \to \mathbb{R}^{n_{\tilde{\varphi}}}$ satisfying

$$0 = \tilde{\Psi}(w)\, w + \tilde{\Omega}(w)\, \tilde{\varphi}(w) \tag{262}$$

such that:

(i) Set $\mathcal{W}^+$ satisfy $\mathcal{W} \subseteq \mathcal{W}^+ \subseteq \mathbb{R}^{n_w}$.

(ii) Matrices $\tilde{Q} : \mathcal{W}^+ \to \mathbb{R}^{n_w \times n_w}$, $\tilde{\Upsilon} : \mathcal{W}^+ \to \mathbb{R}^{n_w \times n_{\tilde{\varphi}}}$, $\tilde{\Psi} : \mathcal{W}^+ \to \mathbb{R}^{n_{\tilde{\varphi}} \times n_w}$ and $\tilde{\Omega} : \mathcal{W}^+ \to \mathbb{R}^{n_{\tilde{\varphi}} \times n_{\tilde{\varphi}}}$ are affine with respect to w.

(iii) Matrix $\tilde{\Omega}(w)$ is non-singular $\forall\, w \in \mathcal{W}^+$.

Without loss of generality, it is additionally required to define an ellipsoidal set

$$\mathcal{W}_{\mathcal{E}} = \left\{ w \in \mathbb{R}^{n_w} : w^{\mathsf{T}} \tilde{P}\, w \leq 1 \right\} , \tag{263}$$

for some symmetric matrix $\tilde{P} \in \mathbb{R}^{n_w \times n_w}$ such that $\mathcal{W} \subseteq \mathcal{W}_{\mathcal{E}} \subseteq \mathcal{W}^+$.

Provided these assumptions, the solution of Problem 4.2 may be obtained throughout the following proposed conditions.

Lemma 4.3. *Suppose* $\forall\, j \in \{1, 2, \ldots, n_u\}$ *there exist matrices* $\tilde{L}_j \in \mathbb{R}^{n_{\tilde{\varphi}} \times n_{\tilde{\varphi}}}$ *and scalars* $a_j \in \mathbb{R}$ *such that :*

$$a_j > 0 \, , \tag{264}$$

$$\begin{bmatrix} a_j & \tilde{Q}_{[j]}(w) & \tilde{\Upsilon}_{[j]}(w) \\ \star & \tilde{P} & -\tilde{\Psi}^{\mathsf{T}}(w) \tilde{L}_j^{\mathsf{T}} \\ \star & \star & -\mathcal{H}\{\tilde{L}_j \tilde{\Omega}(w)\} \end{bmatrix} \succ 0 \ \ \forall\, w \in \mathcal{V}_w \, . \tag{265}$$

Then (260) *is satisfied with* $\overline{c}_j = \sqrt{a_j}$.

Proof. Suppose the following inequality is true:

$$\begin{gathered}\mathcal{H}\big\{\tilde{\varphi}^{\mathrm{T}}(w)\tilde{L}_j\big(\tilde{\Psi}(w)\,w+\tilde{\Omega}(w)\,\tilde{\varphi}(w)\big)\big\}+\ldots\\ \ldots\pm\overline{c}_j^{-1}\,\mathcal{H}\big\{\tilde{Q}_{[j]}(w)\,w+\tilde{\Upsilon}_{[j]}(w)\,\tilde{\varphi}(w)\big\}\leq 1+w^{\mathrm{T}}\tilde{P}\,w\\ \forall\, w\in\mathcal{W}^{+}\,,\ j\in\{1,2,\ldots,n_u\}\,.\end{gathered}\tag{266}$$

By considering $w\in\mathcal{W}_{\mathcal{E}}\subset\mathcal{W}^{+}$ and because $\tilde{\Psi}(w)\,w+\tilde{\Omega}(w)\,\tilde{\varphi}(w)=0$, it follows that

$$\pm\overline{c}_j^{-1}\,\mathcal{H}\big\{\tilde{Q}_{[j]}(w)\,w+\tilde{\Upsilon}_{[j]}(w)\,\tilde{\varphi}(w)\big\}\leq 2\ \ \forall\, w\in\mathcal{W}^{+}\,,\ j\in\{1,2,\ldots,n_u\}\,.\tag{267}$$

Since $\tilde{Q}_{[j]}(w)\,w+\tilde{\Upsilon}_{[j]}(w)\,\tilde{\varphi}(w)=c_j(w)$, relation (267) implies

$$|c_j(w)|\leq\overline{c}_j\ \ \forall\, w\in\mathcal{W}^{+}\,,\ j\in\{1,2,\ldots,n_u\}\,.\tag{268}$$

Because it was supposed that $w\in\mathcal{W}_{\mathcal{E}}\subseteq\mathcal{W}^{+}$, one deduces

$$(266)\ \ \Rightarrow\ \ \sup_{w\in\mathcal{W}_{\mathcal{E}}}|c_j(w)|\leq\overline{c}_j\ \ \forall\, j\in\{1,2,\ldots,n_u\}\,,\tag{269}$$

and consequently that (266) $\Rightarrow$ (260) since $\mathcal{W}\subseteq\mathcal{W}_{\mathcal{E}}$.

Now observe that (266) can be equivalently expressed as

$$\zeta^{\mathrm{T}}(w)\,\Delta_j(w)\,\zeta(w)\geq 0\ \ \forall\, w\in\mathcal{W}^{+}\,,\ j\in\{1,2,\ldots,n_u\}\,,\tag{270}$$

where $\zeta(w)\triangleq\big[\mp\overline{c}_j^{-1}\quad w^{\mathrm{T}}\quad\varphi_c^{\mathrm{T}}(w)\big]^{\mathrm{T}}$ and $\Delta_j(w)$ denotes

$$\Delta_j(w)\triangleq\begin{bmatrix}\overline{c}_j{}^2 & \tilde{Q}_{[j]}(w) & \tilde{\Upsilon}_{[j]}(w)\\ \star & \tilde{P} & -\tilde{\Psi}^{\mathrm{T}}(w)\tilde{L}_j^{\mathrm{T}}\\ \star & \star & -\mathcal{H}\{\tilde{L}_j\tilde{\Omega}(w)\}\end{bmatrix}.\tag{271}$$

If $\Delta_j(w)\succ 0\ \forall\, w\in\mathcal{W}^{+}$, $j\in\{1,2,\ldots,n_u\}$ then (270) is satisfied $\forall\,\zeta(w)$. Lastly, from Lemma A.3 and since $\mathcal{W}^{+}$ was defined as (145), one gets (265), where the variable change $a_j\triangleq\overline{c}_j{}^2$ was introduced. □

Based on Lemma 4.3, the lowest j-th bound $\overline{c}_j$ can be estimated by solving a semidefinite optimization problem of the form:

$$\min_{L_j\,,\,a_j}\ \ a_j\ \ \text{s.t.}\ \ \big\{(264)\,,\,(265)\big\}\,.\tag{272}$$

4.3.4 Analysis Conditions

Prior to the formulation of design procedures for stabilizing and anti-windup parameters F_0 , … , W_{n}, it is suitable to initially develop analysis conditions related to the attraction requirement (141), as previously done in Chapter 3. The starting point is to consider Lyapunov's stability conditions from Lemma 3.2 and the extended sector condition from Lemma 4.2 just proposed.

Given these considerations, Theorem 4.1 presents the main result of the chapter which addresses the output regulation of the closed-loop system (113), (114) with the anti-windup controller defined by (232), (233) and (241). The additional performance criteria (P1) and (P2) from Definitions 3.1 and 3.2 are again considered.

Theorem 4.1. *Suppose there exist a symmetric matrix $P \in \mathbb{R}^{n_a \times n_a}$, a diagonal matrix $T \in \mathbb{R}^{n_u \times n_u}$ and matrices $L \in \mathbb{R}^{n_\varphi \times n_\varphi}$, $\mathrm{R}_0, \ldots, \mathrm{R}_\mathrm{m} \in \mathbb{R}^{n_u \times n_z}$, $\Xi_0, \ldots, \Xi_\mathrm{m} \in \mathbb{R}^{n_u \times n_s}$ and $\Pi_0, \ldots, \Pi_\mathrm{m} \in \mathbb{R}^{n_u \times n_\varphi}$ such that* (153)*,* (154)*,* (156)*,*

$$T \succ 0 \,, \tag{273}$$

$$\begin{bmatrix} (\overline{u}_j - \overline{c}_j)^2 & \boldsymbol{Q}_{[j]}(z,w) - \boldsymbol{R}_{[j]}(z,w) & \boldsymbol{\Upsilon}_{[j]}(z,w) - \boldsymbol{\Pi}_{[j]}(z,w) \\ \star & P & -\boldsymbol{\Psi}^\intercal(z,w) L^\intercal \\ \star & \star & -\mathcal{H}\{L\boldsymbol{\Omega}(z,w)\} \end{bmatrix} \succ 0 \\ \forall\, (z,w) \in \mathcal{V}_z \times \mathcal{V}_w \,,\ j \in \{1,2,\ldots,n_u\} \,, \tag{274}$$

$$\mathcal{H}\left\{ \begin{bmatrix} P\boldsymbol{A}(z,w) + \alpha P & P\boldsymbol{\Phi}(z,w) & P\boldsymbol{J}(z,w) \\ L\boldsymbol{\Psi}(z,w) & L\boldsymbol{\Omega}(z,w) & 0 \\ T\boldsymbol{R}(z,w) & T\boldsymbol{\Pi}(z,w) & -T \end{bmatrix} \right\} \prec 0 \ \ \forall\, (z,w) \in \mathcal{V}_z \times \mathcal{V}_w \,, \tag{275}$$

where $\boldsymbol{R}(z,w) \triangleq \begin{bmatrix} R(z,w) & \Xi(z,w) \end{bmatrix}$, $\boldsymbol{\Pi}(z,w) \triangleq \mathit{\Pi}(z,w)$ *and*

$$\begin{bmatrix} R(z,w) & \Xi(z,w) & \mathit{\Pi}(z,w) \end{bmatrix} \triangleq \begin{bmatrix} \mathrm{R}_0 & \Xi_0 & \Pi_0 \end{bmatrix} + \sum_{i=1}^{\mathrm{m}} \begin{bmatrix} \mathrm{R}_i & \Xi_i & \Pi_i \end{bmatrix} \nu_i(z,w) \,, \tag{276}$$

for any linear function $\nu : \mathcal{Z}^+ \times \mathcal{W}^+ \to \mathbb{R}^\mathrm{m}$, $\mathrm{m} \in \mathbb{N}$. Then the closed-loop system (113)*,* (114) *with controller* (232)*,* (233)*,* (241) *achieves output regulation and satisfies* (P1) *and* (P2) *for every initial condition in* (157)*.*

Proof. Consider the Lyapunov candidate function $V(\mathbf{z})$ as in (158) for a symmetric and positive-definite matrix P, implying that $V(\mathbf{z}) > 0 \ \forall\, \mathbf{z} \in \mathbb{R}^{n_a}$, $\mathbf{z} \neq 0$. The derivative of (158) along the trajectories of the system (253) is $\dot{V}(\mathbf{z}, w) = \mathcal{H}\{\mathbf{z}^\intercal \boldsymbol{\Delta}_1(z,w)\, \zeta(\mathbf{z}, w)\}$, where

$$\boldsymbol{\Delta}_1(z,w) \triangleq \begin{bmatrix} P\boldsymbol{A}(z,w) & P\boldsymbol{\Phi}(z,w) & P\boldsymbol{J}(z,w) \end{bmatrix} \,, \quad \zeta(\mathbf{z}, w) \triangleq \begin{bmatrix} \mathbf{z} \\ \varphi(z,w) \\ \psi(\mu) \end{bmatrix} \,, \tag{277}$$

with $\mu = \boldsymbol{Q}(z,w)\, \mathbf{z} + \boldsymbol{\Upsilon}(z,w)\, \varphi(z,w) + c(w)$. Utilizing this same notation, the algebraic equality constraint in (253) can be expressed by $\boldsymbol{\Delta}_2(z,w)\, \zeta(\mathbf{z}, w) = 0$, where

$$\boldsymbol{\Delta}_2(z,w) \triangleq \begin{bmatrix} \boldsymbol{\Psi}(z,w) & \boldsymbol{\Omega}(z,w) & 0 \end{bmatrix} \,. \tag{278}$$

Consider now the statement from Lemma 4.2 particularly with functions $\boldsymbol{\theta}(\mathbf{z}, w)$ and $\boldsymbol{\vartheta}(\mathbf{z}, w)$ expanded as

$$\begin{cases} \boldsymbol{\theta}(\mathbf{z}, w) &= \boldsymbol{Q}(z,w)\, \mathbf{z} + \boldsymbol{\Upsilon}(z,w)\, \varphi(z,w) \\ \boldsymbol{\vartheta}(\mathbf{z}, w) &= \boldsymbol{R}(z,w)\, \mathbf{z} + \boldsymbol{\Pi}(z,w)\, \varphi(z,w) \end{cases} \,, \tag{279}$$

where matrices $\boldsymbol{Q}(z,w)$ and $\boldsymbol{\Upsilon}(z,w)$ are the same ones that compose signal μ in (253) and the new matrices $\boldsymbol{R} : \mathcal{Z}^+ \times \mathcal{W}^+ \to \mathbb{R}^{n_u \times n_a}$ and $\boldsymbol{\Pi} : \mathcal{Z}^+ \times \mathcal{W}^+ \to \mathbb{R}^{n_u \times n_\varphi}$ are free affine functions with respect (z,w). These matrices are equivalently defined as $\boldsymbol{R}(z,w) \triangleq \begin{bmatrix} R(z,w) & \Xi(z,w) \end{bmatrix}$ and $\boldsymbol{\Pi}(z,w) \triangleq \mathit{\Pi}(z,w)$, where $R(z,w)$, $\Xi(z,w)$ and $\mathit{\Pi}(z,w)$ are constructed as in (276) for any linear function $\nu : \mathcal{Z}^+ \times \mathcal{W}^+ \to \mathbb{R}^\mathrm{m}$, $\mathrm{m} \in \mathbb{N}$. According to Lemma 4.2, if $(\mathbf{z}, w) \in \mathcal{S}$ then (257) is true, which can be written in the form $\psi^\intercal(\mu)\, \boldsymbol{\Delta}_3(z,w)\, \zeta(\mathbf{z}, w) \geq 0$ where

$$\boldsymbol{\Delta}_3(z,w) \triangleq \begin{bmatrix} T\boldsymbol{R}(z,w) & T\boldsymbol{\Pi}(z,w) & -T \end{bmatrix} \,, \tag{280}$$

for some diagonal matrix T satisfying (273). Now suppose the following inequality holds for a matrix $L \in \mathbb{R}^{n_\varphi \times n_\varphi}$ and some scalar $\alpha \geq 0$:

$$\begin{gathered}\dot{V}(\mathbf{z},w) + 2\alpha\, V(\mathbf{z}) + \mathcal{H}\big\{\varphi^{\intercal}(z,w)\, L \boldsymbol{\Delta}_2(z,w)\, \zeta(\mathbf{z},w)\big\} + \ldots \\ \ldots + \mathcal{H}\big\{\psi^{\intercal}(\mu)\ \boldsymbol{\Delta}_3(z,w)\, \zeta(\mathbf{z},w)\big\} < 0 \ \ \forall\, (\mathbf{z},w) \in \boldsymbol{\mathcal{Z}}^{+} \times \mathcal{W}^{+}\,,\ \mathbf{z} \neq 0\,.\end{gathered} \tag{281}$$

Then, if this relation is verified, it readily follows that $\dot{V}(\mathbf{z},w) < 0\ \forall\, (\mathbf{z},w) \in (\boldsymbol{\mathcal{Z}}^{+} \times \mathcal{W}^{+}) \cap \mathcal{S}$, $\mathbf{z} \neq 0$, where $\boldsymbol{\mathcal{Z}}^{+} = \mathcal{Z}^{+} \times \mathbb{R}^{n_s}$. By factorizing $\zeta(\mathbf{z},w)$ and applying Lemma A.3 in expression (281), one obtains the matrix inequality (275). Conditions (153), (273) and (275) consequently ensure that the candidate Lyapunov function $V(\mathbf{z})$ is positive-definite and its derivative is negative-definite $\forall\, (\mathbf{z},w) \in (\boldsymbol{\mathcal{Z}}^{+} \times \mathcal{W}^{+}) \cap \mathcal{S}$. Therefore, it remains to show that $\mathcal{D} \subset \boldsymbol{\mathcal{Z}}^{+} \times \mathcal{W}^{+}$ and $\mathcal{D} \subset \mathcal{S}$, where $\mathcal{D}$, defined as in (157), is the domain of attraction estimate and positively invariant region with respect to the system trajectories.

According to proof from Theorem 3.1, the criterion $\mathcal{D} \subset \boldsymbol{\mathcal{Z}}^{+} \times \mathcal{W}^{+}$ is satisfied if the condition (154) holds. Furthermore, in order to deal with the requirement $\mathcal{D} \subset \mathcal{S}$ for the validity of the sector condition from Lemma 4.2, suppose

$$\begin{gathered}\mathcal{H}\big\{\varphi^{\intercal}(\mathbf{z},w)\, L \boldsymbol{\Delta}_2(z,w)\, \zeta(\mathbf{z},w) \pm (\overline{u}_j - \overline{c}_j)^{-1} \boldsymbol{\Delta}_{4[j]}(z,w)\, \zeta(\mathbf{z},w)\big\} \leq 1 + \mathbf{z}^{\intercal} P\, \mathbf{z} \\ \forall\, (\mathbf{z},w) \in \boldsymbol{\mathcal{Z}}^{+} \times \mathcal{W}^{+}\,,\ j \in \{1,2,\ldots,n_u\}\,,\end{gathered} \tag{282}$$

where $\boldsymbol{\Delta}_{4[j]}$ denotes the j-th row of the matrix

$$\boldsymbol{\Delta}_4(z,w) = \begin{bmatrix}\boldsymbol{Q}(z,w) - \boldsymbol{R}(z,w) & \boldsymbol{\Upsilon}(z,w) - \boldsymbol{\Pi}(z,w) & 0\end{bmatrix}\,. \tag{283}$$

If $(\mathbf{z}(0), w(0)) \in \mathcal{D}$ then $\mathbf{z}^{\intercal}\, P\, \mathbf{z} \leq 1$, therefore from (282) one gets

$$\big|\boldsymbol{\Delta}_{4[j]}(z,w)\, \zeta(\mathbf{z},w)\big| \leq (\overline{u}_j - \overline{c}_j)\ \ \forall\, (\mathbf{z},w) \in \boldsymbol{\mathcal{Z}}^{+} \times \mathcal{W}^{+}\,,\ j \in \{1,2,\ldots,n_u\}\,, \tag{284}$$

recalling that $\boldsymbol{\Delta}_2(z,w)\, \zeta(\mathbf{z},w) = 0$. Since $(\mathbf{z},w) \in \mathcal{D} \Rightarrow w \in \mathcal{W}$, it follows that (282) implies $\mathcal{D} \subset \mathcal{S}$, where set $\mathcal{S}$ is defined as (256) using functions $\boldsymbol{\theta}(\mathbf{z},w)$ and $\boldsymbol{\vartheta}(\mathbf{z},w)$ from (279). By factorizing the vector $\begin{bmatrix}\mp(\overline{u}_j - \overline{c}_j)^{-1} & \mathbf{z}^{\intercal} & \varphi^{\intercal}(\mathbf{z},w)\end{bmatrix}^{\intercal}$ in inequality (282) and again using Lemma A.3, one should obtain the condition (274).

All conditions from Lemma 3.2 are therefore satisfied if (153), (154), (273), (274) and (275) are true. Consequently, the trajectory $\mathbf{z}(t)$ of the system (253) asymptotically converges to the origin for every initial condition $(\mathbf{z}(0), w(0)) \in \mathcal{D}$, satisfying (141) which is equivalent to (123). According to Lemma 4.1, it then follows that the original closed-loop system (113), (114) with controller (232), (233) (241) achieves output regulation for every initial condition in (157). Moreover, inequality (281) here also implies that $\dot{V}(\mathbf{z},w) < -2\alpha\, V(\mathbf{z})\ \forall\, (\mathbf{z},w) \in \mathcal{D}$, $\mathbf{z} \neq 0$, thus implying that (165) and (166) are true. Consequently, (P1) satisfies for the established conditions, and the second criterion (P2) is addressed equivalently by (156). □

According to Theorem 4.1, the domain of attraction estimate (157) with maximized volume can be numerically computed by the SDP problem

$$\min_{P,L,\mathrm{R}_0,\ldots,\hat{\Pi}_{\mathrm{m}}} \ \mathrm{tr}(P)\ \ \text{s.t.}\ \ \big\{(153)\,,\,(154)\,,\,(156)\,,\,(273)\,,\,(274)\,,\,(275)\big\}\,, \tag{285}$$

noting that just P, L, R_0, …, Π_{m} are being regarded as decision variables, not including the stabilizing and anti-windup parameters F_0, …, W_{n} and the diagonal matrix T. The optimization problem can be employed as an stability analysis tool, provided there are some candidate parameters $T, \mathrm{F}_0, \ldots, \mathrm{W}_{\mathrm{n}}$ fixed *a priori*. The next pages will focus on extending the methodology so as to additionally regard these parameters as free decision variables, thus providing a synthesis procedure.

4.3.5 Design Conditions

Towards obtaining stability and performance conditions for synthesis purposes, the output feedback congruence transformations proposed by SCHERER; GAHINET; CHILALI (1997) can be adapted to the current scope. This approach led to the development of new conditions as stated by the following theorem, where the stabilizing controller order is now being fixed as $n_s = n_z$.

Theorem 4.2. *Suppose there exist symmetric matrices $X, Y \in \mathbb{R}^{n_z \times n_z}$, a diagonal matrix $\hat{T} \in \mathbb{R}^{n_u \times n_u}$ and matrices $L \in \mathbb{R}^{n_\varphi \times n_\varphi}$, $\hat{\mathrm{R}}_0, \ldots, \hat{\mathrm{R}}_\mathrm{m} \in \mathbb{R}^{n_u \times n_z}$, $\hat{\Xi}_0, \ldots, \hat{\Xi}_\mathrm{m} \in \mathbb{R}^{n_u \times n_z}$, $\hat{\Pi}_0, \ldots, \hat{\Pi}_\mathrm{m} \in \mathbb{R}^{n_u \times n_\varphi}$, $\hat{\mathrm{F}}_0, \ldots, \hat{\mathrm{F}}_\mathrm{n} \in \mathbb{R}^{n_z \times n_z}$, $\hat{\mathrm{G}}_0, \ldots, \hat{\mathrm{G}}_\mathrm{n} \in \mathbb{R}^{n_z \times n_\varepsilon}$, $\hat{\mathrm{H}}_0, \ldots, \hat{\mathrm{H}}_\mathrm{n} \in \mathbb{R}^{n_v \times n_z}$, $\hat{\mathrm{K}}_0, \ldots, \hat{\mathrm{K}}_\mathrm{n} \in \mathbb{R}^{n_v \times n_\varepsilon}$, $\hat{\mathrm{E}}_0, \ldots, \hat{\mathrm{E}}_\mathrm{n} \in \mathbb{R}^{n_m \times n_u}$ and $\hat{\mathrm{W}}_0, \ldots, \hat{\mathrm{W}}_\mathrm{n} \in \mathbb{R}^{n_z \times n_u}$ such that* (168)*,* (169)*,* (171)*,*

$$\hat{T} \succ 0 \,, \tag{286}$$

$$\begin{bmatrix} (\overline{u}_j - \overline{c}_j)^2 & \begin{matrix} Q_{[j]}(z,w)X + \\ D_{[j]}\hat{H}(z,w) - \\ \hat{R}_{[j]}(z,w) \end{matrix} & \begin{matrix} Q_{[j]}(z,w) + \\ D_{[j]}K(z,w)C - \\ \hat{\Xi}_{[j]}(z,w) \end{matrix} & \begin{matrix} \Upsilon_{[j]}(z,w) + \\ D_{[j]}K(z,w)\Gamma - \\ \hat{\Pi}_{[j]}(z,w) \end{matrix} \\ \star & X & I & -X\,\Psi^\intercal(z,w)L^\intercal \\ \star & \star & Y & -\Psi^\intercal(z,w)L^\intercal \\ \star & \star & \star & -\mathcal{H}\{L\Omega(z,w)\} \end{bmatrix} \succ 0 \tag{287}$$

$$\forall\,(z,w) \in \mathcal{V}_z \times \mathcal{V}_w \;,\; j \in \{1,2,\ldots,n_u\}\,,$$

$$\mathcal{H}\left\{\begin{bmatrix} \begin{matrix} A(z,w)X + \\ B\hat{H}(z,w) + \\ \alpha X \end{matrix} & \begin{matrix} A(z,w) + \\ B\hat{K}(z,w)C + \\ \alpha I \end{matrix} & \begin{matrix} \Phi(z,w) + \\ B\hat{K}(z,w)\Gamma \end{matrix} & \begin{matrix} BD_m^\intercal\hat{E}(z,w) - \\ BD^\intercal\hat{T} \end{matrix} \\ \begin{matrix} \hat{F}(z,w) + \\ \alpha I \end{matrix} & \begin{matrix} YA(z,w) + \\ \hat{G}(z,w)C + \\ \alpha Y \end{matrix} & \begin{matrix} Y\Phi(z,w) + \\ \hat{G}(z,w)\Gamma \end{matrix} & \hat{W}(z,w) \\ L\Psi(z,w)X & L\Psi(z,w) & L\Omega(z,w) & 0 \\ \hat{R}(z,w) & \hat{\Xi}(z,w) & \hat{\Pi}(z,w) & -\hat{T} \end{bmatrix}\right\} \prec 0$$

$$\forall\,(z,w) \in \mathcal{V}_z \times \mathcal{V}_w \,, \tag{288}$$

where $\hat{F}(z,w)$, ... , $\hat{K}(z,w)$ are defined as in (172)*, $\hat{E}(z,w)$ and $\hat{W}(z,w)$ are*

$$\begin{bmatrix} \hat{E}(z,w) \\ \hat{W}(z,w) \end{bmatrix} \triangleq \begin{bmatrix} \hat{\mathrm{E}}_0 \\ \hat{\mathrm{W}}_0 \end{bmatrix} + \sum_{i=1}^{\mathrm{n}} \begin{bmatrix} \hat{\mathrm{E}}_i \\ \hat{\mathrm{W}}_i \end{bmatrix} \lambda_i(z,w) \,, \tag{289}$$

and matrices $\hat{R}(z,w)$, $\hat{\Xi}(z,w)$ and $\hat{\Pi}(z,w)$ denote

$$\begin{bmatrix} \hat{R}(z,w) & \hat{\Xi}(z,w) & \hat{\Pi}(z,w) \end{bmatrix} \triangleq \begin{bmatrix} \hat{\mathrm{R}}_0 & \hat{\Xi}_0 & \hat{\Pi}_0 \end{bmatrix} + \sum_{i=1}^{\mathrm{m}} \begin{bmatrix} \hat{\mathrm{R}}_i & \hat{\Xi}_i & \hat{\Pi}_i \end{bmatrix} \nu_i(z,w) \,, \tag{290}$$

for any linear function $\nu : \mathcal{Z}^+ \times \mathcal{W}^+ \to \mathbb{R}^\mathrm{m}$, $\mathrm{m} \in \mathbb{N}$. Then the closed-loop system (113)*,* (114) *with controller* (232)*,* (233)*,* (241) *achieves output regulation ans satisfies* (P1) *and* (P2) *for every initial condition in* (157) *with P given by* (173)*, stabilizing controller parameters F_i, G_i, H_i and K_i $\forall\, i \in \{0,1,\ldots,\mathrm{n}\}$ obtained by* (174) *and anti-windup*

parameters E_i *and* $\mathrm{W}_i \; \forall \, i \in \{0, 1, \ldots, \mathrm{n}\}$ *constructed as*

$$\left\{ \begin{array}{rcl} \mathrm{E}_i & = & \hat{\mathrm{E}}_i \, \hat{T}^{-1} \, , \; i = 0, 1, \ldots, \mathrm{n} \, , \\ \mathrm{W}_0 & = & N^{-1}(\hat{\mathrm{W}}_0 - YBD_m^{\mathsf{T}} \hat{\mathrm{E}}_0)\hat{T}^{-1} + N^{-1}YBD^{\mathsf{T}} \, , \\ \mathrm{W}_i & = & N^{-1}(\hat{\mathrm{W}}_i - YBD_m^{\mathsf{T}} \hat{\mathrm{E}}_i)\hat{T}^{-1} \, , \; i = 1, \ldots, \mathrm{n} \, , \end{array} \right. \tag{291}$$

where the pair $M, N \in \mathbb{R}^{n_z \times n_z}$ *is a non-singular solution to* (175)*.*

Proof. Suppose conditions from Theorem 4.1 hold for $n_s = n_z$ and for P decomposed as (176), where $X, Y \in \mathbb{R}^{n_z \times n_z}$ are symmetric matrices and $M, N \in \mathbb{R}^{n_z \times n_z}$ are generic square matrices. Since $P^{-1}P = I$, then condition (175) must be satisfied. Consider the same blocks $Z_1, Z_2 \in \mathbb{R}^{n_a \times n_a}$ shown in (177), where $PZ_1 = Z_2$. Applying the congruence transformations Z_1, $\mathrm{diag}\{1, Z_1\}$, $\mathrm{diag}\{Z_1, Z_1\}$, T^{-1}, $\mathrm{diag}\{1, Z_1, I\}$ and $\mathrm{diag}\{Z_1, I, T^{-1}\}$ into (153), (154), (156), (273), (274) (275) leads respectively to (168), (169), (171), (286), (287) and (288) when considering the change of variables (178),

$$\left\{ \begin{array}{rcl} \hat{E}(z,w) & = & E(z,w)T^{-1} \\ \hat{W}(z,w) & = & YBD_m^{\mathsf{T}} E(z,w)T^{-1} - YBD^{\mathsf{T}}T^{-1} + NW(z,w)T^{-1} \end{array} \right. , \tag{292}$$

$\hat{T} = T^{-1}$, $\hat{R}(z,w) = R(z,w)X + \Xi(z,w)M^{\mathsf{T}}$, $\hat{\Xi}(z,w) = R(z,w)$ and $\hat{\Pi}(z,w) = \Pi(z,w)$. From straightforward inversion of (178) and (292), one obtains respectively (179) and

$$\left\{ \begin{array}{rcl} E(z,w) & = & \hat{E}(z,w)\hat{T}^{-1} \\ W(z,w) & = & N^{-1}\hat{W}(z,w)\hat{T}^{-1} - N^{-1}YBD_m^{\mathsf{T}}\hat{E}(z,w)\hat{T}^{-1} + N^{-1}YBD^{\mathsf{T}} \end{array} \right. , \tag{293}$$

which leads to (174) and (291) by considering the definitions of $A(z,w)$ from (144), of $F(z,w)$, ... , $K(z,w)$ from (136), of $\hat{F}(z,w)$, ... , $\hat{K}(z,w)$ from (172), of $E(z,w)$ and $W(z,w)$ from (247) and of $\hat{E}(z,w)$ and $\hat{W}(z,w)$ from (289). Also, matrix P can be reconstructed as (173) since $P = Z_2 \, Z_1^{-1}$. In closing, conditions from Theorem 4.1 are then equivalent to Theorem 4.2 when considering a full order stabilizing controller $n_s = n_z$. □

Similar to the methodology described in the previous chapter, the stabilizing and anti-windup parameters can be synthesized by the following optimization problem in order to maximize the volume of the domain of attraction estimate:

$$\min_{X,Y,L,\hat{T},\hat{\mathrm{R}}_0,\ldots,\hat{\Pi}_\mathrm{m},\hat{\mathrm{F}}_0,\ldots,\hat{\mathrm{W}}_\mathrm{n}} \; \mathrm{tr}(Y) \;\; \text{s.t.} \; \Big\{ (168) \, , \, (169) \, , \, (288) \, , \, (286) \, , \, (287) \, , \, (288) \Big\} \, . \tag{294}$$

This optimization problem notably contains bilinear terms in (287) and (288) with respect to the pair of variables L and X, similar as problem (180) presented before. Recall that Appendix A.2 shows a procedure capable of searching for a local solution to this class of optimization problems.

Remark 4.1. Linear function $\nu(z,w)$ contained in (290) can always be set as $\nu(z,w) = 0$ in order to reduce the numerical complexity of stability conditions (287) and (288). On the other hand, it is suggested to consider $\nu(z,w) = [z^{\mathsf{T}} \;\; w^{\mathsf{T}}]^{\mathsf{T}}$ in order to obtain less conservative results.

In case the additional Assumption 3.3 is true, as detailed in the previous chapter, it is suggested again to include function $\varphi(y)$ into the stabilizing stage (241):

$$\left\{ \begin{array}{rcl} \dot{\xi}_s & = & \mathrm{F}(y)\,\xi_s + \mathrm{G}(y)\,\varepsilon + \Lambda(y)\,\varphi(y) + \mathrm{W}(y)\,\psi(\mu) \\ v & = & \mathrm{H}(y)\,\xi_s + \mathrm{K}(y)\,\varepsilon + \Theta(y)\,\varphi(y) \end{array} \right. . \tag{295}$$

The complementary terms $\Lambda : \mathbb{R}^{n_y} \to \mathbb{R}^{n_s \times n_\varphi}$ and $\Theta : \mathbb{R}^{n_y} \to \mathbb{R}^{n_v \times n_\varphi}$ can be parametrized according to (184), where $\Lambda_0, \ldots, \Lambda_\mathrm{n} \in \mathbb{R}^{n_s \times n_\varphi}$ and $\Theta_0, \ldots, \Theta_\mathrm{n} \in \mathbb{R}^{n_v \times n_\varphi}$ are free design matrices. The modified stabilized stage (295) can be also verified to satisfy the regulation requirement (122) from Lemma 4.1, since $\varphi(d(w)) = \varphi(0, w) = 0 \; \forall \, w \in \mathcal{W}$.

By substituting the original stabilizing stage (241) with (295), not only additional degree of freedom is provided for the design, but also (294) can be reframed as a convex optimization problem. In this modified case, matrices $\boldsymbol{\Phi}(z, w)$ and $\boldsymbol{\Upsilon}(z, w)$ of the augmented system representation (253) are redefined according to

$$\begin{array}{rcl} \boldsymbol{\Phi}(z, w) & = & \begin{bmatrix} \Phi(z, w) + BK(z, w)\Gamma + B\Theta(z, w) \\ \Lambda(z, w) + G(z, w)\Gamma \end{bmatrix}, \\ \boldsymbol{\Upsilon}(z, w) & = & \Upsilon(z, w) + DK(z, w)\Gamma + D\Theta(z, w)\,. \end{array} \tag{296}$$

From these observations, Theorem 4.2 can be restated according to the next corollary.

Corollary 4.1. *Suppose there exist symmetric matrices $X, Y \in \mathbb{R}^{n_z \times n_z}$, a diagonal matrix $\hat{T} \in \mathbb{R}^{n_u \times n_u}$ and matrices $\hat{L} \in \mathbb{R}^{n_\varphi \times n_\varphi}$, $\hat{\mathrm{R}}_0, \ldots, \hat{\mathrm{R}}_\mathrm{m} \in \mathbb{R}^{n_u \times n_z}$, $\hat{\Xi}_0, \ldots, \hat{\Xi}_\mathrm{m} \in \mathbb{R}^{n_u \times n_z}$, $\hat{\Pi}_0, \ldots, \hat{\Pi}_\mathrm{m} \in \mathbb{R}^{n_u \times n_\varphi}$, $\hat{\mathrm{F}}_0, \ldots, \hat{\mathrm{F}}_\mathrm{n} \in \mathbb{R}^{n_z \times n_z}$, $\hat{\mathrm{G}}_0, \ldots, \hat{\mathrm{G}}_\mathrm{n} \in \mathbb{R}^{n_z \times n_\varepsilon}$, $\hat{\mathrm{H}}_0, \ldots, \hat{\mathrm{H}}_\mathrm{n} \in \mathbb{R}^{n_v \times n_z}$, $\hat{\mathrm{K}}_0, \ldots, \hat{\mathrm{K}}_\mathrm{n} \in \mathbb{R}^{n_v \times n_\varepsilon}$, $\hat{\Lambda}_0, \ldots, \hat{\Lambda}_\mathrm{n} \in \mathbb{R}^{n_z \times n_\varphi}$, $\hat{\Theta}_0, \ldots, \hat{\Theta}_\mathrm{n} \in \mathbb{R}^{n_v \times n_\varphi}$, $\hat{\mathrm{E}}_0, \ldots, \hat{\mathrm{E}}_\mathrm{n} \in \mathbb{R}^{n_m \times n_u}$ and $\hat{\mathrm{W}}_0, \ldots, \hat{\mathrm{W}}_\mathrm{n} \in \mathbb{R}^{n_z \times n_u}$ such that* (168)*,* (169)*,* (171)*,* (286)*,*

$$\begin{bmatrix} & Q_{[j]}(z, w)X + & Q_{[j]}(z, w) + & \Upsilon_{[j]}(z, w)\hat{L} + \\ (\overline{u}_j - \overline{c}_j)^2 & D_{[j]}\hat{H}(z, w) - & D_{[j]}K(z, w)C - & D_{[j]}\hat{\Theta}(z, w) - \\ & \hat{R}_{[j]}(z, w) & \hat{\Xi}_{[j]}(z, w) & \hat{\Pi}_{[j]}(z, w) \\ \star & X & I & -X\,\Psi^{\intercal}(z, w) \\ \star & \star & Y & -\Psi^{\intercal}(z, w) \\ \star & \star & \star & -\mathcal{H}\{\Omega(z, w)\hat{L}\} \end{bmatrix} \succ 0 \tag{297}$$

$$\forall\,(z, w) \in \mathcal{V}_z \times \mathcal{V}_w \;,\; j \in \{1, 2, \ldots, n_u\}\,,$$

$$\mathcal{H}\left\{ \begin{bmatrix} A(z, w)X + B\hat{H}(z, w) + \alpha X & A(z, w) + B\hat{K}(z, w)C + \alpha I & \Phi(z, w)\hat{L} + B\hat{\Theta}(z, w) & BD_m^{\intercal}\hat{E}(z, w) - BD^{\intercal}\hat{T} \\ \hat{F}(z, w) + \alpha I & YA(z, w) + \hat{G}(z, w)C + \alpha Y & \hat{\Lambda}(z, w) & \hat{W}(z, w) \\ \Psi(z, w)X & \Psi(z, w) & \Omega(z, w)\hat{L} & 0 \\ \hat{R}(z, w) & \hat{\Xi}(z, w) & \hat{\Pi}(z, w) & -\hat{T} \end{bmatrix} \right\} \prec 0$$

$$\forall\,(z, w) \in \mathcal{V}_z \times \mathcal{V}_w \;, \tag{298}$$

where $\hat{F}(z, w)$, ..., $\hat{K}(z, w)$ are defined as in (172)*, $\hat{\Theta}(z, w)$ and $\hat{\Lambda}(z, w)$ are identical to* (187)*, $\hat{E}(z, w)$ and $\hat{W}(z, w)$ are represented by* (289) *and matrices $\hat{R}(z, w)$, $\hat{\Xi}(z, w)$ and $\hat{\Pi}(z, w)$ are the same as in* (290) *for any linear function $\nu : \mathcal{Z}^+ \times \mathcal{W}^+ \to \mathbb{R}^\mathrm{m}$, $\mathrm{m} \in \mathbb{N}$.*

Then the closed-loop system (113)*,* (114) *with controller* (232)*,* (233)*,* (295) *achieves output regulation and satisfies* (P1) *and* (P2) *for every initial condition in* (157) *with* P *given by* (173)*, stabilizing controller parameters* F_i *, . . . ,* $\Theta_i \; \forall \, i \in \{0, 1, \ldots, \mathrm{n}\}$ *obtained by* (174) *and* (188)*, and with anti-windup parameters* E_i *and* $\mathrm{W}_i \; \forall \, i \in \{0, 1, \ldots, \mathrm{n}\}$ *constructed by* (291)*, where the pair* $M, N \in \mathbb{R}^{n_z \times n_z}$ *is a non-singular solution to* (175)*.*

Proof. Consider the same proof presented for Theorem 4.2, except post- and pre-multiply (274) and (275) respectively with $\mathrm{diag}\{1, Z_1, L^{-\intercal}\}$, $\mathrm{diag}\{Z_1, L^{-\intercal}, T^{-1}\}$ and their transposes, which yield (297) and (298) when considering (296) and the change of variables (178), (189), $\hat{T} = T^{-1}$, $\hat{L} = L^{-\intercal}$, $\hat{R}(z, w) = R(z, w)X + \Xi(z, w)M^{\intercal}$, $\hat{\Xi}(z, w) = R(z, w)$ and $\hat{\Pi}(z, w) = \Pi(z, w)L^{-\intercal}$. From straightforward inversion of the variable transformations (178) and (189), one obtains respectively (174) and (188). □

According to Corollary 4.1, the parameters from stabilizing controller (295) and the anti-windup parameters can be synthesized by the convex optimization problem

$$\min_{X, Y, \hat{L}, \hat{T}, \hat{\mathrm{R}}_0, \ldots, \hat{\Pi}_\mathrm{m}, \hat{\mathrm{F}}_0, \ldots, \hat{\mathrm{W}}_\mathrm{n}} \; \mathrm{tr}(Y) \;\; \text{s.t.} \; \Big\{ (168)\,,\, (169)\,,\, (171)\,,\, (286)\,,\, (297)\,,\, (298) \Big\}\,, \quad (299)$$

where (297) and (298) now verify to be LMIs with respect to all decision variables.

4.4 Numerical Examples

This section illustrates the proposed control design methodology with two numerical control design examples. The cases to be shown here are the same ones from Section 3.4, where it was considered a polynomial nonlinear plant subject to a harmonic exosystem and a strictly rational nonlinear system subject to a chaotic exosystem.

4.4.1 Polynomial Nonlinear Plant with a Harmonic Exosystem

Consider here the same scenario explained in Subsection 3.4.1, where the plant to be output regulated is given by (192) and the exosystem dynamics is as in (193). The only difference here is that the control input $u \in \mathcal{U} \subset \mathbb{R}$ is now bounded by a compact constraining set $\mathcal{U} = [-\overline{u}, \overline{u}]$, for some $\overline{u} > 0$.

The overall objective of this example is to design an output feedback controller such that the error signal $e(t)$ asymptotically approaches zero and $u(t) \in \mathcal{U} \; \forall \, t \geq 0$. In order to properly deal with such problem, the anti-windup regulation framework explained on Section 4.2 will be illustrated.

The design of internal model functions $\phi_m(\xi_m, y)$ and $\theta_m(\xi_m, y)$ here is identical to the original case detailed in Subsection 3.4.1. Therefore, the sequel will jump straight to the stabilizing stage and anti-windup design.

4.4.1.1 Stabilizing stage and anti-windup design

The preliminary stabilizing stage design considerations are assumed equal to the previous chapter, namely $\varepsilon = \delta(y) = y$ and $\lambda(y) = 0$.

The initial step in this design procedure is to represent the system equations in the regulation error form (133) using coordinate change (132), which for the example is (200). By developing all the regulation error system functions $f_z(z, w, \hat{v})$, $\theta_z(z, w)$, $g_z(z, w)$,

$h_z(z,w)$ and $\delta_z(z,w)$, one should obtain

$$f_z(z,w,\hat{v}) = \begin{bmatrix} z_2 \\ \mathrm{a}\,(z_1^2 z_2 + \omega\, z_1^2 w_2 + 2\omega\, z_1 w_1 w_2 + z_2 w_1^2 + 2\, z_1 z_2 w_1) + \mathrm{b}\,(z_3 + \hat{v}_1) \\ z_4 + \hat{v}_2 \\ z_5 + \hat{v}_3 \\ z_6 + \hat{v}_4 \\ -9\omega^4\, z_3 - 10\omega^2\, z_5 + \hat{v}_5 \end{bmatrix}, \tag{300}$$

$\theta_z(z) = z_3$ and $g_z(z) = h_z(z) = \delta_z(z) = z_1$, where in comparison to (300) the original variable v has simply changed to $\hat{v}$, noting that $\hat{v}$ denotes the definition from (243).

The second step is to choose an appropriate differential-algebraic representation for the functions $f_z(z,w,\hat{v})$, $\delta_z(z)$ and now additionally for $\theta_z(z)$. The same vector of rational nonlinearities $\varphi(z,w)$ from (202) may be used for this purpose. In turn, functions $f_z(z,w,\hat{v})$, $\delta_z(z)$ and $\theta_z(z)$ may be expressed in the DAR framework of (250) and (251) with the same matrices from (203) and the following complementary ones for $\theta_z(z)$:

$$Q = \begin{bmatrix} 0 & 0 & 1 & 0 & 0 & 0 \end{bmatrix}, \quad \Upsilon = \begin{bmatrix} 0 & 0 \end{bmatrix}. \tag{301}$$

The third step is to define the bounding sets $\mathcal{W} \subseteq \mathcal{W}^+ \subseteq \mathbb{R}^2$ and $\{0\} \subset \mathrm{int}\{\mathcal{Z}^+\} \subseteq \mathbb{R}^6$ in order to numerically approach the synthesis problem. The definition for these sets is here considered identical to the original case explained in Subsection 3.4.1.

An extra design choice in the current input constrained case is the function $\nu(z,w)$, which defines the affinity of free decision variables $R(z,w)$, $\Xi(z,w)$ and $\Pi(z,w)$ mentioned throughout the chapter. Since the considered sets $\mathcal{Z}^+$ and $\mathcal{W}^+$ impose restrictions on the dimensions z_1, w_1 and w_2, the function $\nu(z,w)$ may be defined accordingly as

$$\nu(z,w) = \begin{bmatrix} z_1 & w_1 & w_2 \end{bmatrix}^{\mathsf{T}}. \tag{302}$$

The system parameters here are the same as those used in Subsection 3.4.1. The design constraints for lower bound decay rate and upper bound system matrix eigenvalue are being set respectively as $\alpha = 5 \cdot 10^{-2}$ and $r = 1.2 \cdot 10^2$. It is being also defined $\overline{w} = 1$ and $\overline{e} = 3$ with respect to the bounding sets $\mathcal{Z}^+$ and $\mathcal{W}^+$. Lastly, the new input amplitude constraint is being configured as $\overline{u} = 20$. In order to compute the required magnitude bound of the steady-state control $c(w)$, the optimization problem (272) was evaluated, which resulted $|c(w)| \leq \overline{c} = 1.4142\ \forall\, w \in \mathcal{W}$, satisfying the requirement $\overline{c} \leq \overline{u}$.

Given all these numerical values, the optimization problem (294) was considered in order to synthesize the stabilizing and anti-windup gains. The iterative procedure in Appendix A.2 was again employed so as to handle the bilinear terms involving some of the decision variables. It was necessary to perform 2 iterations in the feasibility phase until achieving an strictly feasible solution, and it took 8 iterations in the optimization phase in order to achieve an objective value decrement smaller than 10^{-4} over the last 4 iterations. The ultimately obtained solution has the objective value $\mathrm{tr}(Y) = 0.4502$, the stabilizing

parameters

$$\mathrm{F} = \begin{bmatrix} -2.4662 & -1.6244 & 2.1420 & -95.216 & 0.4291 & 0.0007 \\ 0.5743 & -2.3124 & -0.6389 & 11.335 & -0.0389 & -0.0001 \\ -0.1314 & 0.2395 & -1.9264 & 43.426 & 0.4034 & 0.0011 \\ 0.0597 & -0.0422 & -0.6082 & -7.2421 & -0.0810 & -0.0003 \\ -0.4450 & 0.0707 & -2.0177 & 10.120 & -110.23 & 0.0035 \\ -0.0001 & 0.0000 & -0.0014 & 0.0040 & -0.0001 & -107.31 \end{bmatrix}, \quad \mathrm{G} = \begin{bmatrix} -27.958 \\ 2.2850 \\ -36.062 \\ 6.7897 \\ 8880.0 \\ 5.8784 \end{bmatrix},$$

$$\mathrm{H} = \begin{bmatrix} -56.918 & 7.4569 & -7.2729 & -17.390 & 2.0567 & -0.0024 \\ -134.09 & 21.096 & 74.560 & -5629.3 & 13.540 & 0.0049 \\ 12.096 & 226.02 & 42.321 & -1111.9 & 0.3756 & 0.0042 \\ 53.604 & -3.4787 & 737.04 & -4987.3 & 2.1134 & 0.0277 \\ 12.973 & 23.842 & -117.10 & 4557.7 & 2.3670 & -0.0212 \end{bmatrix}, \quad \mathrm{K} = \begin{bmatrix} -187.02 \\ -721.00 \\ 74.995 \\ 441.27 \\ -675.53 \end{bmatrix}, \tag{303}$$

and the following anti-windup gains:

$$\mathrm{E} = \begin{bmatrix} -4.4910 \\ 0.2108 \\ 3.0697 \\ -2.2942 \end{bmatrix}, \quad \mathrm{W} = \begin{bmatrix} -0.1611 \\ 0.0133 \\ -0.1993 \\ 0.0376 \\ 49.498 \\ 0.0363 \end{bmatrix}. \tag{304}$$

4.4.1.2 Numerical results and discussion

Figures 16 and 17 show results obtained from a numerical simulation of the closed-loop system with the proposed controller. For generating these plots, the controller initial condition was set as $\xi(0) = 0$ and the exosystem initial state was defined with the default values $w(0) = [0\ 1]^\intercal$. On the other hand, two different plant initial states were considered, which are $x(0) = [1.1\ \ 6.578]^\intercal$ and $x(0) = [-1.3\ \ -3.809]^\intercal$. The responses for each of these initial conditions are depicted respectively by black and gray shades on Figures 16 and 17. So as to induce control input saturation, these plant initial states were chosen such that $(\mathbf{z}(0), w(0))$ is marginally close to the border of the estimated domain of attraction $\mathcal{D}$, which is subsequently represented by Figure 18.

Figure 16 depicts on top the system output error signals $e(t)$, showing asymptotic convergence for both initial conditions tested. The bottom plot of Figure 16 and the next Figure 17 illustrate the control input signals $u(t)$ generated by the designed controller. In these pictures, one can clearly see the initial saturation effect, followed by a smooth transition to the steady-state regime, when the signals asymptotically approach $c(w(t))$.

Lastly, Figure 18 shows the set of viable plant initial conditions $x(0)$. In this figure, the black contour denotes the border of $\mathcal{D}$ when the other initial states are set at the default scenario, namely $\xi(0) = 0$ and $w(0) = [0\ \ 1]^\intercal$. The gray contours in turn denote a sweep through several exosystem initial states $w(0)$ inside the admissible disk $\mathcal{W}$. Moreover, the black dots represent the same initial states used for evaluation of the trajectories presented by Figures 16 and 17.

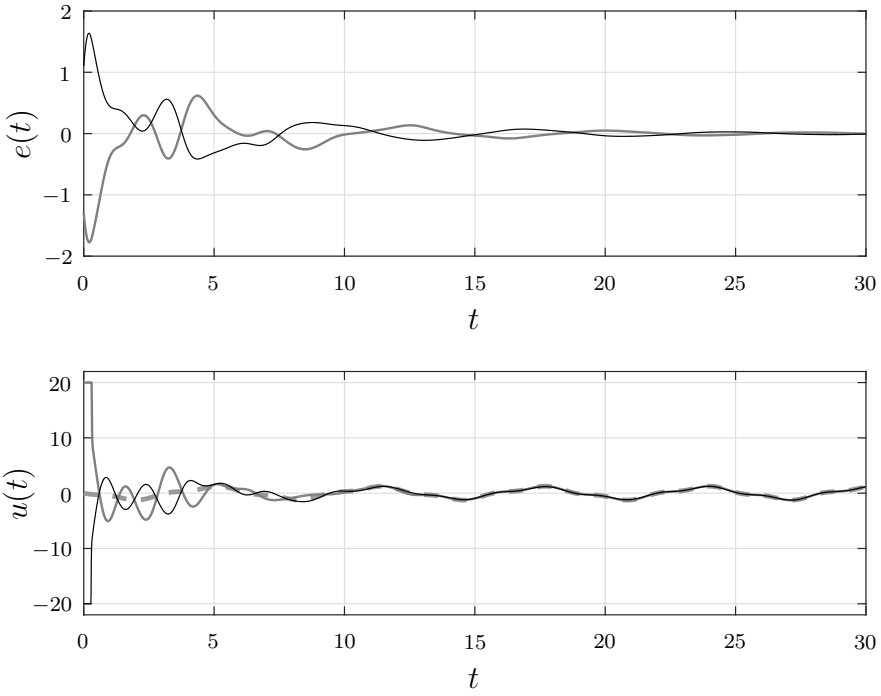

Figure 16: On top: the output regulation error signals $e(t)$. On bottom: the control input signals $u(t)$ compared to the zero-error steady-state signals $c(w(t))$ (dashed line). Shades denote different initial conditions on the border of $\mathcal{D}$. Source: the author.

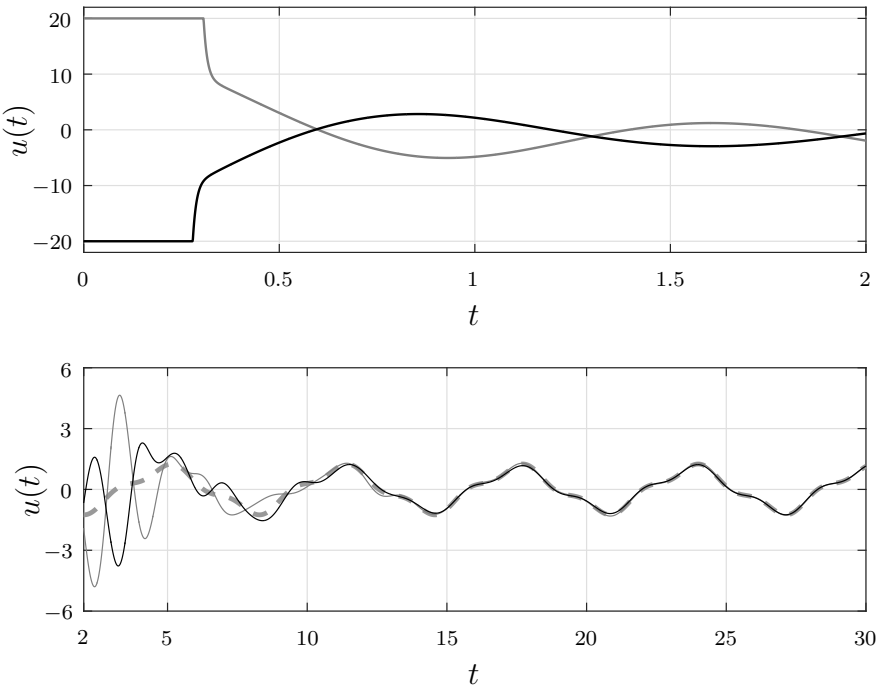

Figure 17: Zoomed in depiction of the control inputs $u(t)$ from Figure 16. The top plot details the initial saturated period, while the bottom graph shows the control signals approaching the steady-state waveform. Source: the author.

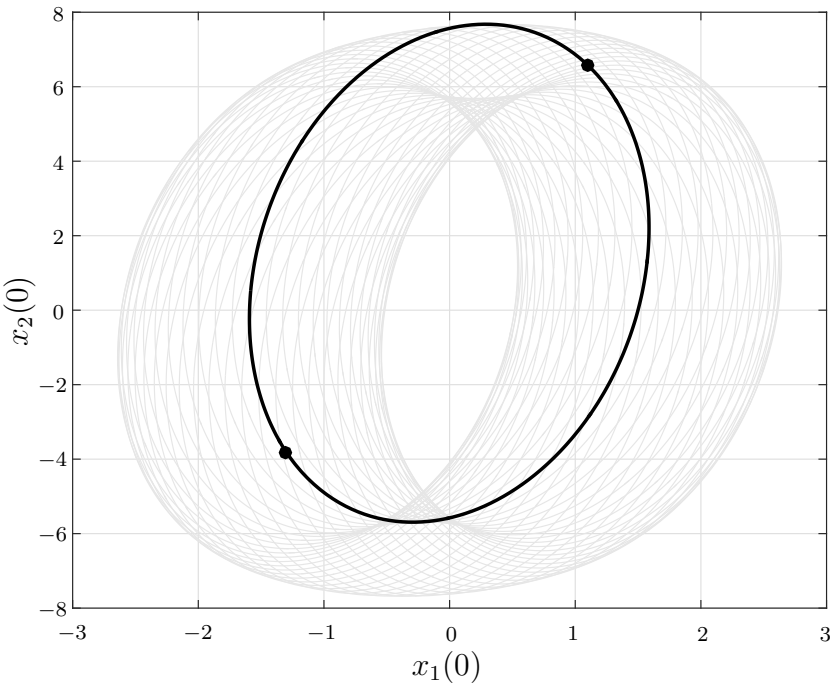

Figure 18: Representation of the set $\mathcal{D}$ in the x-state-space. The black contour is the region border for the default exosystem initial state. The gray contours denote borders for a myriad of exosystem initial states $w(0) \in \mathcal{W}$. Source: the author.

4.4.2 Rational Nonlinear Plant with a Chaotic Exosystem

Consider now the same example from Subsection 3.4.2, where a strictly rational nonlinear plant is considered as in (209) and it is subject to a chaotic exosystem of the form (210). The only difference now is that the control input $u \in \mathcal{U} \subset \mathbb{R}$ is bounded by a compact constraining set $\mathcal{U} = [-\overline{u}, \overline{u}]$, for some $\overline{u} > 0$. The overall objective is again to design an output feedback controller such that the error signal $e(t)$ asymptotically approaches zero, but also ensuring that $u(t) \in \mathcal{U} \; \forall \, t \geq 0$.

In spite of the additional input constraint, the design of internal model functions $\phi_m(\xi_m, y)$ and $\theta_m(\xi_m, y)$ remains identical to the original case detailed in Subsection 3.4.2. Therefore, the sequel will skip to the stabilizing stage and anti-windup design.

4.4.2.1 Stabilizing stage and anti-windup design

The preliminary stabilizing stage setups are assumed equal to the original case from Subsection 3.4.2, where the output measurement vanishing function was defined as $\delta(y) = y_1$ and the candidate gain scheduling function was set as $\lambda(y) = y_2$.

The first step required to design the stabilizing stage is to express the system using coordinate change (132). All functions of the regulation error system (244) now verify to be:

$$f_z(z,w,\hat{v}) = \begin{bmatrix} a_1 \dfrac{z_1^2}{1+z_1^2} + z_2 \\ a_1 \dfrac{z_1}{1+z_1^2} + a_3\,(z_4 - \hat{b}_2\, z_3 + \hat{v}_1) \\ b_1\,(z_4 - z_3) + \hat{v}_2 \\ b_2\, z_3 - z_4 - w_1 z_5 + \hat{v}_3 \\ w_1 z_4 - b_3\, z_5 + \hat{v}_4 \end{bmatrix}, \quad \begin{aligned} \theta_z(z) &= z_4 - \hat{b}_2\, z_3\ , \\ h_z(z) &= \delta_z(z) = z_1\ , \\ g_z(z) &= \begin{bmatrix} z_1 \\ 0 \end{bmatrix}. \end{aligned} \tag{305}$$

The candidate controller scheduling function may also be represented in the regulation error form, which is given by (219).

The second step is to choose an appropriate DAR for the functions $f_z(z,w,\hat{v})$, $\delta_z(z)$ and $\theta_z(z)$. The same vector of rational nonlinearities $\varphi(z,w)$ from (220) may be used for this purpose, and the same matrices from (221) may be employed to represent functions $f_z(z,w,\hat{v})$ and $\delta_z(z)$ according to (250) and (251). On the other hand, one should define the following complementary matrices in regard of $\theta_z(z)$:

$$Q = \begin{bmatrix} 0 & 0 & -\hat{b}_2 & 1 & 0 \end{bmatrix}, \quad \Upsilon = \begin{bmatrix} 0 & 0 \end{bmatrix}. \tag{306}$$

The same DAR properties highlighted in Subsection 3.4.2 remain applicable to the present case. Namely, $\Omega(z)$ is non-singular $\forall\, z \in \mathbb{R}^5$, the identity $A(w) = \mathrm{A}_0 + \mathrm{A}_1\, \lambda(w)$ holds for A_0 and A_1 defined as (222), and lastly, $\varphi(z)$ can be remapped with respect to the output measurement as (223). Such properties allow the implementation of the controller (295) and the synthesis can be addressed by a convex optimization problem, as indicated in (299).

The third step is to define the bounding sets $\mathcal{W} \subseteq \mathcal{W}^+ \subseteq \mathbb{R}^3$ and $\{0\} \subset \{\mathcal{Z}^+\} \subseteq \mathbb{R}^5$ in order to numerically approach the synthesis problem. The definition of these sets is considered identical to the one in Subsection 3.4.2. In this input constrained case, there is an extra design choice with respect to function $\nu(z,w)$ as mentioned previously by Remark 4.1. Because the considered sets $\mathcal{Z}^+$ and $\mathcal{W}^+$ impose restrictions on the dimensions z_1 and w_1 solely, the function $\nu(z,w)$ is recommended to be set as $\nu(z,w) = [z_1 \;\; w_1]^\intercal$.

The same original numeric values are being considered for plant and exosystem parameters. The performance specifications are being set as $\alpha = 5 \cdot 10^{-2}$ and $r = 10^2$, and additionally, the error bound is being defined as $\overline{e} = 10^4$. The new control input amplitude constraint is being configured as $\overline{u} = 4$. In order to compute the required magnitude bound of the steady-state control $c(w)$, the optimization problem (272) was employed, which yielded $|c(w)| \leq \overline{c} = 1.1388\ \forall\, w \in \mathcal{W}$, satisfying the requirement $\overline{c} \leq \overline{u}$. The numerical solution of SDP problem (299) resulted $\mathrm{tr}(Y) = 0.0364$ with the anti-windup parameters:

$$\mathrm{E}_0 = \begin{bmatrix} 10.987 \\ -3.8164 \\ 0.0000 \end{bmatrix}, \quad \mathrm{E}_1 = \begin{bmatrix} -0.0000 \\ 0.0000 \\ -0.1665 \end{bmatrix}, \quad \mathrm{W}_0 = \begin{bmatrix} -0.0000 \\ -7.5848 \\ 10.084 \\ 2.4057 \\ 0.0885 \end{bmatrix}, \quad \mathrm{W}_1 = \begin{bmatrix} 0.0102 \\ -0.0000 \\ 0.0000 \\ -0.0000 \\ -0.0000 \end{bmatrix}, \tag{307}$$

and with the following stabilizing controller matrices:

$$\mathrm{F}_0 = \begin{bmatrix} -2.8319 & 0.0000 & -0.0000 & -0.0000 & 0.0000 \\ 0.0000 & -38.436 & 1.0877 & 37.914 & -0.0416 \\ -0.0000 & 29.892 & -5.5886 & -33.378 & -0.0108 \\ -0.0000 & -0.2409 & -5.3848 & -97.606 & 0.0564 \\ -0.0000 & -0.0006 & 0.0014 & 0.0238 & -70.723 \end{bmatrix} \quad \mathrm{G}_0 = \begin{bmatrix} -0.0000 \\ 22.710 \\ -20.209 \\ -30.002 \\ 0.0073 \end{bmatrix} \quad \Lambda_0 = \begin{bmatrix} -0.0000 & -0.0000 \\ 0.2960 & -0.0068 \\ -0.3090 & 0.0054 \\ -0.2937 & 0.0004 \\ 0.0000 & 0.0000 \end{bmatrix},$$

$$\mathrm{H}_0 = \begin{bmatrix} -0.0000 & 17.319 & -11.013 & -8.5993 & 0.0129 \\ 0.0000 & -0.8341 & 25.962 & 28.724 & 0.0298 \\ 0.0000 & 3.7867 & 22.623 & -9.7841 & 0.1225 \\ 1.4855 & -0.0000 & 0.0000 & 0.0000 & -0.0000 \end{bmatrix} \quad \mathrm{K}_0 = \begin{bmatrix} -11.151 \\ 16.793 \\ 3.0488 \\ 0.0000 \end{bmatrix} \quad \Theta_0 = \begin{bmatrix} -0.0011 & -0.0013 \\ -0.0035 & -0.0065 \\ 0.0014 & 0.0040 \\ 0.0000 & 0.0000 \end{bmatrix},$$

$$\mathrm{F}_1 = \begin{bmatrix} 0.0000 & 0.5995 & 0.6565 & -0.0315 & -0.0000 \\ -0.8578 & 0.0000 & -0.0000 & -0.0000 & -0.0000 \\ -0.5653 & -0.0000 & 0.0000 & 0.0000 & 0.0000 \\ 0.0120 & 0.0000 & -0.0000 & -0.0000 & -0.0000 \\ -0.0000 & 0.0000 & -0.0000 & -0.0000 & 0.0000 \end{bmatrix} \quad \mathrm{G}_1 = \begin{bmatrix} 0.0159 \\ -0.0000 \\ 0.0000 \\ -0.0000 \\ -0.0000 \end{bmatrix} \quad \Lambda_1 = \begin{bmatrix} -0.0000 & -0.0000 \\ -0.0000 & -0.0000 \\ 0.0000 & -0.0000 \\ 0.0000 & 0.0000 \\ -0.0000 & -0.0000 \end{bmatrix},$$

$$\mathrm{H}_1 = \begin{bmatrix} -0.0000 & 0.0000 & -0.0000 & -0.0000 & 0.0000 \\ -0.1675 & 0.0000 & -0.0000 & -0.0000 & -0.0000 \\ -5.1170 & -0.0000 & 0.0000 & 0.0000 & -0.0000 \\ 0.0000 & -2.7107 & -3.1075 & 0.6548 & 0.0002 \end{bmatrix} \quad \mathrm{K}_1 = \begin{bmatrix} -0.0000 \\ -0.0000 \\ 0.0000 \\ 0.0359 \end{bmatrix} \quad \Theta_1 = \begin{bmatrix} 0.0000 & 0.0000 \\ -0.0000 & -0.0000 \\ 0.0000 & 0.0000 \\ -0.0000 & -0.0000 \end{bmatrix}. \tag{308}$$

4.4.2.2 Numerical results and discussion

Figures 19 and 20 present numerical simulations of the closed-loop system with initial conditions marginally close to the border of the estimated domain of attraction $\mathcal{D}$, in order to induce control input saturation. The chosen initial states are in turn $x(0) = [4 \;\; 1851.4]^\intercal$ and $x(0) = [-4 \;\; -1863.9]^\intercal$, where for both cases $\xi(0) = 0$ and the default exosystem initial condition $w(0)$ from (230) were used. The graphical representation of the set $\mathcal{D}$ and the considered initial states are afterwards shown in Figure 23.

Figure 19 shows on top the system output error signals $e(t)$, where asymptotic convergence to the origin is verified. Figure 20 and the bottom frame of Figure 19 also detail the control input signals $u(t)$ produced by the simulation runs, where one can clearly observe the effect of the saturation nonlinearity. Past the initial saturated period, the input signals smoothly approaches the non-vanishing and non-periodic excitation required to achieve output regulation. The tridimensional portraits in Figures 21 and 22 also expose the internal model trajectories generated by the simulations, respectively focusing on the transient and steady-state periods. In Figure 21, bold lines indicate the activation of the control input saturation, whereas thin lines mean the control input is unsaturated. Subsequently in Figure 22, one may observe ξ_m asymptotically approaching the zero-error trajectory $\sigma_m(w) = a_2 a_3^{-1}\, w$, which is the chaotic Lorenz exosystem trajectory scaled by the factor $a_2 a_3^{-1}$.

The set of all plant initial conditions $x(0)$ with assured theoretical convergence is represented in Figure 23. The black contour denotes the border of $\mathcal{D}$ when the other initial states are set at the default scenario, which is $\xi(0) = 0$ and $w(0)$ according to (230). The gray patches in turn represent a sweep through several conditions $w(0)$ inside the positively invariant set $\mathcal{W}$ of the exosystem. Figure 24 is also comparing the region $\mathcal{D}$ with the estimated domain of attraction in case the proposed anti-windup compensation is disabled, in this case evaluated by numerical simulations for a discrete set of initial states. One may clearly observe the gray crossings inside the $\mathcal{D}$ contour, cases where the anti-windup action was verified to be necessary in order to maintain the closed-loop stability.

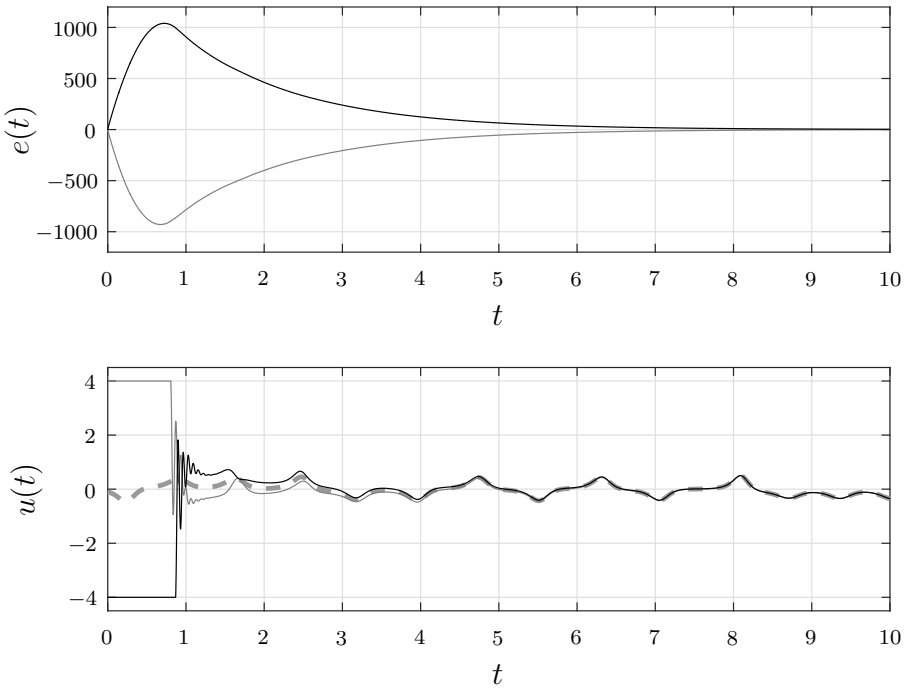

Figure 19: On top: the output regulation error signals $e(t)$. On bottom: the control input signals $u(t)$ compared to the zero-error steady-state signals $c(w(t))$ (dashed line). Shades denote different initial conditions on the border of $\mathcal{D}$. Source: the author.

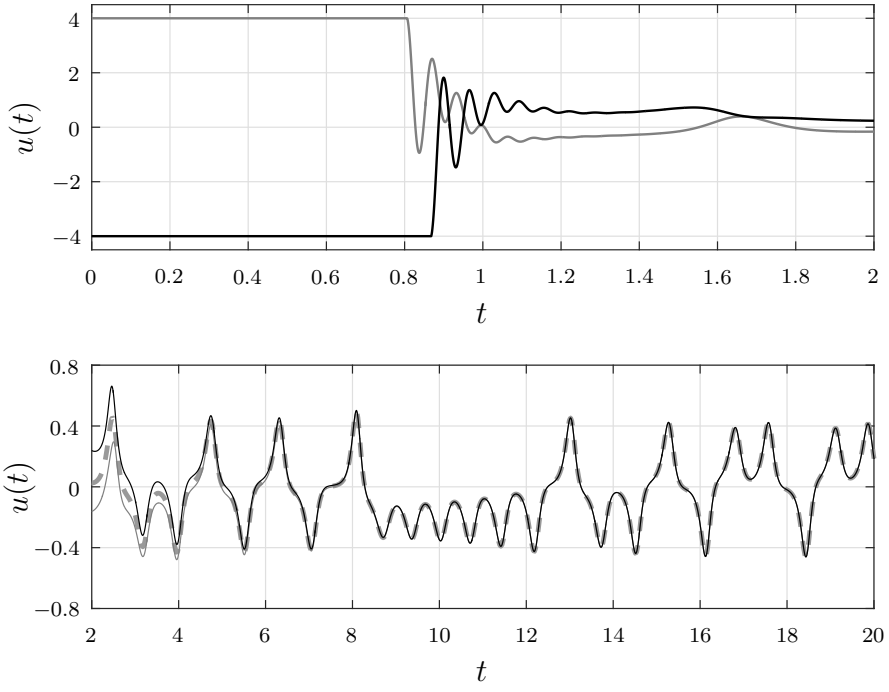

Figure 20: Zoomed in depiction of the control inputs $u(t)$ from Figure 19. Top plot details the initial saturated period, while bottom graph focuses on the steady-state. Source: the author.

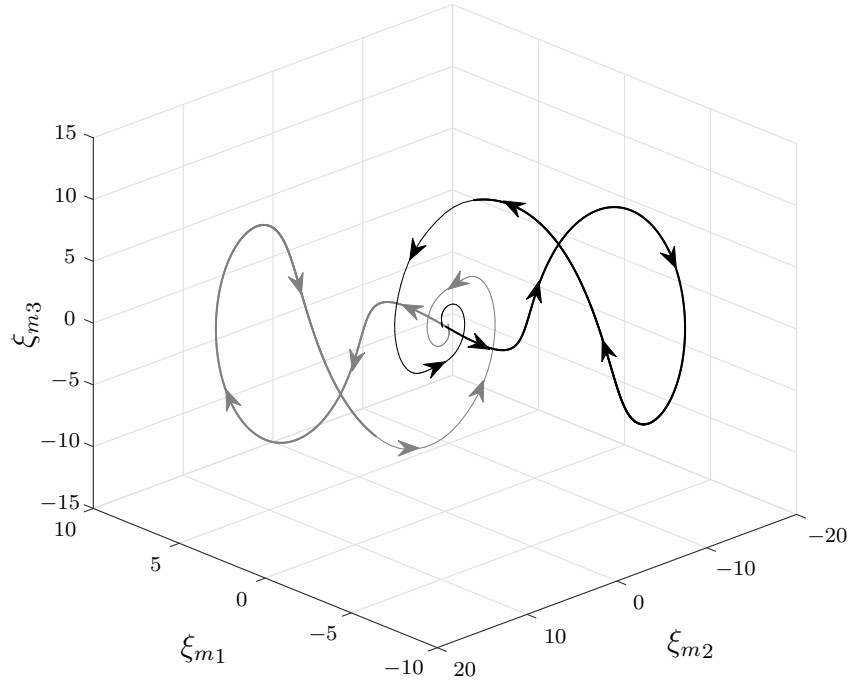

Figure 21: Phase portrait depicting transient internal model trajectories ξ_m for different plant initial conditions. The thick lines indicate activation of the control input saturation. Source: the author.

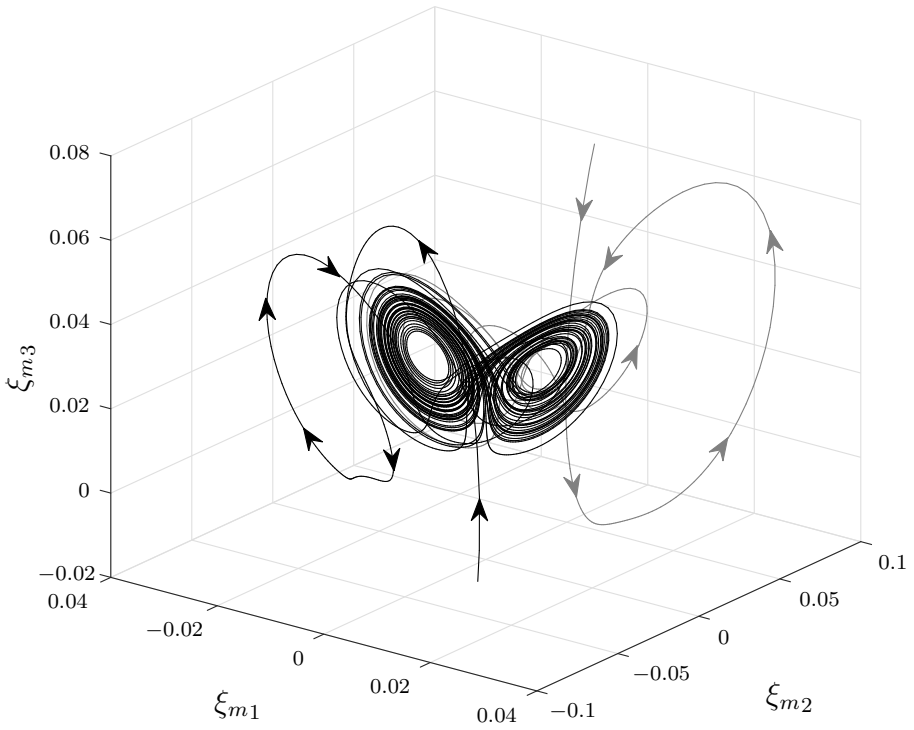

Figure 22: Phase portrait depicting internal model trajectories ξ_m in the steady-state. Source: the author.

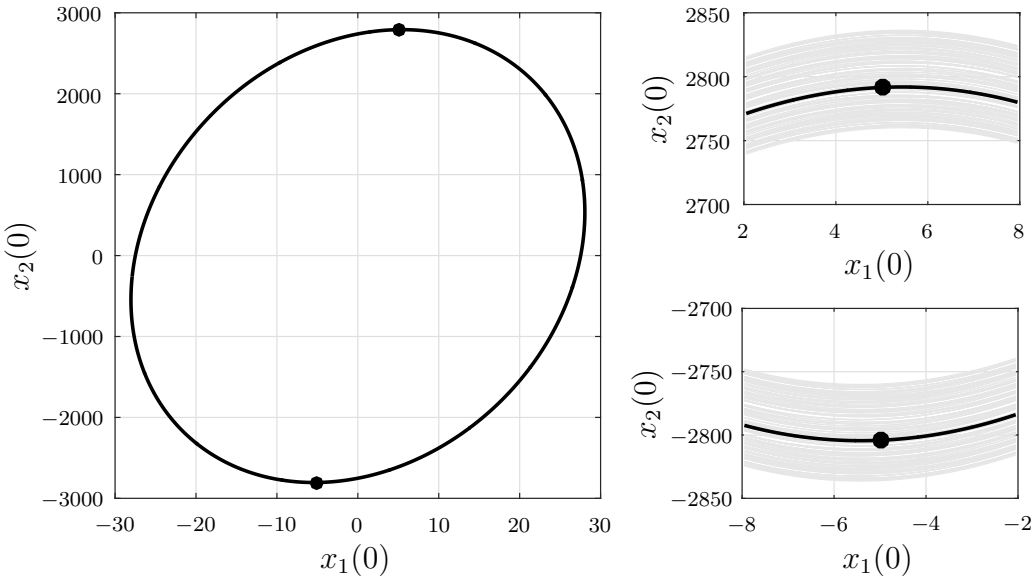

Figure 23: Representation of the set $\mathcal{D}$ in the x-state-space. The black contour is the border of $\mathcal{D}$ for the default exosystem initial state from (230). The gray patches denote borders of $\mathcal{D}$ for a myriad of exosystem initial states $w(0) \in \mathcal{W}$. Source: the author.

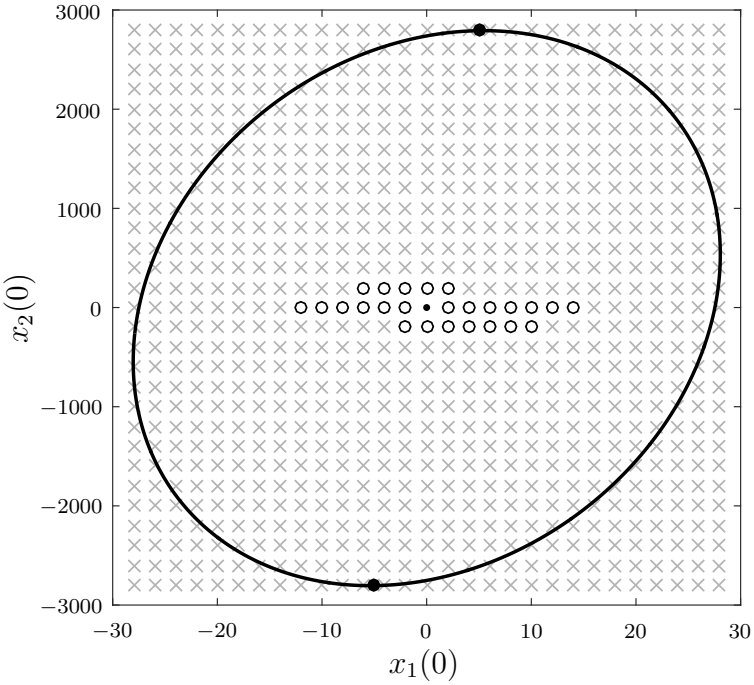

Figure 24: The contour denotes the region $\mathcal{D}$, where output regulation is guaranteed with the complete proposed design. Crosses represent initial conditions for which the closed-loop system simulation becomes unstable if the anti-windup compensation is deactivated. The small dot is an initial condition which does not produce input saturation, whereas circles denote cases which produce saturation and the closed-loop system simulation without anti-windup still achieves output regulation. Source: the author.

4.5 Final Remarks

This chapter dealt with the output regulation problem for rational nonlinear systems subject to input saturation. One important contribution of this study is the adaptation of the anti-windup scheme, originaly developed by GOMES DA SILVA JR et al. (2014), to the nonlinear regulation problem, where the compensation was considered into both internal model and stabilizing stages. Furthermore, the differential-algebraic representation led to stability analysis and synthesis procedures for the stabilizing and anti-windup parameters. The proposed work is expected to have significant scientific relevance, since the literature on nonlinear output regulation mostly neglects the effects of input saturation, e.g. (LU; HUANG, 2015; XU; CHEN; WANG, 2017). The material developed throughout this chapter was organized in the following journal paper to be soon submitted:

- CASTRO, R. S.; FLORES, J. V.; SALTON, A. T.; GOMES DA SILVA JR, J. M. *Anti-Windup Stabilization for Output Regulation of Rational Nonlinear Systems*.

5 EXTENSION FOR THE PRACTICAL OUTPUT REGULATION

This chapter extends the previously developed methodologies for the more general problem called practical output regulation (MARCONI; PRALY, 2008), where the objective of asymptotic output error convergence to zero is relaxed and replaced by an ultimate boundedness requirement. This objective change is referred to as practical because in most real world applications it is highly demanding – and sometimes even unfeasible – to achieve output regulation in the original sense. Moreover, in most practical engineering problems, the desired goal is the best trade-off between residual steady-state error, control implementation complexity and smoothness of the control action. In short, the main features of the practical output regulation framework to be presented in this chapter are the following:

(a) Addressing systems described by non-triangular differential equations;

(b) Implementing reduced order internal model stages;

Item (a) refers to systems with non-triangular dynamical description, which can not be expressed in the form of (76). For these cases, the solution of the regulator partial differential equations is not systematic and might be impracticable to be determined analytically, thus possibly violating the Assumption 3.1. In the practical regulation framework, this assumption can be dropped and it is sufficient to consider approximated steady-state mappings, which can be obtained by a numerical procedure. As the plant zero-error steady-state approximation gets closer to the actual solution, a lower theoretical ultimate error bound will be achievable by the stability conditions to be presented, reaching zero in the limit where the steady-state mappings are exact.

Furthermore, there exist systems where the required internal model order for achieving perfect output regulation is infinite, thus posing a challenge for implementation. Another highly relevant feature of the practical output regulation framework is thus the possibility of considering reduced order internal model stages, as highlighted by (b). In this context, there is usually a trade-off between control complexity and residual steady-state error.

In this chapter, Section 5.1 introduces the new problem to be considered, followed by Section 5.2 where the practical control design framework is detailed. The main theoretical results are contained afterwards in Section 5.3, where stability, performance and boundedness conditions are presented. Lastly, Section 5.4 illustrates the proposed practical regulation framework with a numerical example.

5.1 Problem Statement

Consider the usual closed-loop architecture where the system, exosystem, and output feedback controller are described respectively by (113), (114) and (115), where the control input is constrained inside region $\mathcal{U}$ defined as in (231). The preliminary basic assumptions are the same as considered before (i.e. Assumptions 2.1 and 2.2).

The following definition introduces the concept of achieving practical output regulation which is directly based on MARCONI; PRALY (2008), except for an additional complement so as to distinguish boundedness within a finite time.

Definition 5.1. The closed-loop system (113), (114), (115) is said to:

- achieve *practical output regulation* in $\mathcal{D} \subseteq \mathbb{R}^{n_x} \times \mathbb{R}^{n_\xi} \times \mathbb{R}^{n_w}$ for some *ultimate error bound* $\gamma_\infty \geq 0$ if the closed-loop system is *bounded*[1] in $\mathcal{D}$ and furthermore:

$$\big(x(0), \xi(0), w(0)\big) \in \mathcal{D} \;\; \Rightarrow \;\; \lim_{t \to \infty} ||e(t)|| \leq \gamma_\infty \, . \tag{309}$$

- achieve *practical output regulation* in $\mathcal{D} \subseteq \mathbb{R}^{n_x} \times \mathbb{R}^{n_\xi} \times \mathbb{R}^{n_w}$ for some *ultimate error bound* $\gamma_\tau \geq 0$, within a *finite time* $\tau > 0$, if the closed-loop system is *bounded* in $\mathcal{D}$ and furthermore:

$$\big(x(0), \xi(0), w(0)\big) \in \mathcal{D} \;\; \Rightarrow \;\; ||e(t)|| \leq \gamma_\tau \; \forall \, t \geq \tau \, . \tag{310}$$

One should note that the practical output regulation definition is a relaxation of the standard output regulation introduced by Definition 2.2 (which is the special case where the ultimate error bound is enforced as $\gamma_\infty = 0$). Furthermore, one should see that (310) becomes equivalent to (309) in the limit where τ goes to infinity.

Provided these newly stated concepts, the control design problem is now expressed as follows.

Problem 5.1. Design controller functions $\phi(\xi, y)$ and $\theta(\xi, y)$ such that the closed-loop system (113), (114), (115) achieves practical output regulation in some region $\mathcal{D} \subseteq \mathbb{R}^{n_x} \times \mathbb{R}^{n_\xi} \times \mathcal{W}$ for some ultimate error bound γ_τ with the control input signal restricted to the set (231).

5.2 Practical Control Framework

In order to solve the highlighted practical output regulation design problem, the considered architecture is exactly as shown previously in Figure 15, where the controller is composed by a saturation function (232), by an internal model stage as (233) and by a stabilizing stage as (241). The anti-windup feedback loops, as described in Section 4.2, are also considered here.

Regarding the output regulation in the original sense, it was pointed out by Lemmas 3.1 and 4.1 that an invariant and zero-error steady-state manifold must exist, which is equivalent to the existence of smooth mappings $\pi(w)$, $c(w)$, $d(w)$ and $\sigma_m(w)$, satisfying the set of regulator equations, i.e. (120), (121) and (130). Since the zero-error steady-state

[1] The concept of being *bounded* is described in Definition 2.2.

property is not strictly required now, one may consider regulator equations with residuals for practical design purposes, respectively as[2]

$$\left\{\begin{array}{rcl} \dfrac{\partial\tilde{\pi}(w)}{\partial w}s(w) & = & f(\tilde{\pi}(w),w,\tilde{c}(w))-\Delta_f(w) \\ \tilde{d}(w) & = & g(\tilde{\pi}(w),w) \\ 0 & = & h(\tilde{\pi}(w),w)-\Delta_h(w) \end{array}\right. \quad \forall\, w\in\mathcal{W}\,, \tag{311}$$

$$\left\{\begin{array}{rcl} \dfrac{\partial\tilde{\sigma}_m(w)}{\partial w}s(w) & = & \phi_m(\tilde{\sigma}_m(w),\tilde{d}(w))-\Delta_\phi(w) \\ \tilde{c}(w) & = & \theta_m(\tilde{\sigma}_m(w),\tilde{d}(w)) \end{array}\right. \quad \forall\, w\in\mathcal{W}\,, \tag{312}$$

$$0=\delta(\tilde{d}(w))-\Delta_\delta(w)\ \ \forall\, w\in\mathcal{W}\,. \tag{313}$$

In here, $\Delta_f:\mathcal{W}\to\mathbb{R}^{n_x}$, $\Delta_h:\mathcal{W}\to\mathbb{R}^{n_e}$, $\Delta_\phi:\mathcal{W}\to\mathbb{R}^{n_m}$ and $\Delta_\delta:\mathcal{W}\to\mathbb{R}^{n_\varepsilon}$ are introduced as residual functions, while $\tilde{\pi}:\mathcal{W}\to\mathbb{R}^{n_x}$, $\tilde{c}:\mathcal{W}\to\mathcal{U}$, $\tilde{d}:\mathcal{W}\to\mathbb{R}^{n_y}$ and $\tilde{\sigma}_m:\mathcal{W}\to\mathbb{R}^{n_m}$ are mappings which define an approximated manifold

$$\tilde{\mathcal{M}}=\Big\{(x,\xi_m,\xi_s,w)\in\mathbb{R}^{n_x}\times\mathbb{R}^{n_m}\times\mathbb{R}^{n_s}\times\mathcal{W}\,:\,x=\tilde{\pi}(w)\,,\ \xi_m=\tilde{\sigma}_m(w)\,,\ \xi_s=0\Big\}\,. \tag{314}$$

Due to the introduction of residual terms, it is noticeable that $\tilde{\mathcal{M}}$ is neither invariant nor error-zeroing, however, as $\Delta_f(w)$, $\Delta_h(w)$, $\Delta_\phi(w)$ and $\Delta_\delta(w)$ approach zero, $\tilde{\mathcal{M}}$ approaches the ideal zero-error and invariant manifold $\mathcal{M}$ defined by (75). Moreover, this relaxed formulation allows the usage of numerical algorithms able to compute a proximate solution to the regulator equations, including the internal model functions. Any numerical method able to approximate the solution of partial differential equations can be applied in this case, ranging from a traditional nonlinear programming using interior-point solvers (BERTSEKAS, 1999) to heuristic based procedures such as neural networks (LAGARIS; LIKAS; FOTIADIS, 1998).

It is important to emphasize that the subsequent control design methodology neither requires working with the regulator equations nor using an internal model stage. For instance, with respect to the plant equations (311), one can always consider the trivial solution $\tilde{\pi}(w)=0$ and $\tilde{c}(w)=0$, where in this case the residuals are readily $\Delta_f(w)=f(0,w,0)$ and $\Delta_h(w)=h(0,w)$. However, for improving the control design and possibly attaining lower ultimate error bounds, it is recommended to employ numerical optimization routines so as to find solutions which help to reduce the residuals along the domain of interest $\mathcal{W}$. A procedure able to deal with this problem is described subsequently, where it is only assumed *a priori* knowledge of the plant and exosystem functions $f(x,w,u)$, $g(x,w)$, $h(x,w)$ and $s(w)$:

(a) *Approximation of the plant zero-error steady-state:* search for smooth mappings $\tilde{\pi}(w):\mathcal{W}\to\mathbb{R}^{n_x}$ and $\tilde{c}(w):\mathcal{W}\to\mathbb{R}^{n_u}$ according to the following numerical optimization problem

$$\min_{\tilde{\pi}(w)\,,\,\tilde{c}(w)}\ \int_{\mathcal{W}}\left(||\Delta_f(w)||^2+||\Delta_h(w)||^2\right)\mathrm{d}w\ \ \text{s.t. (311)}\,. \tag{315}$$

[2]Without loss of generality, residual terms are not considered in the equations for $\tilde{d}(w)$ and $\tilde{c}(w)$, since these functions can always be displaced in order to eliminate any residual.

(b) *Internal model synthesis:* given the result from phase (a), search for functions $\phi_m(\xi_m, y)$, $\theta_m(\xi_m, y)$ and for a smooth mapping $\tilde{\sigma}_m(w) : \mathcal{W} \to \mathbb{R}^{n_m}$ according to the following numerical optimization problem:

$$\min_{\phi_m(\xi_m,y)\,,\,\theta_m(\xi_m,y)\,,\,\tilde{\sigma}_m(w)} \int_{\mathcal{W}} ||\Delta_\phi(w)||^2 \,\mathrm{d}w \;\; \text{s.t. (312)} \,. \tag{316}$$

If $\tilde{c}(w) = 0$, skip this step and do not use an internal model stage.

(c) *Approximation of the output vanishing function:* given the result from phase (a), search for a function $\delta(y)$ according to the following numerical optimization problem:

$$\min_{\delta(y)} \int_{\mathcal{W}} ||\Delta_\delta(w)||^2 \,\mathrm{d}w \;\; \text{s.t. (313)} \,. \tag{317}$$

In order to numerically solve the optimization problems (315), (316) and (317), one should perform a parametrization of the unknown functions and residuals using a series of free decision variables $q_1, q_2, \ldots, q_{n_q} \in \mathbb{R}$. A general guideline in this case is to assign a candidate polynomial structure with free coefficients to each unknown function, an approach which will be exemplified in Subsection 5.4.1. Another important consideration for numerical tractability is the discretization of the integrals in (315), (316) and (317), which may be substituted by a sum over a finite grid $\tilde{\mathcal{W}}$ approximating the desired domain $\mathcal{W}$. Given these considerations, a nonlinear programming approach, for instance, is applicable in order to numerically determine the free variables.

For the validity of the regulator equations under the presence of input saturation and also for the subsequent usability in the stabilization phase, one should *a posteriori* check if the supreme bounds of $\tilde{c}(w)$ inside the set $\mathcal{W}$ do not exceed the maximum control amplitudes, i.e.

$$\sup_{w\in\mathcal{W}} |\tilde{c}_j(w)| \leq \overline{c}_j < \overline{u}_j \;\; \forall\, j \in \{1, 2, \ldots, n_u\} \,. \tag{318}$$

The values $\overline{c}_1, \overline{c}_2, \ldots, \overline{c}_{n_u}$ can again be systematically determined by the methodology explained in Subsection 4.3.3.

In possession of solutions $\tilde{\pi}(w)$, $\tilde{c}(w)$, $\sigma_m(w)$, $\tilde{\phi}_m(\xi_m, y)$, $\theta_m(\xi_m, y)$, $\delta(y)$, $\Delta_f(w)$, $\Delta_h(w)$, $\Delta_\phi(w)$ and $\Delta_\delta(w)$ from previous phases (a), (b) and (c), and assuming that (318) holds, one should move to the next step in the control design, which is related to closed-loop stabilization. The methodology related to this last step is the main contribution of this chapter, as presented in the subsequent section.

(d) *Stabilizing stage and anti-windup synthesis*: given the result from phases (a), (b) and (c), and for a given scheduling function $\lambda(y)$, design stabilizing parameters F_0 , ... , K_n and anti-windup parameters E_0 , ... , W_n such that practical output regulation is achieved for some ultimate bound γ_τ.

In the literature, one may find methodologies able to solve steps (a), (b) and (c), similar to those described here. One example is BYRNES; GILLIAM (2007), where the regulator equations are proximatelly solved by fixed point and Newton iteration methods. Another case is KHAILAIE; ADHAMI-MIRHOSSEINI; YAZDANPANAH (2011), where the so-called Galerkin method is considered for determining an approximate system zero-error steady-state. The main innovation presented here is thus the methodology for addressing step (d), where for any given approximate solution to the regulator equations, a systematic ultimately bounded stabilization approach is provided for rational nonlinear dynamics.

5.3 Main Results

In this section, a new methodology is presented in order to systematically approach the design phase (d), which can be seen as a direct extension of the material developed in Chapters 3 and 4. The major difference in the current formulation is the presence of residual non-vanishing terms in the regulation error dynamics, a consequence for allowing approximate solutions to the regulator equations. Moreover, it is necessary now to characterize additional regions defining the ultimate bounds of the regulation error state trajectory.

Initially in Subsection 5.3.1, the system equations are arranged in a practical regulation error form, followed by the employment of the DAR in Subsection 5.3.2. Stability, performance and boundedness conditions are then presented in Subsection 5.3.3, leading to design conditions in Subsection 5.3.4, including a convex special case demonstrated in the end.

5.3.1 Practical Regulation Error System

A change of state-space coordinates $z \in \mathbb{R}^{n_z}$ $(n_z = n_x + n_m)$ is again considered as

$$z \triangleq \begin{bmatrix} z_x \\ z_m \end{bmatrix} \triangleq \begin{bmatrix} x - \tilde{\pi}(w) \\ \xi_m - \tilde{\sigma}_m(w) \end{bmatrix}, \tag{319}$$

which will be subsequently referred to as the practical regulation error states. Unlike the previous chapters, the steady-state approximations $\tilde{\pi}(w)$ and $\tilde{\sigma}_m(w)$ do not represent exact solutions to the regulator equations and are now associated with the relaxed conditions (311) and (312).

By performing the time-derivative of z in (319) and by considering the derivative of $\tilde{\pi}(w)$ and $\tilde{\sigma}_m(w)$ along the exosystem trajectories as in (311) and (312), one should arrive at the following equations:

$$\begin{cases} \dot{z} &= f_z(z, w, \hat{v}) + \Delta_{f_z}(w) \\ e &= h_z(z, w) + \Delta_{h_z}(w) \\ \varepsilon &= \delta_z(z, w) + \Delta_{\delta_z}(w) \end{cases} . \tag{320}$$

Functions $f_z : \mathbb{R}^{n_z} \times \mathbb{R}^{n_w} \times \mathbb{R}^{n_v} \to \mathbb{R}^{n_z}$, $h_z : \mathbb{R}^{n_z} \times \mathbb{R}^{n_w} \to \mathbb{R}^{n_e}$ and $\delta_z : \mathbb{R}^{n_z} \times \mathbb{R}^{n_w} \to \mathbb{R}^{n_\varepsilon}$ are constructed exactly as shown before in (245), where the original mappings $\pi(w)$ and $\sigma_m(w)$ are simply substituted by the approximate ones $\tilde{\pi}(w)$ and $\tilde{\sigma}_m(w)$. The auxiliary definition $\hat{v} \in \mathbb{R}^{n_v}$ is the same as in (243), which denotes the effective plant and internal model stabilizing inputs. In turn, the new system components $\Delta_{f_z} : \mathbb{R}^{n_w} \to \mathbb{R}^{n_z}$, $\Delta_{h_z} : \mathbb{R}^{n_w} \to \mathbb{R}^{n_e}$ and $\Delta_{\delta_z} : \mathbb{R}^{n_w} \to \mathbb{R}^{n_\varepsilon}$ are constructed from the regulator equations residuals as:

$$\Delta_{f_z}(w) = \begin{bmatrix} \Delta_f(w) \\ \Delta_\phi(w) \end{bmatrix}, \;\; \Delta_{h_z}(w) = \Delta_h(w), \;\; \Delta_{\delta_z}(w) = \Delta_\delta(w). \tag{321}$$

These terms represent non-vanishing dynamic components, a consequence for considering the coordinate change with an inexact solution to the regulator equations. Even though it still verifies that $f_z(0, w, 0) = 0$, $h_z(0, w) = 0$ and $\delta_z(0, w) = 0 \; \forall \, w \in \mathcal{W}$, in this case if $\Delta_{f_z}(w) \neq 0$, then the origin $z = 0$ cannot be characterized as an equilibrium point of the system (320) $\forall \, w \in \mathcal{W}$, unlike the exact regulation error system defined in (244). Similarly, if $\Delta_{h_z}(w) \neq 0$ and $\Delta_{\delta_z}(w) \neq 0$, then the output error $h_z(z, w)$ and the auxiliary function $\delta_z(z, w)$ are not zero in the origin point $z = 0$. Nevertheless, it is evident that as the regulator equations residuals approach zero, the practical regulation

error representation (320) approaches the ideal form (244), where $z = 0$ is an exact equilibrium point $\forall\, w \in \mathcal{W}$. The magnitude of $\Delta_{f_z}(w)$, $\Delta_{h_z}(w)$ and $\Delta_{\delta_z}(w)$ will thus have a direct influence in the system ultimate bound estimates, which will be developed relative to coordinates introduced in (319).

In the present context, the stabilizing stage equations are the same as used previously, i.e. (246). Furthermore, the unconstrained control signal μ is still expressed in the same manner as in (244), except for the use of mapping $\tilde{c}(w)$:

$$\mu = \theta_z(z, w) + \tilde{c}(w) + v_u \,. \tag{322}$$

Other previous definitions such as (248) and (249) still remain the same.

5.3.2 Differential-Algebraic Representation

In order to deal with the dynamic representation (320) for design purposes, the system functions are considered to be representable in a DAR as mentioned in Assumption 4.1[3] and as stated in the following assumption with respect to the new residual terms.

Assumption 5.1. Nonlinear functions $\Delta_{f_z}(w)$, $\Delta_{\delta_z}(w)$ and $\Delta_{h_z}(w)$ of the system (320) can be represented as

$$\begin{array}{rcl} \Delta_{f_z}(w) & = & \tilde{A}(w)\, w + \tilde{\Phi}(w)\, \tilde{\varphi}(w) \\ \Delta_{\delta_z}(w) & = & \tilde{C}\, w \; + \tilde{\Gamma}\, \tilde{\varphi}(w) \\ \Delta_{h_z}(w) & = & \tilde{C}_e\, w + \tilde{\Gamma}_e\, \tilde{\varphi}(w) \end{array} \tag{323}$$

with a rational nonlinear function $\tilde{\varphi} : \mathcal{W}^+ \to \mathbb{R}^{n_{\tilde{\varphi}}}$ satisfying

$$0 = \tilde{\Psi}(w)\, w + \tilde{\Omega}(w)\, \tilde{\varphi}(w) \tag{324}$$

such that:

(i) Set $\mathcal{W}^+$ satisfies $\mathcal{W} \subseteq \mathcal{W}^+ \subseteq \mathbb{R}^{n_w}$.

(ii) Matrices $\tilde{A} : \mathcal{W}^+ \to \mathbb{R}^{n_z \times n_w}$, $\tilde{\Phi} : \mathcal{W}^+ \to \mathbb{R}^{n_z \times n_{\tilde{\varphi}}}$, $\tilde{\Psi} : \mathcal{W}^+ \to \mathbb{R}^{n_{\tilde{\varphi}} \times n_w}$ and $\tilde{\Omega} : \mathcal{W}^+ \to \mathbb{R}^{n_{\tilde{\varphi}} \times n_{\tilde{\varphi}}}$ are affine with respect to w.

(iii) Matrices $\tilde{C} \in \mathbb{R}^{n_\varepsilon \times n_w}$, $\tilde{\Gamma} \in \mathbb{R}^{n_\varepsilon \times n_{\tilde{\varphi}}}$, $\tilde{C}_e \in \mathbb{R}^{n_e \times n_w}$ and $\tilde{\Gamma}_e \in \mathbb{R}^{n_e \times n_{\tilde{\varphi}}}$ are constant.

(iv) Matrix $\tilde{\Omega}(w)$ is non-singular $\forall\, w \in \mathcal{W}^+$.

Similarly to earlier cases, there exists a proper DAR according to Assumption 5.1 whenever $\Delta_{f_z}(w)$, $\Delta_{h_z}(w)$ and $\Delta_{\delta_z}(w)$ are regular rational functions $\forall\, w \in \mathcal{W}^+$. In turn, this property is naturally verified whenever the original system functions and the candidate steady-state mappings are also rational. Further details on how to setup a proper DAR have been thoroughly explained in Subsection 3.3.2.

Regions $\mathcal{Z}^+$ and $\mathcal{W}^+$ are again considered as (145), i.e. sets defined by a convex hull of vertices $\mathcal{V}_z$ and $\mathcal{V}_w$. Set $\mathcal{Z}^+$ is also considered in the form (146) for some known vectors $p_1, p_2, \ldots, p_{n_k} \in \mathbb{R}^{n_z}$. At this point, it is important to define an additional ellipsoidal set

$$\mathcal{W}_\mathcal{E} = \left\{ w \in \mathbb{R}^{n_w} : w^\intercal \tilde{P}\, w \leq 1 \right\}, \quad \mathcal{W} \subseteq \mathcal{W}_\mathcal{E} \subseteq \mathcal{W}^+ \,, \tag{325}$$

[3] In here, it is being additionally assumed that $h_z(z, w)$ admits a DAR in the same form of $\delta_z(z, w)$ in Assumption 4.1, with matrices denoted as $C_e \in \mathbb{R}^{n_e \times n_z}$ and $\Gamma_e \in \mathbb{R}^{n_e \times n_\varphi}$.

for a symmetric matrix $\tilde{P} \in \mathbb{R}^{n_w}$. This definition will later allow the use of Lemma A.5 in order to deal with the w-dependence in the residual regulation error dynamics.

Provided the established DAR framework, the practical regulation error system equations can be written as

$$\begin{cases} \dot{z} &= A(z,w)\,z + \Phi(z,w)\,\varphi(z,w) + BJ(z,w)\,\psi(\mu) + \tilde{A}(w)\,w + \tilde{\Phi}(w)\,\tilde{\varphi}(w) + B\,v \\ \mu &= Q(z,w)\,z + \Upsilon(z,w)\,\varphi(z,w) + \tilde{c}(w) + D\,v \\ \varepsilon &= C\,z + \Gamma\,\varphi(z,w) + \tilde{C}\,w + \tilde{\Gamma}\,\tilde{\varphi}(w) \\ e &= C_e\,z + \Gamma_e\,\varphi(z,w) + \tilde{C}_e\,w + \tilde{\Gamma}_e\,\tilde{\varphi}(w) \\ 0 &= \Psi(z,w)\,z + \Omega(z,w)\,\varphi(z,w) \\ 0 &= \tilde{\Psi}(w)\,w + \tilde{\Omega}(w)\,\tilde{\varphi}(w) \end{cases} \tag{326}$$

By then considering an augmented system state vector in the form of (138) and by joining the stabilizing controller equations, one is able to express the closed-loop system dynamics as:

$$\begin{cases} \dot{\mathbf{z}} &= \boldsymbol{A}(z,w)\,\mathbf{z} + \boldsymbol{\Phi}(z,w)\,\varphi(z,w) + \boldsymbol{J}(z,w)\,\psi(\mu) + \tilde{\boldsymbol{A}}(z,w)\,w + \tilde{\boldsymbol{\Phi}}(z,w)\,\tilde{\varphi}(w) \\ \mu &= \boldsymbol{Q}(z,w)\,\mathbf{z} + \boldsymbol{\Upsilon}(z,w)\,\varphi(z,w) + \tilde{c}(w) \\ e &= \boldsymbol{C}\,\mathbf{z} + \boldsymbol{\Gamma}\,\varphi(z,w) + \tilde{\boldsymbol{C}}\,w + \tilde{\boldsymbol{\Gamma}}\,\tilde{\varphi}(w) \\ 0 &= \boldsymbol{\Psi}(z,w)\,\mathbf{z} + \boldsymbol{\Omega}(z,w)\,\varphi(z,w) \\ 0 &= \tilde{\boldsymbol{\Psi}}(w)\,w + \tilde{\boldsymbol{\Omega}}(w)\,\tilde{\varphi}(w) \end{cases} \tag{327}$$

The matrices in here that also appear in (253) are defined exactly as in (149) and (254), whereas the new augmented matrices $\tilde{\boldsymbol{A}} : \mathcal{Z}^+ \times \mathcal{W}^+ \to \mathbb{R}^{n_a \times n_w}$, $\tilde{\boldsymbol{\Phi}} : \mathcal{Z}^+ \times \mathcal{W}^+ \to \mathbb{R}^{n_a \times n_{\tilde{\varphi}}}$, $\tilde{\boldsymbol{\Psi}} : \mathcal{Z}^+ \times \mathcal{W}^+ \to \mathbb{R}^{n_{\tilde{\varphi}} \times n_w}$ and $\tilde{\boldsymbol{\Omega}} : \mathcal{Z}^+ \times \mathcal{W}^+ \to \mathbb{R}^{n_{\tilde{\varphi}} \times n_{\tilde{\varphi}}}$, $\boldsymbol{C} \in \mathbb{R}^{n_e \times n_a}$, $\boldsymbol{\Gamma} \in \mathbb{R}^{n_e \times n_\varphi}$, $\tilde{\boldsymbol{C}} \in \mathbb{R}^{n_e \times n_w}$ and $\tilde{\boldsymbol{\Gamma}} \in \mathbb{R}^{n_e \times n_{\tilde{\varphi}}}$ are denoting:

$$\begin{gathered} \tilde{\boldsymbol{A}}(z,w) = \begin{bmatrix} \tilde{A}(w) + BK(z,w)\tilde{C} \\ G(z,w)\tilde{C} \end{bmatrix}, \quad \tilde{\boldsymbol{\Phi}}(z,w) = \begin{bmatrix} \tilde{\Phi}(w) + BK(z,w)\tilde{\Gamma} \\ G(z,w)\tilde{\Gamma} \end{bmatrix}, \\ \tilde{\boldsymbol{\Psi}}(w) = \tilde{\Psi}(w)\,, \quad \tilde{\boldsymbol{\Omega}}(w) = \tilde{\Omega}(w)\,, \quad \boldsymbol{C} = \begin{bmatrix} C_e & 0 \end{bmatrix}, \quad \boldsymbol{\Gamma} = \Gamma_e\,, \quad \tilde{\boldsymbol{C}} = \tilde{C}_e\,, \quad \tilde{\boldsymbol{\Gamma}} = \tilde{\Gamma}_e\,. \end{gathered} \tag{328}$$

Similarly to previous chapters, it is considered an *a priori* given controller scheduling function $\lambda(y)$ such that (137) is linear with respect to (z,w), ensuring that all matrix functions in (327) are affine with respect to (z,w).

5.3.3 Analysis Conditions

Towards developing stability, performance and boundedness analysis conditions for the practical output regulation problem in hand, the following complementary definition is introduced with respect to the system representation (327).

Definition 5.2. For every initial condition in $\mathcal{D} \subseteq \mathbb{R}^{n_a} \times \mathcal{W}$, the practical regulation error system (327) is said to be[4]:

- *ultimately bounded* in $\mathcal{B}_\infty \subset \mathcal{D}$ if

$$\big(\mathbf{z}(0), w(0)\big) \in \mathcal{D} \;\Rightarrow\; \lim_{t\to\infty} \mathbf{z}(t) \in \boldsymbol{\mathcal{Z}}_\infty\,, \quad \mathcal{B}_\infty \triangleq \boldsymbol{\mathcal{Z}}_\infty \times \mathcal{W}\,; \tag{329}$$

- *ultimately bounded* in $\mathcal{B}_\tau \subset \mathcal{D}$ within a *finite time* $\tau > 0$ if

$$\big(\mathbf{z}(0), w(0)\big) \in \mathcal{D} \;\Rightarrow\; \mathbf{z}(t) \in \boldsymbol{\mathcal{Z}}_\tau \;\forall\, t \geq \tau\,, \quad \mathcal{B}_\tau \triangleq \boldsymbol{\mathcal{Z}}_\tau \times \mathcal{W}\,. \tag{330}$$

[4]In this definition, it is implicit that $w(t) \in \mathcal{W} \;\forall\, w(0) \in \mathcal{W}$, according to Assumption 2.2.

Given this new definition, the logical formulation of stability, performance and boundedness relations are divided into two categories. Primarily, conditions for input-to-state boundedness (i.e. from w to $\mathbf{z}$) are derived, where an ultimate bounding set $\mathcal{B}_\infty$ is characterized. Secondly, conditions for state-to-output boundedness (i.e. from $\mathbf{z}$ to e) are obtained, where an ultimate error bound γ_∞ is established according to Definition 5.1. Thus, the basic overall procedure is summarized as follows:

$$\big(\mathbf{z}(0), w(0)\big) \in \mathcal{D} \;\Rightarrow\; \lim_{t\to\infty} \mathbf{z}(t) \in \boldsymbol{\mathcal{Z}}_\infty \;\Rightarrow\; \lim_{t\to\infty} ||e(t)|| \leq \gamma_\infty \,. \tag{331}$$

The conditions to be presented are in fact more general then (331) and also characterize ultimate bounds within some finite time $\tau > 0$, i.e.

$$\big(\mathbf{z}(0), w(0)\big) \in \mathcal{D} \;\Rightarrow\; \mathbf{z}(t) \in \boldsymbol{\mathcal{Z}}_\tau \;\forall\, t \geq \tau \;\Rightarrow\; ||e(t)|| \leq \gamma_\tau \;\forall\, t \geq \tau \,. \tag{332}$$

Even further, an exponential transitory performance condition is addressed according to Definition 5.3 presented in the sequence. This criterion is based on (P1) from Definition 3.1, now generalized for the current practical context.

Definition 5.3. *Practical Exponential Performance* (P3): the trajectories $\mathbf{z}(t)$ exponentially approach $\boldsymbol{\mathcal{Z}}_\infty$ with decay rate faster than $\alpha > 0$, i.e. $\exists\, \epsilon > 0$ such that $||\mathbf{z}(t)||^2 \leq \epsilon\, \mathrm{e}^{-2\alpha t} + \epsilon_\infty \;\forall\, t \geq 0$ for every initial condition $(\mathbf{z}(0), w(0)) \in \mathcal{D}$, where $\epsilon_\infty \geq 0$ is the smallest scalar such that $||\mathbf{z}||^2 \leq \epsilon_\infty \;\forall\, \mathbf{z} \in \boldsymbol{\mathcal{Z}}_\infty$.

Given all these preliminary considerations, Theorem 5.1 presents the main result of the chapter.

Theorem 5.1. *Suppose there exist a symmetric matrix $P \in \mathbb{R}^{n_a \times n_a}$, a diagonal matrix $T \in \mathbb{R}^{n_u \times n_u}$, matrices $L \in \mathbb{R}^{n_\varphi \times n_\varphi}$, $\tilde{L} \in \mathbb{R}^{n_{\tilde{\varphi}} \times n_{\tilde{\varphi}}}$, $\mathrm{R}_0, \ldots, \mathrm{R}_\mathrm{m} \in \mathbb{R}^{n_u \times n_z}$, $\Xi_0, \ldots, \Xi_\mathrm{m} \in \mathbb{R}^{n_u \times n_s}$, $\Pi_0, \ldots, \Pi_\mathrm{m} \in \mathbb{R}^{n_u \times n_\varphi}$ and scalars $\tilde{\alpha}, \eta_\infty \in \mathbb{R}$ such that* (153)*,* (154)*,* (156)*,* (273)*,* (274)*,*

$$\alpha\, \eta_\infty > \tilde{\alpha} > 0 \,, \;\; 1 > \eta_\infty > 0 \,, \tag{333}$$

$$\mathcal{H} \left\{ \begin{bmatrix} P\boldsymbol{A}(z,w) + \alpha P & P\boldsymbol{\Phi}(z,w) & P\boldsymbol{J}(z,w) & P\tilde{\boldsymbol{A}}(z,w) & P\tilde{\boldsymbol{\Phi}}(z,w) \\ L\boldsymbol{\Psi}(z,w) & L\boldsymbol{\Omega}(z,w) & 0 & 0 & 0 \\ T\boldsymbol{R}(z,w) & T\boldsymbol{\Pi}(z,w) & -T & 0 & 0 \\ 0 & 0 & 0 & -\tilde{\alpha}\tilde{P} & 0 \\ 0 & 0 & 0 & \tilde{L}\tilde{\boldsymbol{\Psi}}(w) & \tilde{L}\tilde{\boldsymbol{\Omega}}(w) \end{bmatrix} \right\} \prec 0 \tag{334}$$

$$\forall\, (z,w) \in \mathcal{V}_z \times \mathcal{V}_w \,,$$

where $\boldsymbol{R}(z,w) \triangleq \big[R(z,w) \;\; \Xi(z,w)\big]$, $\boldsymbol{\Pi}(z,w) \triangleq \Pi(z,w)$ and (276) *for any linear function $\nu : \mathcal{Z}^+ \times \mathcal{W}^+ \to \mathbb{R}^\mathrm{m}$, $\mathrm{m} \in \mathbb{N}$. Then the system* (327) *is ultimately bounded in*

$$\begin{aligned} \mathcal{B}_\infty &= \big\{(\mathbf{z}, w) \in \mathbb{R}^{n_a} \times \mathcal{W} : \mathbf{z}^\intercal P\, \mathbf{z} \leq \eta_\infty\big\} \,, \\ \mathcal{B}_\tau &= \big\{(\mathbf{z}, w) \in \mathbb{R}^{n_a} \times \mathcal{W} : \mathbf{z}^\intercal P\, \mathbf{z} \leq \eta_\tau\big\} \,,\; \eta_\tau \triangleq (1 - \eta_\infty)\, \mathrm{e}^{-2\alpha\tau} + \eta_\infty \,,\; \tau > 0 \,, \end{aligned} \tag{335}$$

and satisfies (P2) *and* (P3) *for every initial condition in* (157)*. Moreover, suppose for some $\tau > 0$ there exist matrices $U \in \mathbb{R}^{n_\varphi \times n_\varphi}$, $\tilde{U} \in \mathbb{R}^{n_{\tilde{\varphi}} \times n_{\tilde{\varphi}}}$ and scalars $\beta, \tilde{\beta}, \gamma_\tau^2 \in \mathbb{R}$ such that*

$$\beta > 0 \,, \;\; 1 - \beta\, \eta_\tau > \tilde{\beta} > 0 \,, \;\; \gamma_\tau^2 > 0 \,, \tag{336}$$

$$\begin{bmatrix} \gamma_\tau^2 & \boldsymbol{C} & \boldsymbol{\Gamma} & \tilde{\boldsymbol{C}} & \tilde{\boldsymbol{\Gamma}} \\ \star & \beta P & -\boldsymbol{\Psi}^{\mathsf{T}}(z,w)U^{\mathsf{T}} & 0 & 0 \\ \star & \star & -\mathcal{H}\{U\boldsymbol{\Omega}(z,w)\} & 0 & 0 \\ \star & \star & \star & \tilde{\beta}\tilde{P} & -\tilde{\boldsymbol{\Psi}}^{\mathsf{T}}(w)\tilde{U}^{\mathsf{T}} \\ \star & \star & \star & \star & -\mathcal{H}\{\tilde{U}\tilde{\boldsymbol{\Omega}}(w)\} \end{bmatrix} \succ 0 \;\; \forall\, (z,w) \in \mathcal{V}_z \times \mathcal{V}_w \,. \quad (337)$$

Then the closed-loop system (113)*,* (114) *with controller* (232)*,* (233)*,* (241) *also achieves practical output regulation with ultimate error bound* γ_τ *for every initial condition in* (157)*.*

Proof. Consider the usual quadratic Lyapunov function (158), for a symmetric and positive-definite matrix P, noting that $V(\mathbf{z}) > 0 \;\forall\, \mathbf{z} \in \mathbb{R}^{n_a}$, $\mathbf{z} \neq 0$. The derivative of (158) along the trajectories of the system (327) is given by $\dot{V}(\mathbf{z},w) = \mathcal{H}\{\mathbf{z}^{\mathsf{T}}\,\boldsymbol{\Theta}_1(z,w)\,\zeta(\mathbf{z},w)\}$, where $\boldsymbol{\Theta}_1(z,w)$ and $\zeta(\mathbf{z},w)$ are defined as

$$\boldsymbol{\Theta}_1(z,w) \triangleq \begin{bmatrix} P\boldsymbol{A}(z,w) & P\,\boldsymbol{\Phi}(z,w) & P\boldsymbol{J}(z,w) & P\tilde{\boldsymbol{A}}(z,w) & P\,\tilde{\boldsymbol{\Phi}}(z,w) \end{bmatrix} , \quad (338)$$

$$\zeta(\mathbf{z},w) \triangleq \begin{bmatrix} \mathbf{z}^{\mathsf{T}} & \varphi^{\mathsf{T}}(z,w) & \psi^{\mathsf{T}}(\mu) & w^{\mathsf{T}} & \tilde{\varphi}^{\mathsf{T}}(w) \end{bmatrix}^{\mathsf{T}} , \quad (339)$$

with $\mu = \boldsymbol{Q}(z,w)\,\mathbf{z} + \boldsymbol{\Upsilon}(z,w)\,\varphi(z,w) + \tilde{c}(w)$. From notation (339), the algebraic equality constraints in (327) can be expressed as $\boldsymbol{\Theta}_2(z,w)\,\zeta(\mathbf{z},w) = 0$ and $\boldsymbol{\Theta}_3(w)\,\zeta(\mathbf{z},w) = 0$, where

$$\boldsymbol{\Theta}_2(z,w) \triangleq \begin{bmatrix} \boldsymbol{\Psi}(z,w) & \boldsymbol{\Omega}(z,w) & 0 & 0 & 0 \end{bmatrix} , \;\; \boldsymbol{\Theta}_3(w) \triangleq \begin{bmatrix} 0 & 0 & 0 & \tilde{\boldsymbol{\Psi}}(w) & \tilde{\boldsymbol{\Omega}}(w) \end{bmatrix} . \quad (340)$$

Consider also Lemma 4.2 with functions $\boldsymbol{\theta}(\mathbf{z},w)$ and $\boldsymbol{\vartheta}(\mathbf{z},w)$ expanded as (279), where matrices $\boldsymbol{R}(z,w) \triangleq \begin{bmatrix} R(z,w) & \Xi(z,w) \end{bmatrix}$ and $\boldsymbol{\Pi}(z,w) \triangleq \Pi(z,w)$ are constructed by (276) for any linear function $\nu : \mathcal{Z}^+ \times \mathcal{W}^+ \to \mathbb{R}^{\mathrm{m}}$, $\mathrm{m} \in \mathbb{N}$. According to Lemma 4.2, if $(\mathbf{z},w) \in \mathcal{S}$ then (257) is satisfied, which is identical to $\mathcal{H}\{\psi^{\mathsf{T}}(\mu)\,\boldsymbol{\Theta}_4(z,w)\,\zeta(\mathbf{z},w)\} \geq 0$ where

$$\boldsymbol{\Theta}_4(z,w) \triangleq \begin{bmatrix} T\boldsymbol{R}(z,w) & T\boldsymbol{\Pi}(z,w) & -T & 0 & 0 \end{bmatrix} , \quad (341)$$

for some diagonal and positive-definite matrix T. Furthermore, consider the candidate domain of attraction estimate $\mathcal{D} = \{(\mathbf{z},w) \in \mathbb{R}^{n_a} \times \mathcal{W} : V(\mathbf{z}) \leq 1\}$ and suppose that $\mathcal{D} \subset \boldsymbol{\mathcal{Z}}^+ \times \mathcal{W}^+$ and $\mathcal{D} \subset \mathcal{S}$, conditions which are satisfied if (154) and (274), as discussed in the proof of Theorem 4.1. Now suppose there exist matrices $L \in \mathbb{R}^{n_\varphi \times n_\varphi}$, $\tilde{L} \in \mathbb{R}^{n_{\tilde{\varphi}} \times n_{\tilde{\varphi}}}$ and scalars $\alpha > 0$, $\tilde{\alpha} > 0$ and $1 > \eta_\infty > 0$ such that the following inequality holds:

$$\begin{aligned} &\dot{V}(\mathbf{z},w) \,+\, 2\alpha\,(V(\mathbf{z}) - \eta_\infty) + 2\tilde{\alpha}\,(1 - w^{\mathsf{T}}\tilde{P}\,w) \,+\, \ldots \\ &\ldots \,+\, \mathcal{H}\big\{\varphi^{\mathsf{T}}(z,w)\,L\boldsymbol{\Theta}_2(z,w)\,\zeta(\mathbf{z},w) + \tilde{\varphi}^{\mathsf{T}}(w)\,\tilde{L}\boldsymbol{\Theta}_3(w)\,\zeta(\mathbf{z},w)\big\} \,+\, \ldots \\ &\ldots \,+\, \mathcal{H}\big\{\psi^{\mathsf{T}}(\mu)(\mathbf{z},w)\,\boldsymbol{\Theta}_4(z,w)\,\zeta(\mathbf{z},w)\big\} < 0 \;\forall\, (\mathbf{z},w) \in \boldsymbol{\mathcal{Z}}^+ \times \mathcal{W}^+ \,,\; \mathbf{z} \neq 0 \,. \end{aligned} \quad (342)$$

Since $\boldsymbol{\Theta}_2(z,w)\,\zeta(\mathbf{z},w) = 0$, $\boldsymbol{\Theta}_3(w)\,\zeta(\mathbf{z},w) = 0$, $\psi^{\mathsf{T}}(\mu)(\mathbf{z},w)\,\boldsymbol{\Theta}_4(z,w)\,\zeta(\mathbf{z},w) \geq 0$ and $(1 - w^{\mathsf{T}}\tilde{P}\,w) \geq 0 \;\forall\, (\mathbf{z},w) \in \mathcal{D}$, it follows that (342) implies:

$$\dot{V}(\mathbf{z},w) < -2\alpha\,(V(\mathbf{z}) - \eta_\infty) \;\forall\, (\mathbf{z},w) \in \mathcal{D} \,,\; \mathbf{z} \neq 0 \,, \quad (343)$$

$$\dot{V}(\mathbf{z},w) < 0 \;\forall\, (\mathbf{z},w) \in (\mathcal{D} - \mathcal{B}_\infty) \triangleq \big\{(\mathbf{z},w) \in \mathbb{R}^{n_a} \times \mathcal{W} : \eta_\infty \leq V(\mathbf{z}) \leq 1\big\} \,. \quad (344)$$

From this development, it is noticeable that

$$(\mathbf{z}(0)\,w(0)) \in \mathcal{D} \;\;\Rightarrow\;\; \lim_{t\to\infty} (\mathbf{z}(t), w(t)) \in \mathcal{B}_\infty \triangleq \big\{(\mathbf{z},w) \in \mathbb{R}^{n_a} \times \mathcal{W} : V(\mathbf{z}) \leq \eta_\infty\big\} \,, \quad (345)$$

and thus, the system (327) is ultimately bounded in $\mathcal{B}_\infty$ for every initial condition in $\mathcal{D}$. Moreover, from the previous condition (343), it follows that

$$
\begin{gathered}
(V(\mathbf{z}(t)) - \eta_\infty) \leq (V(\mathbf{z}(0)) - \eta_\infty)\, \mathrm{e}^{-2\alpha t} \leq (1 - \eta_\infty)\, \mathrm{e}^{-2\alpha t}\ \forall\, (\mathbf{z}(0), w(0)) \in \mathcal{D}\,, \\
V(\mathbf{z}(t)) \leq \eta_t\ \forall\, (\mathbf{z}(0), w(0)) \in \mathcal{D}\,,\ \eta_t \triangleq (1 - \eta_\infty)\, \mathrm{e}^{-2\alpha t} + \eta_\infty\,,\ t \geq 0\,, \\
(\mathbf{z}(0)\, w(0)) \in \mathcal{D}\ \ \Rightarrow\ \ (\mathbf{z}(t), w(t)) \in \mathcal{B}_\tau \triangleq \left\{(\mathbf{z}, w) \in \mathbb{R}^{n_a} \times \mathcal{W} : V(\mathbf{z}) \leq \eta_\tau\right\} \forall\, t \geq \tau\,,
\end{gathered}
\tag{346}
$$

and therefore, the system (327) is also ultimately bounded in $\mathcal{B}_\tau$ within finite time $\tau > 0$ for every initial condition in $\mathcal{D}$. In addition, since $\lambda_{min}(P)\, ||\mathbf{z}||^2 \leq V(\mathbf{z}) = \mathbf{z}^\mathsf{T} P\, \mathbf{z}$, where $\lambda_{min}(P) \in \mathbb{R}$ is the smallest eigenvalue of P, the following relation is also true:

$$
||\mathbf{z}(t)||^2 \leq \lambda_{min}(P)^{-1}\, (1 - \eta_\infty)\, \mathrm{e}^{-2\alpha t} + \lambda_{min}(P)^{-1}\, \eta_\infty\ \forall\, (\mathbf{z}(0), w(0)) \in \mathcal{D}\,. \tag{347}
$$

Thus according to Definition 5.3, the practical exponential performance criteria (P3) is satisfied. Finally, by developing (342) with $\boldsymbol{\Theta}_1(z, w)\,, \ldots, \boldsymbol{\Theta}_4(z, w)$ and factorizing out $[1\ \ \zeta^\mathsf{T}(\mathbf{z}, w)]^\mathsf{T}$, one should obtain the conditions in (333) and (334) .

Additionally, suppose for a given η_τ there exist matrices $U \in \mathbb{R}^{n_\varphi \times n_\varphi}$, $\tilde{U} \in \mathbb{R}^{n_{\tilde{\varphi}} \times n_{\tilde{\varphi}}}$ and scalars $\beta > 0$, $\tilde{\beta} > 0$ and $\gamma_\tau > 0$ such that:

$$
\begin{gathered}
\gamma_\tau^{-2}\, ||e||^2 + \beta\, (\eta_\tau - \mathbf{z}^\mathsf{T} P\, \mathbf{z}) + \tilde{\beta}\, (1 - w^\mathsf{T} \tilde{P}\, w) + \mathcal{H}\big\{\varphi^\mathsf{T}(z, w)\, U \boldsymbol{\Theta}_2(z, w)\, \zeta(\mathbf{z}, w)\big\}\ +\ \ldots \\
\ldots\ +\ \mathcal{H}\big\{\tilde{\varphi}^\mathsf{T}(w)\, \tilde{U} \boldsymbol{\Theta}_3(w)\, \zeta(\mathbf{z}, w)\big\} \leq 1\ \forall\, (\mathbf{z}, w) \in \boldsymbol{\mathcal{Z}}^+ \times \mathcal{W}^+\,.
\end{gathered}
\tag{348}
$$

Since $\boldsymbol{\Theta}_2(z, w)\, \zeta(\mathbf{z}, w) = 0$, $\boldsymbol{\Theta}_3(w)\, \zeta(\mathbf{z}, w) = 0$, $(1 - w^\mathsf{T} \tilde{P}\, w) \geq 0$ and $(\eta_\tau - \mathbf{z}^\mathsf{T} P\, \mathbf{z}) \geq 0$ $\forall\, (\mathbf{z}, w) \in \mathcal{B}_\tau$, it verifies from (348) that

$$
||e|| \leq \gamma_\tau\ \forall\, (\mathbf{z}, w) \in \mathcal{B}_\tau\,. \tag{349}
$$

So, according to Definition 5.1, the closed-loop system (113), (114), (232), (233), (241) achieves practical output regulation within finite time τ and with ultimate error bound γ_τ for every initial condition in (157). Finally, by re-arranging the expression (348) and factorizing $[1\ \ \mathbf{z}^\mathsf{T}\ \ \varphi^\mathsf{T}(z, w)\ \ w^\mathsf{T}\ \ \tilde{\varphi}^\mathsf{T}(w)]$, one obtains the conditions in (336) and:

$$
\begin{bmatrix}
\beta P & -\boldsymbol{\Psi}^\mathsf{T}(z, w) U^\mathsf{T} & 0 & 0 \\
\star & -\mathcal{H}\{U \boldsymbol{\Omega}(z, w)\} & 0 & 0 \\
\star & \star & \tilde{\beta} \tilde{P} & -\tilde{\boldsymbol{\Psi}}^\mathsf{T}(w) \tilde{U}^\mathsf{T} \\
\star & \star & \star & -\mathcal{H}\{\tilde{U} \tilde{\boldsymbol{\Omega}}(w)\}
\end{bmatrix}
- \boldsymbol{\Theta}_5^\mathsf{T}\, \gamma_\tau^{-2}\, \boldsymbol{\Theta}_5 \succ 0\ \ \forall\, (z, w) \in \mathcal{V}_z \times \mathcal{V}_w\,,
\tag{350}
$$

where $\boldsymbol{\Theta}_5 = [\boldsymbol{C}\ \ \boldsymbol{\Gamma}\ \ \tilde{\boldsymbol{C}}\ \ \tilde{\boldsymbol{\Gamma}}]$. At last, relation (337) is obtained by applying Schur's Complement (Lemma A.2) into (350). □

Based on Theorem 5.1, it is possible to analyze if the closed-loop achieves practical output regulation, to determine a set of admissible initial conditions and also to determine ultimate bounds for the regulation error states and output error. In order to cast such analysis problem in the form of a traditional SDP, one must consider *a priori* given stabilizing and anti-windup parameters $\mathrm{F}_0, \ldots, \mathrm{W}_\mathrm{n}$, a diagonal matrix T and a decay-rate performance target $\alpha > 0$. Differently from the previous chapters, an ultimate bounding set $\mathcal{B}_\infty$ is being characterized in here, which is simply a scaled down version of domain of attraction estimate $\mathcal{D}$ by the factor $\eta_\infty < 1$. Thus, by minimizing the scalar η_∞, the gap between $\mathcal{D}$ and $\mathcal{B}_\infty$ is increased, i.e. the volume of the region $(\mathcal{D} - \mathcal{B}_\infty)$ is maximized.

In order to achieve equivalence with the previous methodologies, the following SDP is proposed:

$$\min_{P,L,\tilde{L},\tilde{\alpha},\eta_\infty,\mathrm{R}_0,\ldots,\Pi_\mathrm{m}} \kappa\,\eta_\infty + (1-\kappa)\,\mathrm{tr}(P) \;\text{ s.t. }\; \begin{Bmatrix} (153)\,,\,(154)\,,\,(156)\,,\,(273)\,,\,\ldots \\ \ldots\,,\,(274)\,,\,(333)\,,\,(334) \end{Bmatrix}, \tag{351}$$

where the free scalar $\kappa \in [0\,,\,1]$ establishes the priority between maximization of the $(\mathcal{D}-\mathcal{B}_\infty)$ gap and the pure maximization of $\mathcal{D}$ as previously considered. Given a solution pair P and η_∞ from (351), an additional SDP should also be performed *a posteriori* in order to determine an estimate for the ultimate error bound γ_τ for a given $\tau > 0$:

$$\min_{U,\tilde{U},\gamma_\tau^2,\beta,\tilde{\beta}} \gamma_\tau^2 \;\text{ s.t. }\; \big\{(336)\,,\,(337)\big\}\,. \tag{352}$$

5.3.4 Design Conditions

So as to deal with the design of stabilizing and anti-windup parameters, the usual congruence transformations for output feedback synthesis can be applied into conditions from Theorem 5.1. This additional development is detailed in the following theorem. As considered in the previous chapters, the stabilizing controller order is henceforth enforced as $n_s = n_z$.

Theorem 5.2. *Suppose there exist symmetric matrices $X, Y \in \mathbb{R}^{n_z\times n_z}$, a diagonal matrix $\hat{T} \in \mathbb{R}^{n_u\times n_u}$, matrices $L \in \mathbb{R}^{n_\varphi\times n_\varphi}$, $\tilde{L} \in \mathbb{R}^{n_{\tilde{\varphi}}\times n_{\tilde{\varphi}}}$, $\hat{\mathrm{R}}_0,\ldots,\hat{\mathrm{R}}_\mathrm{m} \in \mathbb{R}^{n_u\times n_z}$, $\hat{\Xi}_0,\ldots,\hat{\Xi}_\mathrm{m} \in \mathbb{R}^{n_u\times n_z}$, $\hat{\Pi}_0,\ldots,\hat{\Pi}_\mathrm{m} \in \mathbb{R}^{n_u\times n_\varphi}$, $\hat{\mathrm{F}}_0,\ldots,\hat{\mathrm{F}}_\mathrm{n} \in \mathbb{R}^{n_z\times n_z}$, $\hat{\mathrm{G}}_0,\ldots,\hat{\mathrm{G}}_\mathrm{n} \in \mathbb{R}^{n_z\times n_\varepsilon}$, $\hat{\mathrm{H}}_0,\ldots,\hat{\mathrm{H}}_\mathrm{n} \in \mathbb{R}^{n_v\times n_z}$, $\hat{\mathrm{K}}_0,\ldots,\hat{\mathrm{K}}_\mathrm{n} \in \mathbb{R}^{n_v\times n_\varepsilon}$, $\hat{\mathrm{E}}_0,\ldots,\hat{\mathrm{E}}_\mathrm{n} \in \mathbb{R}^{n_m\times n_u}$, $\hat{\mathrm{W}}_0,\ldots,\hat{\mathrm{W}}_\mathrm{n} \in \mathbb{R}^{n_z\times n_u}$ and scalars $\tilde{\alpha}, \eta_\infty \in \mathbb{R}$ such that* (168)*,* (169)*,* (171)*,* (286)*,* (287)*,* (333)*,*

$$\mathcal{H}\left\{\begin{bmatrix} A(z,w)X + B\hat{H}(z,w) + \alpha X & A(z,w) + B\hat{K}(z,w)C + \alpha I & \Phi(z,w) + B\hat{K}(z,w)\Gamma & BD_m^\intercal\hat{E}(z,w) - BD^\intercal\hat{T} & \tilde{A}(w) + B\hat{K}(z,w)\tilde{C} & \tilde{\Phi}(w) + B\hat{K}(z,w)\tilde{\Gamma} \\ \hat{F}(z,w) + \alpha I & YA(z,w) + \hat{G}(z,w)C + \alpha Y & Y\Phi(z,w) + \hat{G}(z,w)\Gamma & \hat{W}(z,w) & Y\tilde{A}(w) + \hat{G}(z,w)\tilde{C} & Y\tilde{\Phi}(w) + \hat{G}(z,w)\tilde{\Gamma} \\ L\Psi(z,w)X & L\Psi(z,w) & L\Omega(z,w) & 0 & 0 & 0 \\ \hat{R}(z,w) & \hat{\Xi}(z,w) & \hat{\Pi}(z,w) & -\hat{T} & 0 & 0 \\ 0 & 0 & 0 & 0 & -\tilde{\alpha}\tilde{P} & 0 \\ 0 & 0 & 0 & 0 & \tilde{L}\tilde{\Psi}(w) & \tilde{L}\tilde{\Omega}(w) \end{bmatrix}\right\} \prec 0 \\ \forall\,(z,w) \in \mathcal{V}_z \times \mathcal{V}_w\,, \tag{353}$$

where $\hat{F}(z,w)$, ... , $\hat{K}(z,w)$ are defined as in (172)*, $\hat{E}(z,w)$ and $\hat{W}(z,w)$ are represented by* (289) *and matrices $\hat{R}(z,w)$, $\hat{\Xi}(z,w)$ and $\hat{\Pi}(z,w)$ are the same as in* (290) *for any linear function $\nu : \mathcal{Z}^+ \times \mathcal{W}^+ \to \mathbb{R}^\mathrm{m}$, $\mathrm{m} \in \mathbb{N}$. Then the system* (327) *is ultimately bounded in* (335) *and satisfies* (P2) *and* (P3) *for every initial condition in* (157) *with P given by* (173)*, with stabilizing controller parameters F_i , ... , K_i $\forall\, i \in \{0,1,\ldots,\mathrm{n}\}$ obtained by* (174) *and anti-windup parameters E_i and W_i $\forall\, i \in \{0,1,\ldots,\mathrm{n}\}$ constructed by* (291)*, where the pair $M, N \in \mathbb{R}^{n_z\times n_z}$ is a non-singular solution to* (175)*. Moreover, suppose for some $\tau > 0$ there exist matrices $U \in \mathbb{R}^{n_\varphi\times n_\varphi}$, $\tilde{U} \in \mathbb{R}^{n_{\tilde{\varphi}}\times n_{\tilde{\varphi}}}$ and scalars $\beta, \tilde{\beta}, \gamma_\tau^2 \in \mathbb{R}$ such that* (337)*. Then the closed-loop system* (113)*,* (114) *with controller* (232)*,* (233)*,* (241) *also achieves practical output regulation with ultimate error bound γ_τ for every initial condition in* (157)*.*

Proof. Suppose conditions from Theorem 5.1 hold for $n_s = n_z$ and for P decomposed as (176), where $X, Y \in \mathbb{R}^{n_z \times n_z}$ are symmetric matrices and $M, N \in \mathbb{R}^{n_z \times n_z}$ are generic square matrices. Since $P^{-1}P = I$, then condition (175) must be satisfied. Consider the same blocks $Z_1, Z_2 \in \mathbb{R}^{n_a \times n_a}$ shown in (177), where $PZ_1 = Z_2$. Applying the congruence transformations Z_1, $\mathrm{diag}\{1, Z_1\}$, $\mathrm{diag}\{Z_1, Z_1\}$, T^{-1}, $\mathrm{diag}\{1, Z_1, I\}$ and $\mathrm{diag}\{Z_1, I, T^{-1}, I, I\}$ into (153), (154), (156), (273), (274) and (334) leads respectively to (168), (169), (171), (286), (287) and (353) when considering the change of variables (178), (292), $\hat{T} = T^{-1}$, $\hat{R}(z,w) = R(z,w)X + \Xi(z,w)M^{\intercal}$, $\hat{\Xi}(z,w) = R(z,w)$ and $\hat{\Pi}(z,w) = \Pi(z,w)$. By inversion of (178) and (292), one obtains respectively (179) and (293), which leads to (174) and (291). Also, matrix P can be reconstructed as (173) since $P = Z_2\, Z_1^{-1}$. Thus, conditions from Theorem 5.1 are then equivalent to Theorem 5.2 when considering a full order controller $n_s = n_z$. □

Using the conditions of Theorem 5.2, the optimization problem (351), originally constructed for analyzes purposes, can be reframed as

$$\min_{\substack{X,Y,L,\tilde{L},\tilde{\alpha},\eta_\infty,\hat{T},\\ \hat{\mathrm{R}}_0,\ldots,\hat{\Pi}_\mathrm{m},\hat{\mathrm{F}}_0,\ldots,\hat{\mathrm{W}}_\mathrm{n}}} \kappa\,\eta_\infty + (1-\kappa)\,\mathrm{tr}(Y) \;\text{ s.t. }\; \begin{Bmatrix} (168)\,,\,(169)\,,\,(171)\,,\,(286)\,,\,\ldots \\ \ldots\,,\,(287)\,,\,(333)\,,\,(353) \end{Bmatrix}, \tag{354}$$

where stabilizing and anti-windup parameters are here included as decision variables. After the controller parameters have been synthesized by (354), one can evaluate (352) so as to determine an ultimate error bound estimate γ_τ for a given τ.

It is noticeable that (354) contains the usual bilinearity involving variables L and X, similar to what have been presented in the previous chapters. Although, whenever Assumption 3.3 is true, it is again possible to substitute the original stabilizing stage (241) with the modified one (295), so as to eliminate the before-mentioned bilinearity. The adaptation of Theorem 5.2 for this convex special case is presented by the subsequent corollary.

Corollary 5.1. *Suppose there exist symmetric matrices $X, Y \in \mathbb{R}^{n_z \times n_z}$, a diagonal matrix $\hat{T} \in \mathbb{R}^{n_u \times n_u}$, matrices $\hat{L} \in \mathbb{R}^{n_\varphi \times n_\varphi}$, $\tilde{L} \in \mathbb{R}^{n_{\tilde{\varphi}} \times n_{\tilde{\varphi}}}$, $\hat{\mathrm{R}}_0, \ldots, \hat{\mathrm{R}}_\mathrm{m} \in \mathbb{R}^{n_u \times n_z}$, $\hat{\Xi}_0, \ldots, \hat{\Xi}_\mathrm{m} \in \mathbb{R}^{n_u \times n_z}$, $\hat{\Pi}_0, \ldots, \hat{\Pi}_\mathrm{m} \in \mathbb{R}^{n_u \times n_\varphi}$, $\hat{\mathrm{F}}_0, \ldots, \hat{\mathrm{F}}_\mathrm{n} \in \mathbb{R}^{n_z \times n_z}$, $\hat{\mathrm{G}}_0, \ldots, \hat{\mathrm{G}}_\mathrm{n} \in \mathbb{R}^{n_z \times n_\varepsilon}$, $\hat{\mathrm{H}}_0, \ldots, \hat{\mathrm{H}}_\mathrm{n} \in \mathbb{R}^{n_v \times n_z}$, $\hat{\mathrm{K}}_0, \ldots, \hat{\mathrm{K}}_\mathrm{n} \in \mathbb{R}^{n_v \times n_\varepsilon}$, $\hat{\Lambda}_0, \ldots, \hat{\Lambda}_\mathrm{n} \in \mathbb{R}^{n_z \times n_\varphi}$, $\hat{\Theta}_0, \ldots, \hat{\Theta}_\mathrm{n} \in \mathbb{R}^{n_v \times n_\varphi}$, $\hat{\mathrm{E}}_0, \ldots, \hat{\mathrm{E}}_\mathrm{n} \in \mathbb{R}^{n_m \times n_u}$, $\hat{\mathrm{W}}_0, \ldots, \hat{\mathrm{W}}_\mathrm{n} \in \mathbb{R}^{n_z \times n_u}$ and scalars $\tilde{\alpha}, \eta_\infty \in \mathbb{R}$ such that* (168)*,* (169)*,* (171)*,* (286)*,* (297)*,* (333)*,*

$$\mathcal{H}\left\{\begin{bmatrix} A(z,w)X + B\hat{H}(z,w) + \alpha X & A(z,w) + B\hat{K}(z,w)C + \alpha I & \Phi(z,w)\hat{L} + B\hat{\Theta}(z,w) & BD_m^{\intercal}\hat{E}(z,w) - BD^{\intercal}\hat{T} & \tilde{A}(w) + B\hat{K}(z,w)\tilde{C} & \tilde{\Phi}(w) + B\hat{K}(z,w)\tilde{\Gamma} \\ \hat{F}(z,w) + \alpha I & YA(z,w) + \hat{G}(z,w)C + \alpha Y & \hat{\Lambda}(z,w) & \hat{W}(z,w) & Y\tilde{A}(w) + \hat{G}(z,w)\tilde{C} & Y\tilde{\Phi}(w) + \hat{G}(z,w)\tilde{\Gamma} \\ \Psi(z,w)X & \Psi(z,w) & \Omega(z,w)\hat{L} & 0 & 0 & 0 \\ \hat{R}(z,w) & \hat{\Xi}(z,w) & \hat{\Pi}(z,w) & -\hat{T} & 0 & 0 \\ 0 & 0 & 0 & 0 & -\tilde{\alpha}\tilde{P} & 0 \\ 0 & 0 & 0 & 0 & \tilde{L}\tilde{\Psi}(w) & \tilde{L}\tilde{\Omega}(w) \end{bmatrix}\right\} \prec 0$$
$$\forall\,(z,w) \in \mathcal{V}_z \times \mathcal{V}_w\,, \tag{355}$$

where $\hat{F}(z,w)\,,\,\ldots\,,\,\hat{K}(z,w)$ are defined as in (172)*, $\hat{\Theta}(z,w)$ and $\hat{\Lambda}(z,w)$ are identical to* (187)*, $\hat{E}(z,w)$ and $\hat{W}(z,w)$ are represented by* (289) *and matrices $\hat{R}(z,w)$, $\hat{\Xi}(z,w)$ and*

$\hat{\Pi}(z,w)$ are the same as in (290) *for any linear function $\nu : \mathcal{Z}^+ \times \mathcal{W}^+ \to \mathbb{R}^{\mathrm{m}}$, $\mathrm{m} \in \mathbb{N}$. Then the system* (327) *is ultimately bounded in* (335) *and satisfies* (P2) *and* (P3) *for every initial condition in* (157) *with P given by* (173)*, with stabilizing controller parameters $\mathrm{F}_i, \ldots, \Theta_i \; \forall \, i \in \{0, 1, \ldots, \mathrm{n}\}$ obtained by* (174) *and* (188) *and anti-windup parameters E_i and $\mathrm{W}_i \; \forall \, i \in \{0, 1, \ldots, \mathrm{n}\}$ constructed by* (291)*, where the pair $M, N \in \mathbb{R}^{n_z \times n_z}$ is a non-singular solution to* (175)*. Moreover, suppose for some $\tau > 0$ there exist matrices $U \in \mathbb{R}^{n_\varphi \times n_\varphi}$, $\tilde{U} \in \mathbb{R}^{n_{\tilde{\varphi}} \times n_{\tilde{\varphi}}}$ and scalars $\beta, \tilde{\beta}, \gamma_\tau^2 \in \mathbb{R}$ such that* (337)*. Then the closed-loop system* (113)*,* (114) *with controller* (232)*,* (233)*,* (295) *also achieves practical output regulation with ultimate error bound γ_τ for every initial condition in* (157)*.*

Proof. Consider the same proof presented for Theorem 5.2, except post- and pre-multiply (274) and (334) respectively with $\mathrm{diag}\{1, Z_1, L^{-\intercal}\}$, $\mathrm{diag}\{Z_1, L^{-\intercal}, T^{-1}, I, I\}$ and their transposes, which yield (297) and (355) when considering the change of variables (178), (189), $\hat{T} = T^{-1}$, $\hat{L} = L^{-\intercal}$, $\hat{R}(z,w) = R(z,w)X + \Xi(z,w)M^{\intercal}$, $\hat{\Xi}(z,w) = R(z,w)$ and $\hat{\Pi}(z,w) = \Pi(z,w)L^{-\intercal}$. From straightforward inversion of the variable transformations (178) and (189), one obtains respectively (174) and (188). □

Considering the stabilizing stage (295) and the conditions from Corollary 5.1, the previous optimization problem (354) is reformulated as

$$\min_{\substack{X, Y, L, \tilde{L}, \tilde{\alpha}, \eta_\infty, \hat{T}, \\ \hat{\mathrm{R}}_0, \ldots, \hat{\Pi}_{\mathrm{m}}, \hat{\mathrm{F}}_0, \ldots, \hat{\mathrm{W}}_{\mathrm{n}}}} \kappa\,\eta_\infty + (1-\kappa)\,\mathrm{tr}(Y) \;\; \text{s.t.} \;\; \begin{Bmatrix} (168)\,,\; (169)\,,\; (171)\,,\; (286)\,,\; \ldots \\ \ldots\,,\; (297)\,,\; (333)\,,\; (355) \end{Bmatrix}, \tag{356}$$

which is now subject to LMI constraints.

5.4 Numerical Example

This section is dedicated to illustrating the proposed practical output regulation methodology using a numerical example. The plant to be regulated is considered here as

$$\begin{cases} \dot{x}_1 &= x_2 + a_1\,u \\ \dot{x}_2 &= a_3\,w_1^2 x_2 + a_3\,w_2 (x_1 - w_1)^2 + a_2\,u \end{cases}, \qquad y = e = x_1 - w_1\,, \tag{357}$$

where $x \in \mathbb{R}^2$ is the system state vector, $u \in \mathbb{R}$ is the control input, $y \in \mathbb{R}$ is the output measurement, $e \in \mathbb{R}$ is the output error and $a_1, a_2, a_3 \in \mathbb{R}$ are constant parameters. The system is directly influenced by a harmonic exosystem described by (193), where $w \in \mathbb{R}^2$ is the exosystem state and $\omega \in \mathbb{R}$ is a constant parameter denoting the disturbance frequency.

So as to motivate the use of a practical output regulation approach in this example, a preliminary analytic inspection of the problem is performed. In comparison to the previous numerical examples showed in Chapters 3 and 4, the plant dynamics in (357) contains a fundamental difference, which is the presence of a control input term in all the plant states time-derivatives. If $a_1 \neq 0$, the system equations do not match the triangular form presented by (76) and, consequently, the plant zero-error steady-state solution cannot be recursively determined by (77).

By verifying the plant regulator equations, one is able to conclude that $\pi_1(w) = w_1$, in order to satisfy the condition $0 = h(\pi(w), w) = \pi_1(w) - w_1$. The remaining condition $\dot{\pi}(w) = f(\pi(w), w, c(w))$ then yields the following partial differential equations:

$$\begin{cases} \omega\,w_2 &= \pi_2(w) + a_1\,c(w) \\ \omega\,w_2\,\dfrac{\partial \pi_2(w)}{\partial w_1} - \omega\,w_1\,\dfrac{\partial \pi_2(w)}{\partial w_2} &= a_3\,w_1^2\,\pi_2(w) + a_2\,c(w) \end{cases}. \tag{358}$$

By setting $\pi_2(w) = \omega\, w_2 - a_1\, c(w)$ and plugging into the second equation in (358), it results:

$$-a_1\omega\, w_2\, \frac{\partial c(w)}{\partial w_1} + a_1\omega\, w_1\, \frac{\partial c(w)}{\partial w_2} \;=\; a_3\, \omega\, w_1^2 w_2 + \omega^2\, w_1 + (a_2 - a_3\, w_1^2)\, c(w)\;. \quad (359)$$

Now suppose the solution $c(w)$ for equation (359) is a polynomial function of degree $n_c \in \mathbb{N}$. Note that $a_3\, \omega\, w_1^2 w_2 + \omega^2\, w_1$ is of degree 3, that $\partial c(w)/\partial w_1$ and $\partial c(w)/\partial w_2$ are of degree $n_c - 1$, and that $(a_2 - a_3\, w_1^2)\, c(w)$ is of degree $n_c + 2$. The left and right side of equation (359) are thus respectively of degree n_c and $\max\{3, n_c + 2\}$. Therefore $\forall\, n_c \in \mathbb{N}$, both sides of (359) have different degrees, and there is no polynomial solution $c(w)$ with finite degree. Consequently, the exact theoretical solution $c(w)$ must be an infinite order polynomial series. This observation represents a challenge not only for the evaluation of $c(w)$, but also for designing a proper internal model capable of rendering this steady-state control signal, since and infinite order immersion would be required. Moreover, these arguments motivate the use of a practical output regulation methodology, where the steady-state mappings can be approximated and a reduced internal model stage can be considered.

5.4.1 Approximate Solution of the Regulator Equations

In the following pages, the proposed methodology is demonstrated with three different cases. In the first, no internal model stage is considered, providing a baseline for the comparative analysis. On the other hand, the second and third cases will contain an internal model stage, respectively of second and fourth-order. In all configurations, the approximate solution to $\pi_1(w)$ will be fixed as the exact analytic solution previously discussed, i.e.

$$\tilde{\pi}_1(w) = w_1\;. \quad (360)$$

Remaining mapping variables, such as $\pi_2(w)$ and $c(w)$, and even the internal model functions are to be numerically determined, following the procedures mentioned in Section 5.2. Parametrized candidate solutions are initially set for each case, where $q_1, q_2, \ldots, q_{n_q} \in \mathbb{R}$ denote free decision variables to be computed by numerical optimization.

- No internal model case:

$$\tilde{\pi}_2(w) = q_1\, w_1 + q_2\, w_2\;,\;\; \tilde{c}(w) = 0\;. \quad (361)$$

- Second-order internal model case:

$$\tilde{\pi}_2(w) = q_1\, w_1 + q_2\, w_2\;,\;\; \tilde{c}(w) = q_3\, w_1 + q_4\, w_2\;,$$
$$\theta_m(\xi_m) = \xi_{m1}\;,\quad \phi_m(\xi_m) = \begin{bmatrix} \xi_{m2} \\ q_5\, \xi_{m1} + q_6\, \xi_{m2} \end{bmatrix}\;,\quad \tilde{\sigma}_m(w) = \begin{bmatrix} \tilde{c}(w) \\ \dot{\tilde{c}}(w) \end{bmatrix}\;. \quad (362)$$

- Fourth-order internal model case:

$$\tilde{\pi}_2(w) = q_1\, w_1 + q_2\, w_2 + q_3\, w_1^3 + q_4\, w_2^3 + q_5\, w_1^2 w_2 + q_6\, w_1 w_2^2\;,$$
$$\tilde{c}(w) = q_7\, w_1 + q_8\, w_2 + q_9\, w_1^3 + q_{10}\, w_2^3 + q_{11}\, w_1^2 w_2 + q_{12}\, w_1 w_2^2\;,$$
$$\theta_m(\xi_m) = \xi_{m1}\;,\quad \phi_m(\xi_m) = \begin{bmatrix} \xi_{m2} \\ \xi_{m3} \\ \xi_{m4} \\ q_{13}\, \xi_{m1} + q_{14}\, \xi_{m2} + \ldots \\ \ldots + q_{15}\, \xi_{m3} + q_{16}\, \xi_{m4} \end{bmatrix}\;,\;\; \tilde{\sigma}_m(w) = \begin{bmatrix} \tilde{c}(w) \\ \dot{\tilde{c}}(w) \\ \overset{(2)}{\tilde{c}}(w) \\ \overset{(3)}{\tilde{c}}(w) \end{bmatrix}\;. \quad (363)$$

The candidate solutions $\tilde{\pi}_2(w)$ and $\tilde{c}(w)$ are being defined as generic polynomials with unknown coefficients and different degrees, where in this case, even-degree terms were skipped because the solutions $c(w)$ and $\pi_2(w)$ have odd symmetry. In turn, the internal model candidates are being constructed according to the traditional immersion structure explained in Lemma 2.3, however now with *a priori* unknown coefficients. In each case, the degree of $\tilde{c}(w)$ is in accordance to the established internal model order.

For each scenario, it is also necessary to parametrize the residual functions $\Delta_f(w)$, $\Delta_h(w)$ and $\Delta_\phi(w)$ with respect to the relaxed regulator equations. To do so, additional free decision variables q are being considered, as presented next.

- No internal model case:

$$\Delta_f(w) = \begin{bmatrix} q_3\, w_1 + q_4\, w_2 \\ q_5\, w_1 + q_6\, w_2 + q_7\, w_1^3 + q_8\, w_1^2 w_2 \end{bmatrix} \tag{364}$$

- Second-order internal case:

$$\Delta_f(w) = \begin{bmatrix} q_7\, w_1 + q_8\, w_2 \\ q_9\, w_1 + q_{10}\, w_2 + q_{11}\, w_1^3 + q_{12}\, w_1^2 w_2 \end{bmatrix}, \;\; \Delta_\phi(w) = \begin{bmatrix} 0 \\ q_{13}\, w_1 + q_{14}\, w_2 \end{bmatrix}. \tag{365}$$

- Fourth-order internal model case:

$$\Delta_f(w) = \begin{bmatrix} q_{17}\, w_1 + q_{18}\, w_2 + q_{19}\, w_1^3 + q_{20}\, w_2^3 + q_{21}\, w_1^2 w_2 + q_{22}\, w_1 w_2^2 \\ q_{23}\, w_1 + q_{24}\, w_2 + q_{25}\, w_1^3 + q_{26}\, w_2^3 + q_{27}\, w_1^2 w_2 + \ldots \\ \ldots + q_{28}\, w_1 w_2^2 + q_{29}\, w_1^5 + q_{30}\, w_1^4 w_2 + q_{31}\, w_1^3 w_2^2 + q_{32}\, w_1^2 w_2^3 \end{bmatrix},$$

$$\Delta_\phi(w) = \begin{bmatrix} 0 \\ 0 \\ 0 \\ q_{33}\, w_1 + q_{34}\, w_2 + q_{35}\, w_1^3 + q_{36}\, w_2^3 + q_{37}\, w_1^2 w_2 + q_{38}\, w_1 w_2^2 \end{bmatrix}. \tag{366}$$

In every case it follows that $\Delta_h(w) = 0$ since $\tilde{\pi}_1(w) = w_1$. One should also note that, in all cases, $\Delta_{f_2}(w)$ contains polynomial terms of fifth-degree, which are originated by the term $w_1^2\, \tilde{\pi}_2(w)$ in the regulator equations. Moreover, the output measurement vanishing function is defined for all cases as the identity $\varepsilon = \delta(y) = y$, which readily satisfies the last regulator equation (313) with $\Delta_\delta(w) = 0$, since $\tilde{d}(w) = 0$.

Regarding the harmonic exosystem (193), it verifies that $w(0) \in \mathcal{W} \Rightarrow w(t) \in \mathcal{W}$ $\forall\, t > 0$ for any circular region of the form

$$\mathcal{W} = \left\{ w \in \mathbb{R}^2 : ||w|| \leq \overline{w} \right\}, \tag{367}$$

where $\overline{w} > 0$ represents the maximum admissible exogenous state amplitude. In order to numerically solve the plant zero-error steady-state and synthesize the internal model functions, the target domain $\tilde{\mathcal{W}}$ is set as an uniform grid on top of the disk $\mathcal{W}$, according to $\tilde{\mathcal{W}} = \tilde{\mathcal{W}}_1 \times \tilde{\mathcal{W}}_2$, where $\tilde{\mathcal{W}}_1$ and $\tilde{\mathcal{W}}_2$ denote

$$\tilde{\mathcal{W}}_1 = \tilde{\mathcal{W}}_2 = \left\{ -\overline{w},\, -0.75\,\overline{w},\, -0.5\,\overline{w},\, -0.25\,\overline{w},\, 0,\, 0.25\,\overline{w},\, 0.5\,\overline{w},\, 0.75\,\overline{w},\, \overline{w} \right\}. \tag{368}$$

Considering the system parameters $a_1 = a_2 = 1$, $a_3 = -1$, $\omega = 1$ and $\overline{w} = 1$, the optimization problems (315) and (316) were cast in the form of a nonlinear programming and evaluated in the software MATLAB using an interior-point solver. For each case, the obtained solutions q_1,q_2,. . .,q_{n_q} are shown next.

- No internal model case: $q_1 = 3.3894 \cdot 10^{-3}$, $q_2 = 9.8596 \cdot 10^{-1}$, $q_3 = 3.3894 \cdot 10^{-3}$, $q_4 = -1.4038 \cdot 10^{-2}$, $q_5 = 9.8596 \cdot 10^{-1}$, $q_6 = -3.3894 \cdot 10^{-3}$, $q_7 = -3.3894 \cdot 10^{-3}$ and $q_8 = -9.8596 \cdot 10^{-1}$.

- Second-order internal model case: $q_1 = 2.5754 \cdot 10^{-1}$, $q_2 = 4.6403 \cdot 10^{-1}$, $q_3 = 5.3550 \cdot 10^{-1}$, $q_4 = -2.5742 \cdot 10^{-1}$, $q_5 = -1$, $q_6 = 0$, $q_7 = 1.2301 \cdot 10^{-4}$, $q_8 = -4.5936 \cdot 10^{-4}$, $q_9 = 2.0661 \cdot 10^{-1}$, $q_{10} = 2.7795 \cdot 10^{-1}$, $q_{11} = -2.5754 \cdot 10^{-1}$, $q_{12} = -4.6403 \cdot 10^{-1}$, $q_{13} = 0$ and $q_{14} = 0$.

- Fourth-order internal model case: $q_1 = 4.6767 \cdot 10^{-1}$, $q_2 = 5.3452 \cdot 10^{-1}$, $q_3 = -1.9442 \cdot 10^{-1}$, $q_4 = 5.8339 \cdot 10^{-3}$, $q_5 = 1.5364 \cdot 10^{-2}$, $q_6 = -7.1938 \cdot 10^{-3}$, $q_7 = -4.6771 \cdot 10^{-1}$, $q_8 = 4.6546 \cdot 10^{-1}$, $q_9 = 1.9448 \cdot 10^{-1}$, $q_{10} = -5.8233 \cdot 10^{-3}$, $q_{11} = -1.5354 \cdot 10^{-2}$, $q_{12} = 7.2010 \cdot 10^{-3}$, $q_{13} = -9$, $q_{14} = 0$, $q_{15} = -10$, $q_{16} = 0$, $q_{17} = -4.1732 \cdot 10^{-5}$, $q_{18} = -1.4281 \cdot 10^{-5}$, $q_{19} = 5.0466 \cdot 10^{-5}$, $q_{20} = 1.06042 \cdot 10^{-5}$, $q_{21} = 1.0558 \cdot 10^{-5}$, $q_{22} = 7.2101 \cdot 10^{-6}$, $q_{23} = 6.6805 \cdot 10^{-2}$, $q_{24} = -2.2165 \cdot 10^{-3}$, $q_{25} = -2.5783 \cdot 10^{-1}$, $q_{26} = 1.3704 \cdot 10^{-3}$, $q_{27} = 1.9023 \cdot 10^{-2}$, $q_{28} = -6.0264 \cdot 10^{-3}$, $q_{29} = 1.9442 \cdot 10^{-1}$, $q_{30} = 1.5364 \cdot 10^{-2}$, $q_{31} = 7.1938 \cdot 10^{-3}$, $q_{32} = 5.8339 \cdot 10^{-3}$, $q_{33} = 0$, $q_{34} = 0$, $q_{35} = 0$, $q_{36} = 0$, $q_{37} = 0$ and $q_{38} = 0$.

For each configuration, the solution accuracy can be analyzed by the summation of $||\Delta_{f_z}(w)||^2$ for all points in $\tilde{\mathcal{W}}$, where $\Delta_{f_z}(w)$ was defined in (321). The Table 1 compares this computation for each case. Complementary, Figure 25 depicts the dominant components $\Delta_{f_2}(w)$ using a tridimensional surface plot over the w-domain. From Table 1 and Figure 25, it is evident that the regulator equations residuals are significantly diminished as the parametrization complexity is increased.

Table 1: Accuracy measure of the regulator equations approximate solutions for different internal model orders. Lower values indicate a better approximation. Source: the author.

Internal model order	Zero	Second	Fourth
$\sum_{w \in \tilde{\mathcal{W}}} ||\Delta_{f_z}(w)||^2$	$1.2586 \cdot 10^{1}$	$6.5552 \cdot 10^{-1}$	$6.9572 \cdot 10^{-3}$

5.4.2 Stabilizing Stage Design

The initial step in order to design the stabilizing stage is to represent the system equations in the practical regulation error form (320) using coordinate change (319). For each respective setup case, function $f_z(z, w, \hat{v})$ is according to:

- No internal model case:

$$f_z(z, w, \hat{v}) = \begin{bmatrix} z_2 + a_1 \, \hat{v}_1 \\ a_3 \, (w_1^2 z_2 + w_2 z_1^2) + a_2 \, \hat{v}_1 \end{bmatrix}. \tag{369}$$

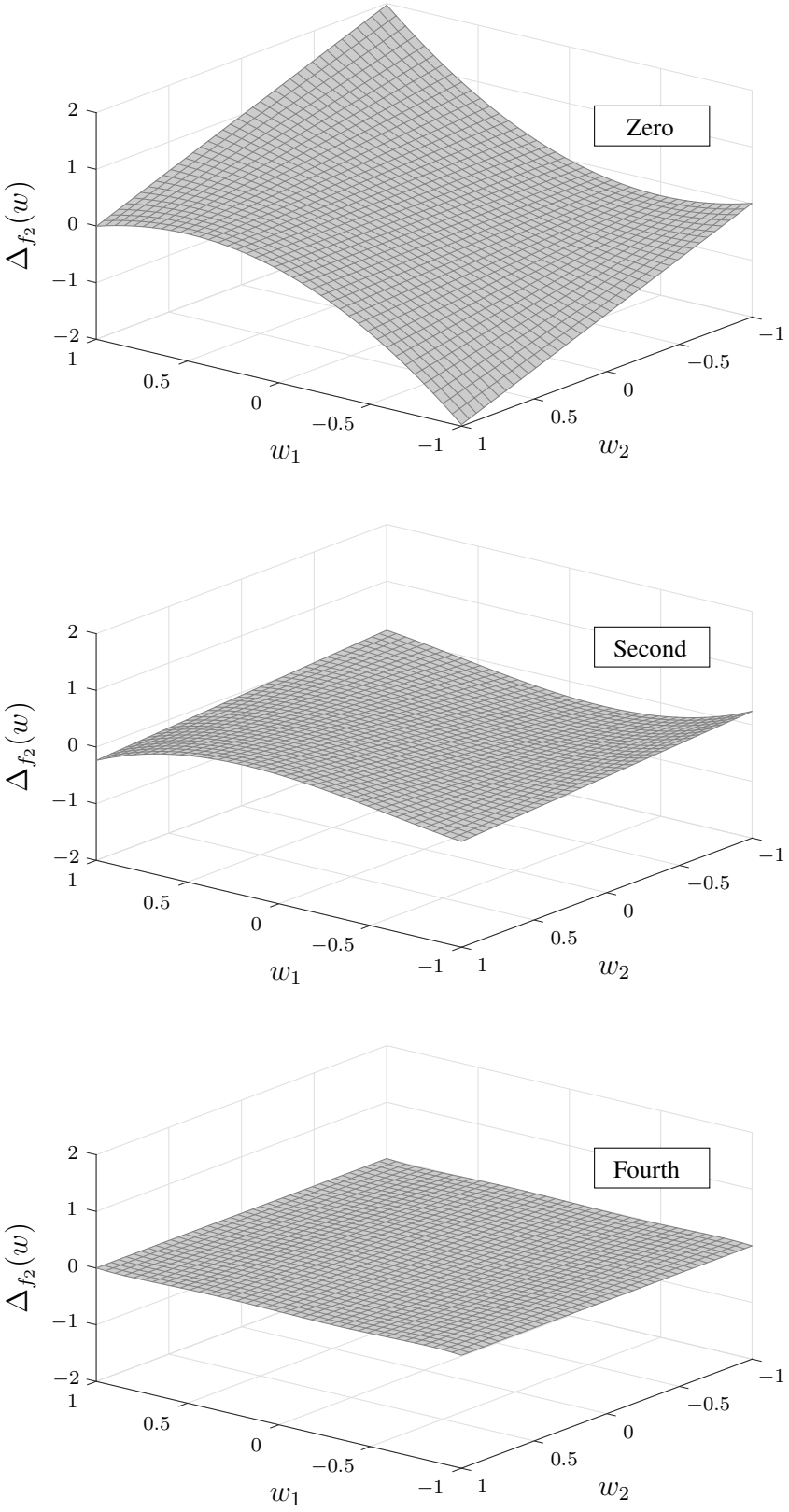

Figure 25: Graphical representation of the residual function $\Delta_{f_2}(w)$ respectively for the zero, second and fourth-order internal model case. Source: the author.

- Second-order internal model case:

$$f_z(z,w,\hat{v}) = \begin{bmatrix} z_2 + a_1\,(z_3+\hat{v}_1) \\ a_3\,(w_1^2 z_2 + w_2 z_1^2) + a_4\,w_2 z_1^2 + a_2\,(z_3+\hat{v}_1) \\ z_4 + \hat{v}_2 \\ q_5\,z_3 + q_6\,z_4 + \hat{v}_3 \end{bmatrix}. \tag{370}$$

- Fourth-order internal model case:

$$f_z(z,w,\hat{v}) = \begin{bmatrix} z_2 + a_1\,(z_3+\hat{v}_1) \\ a_3\,(w_1^2 z_2 + w_2 z_1^2) + a_2\,(z_3+\hat{v}_1) \\ z_4 + \hat{v}_2 \\ z_5 + \hat{v}_3 \\ z_6 + \hat{v}_4 \\ q_{13}\,z_3 + q_{14}\,z_4 + q_{15}\,z_5 + q_{16}\,z_6 + \hat{v}_5 \end{bmatrix}. \tag{371}$$

Moreover, all cases have in common $h_z(z,w) = \delta_z(z,w) = z_1$, $\lambda(y) = 0$ and $\lambda(z,w) = 0$. Also, the last two scenarios are associated with $\theta_z(z,w) = z_3$, whereas $\theta_z(z,w) = 0$ in the first one.

The second step is to choose an appropriate differential-algebraic representation for the functions $f_z(z,w,\hat{v})$, $h_z(z,w)$ and $\delta_z(z,w)$, as detailed in Subsection 5.3.2. For this purpose, it is suffcient to consider, in all configurations, the following vector of rational nonlinearities:

$$\varphi(z,w) = \begin{bmatrix} w_1 z_2 & w_2 z_1 \end{bmatrix}^{\mathsf{T}}. \tag{372}$$

Given this choice, the system matrices, as in Assumption 4.1, may be specified as follows.

- No internal model case:

$$\begin{aligned} A &= \begin{bmatrix} 0 & 1 \\ 0 & 0 \end{bmatrix}, \quad \Phi(z,w) = a_3 \begin{bmatrix} 0 & 0 \\ w_1 & z_1 \end{bmatrix}, \quad B = \begin{bmatrix} a_1 \\ a_2 \end{bmatrix}, \\ C &= \begin{bmatrix} 1 & 0 \end{bmatrix}, \qquad \Gamma = \begin{bmatrix} 0 & 0 \end{bmatrix}, \\ Q &= \begin{bmatrix} 0 & 0 \end{bmatrix}, \qquad \Upsilon = \begin{bmatrix} 0 & 0 \end{bmatrix}, \\ \Psi(w) &= -\begin{bmatrix} 0 & w_1 \\ w_2 & 0 \end{bmatrix}, \qquad \Omega = \begin{bmatrix} 1 & 0 \\ 0 & 1 \end{bmatrix}, \end{aligned} \tag{373}$$

- Second-order internal model case:

$$\begin{aligned} A &= \begin{bmatrix} 0 & 1 & a_1 & 0 \\ 0 & 0 & a_2 & 0 \\ 0 & 0 & 0 & 1 \\ 0 & 0 & q_5 & q_6 \end{bmatrix}, \quad \Phi(z,w) = a_3 \begin{bmatrix} 0 & 0 \\ w_1 & z_1 \\ 0 & 0 \\ 0 & 0 \end{bmatrix}, \quad B = \begin{bmatrix} a_1 & 0 & 0 \\ a_2 & 0 & 0 \\ 0 & 1 & 0 \\ 0 & 0 & 1 \end{bmatrix}, \\ C &= \begin{bmatrix} 1 & 0 & 0 & 0 \end{bmatrix}, \qquad \Gamma = \begin{bmatrix} 0 & 0 \end{bmatrix}, \\ Q &= \begin{bmatrix} 0 & 0 & 1 & 0 \end{bmatrix}, \qquad \Upsilon = \begin{bmatrix} 0 & 0 \end{bmatrix}, \\ \Psi(w) &= -\begin{bmatrix} 0 & w_1 & 0 & 0 \\ w_2 & 0 & 0 & 0 \end{bmatrix}, \qquad \Omega = \begin{bmatrix} 1 & 0 \\ 0 & 1 \end{bmatrix}, \end{aligned} \tag{374}$$

- Fourth-order internal model case:

$$
\begin{aligned}
A &= \begin{bmatrix} 0 & 1 & a_1 & 0 & 0 & 0 \\ 0 & 0 & a_2 & 0 & 0 & 0 \\ 0 & 0 & 0 & 1 & 0 & 0 \\ 0 & 0 & 0 & 0 & 1 & 0 \\ 0 & 0 & 0 & 0 & 0 & 1 \\ 0 & 0 & q_{13} & q_{14} & q_{15} & q_{16} \end{bmatrix}, \; \Phi(z,w) = a_3 \begin{bmatrix} 0 & 0 \\ w_1 & z_1 \\ 0 & 0 \\ 0 & 0 \\ 0 & 0 \end{bmatrix}, B = \begin{bmatrix} a_1 & 0 & 0 & 0 & 0 \\ a_2 & 0 & 0 & 0 & 0 \\ 0 & 1 & 0 & 0 & 0 \\ 0 & 0 & 1 & 0 & 0 \\ 0 & 0 & 0 & 1 & 0 \\ 0 & 0 & 0 & 0 & 1 \end{bmatrix}, \\
C &= \begin{bmatrix} 1 & 0 & 0 & 0 & 0 & 0 \end{bmatrix}, \qquad \Gamma = \begin{bmatrix} 0 & 0 \end{bmatrix}, \\
Q &= \begin{bmatrix} 0 & 0 & 1 & 0 & 0 & 0 \end{bmatrix}, \qquad \Upsilon = \begin{bmatrix} 0 & 0 \end{bmatrix}, \\
\Psi(w) &= -\begin{bmatrix} 0 & w_1 & 0 & 0 & 0 & 0 \\ w_2 & 0 & 0 & 0 & 0 & 0 \end{bmatrix}, \qquad \Omega = \begin{bmatrix} 1 & 0 \\ 0 & 1 \end{bmatrix},
\end{aligned}
\tag{375}
$$

In the practical output regulation problem being addressed, is it furthermore required to choose an appropriate differential-algebraic representation for the residual terms $\Delta_{f_z}(w)$, $\Delta_{h_z}(w)$ and $\Delta_{h_z}(w)$ according to Assumption 5.1. To do so, one may consider the following complementary vector of rational nonlinearities $\tilde{\varphi}(w)$.

- No internal model and second-order internal model cases:

$$
\tilde{\varphi}(w) = \begin{bmatrix} w_1 w_2 & w_1^2 \end{bmatrix}^{\mathsf{T}}. \tag{376}
$$

- Fourth-order internal model case:

$$
\tilde{\varphi}(w) = \begin{bmatrix} w_1 w_2 & w_1^2 & w_2^2 & w_1^2 w_2^2 & w_1^3 w_2 & w_1^4 & w_1^2 w_2 & w_1^3 \end{bmatrix}^{\mathsf{T}}. \tag{377}
$$

The additional system matrices, as in Assumption 5.1, may be specified in the following manner.

- No internal model case:

$$
\begin{aligned}
\tilde{A} &= \begin{bmatrix} q_3 & q_4 \\ q_5 & q_6 \end{bmatrix}, \quad \tilde{\Phi}(w) = \begin{bmatrix} 0 & 0 \\ q_8\, w_1 & q_7\, w_1 \end{bmatrix}, \\
\tilde{C} &= \begin{bmatrix} 0 & 0 \end{bmatrix}, \qquad \tilde{\Gamma} = \begin{bmatrix} 0 & 0 \end{bmatrix}, \\
\tilde{Q} &= \begin{bmatrix} 0 & 0 \end{bmatrix}, \qquad \tilde{\Upsilon} = \begin{bmatrix} 0 & 0 \end{bmatrix}, \\
\tilde{\Psi}(w) &= -\begin{bmatrix} 0 & w_1 \\ w_2 & 0 \end{bmatrix}, \qquad \tilde{\Omega} = \begin{bmatrix} 1 & 0 \\ 0 & 1 \end{bmatrix},
\end{aligned}
\tag{378}
$$

- Second-order internal model case:

$$
\begin{aligned}
\tilde{A} &= \begin{bmatrix} q_7 & q_8 \\ q_9 & q_{10} \\ 0 & 0 \\ q_{13} & q_{14} \end{bmatrix}, \quad \tilde{\Phi}(w) = \begin{bmatrix} 0 & 0 \\ q_{12}\, w_1 & q_{11}\, w_1 \\ 0 & 0 \\ 0 & 0 \end{bmatrix}, \\
\tilde{C} &= \begin{bmatrix} 0 & 0 \end{bmatrix}, \qquad \tilde{\Gamma} = \begin{bmatrix} 0 & 0 \end{bmatrix}, \\
\tilde{Q} &= \begin{bmatrix} q_3 & q_4 \end{bmatrix}, \qquad \tilde{\Upsilon} = \begin{bmatrix} 0 & 0 \end{bmatrix}, \\
\tilde{\Psi}(w) &= -\begin{bmatrix} 0 & w_1 \\ w_2 & 0 \end{bmatrix}, \qquad \tilde{\Omega} = \begin{bmatrix} 1 & 0 \\ 0 & 1 \end{bmatrix},
\end{aligned}
\tag{379}
$$

- Fourth-order internal model case:

$$\tilde{A} = \begin{bmatrix} q_{17} & q_{18} \\ q_{23} & q_{24} \\ 0 & 0 \\ 0 & 0 \\ 0 & 0 \\ q_{33} & q_{34} \end{bmatrix}, \quad \tilde{\Phi}(w) = \begin{bmatrix} q_{21}\,w_1 + q_{22}\,w_2 & q_{35}\,w_1 & q_{36}\,w_2 & 0 & 0 & 0 & 0 & 0 \\ q_{27}\,w_1 + q_{28}\,w_2 & q_{25}\,w_1 & q_{26}\,w_2 & q_{31}\,w_1 + q_{32}\,w_2 & q_{30}\,w_1 & q_{29}\,w_1 & 0 & 0 \\ 0 & 0 & 0 & 0 & 0 & 0 & 0 & 0 \\ 0 & 0 & 0 & 0 & 0 & 0 & 0 & 0 \\ 0 & 0 & 0 & 0 & 0 & 0 & 0 & 0 \\ q_{37}\,w_1 + q_{38}\,w_2 & q_{35}\,w_1 & q_{36}\,w_2 & 0 & 0 & 0 & 0 & 0 \end{bmatrix},$$

$$\tilde{C} = \begin{bmatrix} 0 & 0 \end{bmatrix}, \qquad \tilde{\Gamma} = \begin{bmatrix} 0 & 0 & 0 & 0 & 0 & 0 & 0 & 0 \end{bmatrix},$$

$$\tilde{Q} = \begin{bmatrix} q_7 & q_8 \end{bmatrix}, \quad \tilde{\Upsilon}(w) = \begin{bmatrix} q_{11}\,w_1 + q_{12}\,w_2 & q_9\,w_1 & q_{10}\,w_2 & 0 & 0 & 0 & 0 & 0 \end{bmatrix},$$

$$\tilde{\Psi}(w) = - \begin{bmatrix} 0 & w_1 \\ w_2 & 0 \\ 0 & w_2 \\ 0 & 0 \\ 0 & 0 \\ 0 & 0 \\ 0 & 0 \\ 0 & 0 \end{bmatrix}, \quad \tilde{\Omega}(w) = \begin{bmatrix} 1 & 0 & 0 & 0 & 0 & 0 & 0 & 0 \\ 0 & 1 & 0 & 0 & 0 & 0 & 0 & 0 \\ 0 & 0 & 1 & 0 & 0 & 0 & 0 & 0 \\ 0 & 0 & 0 & 1 & 0 & 0 & -w_2 & 0 \\ 0 & 0 & 0 & 0 & 1 & 0 & -w_1 & 0 \\ 0 & 0 & 0 & 0 & 0 & 1 & 0 & -w_1 \\ -w_1 & 0 & 0 & 0 & 0 & 0 & 1 & 0 \\ 0 & -w_1 & 0 & 0 & 0 & 0 & 0 & 1 \end{bmatrix}, \tag{380}$$

In all scenarios, it also follows that $C_e = C$, $\tilde{C}_e = \tilde{C}$, $\Gamma_e = \Gamma$ and $\tilde{\Gamma}_e = \tilde{\Gamma}$.

Considering the exosystem invariant domain $\mathcal{W}$ declared in (367), the bounding ellipsoid $\mathcal{W}_{\mathcal{E}} \supseteq \mathcal{W}$ in the form of (325) may be set with $\tilde{P} = \overline{w}^{\,-2}\, I$. Moreover, the bounding convex set $\mathcal{W}^+ \supseteq \mathcal{W}_{\mathcal{E}}$ may be specified as $\mathcal{W}^+ = \mathrm{Co}\{\mathcal{V}_{w_1}\} \times \mathrm{Co}\{\mathcal{V}_{w_2}\}$ for the set of vertices $\mathcal{V}_{w_1} = \mathcal{V}_{w_2} = \{-\overline{w}\,,\, \overline{w}\,\}$. On the other hand, the convex region $\mathcal{Z}^+$ may be defined by $\mathcal{Z}^+ = \mathrm{Co}\{\mathcal{V}_{z_1}\} \times \mathbb{R}^{n_z}$, where $\mathcal{V}_{z_1} = \{-\overline{e}\,,\, \overline{e}\,\}$, with $\overline{e}$ denoting the maximum admissible value of $|z_1(t)| = |e(t)|\ \forall\, t \geq 0$.

The parameters a_1, a_2, a_3, ω and $\overline{w}$ are the same as previously considered for the numerical solution of the regulator equations. In turn, the design specifications are being considered here as $\overline{e} = 3$, $\alpha = 0.4$ and $r = 40$, which are identical for all cases in order to provide a fair comparative analysis. Also, in this initial comparison, no control input limit is established. Given these numerical setup, the proposed synthesizing optimization (354) was evaluated for all cases, where the objective selector was set as $\kappa = 1$ so as to fully prioritize the maximization of the region $(\mathcal{D} - \mathcal{B}_\infty)$. The obtained stabilizing controller parameters are presented next.

- No internal model case:

$$\mathrm{F} = \begin{bmatrix} -1.1986 & 0.0532 \\ -0.0054 & -35.808 \end{bmatrix}, \quad \mathrm{G} = \begin{bmatrix} 39.180 \\ 0.0031 \end{bmatrix},$$
$$\mathrm{H} = \begin{bmatrix} -39.180 & -0.1506 \end{bmatrix}, \quad \mathrm{K} = -46.690\,. \tag{381}$$

- Second-order internal model case:

$$\mathrm{F} = \begin{bmatrix} -4.8119 & 28.545 & -0.1580 & -0.0006 \\ -0.0350 & -4.6286 & 0.0003 & -0.0003 \\ -0.0000 & -0.0001 & -0.7016 & 0.0483 \\ -0.0000 & 0.0003 & -0.2453 & -35.835 \end{bmatrix}, \quad \mathrm{G} = \begin{bmatrix} 62.975 \\ -0.1045 \\ -1596.9 \\ 1.7793 \end{bmatrix},$$
$$\mathrm{H} = \begin{bmatrix} -11.914 & -0.2665 & 0.0008 & 0.0001 \\ -57.332 & -6.4064 & -2.1336 & -0.0036 \\ -0.1182 & -1598.2 & 0.8457 & 0.0122 \end{bmatrix}, \quad \mathrm{K} = \begin{bmatrix} -47.125 \\ -842.99 \\ -1891.6 \end{bmatrix}. \tag{382}$$

- Fourth-order internal model case:

$$\mathrm{F} = \begin{bmatrix} -10.167 & 0.1241 & -1.9474 & -0.1083 & 8.2752 & -0.0069 \\ 0.0001 & -10.169 & 0.0405 & 0.2609 & -0.0775 & -0.0127 \\ -0.0002 & 0.0051 & -10.528 & -0.0511 & 0.8353 & 0.0017 \\ -0.0000 & 0.0068 & 0.0007 & -10.776 & -0.2136 & 0.0337 \\ 0.0005 & 0.0167 & 0.0582 & -0.5630 & -0.7580 & 0.0170 \\ 0.0000 & 0.0012 & 0.0019 & -0.0764 & 0.0693 & -35.817 \end{bmatrix}, \quad \mathrm{G} = \begin{bmatrix} 789.59 \\ -5.2093 \\ 76.666 \\ -22.740 \\ 898.32 \\ 3.9626 \end{bmatrix},$$

$$\mathrm{H} = \begin{bmatrix} -0.7302 & -0.0161 & 0.0352 & 0.0052 & -0.0040 & 0.0004 \\ -7.4245 & -19.964 & 6.1958 & 1.9575 & 5.9325 & 0.0127 \\ -0.0020 & -200.09 & 144.06 & 31.905 & -13.803 & 0.1170 \\ -0.0142 & 21.944 & 709.66 & -25.955 & -61.279 & -0.0489 \\ 6.5977 & -27.291 & -623.50 & -914.87 & 29.716 & -1.0878 \end{bmatrix}, \quad \mathrm{K} = \begin{bmatrix} -47.941 \\ -1056.6 \\ -4434.9 \\ -1346.1 \\ 23884 \end{bmatrix}. \tag{383}$$

For each case with zero, second, and fourth-order internal model, the lowest achieved objective η_∞ was respectively $4.9610 \cdot 10^{-6}$, $4.5203 \cdot 10^{-7}$ and $1.1610 \cdot 10^{-8}$. The subsequent Figures 26 and 27 depict the resulting ultimate bounding set $\mathcal{B}_\infty$ and the set of admissible initial conditions $\mathcal{D}$, where both of them are projected into the (z_1, z_2)-plane, i.e. the z_x-plane. While in all cases the domain of attraction $\mathcal{D}$ has a similar volume, a significant reduction is observed in $\mathcal{B}_\infty$ as the internal model order increases. Complementary, Table 2 shows a series of finite time bounds η_τ for $\tau \in \{5, 15, 20, 25, 30, 35\}$, in seconds, calculated as in (335). The optimization problem (352) was also evaluated *a posteriori* so as to determine an ultimate bound γ_∞ for the output error norm $||e||$, which yielded $6.6820 \cdot 10^{-3}$, $2.0170 \cdot 10^{-3}$ and $3.2328 \cdot 10^{-4}$ for zero, second and fourth-order internal models. Since in here z_1 is equal to e, the value of γ_∞ denotes extreme points inside $\mathcal{B}_\infty$ with respect to the z_1 axis, as may be seen in Figure 26. The optimization problem (352) was also checked for finite time periods from Table 2, yielding the numerical results presented in the sequence by Table 3.

In what follows, the closed-loop numerical simulation is analyzed and compared for each designed controller. The considered initial conditions were $x(0) = [-2 \quad -100]^\intercal$, $\xi(0) = 0$ and $w(0) = [0 \ \ 1]^\intercal$, for which practical output regulation is theoretically ensured in all cases with ultimate error bounds as in Table 3. Figure 28 primarily shows transient plots of the output error signal $e(t)$ and the control input $u(t)$, indicating no major differences between the different scenarios. Figure 29 afterwards focuses in the steady-state behavior of the signals $e(t)$ and $u(t)$, where as expected, a visible output error attenuation is observed as the internal model complexity increases.

Figure 30 compares the approximated zero-error steady-state trajectory corresponding to the mappings $\tilde{\pi}_1(w)$, $\tilde{\pi}_2(w)$ and $\tilde{c}(w)$, as defined in (361), (5.4.1) and (5.4.1) respectively for the zero, second and fourth-order internal model case. In the last case, the mappings $\tilde{\pi}(w)$ and $\tilde{c}(w)$ were set as polynomials of third-degree, which yielded a very close proximity to the actual simulated steady-state trajectory, showed in thin black line.

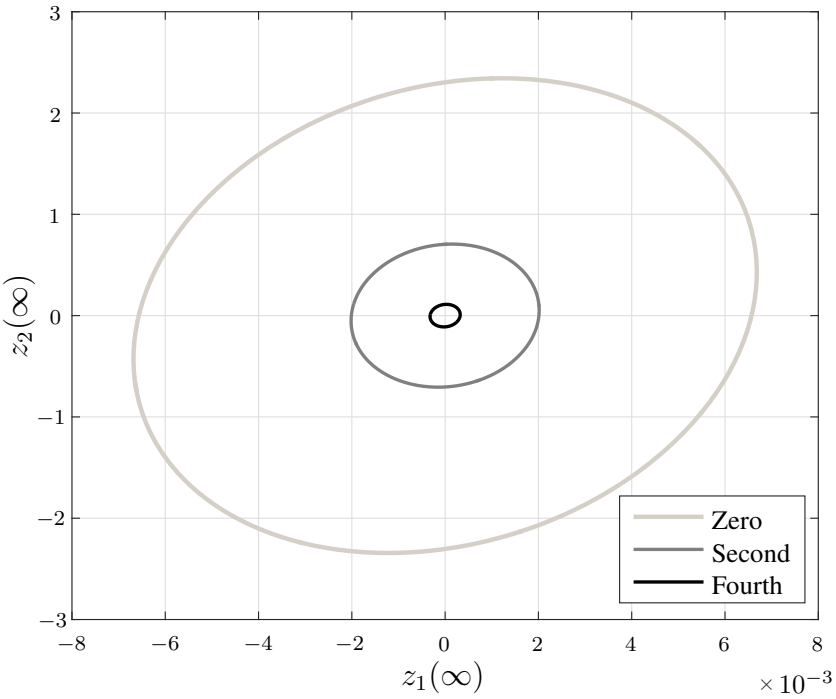

Figure 26: Projection of the ultimate bound region $\mathcal{B}_\infty$ into the z_x-plane for different internal model orders. Source: the author.

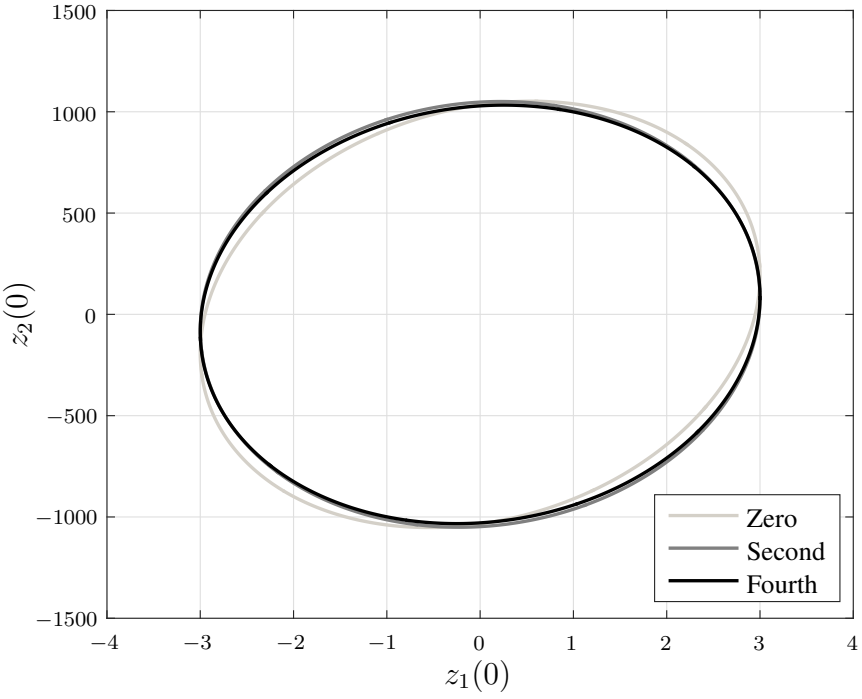

Figure 27: Projection of the initial condition region $\mathcal{D}$ into the z_x-plane for different internal model orders. Source: the author.

Table 2: Theoretical upper bounds η_τ of the Lypunov function $V(\mathbf{z})$ according to the internal model order. Source: the author.

Internal model order	Zero	Second	Fourth
Initial V-level bound (η_0)	1	1	1
V*-level bound after* $5\,\mathrm{s}$ (η_5)	$1.8321 \cdot 10^{-2}$	$1.8316 \cdot 10^{-2}$	$1.8316 \cdot 10^{-2}$
V*-level bound after* $10\,\mathrm{s}$ (η_{10})	$3.4042 \cdot 10^{-4}$	$3.3591 \cdot 10^{-4}$	$3.3547 \cdot 10^{-4}$
V*-level bound after* $15\,\mathrm{s}$ (η_{15})	$1.1105 \cdot 10^{-5}$	$6.5962 \cdot 10^{-6}$	$6.1558 \cdot 10^{-6}$
V*-level bound after* $20\,\mathrm{s}$ (η_{20})	$5.0735 \cdot 10^{-6}$	$5.6456 \cdot 10^{-7}$	$1.2415 \cdot 10^{-7}$
V*-level bound after* $25\,\mathrm{s}$ (η_{25})	$4.9631 \cdot 10^{-6}$	$4.5409 \cdot 10^{-7}$	$1.3671 \cdot 10^{-8}$
V*-level bound after* $30\,\mathrm{s}$ (η_{30})	$4.9610 \cdot 10^{-6}$	$4.5206 \cdot 10^{-7}$	$1.1648 \cdot 10^{-8}$
V*-level bound after* $35\,\mathrm{s}$ (η_{35})	$4.9610 \cdot 10^{-6}$	$4.5203 \cdot 10^{-7}$	$1.1611 \cdot 10^{-8}$
Ultimate V-level bound (η_∞)	$4.9610 \cdot 10^{-6}$	$4.5203 \cdot 10^{-7}$	$1.1610 \cdot 10^{-8}$

Table 3: Theoretical upper bounds γ_τ of the output error norm $||e||$ according to the internal model order. Source: the author.

Internal model order	Zero	Second	Fourth
Initial error bound (γ_0)	3	3	3
Error bound after $5\,\mathrm{s}$ (γ_5)	$4.0606 \cdot 10^{-1}$	$4.0601 \cdot 10^{-1}$	$4.0600 \cdot 10^{-1}$
Error bound after $10\,\mathrm{s}$ (γ_{10})	$5.5352 \cdot 10^{-2}$	$5.4984 \cdot 10^{-2}$	$5.4947 \cdot 10^{-2}$
Error bound after $15\,\mathrm{s}$ (γ_{15})	$9.9973 \cdot 10^{-3}$	$7.7049 \cdot 10^{-3}$	$7.4431 \cdot 10^{-3}$
Error bound after $20\,\mathrm{s}$ (γ_{20})	$6.7574 \cdot 10^{-3}$	$2.2541 \cdot 10^{-3}$	$1.0570 \cdot 10^{-3}$
Error bound after $25\,\mathrm{s}$ (γ_{25})	$6.6834 \cdot 10^{-3}$	$2.0216 \cdot 10^{-3}$	$3.5079 \cdot 10^{-4}$
Error bound after $30\,\mathrm{s}$ (γ_{30})	$6.6820 \cdot 10^{-3}$	$2.0171 \cdot 10^{-3}$	$3.2382 \cdot 10^{-4}$
Error bound after $35\,\mathrm{s}$ (γ_{35})	$6.6820 \cdot 10^{-3}$	$2.0170 \cdot 10^{-3}$	$3.2330 \cdot 10^{-4}$
Ultimate error bound (γ_∞)	$6.6820 \cdot 10^{-3}$	$2.0170 \cdot 10^{-3}$	$3.2328 \cdot 10^{-4}$

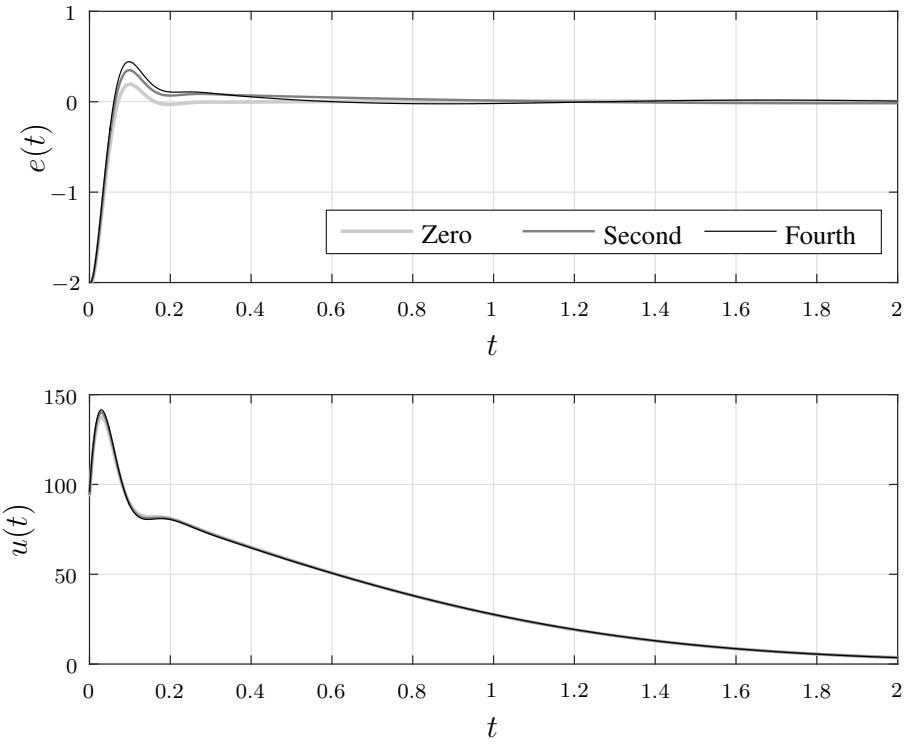

Figure 28: Transient output error signals $e(t)$ (on top) and control signals $u(t)$ (on bottom). Source: the author.

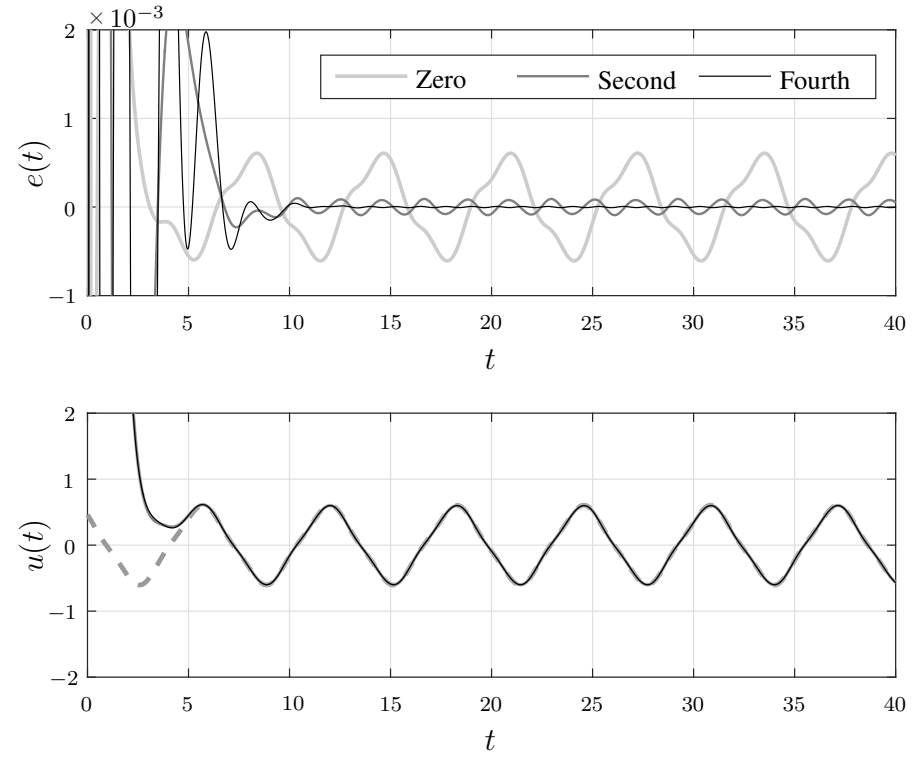

Figure 29: Steady-state output error signals $e(t)$ (on top) and control signals $u(t)$ (on bottom). The dashed line denotes the steady-state approximation $\tilde{c}(w(t))$ as used in the last scenario. Source: the author.

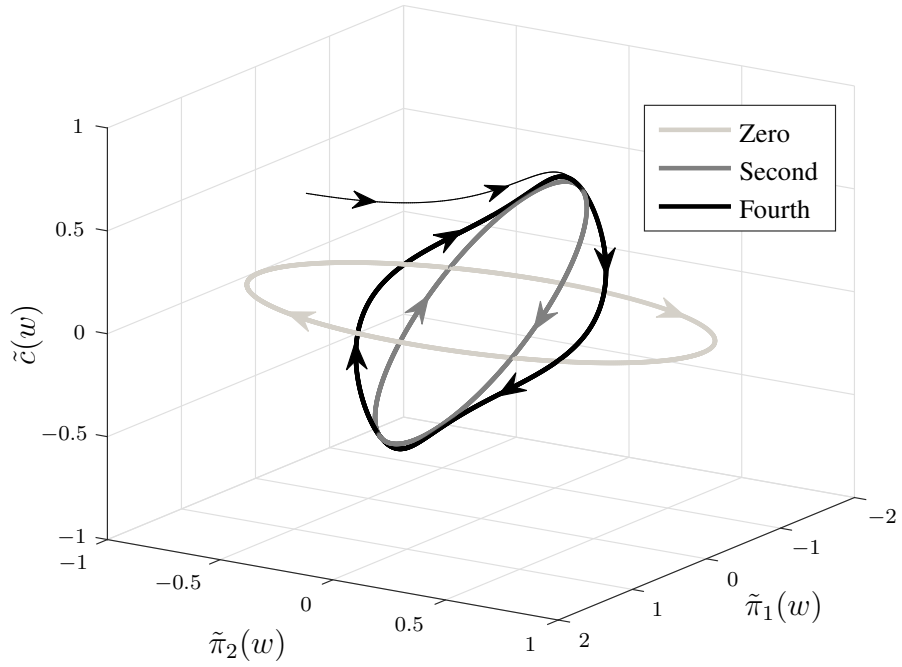

Figure 30: Approximated zero-error steady-state trajectories $(\tilde{\pi}_1(w), \tilde{\pi}_2(w), \tilde{c}(w))$ for the different evaluated cases. The thin black line denotes an actual simulated trajectory considering the last scenario. Source: the author.

5.4.3 Extended Design with Input Saturation and Anti-Windup

So as to demonstrate the full extent of the proposed methodology, the stabilizing stages are here redesigned considering input saturation and anti-windup compensation, where the maximum control amplitude is now enforced as $\overline{u} = 50$.

In order to synthesize the controllers in the presence of saturating inputs, it is furthermore necessary to determine magnitude bounds for the steady-state control mapping approximations, i.e. $\sup_{w\in\mathcal{W}} |\tilde{c}(w)| \leq \overline{c}$. By employing the optimization problem (272), it was determined $\overline{c} = 0$, $\overline{c} = 0.5942$ and $\overline{c} = 0.6599$ respectively for the zero, second and fourth internal model case. An additional design choice here is the function $\nu(z, w)$, which defines the affine relation of free decision variables related to the sector condition. Following previous considerations, the function $\nu(z, w)$ was accordingly set as $\nu(z, w) = [z_1 \;\; w_1 \;\; w_2]^\intercal$. Given this extended numerical setup, the synthesizing optimization (354) was reevaluated for all cases, where the newly obtained stabilizing controller parameters are presented next.

- No internal model case:

$$\begin{aligned} \mathrm{F} &= \begin{bmatrix} 8.7557 & 2.6972 \\ -0.3120 & -35.839 \end{bmatrix}, \quad \mathrm{G} = \begin{bmatrix} 27.490 \\ -0.1882 \end{bmatrix}, \\ \mathrm{H} &= \begin{bmatrix} -27.407 & -2.1450 \end{bmatrix}, \quad \mathrm{K} = -41.116\,. \end{aligned} \tag{384}$$

- Second-order internal model case:

$$\mathrm{F} = \begin{bmatrix} -4.1350 & 0.0023 & 0.6670 & -0.4459 \\ 0.0001 & -4.1365 & -0.5442 & 0.4420 \\ -0.0005 & 0.0283 & 6.9127 & -8.8513 \\ 0.0001 & -0.0001 & 0.6404 & -35.948 \end{bmatrix}, \quad \mathrm{G} = \begin{bmatrix} 22.830 \\ -18.377 \\ 369.87 \\ 7.2463 \end{bmatrix},$$
$$\mathrm{H} = \begin{bmatrix} -26.890 & 15.020 & 1.0482 & 0.2557 \\ -106.48 & 147.96 & 8.9083 & -0.0790 \\ 46.369 & 339.78 & 8.9715 & 0.3184 \end{bmatrix}, \quad \mathrm{K} = \begin{bmatrix} -38.564 \\ -199.83 \\ -218.46 \end{bmatrix}. \tag{385}$$

- Fourth-order internal model case:

$$\mathrm{F} = \begin{bmatrix} -4.1348 & 0.0000 & -0.0002 & 0.0032 & -0.3282 & -0.0564 \\ 0.0000 & -4.1349 & 0.0001 & -0.0023 & 0.2701 & 0.0536 \\ 0.0000 & 0.0001 & -4.1349 & 0.0072 & -0.9583 & -0.1853 \\ -0.0000 & -0.0000 & -0.0002 & -4.1430 & 1.1815 & 0.2691 \\ -0.0001 & -0.0003 & -0.0037 & -0.0649 & 7.7528 & 2.1583 \\ 0.0000 & -0.0000 & 0.0005 & -0.0044 & -0.3474 & -35.842 \end{bmatrix}, \quad \mathrm{G} = \begin{bmatrix} 52.712 \\ -43.156 \\ 152.51 \\ -187.50 \\ -1883.6 \end{bmatrix},$$
$$\mathrm{H} = \begin{bmatrix} -13.179 & 7.5166 & -0.7280 & 5.4249 & -0.8482 & 0.0286 \\ -51.812 & 67.108 & 8.0407 & 61.939 & -6.2685 & 0.1116 \\ 10.653 & 144.14 & 136.19 & 194.65 & -6.9990 & 0.2932 \\ -1.7635 & -15.798 & 384.40 & -185.98 & 43.307 & -0.4923 \\ 123.30 & -2.3364 & -854.95 & -1673.5 & 70.563 & -2.4519 \end{bmatrix}, \quad \mathrm{K} = \begin{bmatrix} -33.890 \\ -427.82 \\ -910.52 \\ 1198.2 \\ 6359.6 \end{bmatrix}. \tag{386}$$

Moreover, the following anti-windup gains were synthesized, recalling that E is related to the internal model stage, while W is associated with the stabilizer.

- No internal model case:

$$\mathrm{W} = \begin{bmatrix} 0.8878 \\ -0.1803 \end{bmatrix}. \tag{387}$$

- Second-order internal model case:

$$\mathrm{E} = \begin{bmatrix} -6.3297 \\ -5.9531 \end{bmatrix}, \quad \mathrm{W} = \begin{bmatrix} 0.8371 \\ -0.6858 \\ 13.833 \\ 3.9579 \end{bmatrix}. \tag{388}$$

- Fourth-order internal model case:

$$\mathrm{E} = \begin{bmatrix} -16.477 \\ -33.129 \\ 44.974 \\ 234.59 \end{bmatrix}, \quad \mathrm{W} = \begin{bmatrix} 2.3023 \\ -1.8902 \\ 6.6868 \\ -8.2399 \\ -82.662 \\ 10.449 \end{bmatrix}. \tag{389}$$

For each internal model scenario in consideration, the achieved theoretical bounds η_∞ is presented by Table 4 and the *a posteriori* determined bounds for the output error norm is also shown in Table 5. The graphical representation of the ultimate bounding set $\mathcal{B}_\infty$ and the set of admissible initial conditions $\mathcal{D}$ are complementary exposed in Figures 31 and 32. A major reduction in the volume of $\mathcal{B}_\infty$ is still observed as the internal model order increases, whereas the change in the volume of $\mathcal{D}$ is insignificant between all cases.

The subsequent Figures 33 and 34 present a numerical simulation of the closed-loop system for each designed controller when subject to input saturation. The considered initial conditions were $x(0) = [-2.5 \quad -10]^\intercal$, $\xi(0) = 0$ and $w(0) = [0 \quad 1]^\intercal$, for which $(\mathbf{z}(0), w(0))$ is inside and near the frontier of $\mathcal{D}$ in every scenario. In Figure 33, where the transient behavior is being focused, one may clearly see the input saturation effect acting in the control signal. In Figure 34, where the steady-state response is zoomed in, the same expect result is verified, i.e. the residual error diminishes according to the internal model order.

Table 4: Theoretical ultimate bound η_∞ of the Lypunov function $V(\mathbf{z})$ for each internal model order case when the controllers are subject to input saturation. Source: the author.

Internal model order	Zero	Second	Fourth
Ultimate V-level bound (η_∞)	$2.1222 \cdot 10^{-3}$	$2.0394 \cdot 10^{-4}$	$5.0034 \cdot 10^{-6}$

Table 5: Theoretical ultimate bound γ_∞ of the output error norm $||e||$ for each internal model order case when the controllers are subject to input saturation. Source: the author.

Internal model order	Zero	Second	Fourth
Ultimate error bound (γ_∞)	$1.3820 \cdot 10^{-1}$	$4.2842 \cdot 10^{-2}$	$6.7105 \cdot 10^{-3}$

5.5 Final Remarks

In this chapter, a novel ultimately bounded stabilization framework was developed for the practical output regulation of rational nonlinear systems, which represents a direct extension of the original methodology devised in Chapters 3 and 4. One of the main features of this extended work is the possibility to deal with systems without an exact knowledge of the zero-error steady-state conditions, thus relaxing previous assumptions regarding the analytic solution of the regulator equations. Another important feature, as emphasized earlier, is the possibility to use reduced order internal models, so as to simplify the implementation of the control law. In comparison to practical nonlinear output regulation design methods in the literature (MARCONI; PRALY, 2008), the contribution of this work is the consideration of systems that cannot be expressed in a normal form, which may also be subject to input saturation. The utilized methodology can also be extended for a wide range of future studies, including digitalization effects such as time-sampling and quantization.

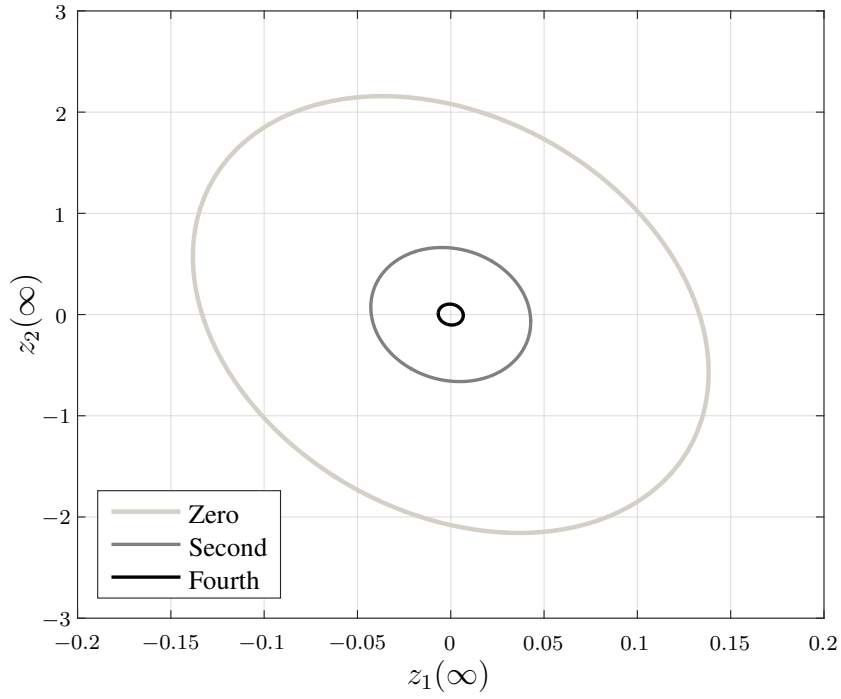

Figure 31: Projection of the ultimate bound region $\mathcal{B}_\infty$ into the z_x-plane for different internal model orders when the controllers are subject to input saturation. Source: the author.

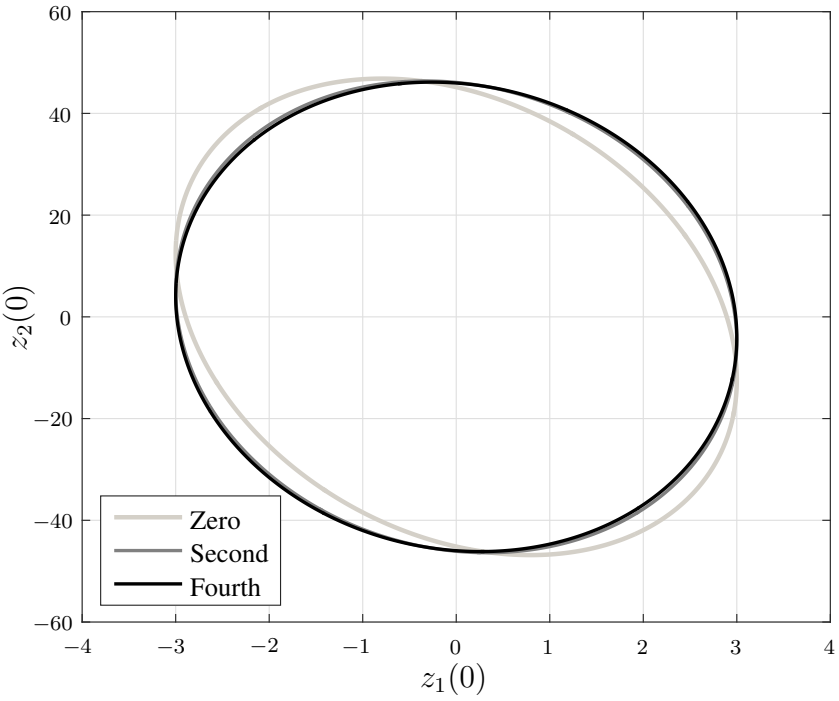

Figure 32: Projection of the initial condition region $\mathcal{D}$ into the z_x-plane for different internal model orders when the controllers are subject to input saturation. Source: the author.

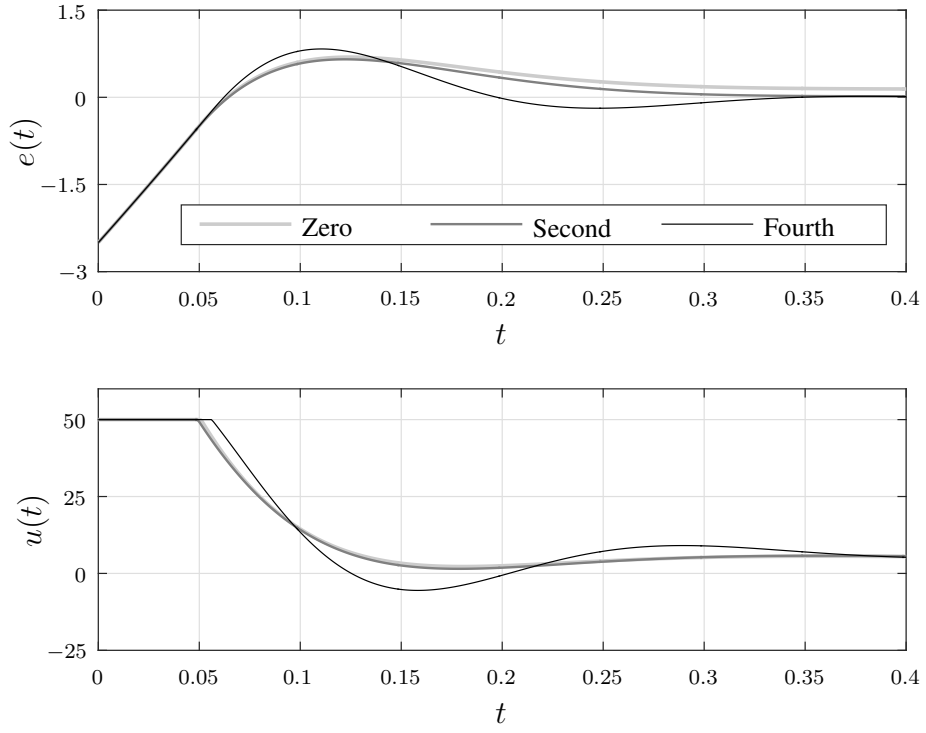

Figure 33: Transient output error signals $e(t)$ (on top) and control signals $u(t)$ (on bottom) when the controllers are subject to input saturation. Source: the author.

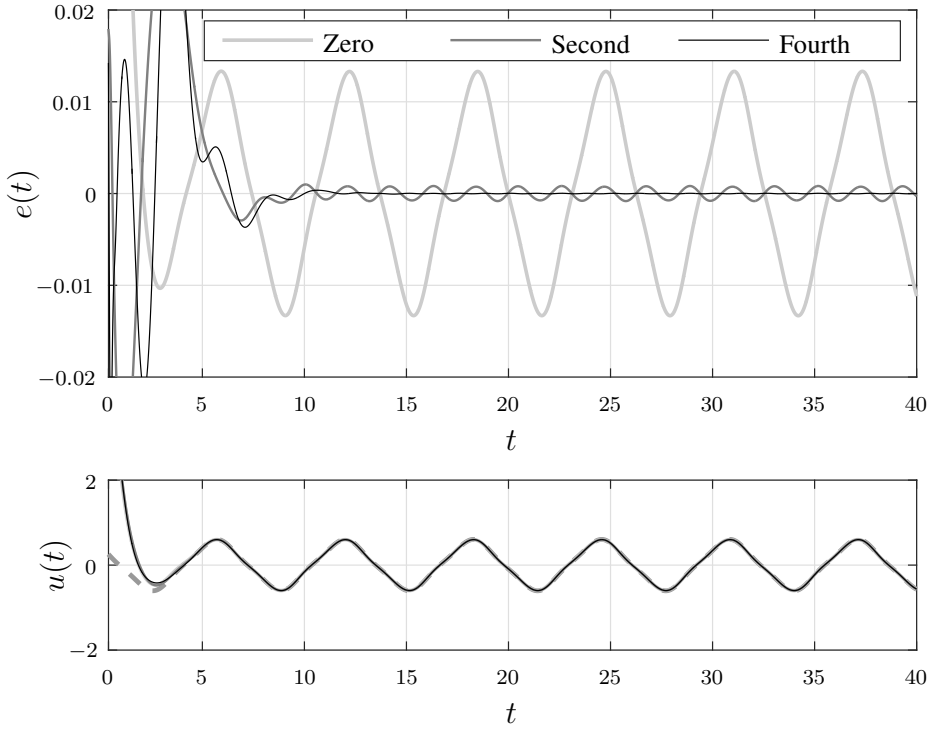

Figure 34: Steady-state output error signals $e(t)$ (on top) and control signals $u(t)$ (on bottom) when the controllers are subject to input saturation. Source: the author.

6 CONCLUSION AND PERSPECTIVES

In closing, this chapter brings an overview of the research highlighting the fulfillment of the established objectives and the main contributing aspects. The perspective for related future works is also exposed afterwards.

6.1 Overview of the Thesis

The overall objective of this thesis was to explore the usage of the differential-algebraic representation in order to systematically approach the output regulation design problem for rational nonlinear systems. Towards this goal, several theoretical results have been obtained as presented throughout the text.

Chapter 3 initially devised the basic foundation of the proposed framework, focusing on systems with rational regulation error dynamics with unbounded control input. In this first chapter, the text detailed the fundamental proposal for incorporating the differential-algebraic representation into a nonlinear output regulation problem, subsequently leading to stability and performance conditions, both for analysis purposes and for stabilization by output feedback. Subsequently Chapter 4 addressed systems subject to input saturation and, moreover, considered the design of anti-windup compensation for both internal model and stabilizing stages. Afterwards, in Chapter 5, the scope was extended for the practical output regulation context, where an ultimately bounded stabilization method was developed for the use of reduced order internal models and approximate solutions of the regulator equations.

As emphasized earlier, state-of-art methods on nonlinear output regulation commonly impose restrictions with respect to the structure of the controlled plant, for instance normal form representation, minimum-phase and affinity with respect to the control input. On the other hand, the developed work only requires rational regulation error dynamics and is also capable of dealing with the input saturation effect. On top of that, this work considered the anti-windup design for internal models and stabilizing controllers, which is a novel approach in the nonlinear output regulation field.

6.2 Future Perspectives

Among future investigations, one possibility is employing the proposed method in order to solve the master-slave synchronization problem (WIELAND; ALLGÖWER, 2009). In this context, the objective is to ensure that the state of a controlled slave system asymptotically tracks the state of an autonomous master system. Naturally, this is a particular case of the general output regulation, noting that the master system is an exosystem and

the slave system is a controlled plant. The proposed methodology is therefore readily applicable to this scenario. Nevertheless, a dedicated approach could take advantage of particular characteristics of the synchronization problem, for instance the identical dynamic structure between master and slave systems.

Another relevant but challenging extension would be the extension of the methodology in this thesis for multi-agent output regulation and syncronization cases considering cooperative control systems (SU; HUANG, 2012). In this scenario, one opportunity is dealing with the consensus problem (HU et al., 2014), where the objective is to ensure the trajectories of every agent system are ultimately synchronized with respect to each other.

A subject of particular interest is the study of ways to achieve less conservative domain of attraction estimates and ultimate bound regions. In this sense, one possibility is to employ refined *a posteriori* analyzes methods with state-dependent Lyapunov functions and annihilators, based on work of TROFINO; DEZUO (2014). Regarding the practical output regulation context, it is also possible to consider an additional numerical evaluation of the steady-state manifold, after the proposed synthesis procedure is completed. This approach may further reduce the regulation error system residuals in order to perform the analyzes.

Lastly, the theoretical methodology devised in thesis could be investigated in a miryad of real world applications. One perspective in this context is the regulation of offshore actuated platforms (FARIA et al., 2016), in order to smoothly compensate for the motion produced by sea waves. Another related practical case is the blade pitch regulation of wind turbines (CASTRO et al., 2017), where the objective is to alleviate periodic mechanical loads in the structure. Furthermore, an interesting perspective is spacecraft control (SALTON et al., 2017), where one could explore the problem of orbit synchronization for rendezvous and docking.

REFERENCES

BERTSEKAS, D. P. **Nonlinear programming**. Nashua: Athena Scientific Belmont, 1999. 780 p.

BOYD, S. et al. **Linear matrix inequalities in system and control theory**. Philadelphia: SIAM, 1994. 193 p.

BYRNES, C. I.; GILLIAM, D. S. Approximate solutions of the regulator equations for nonlinear DPS. In: IEEE CONFERENCE ON DECISION AND CONTROL (CDC'07), 46., 2007, New Orleans. **Proceedings...** New York: IEEE, 2007. p.854–859.

CASTRO, R. S. et al. Variable frequency resonant controller for load reduction in wind turbines. **Control Engineering Practice**, Amsterdam, v.66, p.76–88, 2017.

CASTRO, R. S.; FLORES, J. V.; SALTON, A. T. Robust Discrete-Time Spatial Repetitive Controller. **IEEE Transactions on Control Systems Technology**, New York, n.99, p.1–7, 2018.

CHEN, C.-T. **Linear system theory and design**. 2nd ed. New York: Holt, Rinehart and Winston, 1970. 679 p.

CHEN, Z.; HUANG, J. **Stabilization and regulation of nonlinear systems**. Berlin: Springer, 2015. 356 p.

CICEK, E.; DASDEMIR, J.; ZERGEROGLU, E. Coordinated synchronization of multiple robot manipulators with dynamical uncertainty. **Transactions of the Institute of Measurement and Control**, London, v.37, n.5, p.672–683, 2015.

COUTINHO, D. F. et al. Stability analysis and control of a class of differential-algebraic nonlinear systems. **International Journal of Robust and Nonlinear Control**, New Jersey, v.14, n.16, p.1301–1326, 2004.

COUTINHO, D. F.; GOMES DA SILVA JR, J. M. Estimating the region of attraction of nonlinear control systems with saturating actuators. In: AMERICAN COTNROL CONFERENCE (ACC'07), 26., 2007, New York. **Proceedings...** New York: IEEE, 2007. p.4715–4720.

FARIA, P. F. et al. Quaternion-based dynamic control of a 6-DOF Stewart platform for periodic disturbance rejection. In: IEEE CONFERENCE ON CONTROL APPLICATIONS (CCA'16), 2016, Buenos Aires. **Proceedings...** New York: IEEE, 2016. p.1191–1196.

FRANCIS, B. A.; WONHAM, W. M. The internal model principle of control theory. **Automatica**, Amsterdam, v.12, n.5, p.457–465, 1976.

FRIDMAN, E. Output regulation of nonlinear systems with delay. **Systems & Control Letters**, Amsterdam, v.50, n.2, p.81–93, 2003.

GAHINET, P. et al. The LMI control toolbox. In: IEEE CONFERENCE ON DECISION AND CONTROL (CDC'94), 33., 1994, Lake Buena Vista. **Proceedings...** New York: IEEE, 1994. v.3, p.2038–2041.

GOMES DA SILVA JR, J. M. et al. Dynamic output feedback stabilization for systems with sector-bounded nonlinearities and saturating actuators. **Journal of the Franklin Institute**, Amsterdam, v.350, n.3, p.464–484, 2013.

GOMES DA SILVA JR, J. M. et al. Static anti-windup design for a class of nonlinear systems. **International Journal of Robust and Nonlinear Control**, New Jersey, v.24, n.5, p.793–810, 2014.

GOMES DA SILVA JR, J. M.; LONGHI, M. B.; OLIVEIRA, M. Z. Dynamic anti-windup design for a class of nonlinear systems. **International Journal of Control**, Abingdon, v.89, n.12, p.2406–2419, 2016.

GOMES DA SILVA JR, J. M.; TARBOURIECH, S. Antiwindup design with guaranteed regions of stability: an LMI-based approach. **IEEE Transactions on Automatic Control**, New York, v.50, n.1, p.106–111, 2005.

HU, J. et al. Consensus of nonlinear multi-agent systems with observer-based protocols. **Systems & Control Letters**, Amsterdam, v.72, p.71–79, 2014.

HUANG, J. **Nonlinear output regulation**: theory and applications. Philadelphia: SIAM, 2004. 334 p.

HUANG, J.; CHEN, Z. A general framework for tackling the output regulation problem. **IEEE Transactions on Automatic Control**, New York, v.49, n.12, p.2203–2218, 2004.

ISIDORI, A.; BYRNES, C. I. Output regulation of nonlinear systems. **IEEE Transactions on Automatic Control**, New York, v.35, n.2, p.131–140, 1990.

ISIDORI, A.; MARCONI, L.; SERRANI, A. **Robust autonomous guidance**: an internal model approach. Berlin: Springer, 2012. 229 p.

KANEV, S. et al. Robust output-feedback controller design via local BMI optimization. **Automatica**, Amsterdam, v.40, n.7, p.1115–1127, 2004.

KHAILAIE, S.; ADHAMI-MIRHOSSEINI, A.; YAZDANPANAH, M. J. Analytic approximate solution to the nonlinear output regulation problem using Galerkin approximation method. In: IFAC WORLD CONGRESS, 18., 2011, Milano. **Proceedings...** Amsterdam: Elsevier, 2011. v.44, n.1, p.1392–1397.

KHALIL, H. **Nonlinear Systems**. New Jersey: Prentice Hall, 2002. 768 p.

KIM, S.-K. et al. Disturbance-observer-based model predictive control for output voltage regulation of three-phase inverter for uninterruptible-power-supply applications. **European Journal of Control**, Amsterdam, v.23, p.71–83, 2015.

LAGARIS, I. E.; LIKAS, A.; FOTIADIS, D. I. Artificial neural networks for solving ordinary and partial differential equations. **IEEE Transactions on Neural Networks**, New York, v.9, n.5, p.987–1000, 1998.

LI, D. et al. Estimating the bounds for the Lorenz family of chaotic systems. **Chaos, Solitons & Fractals**, Amsterdam, v.23, n.2, p.529–534, 2005.

LU, M.; HUANG, J. A class of nonlinear internal models for global robust output regulation problem. **International Journal of Robust and Nonlinear Control**, New Jersey, v.25, n.12, p.1831–1843, 2015.

MARCONI, L.; PRALY, L. Uniform practical nonlinear output regulation. **IEEE Transactions on Automatic Control**, New York, v.53, n.5, p.1184–1202, 2008.

MARINO, R.; TOMEI, P. Global adaptive regulation of uncertain nonlinear systems in output feedback form. **IEEE Transactions on Automatic Control**, New York, v.58, n.11, p.2904–2909, 2013.

MOREIRA, L. et al. Event-triggered Control for Nonlinear Rational Systems. In: IFAC WORLD CONGRESS, 20., 2017, Toulouse. **Proceedings...** Amsterdam: Elsevier, 2017. v.50, n.1, p.15307–15312.

PAVLOV, A. V.; WOUW, N. van de; NIJMEIJER, H. **Uniform output regulation of nonlinear systems**: a convergent dynamics approach. Berlin: Springer, 2006. 172 p.

SALTON, A. T. et al. Semidefinite Programming Solution to the Spacecraft Analysis and Control Problem. In: IFAC WORLD CONGRESS, 20., 2017, Toulouse. **Proceedings...** Amsterdam: Elsevier, 2017. v.50, n.1, p.3959–3964.

SCHERER, C.; GAHINET, P.; CHILALI, M. Multiobjective output-feedback control via LMI optimization. **IEEE Transactions on Automatic Control**, New York, v.42, n.7, p.896–911, 1997.

SENOUCI, A. et al. Robust chaotic communication based on indirect coupling synchronization. **Circuits, Systems, and Signal Processing**, Berlin, v.34, n.2, p.393–418, 2015.

SOUZA, C.; COUTINHO, D.; GOMES DA SILVA JR, J. M. Local input-to-state stabilization and ℓ_∞-induced norm control of discrete-time quadratic systems. **International Journal of Robust and Nonlinear Control**, New Jersey, v.25, n.14, p.2420–2442, 2015.

SU, Y.; HUANG, J. Cooperative output regulation of linear multi-agent systems. **IEEE Transactions on Automatic Control**, New York, v.57, n.4, p.1062–1066, 2012.

SUYKENS, J.; VANDEWALLE, J.; DE MOOR, B. An absolute stability criterion for the Lur'e problem with sector and slope restricted nonlinearities. **IEEE Transactions on Circuits and Systems I: Fundamental Theory and Applications**, New York, v.45, n.9, p.1007–1009, 1998.

TARBOURIECH, S. et al. **Stability and stabilization of linear systems with saturating actuators**. Berlin: Springer, 2011. 430 p.

TROFINO, A. Robust stability and domain of attraction of uncertain nonlinear systems. In: AMERICAN COTNROL CONFERENCE (ACC'00), 2000, Chicago. **Proceedings...** New York: IEEE, 2000. v.5, p.3707–3711.

TROFINO, A.; DEZUO, T. LMI stability conditions for uncertain rational nonlinear systems. **International Journal of Robust and Nonlinear Control**, New Jersey, v.24, n.18, p.3124–3169, 2014.

VANANTWERP, J. G.; BRAATZ, R. D. A tutorial on linear and bilinear matrix inequalities. **Journal of Process Control**, Amsterdam, v.10, n.4, p.363–385, 2000.

WIELAND, P.; ALLGÖWER, F. An internal model principle for synchronization. In: IEEE INTERNATIONAL CONFERENCE ON CONTROL AND AUTOMATION (ICCA'09), 2009, Christchurch. **Proceedings...** New York: IEEE, 2009. p.285–290.

XIA, Y. et al. Finite-time tracking control of rigid spacecraft under actuator saturations and faults. In: **Finite Time and Cooperative Control of Flight Vehicles**. Berlin: Springer, 2019. p.141–169.

XU, D.; CHEN, Z.; WANG, X. Global robust stabilization of nonlinear cascaded systems with integral ISS dynamic uncertainties. **Automatica**, Amsterdam, v.80, p.210–217, 2017.

XU, D.; WANG, X.; CHEN, Z. Output regulation of nonlinear output feedback systems with exponential parameter convergence. **Systems & Control Letters**, Amsterdam, v.88, p.81–90, 2016.

YANG, Z.; LI, Y. Active vertical vane control for stabilizing platform roll motion of floating offshore turbines. **Wind Energy**, New Jersey, 2018.

APPENDIX A COMPLEMENTARY MATERIAL

This appendix organizes a complementary material for the main text of the thesis. Primarily, Section A.1 shows a brief introduction on linear matrix inequalities and some useful related lemmas. In the sequence, Section A.2 details an approach for dealing with optimization problems subject to bilinear matrix inequalities.

A.1 Linear Matrix Inequalities

A *linear matrix inequality* (LMI) is a particular type of constraint defined by an affine relation

$$\mathtt{F}(\mathtt{x}) = \mathtt{F}_0 + \sum_{i=1}^{m} \mathtt{F}_i \, \mathtt{x}_i \succ 0 \, , \tag{390}$$

where $\mathtt{x} = [\mathtt{x}_1 \ \mathtt{x}_2 \ \ldots \ \mathtt{x}_m]^\mathsf{T} \in \mathbb{R}^m$ is the vector of decision variables and $\mathtt{F}_i \in \mathbb{R}^{n \times n}$ $\forall \, i \in \{0, 1, \ldots, m\}$ are symmetric matrices. An important property of an LMI is the convexity of its correspondent set $\mathcal{F} = \{\mathtt{x} \in \mathbb{R}^m : \mathtt{F}(\mathtt{x}) \succ 0\}$.

Problems involving LMI constraints are typically a feasibility problem or a convex optimization problem. A feasibility problem consists simply on finding some $\mathtt{x}$ such that $\mathtt{x} \in \mathcal{F}$. On the other hand, an optimization problem consists on minimizing a linear objective function $\mathtt{f}(\mathtt{x}) = \mathtt{c}^\mathsf{T}\mathtt{x}$, $\mathtt{c} \in \mathbb{R}^m$, subject to $\mathtt{x} \in \mathcal{F}$, i.e.

$$\min_{\mathtt{x}} \mathtt{c}^\mathsf{T}\mathtt{x} \ \text{ s.t. } \ \mathtt{F}(\mathtt{x}) \succ 0 \, . \tag{391}$$

This particular kind of convex optimization problem is also referred to as semidefinite programming (SDP) (BOYD et al., 1994).

Over the past years, there was a significant development on numerical tools, such as interior point methods, which are able to efficiently solve LMI feasibility and SDP problems (BOYD et al., 1994). The development of these numerical methods have been specially attractive for the field of control theory because it is possible to cast a wide range of problems in the LMI framework. A classical example is the stability of linear systems $\dot{x} = Ax$ with a quadratic Lyapunov function $V(x) = x^\mathsf{T}Px$, which is equivalent to finding a symmetric and positive-definite matrix P such that $PA + A^\mathsf{T}P \prec 0$ (CHEN, 1970). There also exist software packages able to translate problems such as this, from original matrix form, to the standard form (390) and subsequently apply the solution algorithm (GAHINET et al., 1994).

Some particular lemmas are often used in order to cast problems in the form of LMI constraints. In the following, there is a selection of important LMI related lemmas that are used in this work.

Lemma A.1. *(Congruence transformation) Let $P, Q \in \mathbb{R}^{n\times n}$ be symmetric matrices such that Q is non-singular. Then*

$$P \succ 0 \quad \Leftrightarrow \quad Q\,P\,Q^{\mathsf{T}} \succ 0\,. \tag{392}$$

Proof. Pre- and post-multiplying both sides of $P \succ 0$ by Q and Q^{T} yield $Q\,P\,Q^{\mathsf{T}} \succ 0$. Conversely, pre- and post-multiplying both sides of $Q\,P\,Q^{\mathsf{T}} \succ 0$ by Q^{-1} and $Q^{-\mathsf{T}}$ results $P \succ 0$ back, provided that Q is non-singular. □

Lemma A.2. *(Schur's complement) Consider matrices $P = P^{\mathsf{T}} \in \mathbb{R}^{n\times n}$, $R \in \mathbb{R}^{n\times m}$ and $= Q^{\mathsf{T}} \in \mathbb{R}^{m\times m}$ such that $Q \succ 0$. Then*

$$P - R\,Q^{-1}R^{\mathsf{T}} \succ 0 \quad \Leftrightarrow \quad \begin{bmatrix} P & R \\ R^{\mathsf{T}} & Q \end{bmatrix} \succ 0\,. \tag{393}$$

Proof. The following identity holds:

$$X \triangleq \begin{bmatrix} P & R \\ R^{\mathsf{T}} & Q \end{bmatrix} = Y\,Z\,Y^{\mathsf{T}}\,, \quad Y \triangleq \begin{bmatrix} I & RQ^{-1} \\ 0 & I \end{bmatrix}\,, \quad Z \triangleq \begin{bmatrix} P - RQ^{-1}R^{\mathsf{T}} & 0 \\ 0 & Q \end{bmatrix}\,. \tag{394}$$

From Lemma A.1 and since Y is non-singular, one deduces that $X \succ 0$ if and only if $Y^{-1}XY^{-\mathsf{T}} \succ 0$, which is thus equivalent to $Z \succ 0$. In turn, $Z \succ 0$ if only if $P - RQ^{-1}R^{\mathsf{T}} \succ 0$ and $Q \succ 0$. □

Lemma A.3. *(Affine uncertainties) Let $\mathcal{X} \subset \mathbb{R}^n$ be a convex hull formed by a set of finitely many vertices $\mathcal{V}$, i.e. $\mathcal{X} = \mathrm{Co}\{\mathcal{V}\}$, and let a symmetric matrix $P(x)$ be an affine function with respect to x. Then*

$$P(x) \succ 0 \;\; \forall\, x \in \mathcal{V} \quad \Leftrightarrow \quad P(x) \succ 0 \;\; \forall\, x \in \mathcal{X}\,. \tag{395}$$

Proof. Consider $\mathcal{V} = \{v_1, v_2, \ldots, v_m\}$ where $v_1, \ldots, v_m \in \mathbb{R}^n$, $m \in \mathbb{N}$. Because $P(x)$ is an affine matrix function with respect to x, condition $P(x) \succ 0\; \forall\, x \in \mathrm{Co}\{\mathcal{V}\}$ can be re-arranged in the following polytopic form (BOYD et al., 1994):

$$\sum_{i=1}^{m} \alpha_i\, P(v_i) \succ 0 \;\; \forall\, \alpha \in \mathcal{P} \triangleq \left\{ \alpha \in \mathbb{R}^m : \sum_{i=1}^{m} \alpha_i = 1\,,\; \alpha_i > 0 \right\}\,. \tag{396}$$

If $P(v_i) \succ 0\; \forall\, i \in \{1, 2, \ldots, m\}$, i.e. $P(x) \succ 0\; \forall\, x \in \mathcal{V}$, then it follows that $\alpha_1 P(v_1) + \alpha_2 P(v_2) + \ldots + \alpha_m P(v_m) \succ 0\; \forall\, \alpha \in \mathcal{P}$, or equivalently $P(x) \succ 0\; \forall\, x \in \mathrm{Co}\{\mathcal{V}\}$. Thus $P(x) \succ 0\; \forall\, x \in \mathcal{V} \Rightarrow P(x) \succ 0\; \forall\, x \in \mathcal{X}$ and since $\mathcal{V} \subset \mathcal{X}$ the converse also verifies: $P(x) \succ 0\; \forall\, x \in \mathcal{X} \Rightarrow P(x) \succ 0\; \forall\, x \in \mathcal{V}$. □

Lemma A.4. *(Finsler's lemma) Consider matrices $P = P^{\mathsf{T}} \in \mathbb{R}^{n\times n}$ and $R \in \mathbb{R}^{m\times n}$. Then $x^{\mathsf{T}}Px > 0\; \forall\, x \in \mathcal{L}$, $x \neq 0$ where*

$$\mathcal{L} = \left\{ x \in \mathbb{R}^n : R\,x = 0 \right\}, \tag{397}$$

if there exists a matrix $L \in \mathbb{R}^{n\times m}$ such that

$$P + \mathcal{H}\{LR\} \succ 0\,. \tag{398}$$

Proof. Suppose $x \in \mathcal{L}$. Inequality $x^{\mathsf{T}} P x > 0$ can then be re-expressed as

$$x^{\mathsf{T}} P x + x^{\mathsf{T}} L R\, x + x^{\mathsf{T}} R^{\mathsf{T}} L^{\mathsf{T}} x > 0\,, \tag{399}$$

for any matrix $L \in \mathbb{R}^{n \times m}$, since $R\, x = 0$. If (398) is true, then (399) holds $\forall\, x \neq 0$ and, moreover, $x^{\mathsf{T}} P x > 0\ \forall\, x \in \mathcal{L},\, x \neq 0$ is satisfied. □

Lemma A.5. *(S-Procedure) Consider symmetric matrices $P_0, P_1, \ldots, P_m \in \mathbb{R}^{n \times n}$. Then $x^{\mathsf{T}} P_0\, x > 0\ \forall\, x \in \mathcal{Q},\, x \neq 0$ where*

$$\mathcal{Q} = \left\{ x \in \mathbb{R}^n : x^{\mathsf{T}} P_i\, x \leq 0\,,\ i = 1, 2, \ldots, m \right\}, \tag{400}$$

if there exist non-negative scalars $\tau_1, \tau_2, \ldots, \tau_m \in \mathbb{R}$ such that

$$P_0 + \sum_{i=1}^{m} \tau_i\, P_i \succ 0\,. \tag{401}$$

Proof. Suppose $x \in \mathcal{Q}$. If for some scalars $\tau_1, \tau_2 \ldots, \tau_m \geq 0$ it verifies that

$$x^{\mathsf{T}} P_0\, x + \tau_1\, x^{\mathsf{T}} P_1\, x + \tau_2\, x^{\mathsf{T}} P_2\, x + \ldots + \tau_m\, x^{\mathsf{T}} P_m\, x > 0\,, \tag{402}$$

then $x^{\mathsf{T}} P_0\, x > 0$, because $x^{\mathsf{T}} P_i\, x \leq 0\ \forall\, i \in \{1, 2, \ldots, m\}$. Consequently, if (401) is true then (402) holds $\forall\, x \neq 0$ and $x^{\mathsf{T}} P_0\, x > 0\ \forall\, x \in \mathcal{Q},\, x \neq 0$ is satisfied. □

Lemma A.6. *(Ellipsoid inclusion) Consider a symmetric positive-definite matrix $P \in \mathbb{R}^{n \times n}$, vectors $b_1, b_2, \ldots, p_m \in \mathbb{R}^n$ and scalars $a_1, a_2, \ldots, a_m \in \mathbb{R}$. Let $\mathcal{P}$ be an ellipsoidal set defined as*

$$\mathcal{P} = \left\{ x \in \mathbb{R}^n : x^{\mathsf{T}} P x \leq 1 \right\} \tag{403}$$

and let $\mathcal{X}$ be a polyhedral set defined by

$$\mathcal{X} = \left\{ x \in \mathbb{R}^n : |\, b_i^{\mathsf{T}}\, x\,| \leq a_i\,,\ i = 1, 2, \ldots, m \right\}. \tag{404}$$

Then $\mathcal{P} \subset \mathcal{X}$ if and only if

$$\begin{bmatrix} a_i^2 & b_i^{\mathsf{T}} \\ b_i & P \end{bmatrix} \succ 0\ \ \forall\, i \in \{1, 2, \ldots, m\}\,. \tag{405}$$

Proof. Suppose the following holds:

$$\pm a_i^{-1} (p_i^{\mathsf{T}}\, x + x^{\mathsf{T}} p_i) \leq 1 + x^{\mathsf{T}} P\, x\ \ \forall\, i \in \{1, 2, \ldots, m\}\,. \tag{406}$$

If $x \in \mathcal{P}$ then $\pm a_i^{-1} (b_i^{\mathsf{T}}\, x + x^{\mathsf{T}} b_i) \leq 2 \Rightarrow \pm a_i^{-1} (b_i^{\mathsf{T}}\, x) \leq 1 \Rightarrow \pm (b_i^{\mathsf{T}}\, x) \leq a_i \Rightarrow |b_i^{\mathsf{T}}\, x| \leq a_i$ $\forall\, i \in \{1, 2, \ldots, m\}$, and so $x \in \mathcal{X}$ as well. Notice that (406) can be re-arranged as

$$\begin{bmatrix} \pm a_i^{-1} & x^{\mathsf{T}} \end{bmatrix} \begin{bmatrix} a_i^2 & b_i^{\mathsf{T}} \\ \star & P \end{bmatrix} \begin{bmatrix} \pm a_i^{-1} \\ x \end{bmatrix} \geq 0\ \ \forall\, i \in \{1, 2, \ldots, m\}\,. \tag{407}$$

If condition (405) is true then (407) holds $\forall\, x \in \mathbb{R}^n$ and consequently: (405) $\Rightarrow \mathcal{P} \subset \mathcal{X}$. One can also prove that $\mathcal{P} \subset \mathcal{X} \Rightarrow$ (405) according to BOYD et al. (1994). □

A.2 Bilinear Matrix Inequalities

This complementary section details a procedure capable of addressing optimization problems subject to bilinear matrix inequalities, such as some cases highlighted in the main methodology from Chapters 3, 4 and 5.

In order to illustrate the suggested approach, let $\mathtt{x} \in \mathbb{R}^n$, $\mathtt{y} \in \mathbb{R}^m$ and $\mathtt{z} \in \mathbb{R}^p$ denote decision variables of an optimization problem as $\mathtt{x} = [\mathtt{x}_1 \ \mathtt{x}_2 \ \ldots \ \mathtt{x}_n]^\mathsf{T}$, $\mathtt{y} = [\mathtt{y}_1 \ \mathtt{y}_2 \ \ldots \ \mathtt{y}_m]^\mathsf{T}$ and $\mathtt{z} = [\mathtt{z}_1 \ \mathtt{z}_2 \ \ldots \ \mathtt{z}_p]^\mathsf{T}$. Moreover, consider a matrix inequality constraint in the form of

$$\mathtt{F}(\mathtt{x},\mathtt{y},\mathtt{z}) \triangleq \mathtt{A} + \sum_{i=1}^{n} \mathtt{B}_i\,\mathtt{x}_i + \sum_{i=1}^{m} \mathtt{C}_i\,\mathtt{y}_i + \sum_{i=1}^{p} \mathtt{D}_i\,\mathtt{z}_i + \sum_{i=1}^{m}\sum_{j=i}^{p} \mathtt{E}_{ij}\,\mathtt{y}_i\mathtt{z}_j \succ 0\,, \tag{408}$$

for some symmetric matrices $\mathtt{A}$,$\mathtt{B}_1$,...,$\mathtt{B}_n$,$\mathtt{C}_1$,...,$\mathtt{C}_m$,$\mathtt{D}_1$,...,$\mathtt{D}_p$,$\mathtt{E}_{11}$,...,$\mathtt{E}_{mp} \in \mathbb{R}^{q\times q}$. The inequality expressed by (408) is said to be a *bilinear matrix inequality* (BMI) with respect to decision variables $\mathtt{y}$ and $\mathtt{z}$, which means that if either $\mathtt{y}$ or $\mathtt{z}$ are regarded as fixed (not as decision variables), then (408) becomes a standard *linear matrix inequality* (LMI) such as (390). It should be clear though that the correspondent set of a BMI, i.e.

$$\mathcal{F} = \left\{(\mathtt{x},\mathtt{y},\mathtt{z}) \in \mathbb{R}^n \times \mathbb{R}^m \times \mathbb{R}^p : \mathtt{F}(\mathtt{x},\mathtt{y},\mathtt{z}) \succ 0\right\}\,, \tag{409}$$

is not convex in general, unlike sets formed by LMIs (VANANTWERP; BRAATZ, 2000).

The class of optimization problems to be dealt here is described according to:

$$\min_{\mathtt{x},\mathtt{y},\mathtt{z}} \mathtt{c}^\mathsf{T}\mathtt{x} \ \text{ s.t. } \ \mathtt{F}(\mathtt{x},\mathtt{y},\mathtt{z}) \succ 0\,, \tag{410}$$

for some $\mathtt{c} \in \mathbb{R}^n$ which defines the objective function. In spite of (410) being presented in a standard form, one should see that this optimization problem is equivalent to the ones previously presented as (180), (294) and (354). Take for instance (180):

$$\min_{X,Y,L,\hat{\mathrm{F}}_0,\ldots,\hat{\mathrm{K}}_\mathrm{n}} \ \mathrm{tr}(Y) \ \text{ s.t. } \ \big\{(168)\,,\,(169)\,,\,(170)\,,\,(171)\big\}\,. \tag{411}$$

where there are bilinear terms involving matrices L and X on inequality (170). In this case, "$\mathtt{y}$" may be regarded as the elements of L in vector form, and likewise "$\mathtt{z}$" may be considered as vectorization of the elements in matrix X. Lastly, "$\mathtt{x}$" denote all linearly related variables, which are the ones in Y, $\hat{\mathrm{F}}_0,\ldots,\hat{\mathrm{K}}_\mathrm{n}$. It should also be clear that multiple matrix inequality constraints, such as $\{(168)\,,\,(169)\,,\,(170)\,,\,(171)\}$, can always be represented as a single constraint by block diagonal concatenation.

Towards establishing a procedure able to solve (410), notice that because (408) is a BMI, if either $\mathtt{y}$ or $\mathtt{z}$ are fixed, then (410) become a standard semidefinite optimization problem (SDP), which is convex and can be addressed efficiently by numerical solvers (GAHINET et al., 1994). This simple observation can be used in order to break the problem (410) down into an iterative series of SDP sub-problems, where $\mathtt{y}$ and $\mathtt{z}$ are alternated between decision variables and fixed constants. An approach such as this has been proposed for robust output feedback control synthesis purposes, and it is known as D-K iteration on the literature (KANEV et al., 2004).

Prior to addressing the objective function $\mathtt{c}^\mathsf{T}\mathtt{x}$ of (410) it is necessary to find a feasible solution either for $\mathtt{y}$ or $\mathtt{z}$. So as to tackle this problem, a modified version of problem (410) may be considered:

$$\min_{\mathtt{x},\mathtt{y},\mathtt{z},\gamma} \gamma \ \text{ s.t. } \ \mathtt{F}(\mathtt{x},\mathtt{y},\mathtt{z}) + \gamma I \succ 0\,, \tag{412}$$

where $\gamma \in \mathbb{R}$ is an additional scalar variable. In contrast to the original case, the relaxed condition $\mathtt{F}(\mathtt{x},\mathtt{y},\mathtt{z}) + \gamma I \succ 0$ has the advantage of guaranteed feasibility, since there should always exists some $\gamma \in \mathbb{R}$ such that $\mathtt{F}(\mathtt{x},\mathtt{y},\mathtt{z}) + \gamma I$ becomes positive-definite. Moreover, if one is able to find a solution to (412) for some $\gamma < 0$, then the same solution is guaranteed to be feasible with respect to the original constraint $\mathtt{F}(\mathtt{x},\mathtt{y},\mathtt{z}) \succ 0$. After having found such a feasible solution, one can naturally consider the original objective function $\mathtt{c}^{\mathsf{T}}\mathtt{x}$ of (410) in the pursuance of a proximate locally optimal solution. Provided this explanation, the following iterative algorithm can be employed in order to address (410) in general.

(a) Feasibility phase:

(a.1) Define some initial guess for variable $\mathtt{y}$. One may consider $\mathtt{y} = 0$ by default.

(a.2) Regarding $\mathtt{z}$ as decision variable and $\mathtt{y}$ as fixed with the value obtained from previous step, solve the SDP

$$\min_{\mathtt{x},\mathtt{z},\gamma} \gamma \;\; \text{s.t.} \;\; \mathtt{F}(\mathtt{x},\mathtt{y},\mathtt{z}) + \gamma I \succ 0 \, . \tag{413}$$

(a.3) Regarding now $\mathtt{z}$ as fixed with the value obtained from previous step and $\mathtt{y}$ as decision variable, solve the SDP

$$\min_{\mathtt{x},\mathtt{y},\gamma} \gamma \;\; \text{s.t.} \;\; \mathtt{F}(\mathtt{x},\mathtt{y},\mathtt{z}) + \gamma I \succ 0 \, . \tag{414}$$

(a.4) Return to step (a.2). Stop this loop when γ is negative, meaning that a feasible solution has been found.

(b) Optimization phase:

(b.1) Regarding $\mathtt{z}$ as decision variable and $\mathtt{y}$ as fixed with the value obtained from previous step, solve the SDP

$$\min_{\mathtt{x},\mathtt{z}} \mathtt{c}^{\mathsf{T}}\mathtt{x} \;\; \text{s.t.} \;\; \mathtt{F}(\mathtt{x},\mathtt{y},\mathtt{z}) \succ 0 \, . \tag{415}$$

(b.2) Regarding now $\mathtt{z}$ as fixed with the value obtained from previous step and $\mathtt{y}$ as decision variable, solve the SDP

$$\min_{\mathtt{x},\mathtt{y}} \mathtt{c}^{\mathsf{T}}\mathtt{x} \;\; \text{s.t.} \;\; \mathtt{F}(\mathtt{x},\mathtt{y},\mathtt{z}) \succ 0 \, . \tag{416}$$

(b.3) Return to step (b.1). Stop this loop when $\mathtt{c}^{\mathsf{T}}\mathtt{x}$ does not decrease significantly between iterations, meaning that a proximate locally optimal solution has been found.